LA-UR- 98-5290

LATE QUATERNARY FAULTING ON THE PAJARITO FAULT, WEST OF LOS ALAMOS NATIONAL LABORATORY, NORTH-CENTRAL NEW MEXICO

Results from the Seven-Trench Transect Excavated in Summer of 1997

Final Report

Aug. 31, 1998

Submitted by:
James P. McCalpin
GEO-HAZ Consulting, Inc.
P.O. Box 1377
1221 Graves Avenue
Estes Park, CO 80517

Prepared for:
Douglas E. Volkman, P.E.
EES-1, MS M984
Los Alamos National Laboratory
Los Alamos, NM 87545

LATE QUATERNARY FAULTING ON THE PAJARITO FAULT, WEST OF LOS ALAMOS NATIONAL LABORATORY, NORTH-CENTRAL NEW MEXICO

Results from the Seven-Trench Transect Excavated in Summer of 1997

Final Report

Aug. 31, 1998

Submitted by:
James P. McCalpin
GEO-HAZ Consulting, Inc.
P.O. Box 1377
1221 Graves Avenue
Estes Park, CO 80517

Prepared for:
Douglas E. Volkman, P.E.
EES-1, MS M984
Los Alamos National Laboratory
Los Alamos, NM 87545

Table of Contents **Page**

List of Figures 4
List of Tables 7
List of Appendices 8

1. EXECUTIVE SUMMARY 9

2. INTRODUCTION 10
   2.1 Purpose and Scope of The Trenching Study 10
   2.2 Trench Locations and Rationale 13
   2.3 Field Methods 18
   2.4 Laboratory Methods 20
   2.5 Acknowledgments 24

3. RESULTS 26
   3.1 Pre-Trenching Seismic Refraction Survey 26
   3.2 Trench 1 28
      3.2.1 Stratigraphy 28
      3.2.2 Structure 32
      3.2.3 Geochronology 33
      3.2.4 Paleoseismic Interpretation 34
   3.3 Trench 2 35
      3.3.1 Stratigraphy 35
      3.3.2 Structure 38
      3.3.3 Geochronology 40
      3.3.4 Paleoseismic Interpretation 41
   3.4 Trench 3 42
      3.4.1 Geophysics 42
      3.4.2 Stratigraphy 42
      3.4.3 Structure 47
      3.4.4 Geochronology 50
      3.4.5 Paleoseismic Interpretation 51
   3.5 Trench 4 57
      3.5.1 Stratigraphy 57
      3.5.2 Structure 60
      3.5.3Geochronology 60
      3.5.4 Paleoseismic Inerpretation 62
   3.6 Trench 5 63
      3.6.1 Stratigraphy 63
      3.6.2 Structure 67
      3.6.3 Geochronology 68
      3.6.4 Paleoseismic Interpretation 71

3.7 Trench 6 73
3.7.1 Stratigraphy 73
3.7.2 Structure 77
3.7.3 Geochronology 79
3.7.4 Paleoseismic Interpretation 79
3.8 Trench 7 83
3.8.1 Geophysics 83
3.8.2 Stratigraphy 83
3.8.3 Structure 87
3.8.4 Geochronology 88
3.8.5 Paleoseismic Interpretation 89
3.9 Trench 7A 92
3.9.1 Stratigraphy 92
3.9.2 Structure 95
3.9.3 Geochronology 95
3.9.4 Paleoseismic Interpretation 96

4. INTERPRETATION 98
4.1 Refinement of the Structural Model of the PF 98
4.2 Timing of the Most Recent Faulting Event 100
4.3 Recurrence Intervals Between Paleoearthquakes on the Pajarito Fault 102
4.4 Displacement per Event on the Pajarito Fault 104

5. CONCLUSIONS AND RECOMMENDATIONS 105
5.1 Conclusions 105
5.2 Implications of the 1997 Trenching Results on Quaternary Slip rates for the Pajarito fault 105
5.3 Recommendations 107

6. REFERENCES 109

7. APPENDICES 112
7.1 Report by Dames and Moore Consultants on seismic refraction surveys
7.2 Report by Eric McDonald, Desert Research Institute, on detailed soil profile descriptions and Soil Development Index (SDI) calculations
7.3 Report by Steven L. Reneau, Los Alamos National Laboratory, on radiocarbon sampling and dating results, as of Feb. 11, 1998
7.4 Report by Steven L. Forman, University of Illinois-Chicago, on thermoluminescence (TL) dating

List of Figures

Fig. 1. Location map of Pajarito fault system, showing locations of 1992 trenches (Wong et al, 1993, 1995) and 1997 trenches

Fig. 2. Schematic cross-sections through the Pajarito fault zone. A- schematic diagram showing the crestal tension fissure, east-tilted slab, basal fault zone, and graben. B5 and B4 are subunits of the Tsherige Member of the Bandelier Tuff. Triangles indicate coarse crack fill, dots finer graben sediments; b- scaled cross- section of the PF main scarp across Ski Hill Road. Dips are from field measurements cm, megablock colluvium; Bt, tilted Bandelier Tuff; Bi, intact (untilted) Bandelier Tuff. Circles at far right indicate graben fill (alluvium and colluvium).

Fig. 3. Photograph of a sidewalk subjected to vertical displacement (down to right). Note tensional opening of the expansion joint at the head (left side) of the tilted slab. The right side (toe) of the tilted slab has also subsided slightly relative to the untilted slab on the right, due to soil compaction. This style of deformation is the proposed analogy for the "articulated monocline" model for the PF main scarp.

Fig. 4. Large- scale topographic map showing the seven trenches of the 1997 transect, plus structural features and geophysical lines.

Fig. 5. Aerial stereopair showing the seven- trench transect.

Fig. 6. Subsurface geophysical cross- section through the 200 m- wide graben east of the main scarp of the Pajarito fault. Detailed seismic data are given in Appendix A.

Fig. 7. Ground- level photograph of Trench 1; view is northwest looking up the scarp from the toe.

Fig. 8. Log of Trench 1.

Fig. 9. Photograph of the main deformation zone (fault zone C) in Trench 1, looking down at the logged wall from the surface.

Fig. 10. Log of Trench 2.

Fig. 11. Photograph of Trench 2 looking up the scarp.

Fig. 12. Photograph of Trench 3, looking NE across the trench toward the lip of Los Alamos Canyon. Scarp height increases north of the trench (upper left center) due to stream incision along the scarp.

Fig. 13. Log of Trench 3.

Fig. 14. Photograph of Holocene debris- facies colluvium (unit 15b, upper half of photo) overlying the main fault zone in Trench 3 (slightly to right of center). Red- brown material to right of main fault and beneath the white Holocene colluvium is strongly overprinted by Bt soil formation. To the left of the m[illegible] fault Bandelier Tuff is highly fractured (lower left center). String lines are 1 m apart, rails of shores are 20 cm wide.

Fig. 15. Close-up photograph of the main fault plane (fault A) in Trench 3. The level line at bottom is at - 3.0 mV; compare the two shores to those on Fig. 12. Sheer fabric is apparent in both units 10 and 11 (fissure fill to the right of the fault), expressed as microfractures and oriented clasts parallel to the fault plane. Unit left of fault plane is hard white tuff (unit 1a). Rails of shores are 20 cm wide.

Fig. 16. Hypothetical model for faulting and deposition in a graben, where normal faulting is accompanied by the formation of large fissures at the scarp base.

Fig. 17. Retrodeformation sequence for Trench 3.

Fig. 18. Slip history diagram for Trench 3, based on the retrodeformation sequence.

Fig. 19. Photograph of Trench 4, looking E toward the very low antithetic scarp.

Fig. 20. Log of Trench 4.

Fig. 21. Photograph of the main fault plane in Trench 4, looking down at the south (logged) wall from the surface.

Fig. 22. Photograph of the main fault plane in Trench 4, looking down at the north wall. Note prominent 10 cm-wide fissure.

Fig. 23. Overview photographs of Trench 5. A- base of main scarp of Pajarito fault, with graben to left and Trench 5 to right; b- looking up Trench 5 from the toe of the main scarp. Apparent crest of scarp at upper center is Ski Hill Road; true scarp crest is 15 m higher.

Fig. 24. Head of Trench 5 showing the lowest intact Tuff outcrop on the scarp face, and its subsurface extent (to right of ladder) that defines the head of the trench.

Fig. 25. Log of Trench 5.

Fig. 26. Photograph of fault E in the fault zone of Trench 5. The large pillar of tuff in the floor of the trench is barely visible at bottom center. Note steep clast orientations in trench wall.

Fig. 27. Overview of Trench 6 looking up trench from toe.

Fig. 28. Log of Trench 6.

Fig. 29 Schematic diagram showing how domino-style faulting affects the downthrown block in Trench 6.

Fig. 30. Partial retrodeformation sequence for Trench 6.

Fig. 31. Photograph of Trench 7.

Fig. 32 Log of Trench 7.

Fig. 33. Photograph of the upper part of fault A, where it forms a depositional contact between hard white Bandelier Tuff (at left) and mid-Holocene alluvium (unit 8).

Fig. 34 Retrodeformation sequence for Trench 7.

Fig. 35. Photograph of Trench 7A.

Fig. 36. Log of Trench 7A.

Fig. 37. Schematic diagrams showing how a subsurface normal fault would interact with a rigid surface slab of Tuff.

Fig. 38. Space-time diagram showing the limiting ages on the MREs in Trenches 3, 4, 7, and 7A.

Fig. 39. Empirical probability distribution of the COV of recurrence interval series between characteristic earthquakes, based on a worldwide paleoseismic data set. The mean COV of local recurrence series is 0.36.

List of Tables

Table 1. Comparison of Trenching Approaches for Characterizing the Pajarito Fault

Table 2. Time schedule of trench excavation and logging, summer 1997

Table 3. SDI age estimates for trenches 3, 4, 5, 6, and 7.

Table 4. Summary Table of Thermoluminescence Age Estimates.

Table 5. Summary Table of Radiocarbon Dates.

Table 6. SDI Age Estimates of Soils in Trench 3.

1. EXECUTIVE SUMMARY

In July 1997 we excavated seven trenches across strands of the Pajarito fault zone to characterize the most recent faulting event (MRE), and to refine characterization of previous faulting events. Our strategy for capturing the MRE was to excavate a series of seven trenches along an east-west transect across the fault zone south of Los Alamos Canyon, where parallel faults span a zone nearly 2 km wide. Two of the seven trenches were located on the main 50 m-high scarp of the Pajarito fault, with the remainder on smaller east- and west-facing scarps.

The best paleoseismic records were preserved on scarps that faced west, or upslope (Trenches 3, 4, 7, 7A). Each of these trenches displayed evidence of a mid-to late-Holocene MRE. Due to the anomalous dating results obtained in Trench 7, we excavated a small companion trench (7A) on April 8, 1998.

The MRE in Trenches 3, 4, 7 and 7a appears to fall in a relatively narrow age range between about 1260 and 2290 cal. yr BP, with the tightest bracketing coming from Trench 7A where the constraints are 1500 and 1520 cal. yr BP. If the radiocarbon ages are accurate, there was a large-displacement faulting event (ca. 1 m vertical displacement) at the sites of Trenches 3, 4 and 7. For this amount of displacement to occur on two antithetic faults, the net vertical displacement across the entire fault zone was probably greater. However, due to the monoclinal nature of the main fault scarp, net vertical displacement is difficult to estimate from displacements observed in Trenches 5 and 6 on the main scarp.

The record of older paleoearthquakes was partially reconstructed in Trenches 3, 5, 6, and 7. Trench 3, excavated across a secondary fault, contained evidence for at least six surface-rupturing events in the past ca. 110 ka. Because secondary faults may not record every faulting event, six events in the period 1.5-110 ka implies a maximum long-term mean recurrence interval of about 21 ka. The pre-110 ka part of the stratigraphic record in our trenches may not be complete, as suggested by cumulative SDI-based age estimates of ca. 400 ka at a stratigraphic level known to be 1.1 Ma by Ar-Ar dating. This discordance suggests that as much as 2/3 of the past 1.1 Ma is not represented by either graben sediments or soils, so there must have been significant erosion even in the tectonic sediment traps (tension fissures, grabens) where our trenches were located.

The MRE dated at ca. 1.5 ka does not appear to be contemporaneous with the MRE on the Guaje Mountain fault, dated at Cabra Canyon at 4-6 ka (Gardner et al, 1990). Additionally, the MRE seems to be too young to correlate with the MRE on the Rendija Canyon fault, dated at either 8 ka or 23 ka (Wong et al, 1995). Conversely, our trenches do not show evidence on the Pajarito fault for a second (or third) Holocene earthquake at either 4-6 ka or 8 ka. Thus, if the limiting ages for the MREs on the RCF and GMF (based on only 1 to 3 trenches) can be trusted, it appears that the MREs on each of the three faults in the Pajarito fault system are separate earthquakes.

List of Appendices

Appendix A. Report by Dames and Moore on seismic refraction surveys.

Appendix B. Report by Eric McDonald, Desert Research Institute, on detailed soil profile descriptions and soil development index (SDI) calculations.

Appendix C. Report by Steven L. Reneau, LANL, describing radiocarbon sampling and dating as of Feb. 11, 1998.

Appendix D. Report by Steven L. Forman, University of Illinois- Chicago, on thermoluminescence (TL) dating.

2. INTRODUCTION

This report summarizes the paleoseismic trenching study of the Pajarito fault performed by James P. McCalpin and co-workers during the summer and fall of 1997. Contained herein are the trench log. .d the interpretation of deformation events deduced from these logs.

2.1 Purpose and Scope of The Trenching Study

The primary purpose of this trenching study was to date the most recent faulting event (MRE) on the main trace of the Pajarito fault (PF) (Fig. 1). Previous studies (Gardner et al., 1990; Wong et al., 1993,1995; Olig et al., 1996; Kelson et al., 1996) of the Pajarito fault zone (PFZ) yielded relatively well - constrained ages for the MRE on the two major west-dipping faults, the Rendija Canyon fault (RCF) and Guaje Mountain fault (GMF). On the RCF, the MRE was dated at either 8 ka (based on radiocarbon) or 23 ka (based on TL; Kelson et al., 1996). On the GMF the MRE was dated at 4 - 6 ka (Gardner et al., 1990). In contrast, the MRE deduced on the main trace of the Pajarito fault zone (the Parajito fault PF) pre-dated the El Cajete pumice, and would thus be older than ca. 50 - 60 ka (Wong et al., 1995; Olig et al, 1996). Thus the Holocene (or late Pleistocene) MREs on the RCF and GMF evidently had no counterpart events on the main Pajarito fault.

The paleoearthquake chronology outlined above could be explained in three ways: (1) The dates of MREs on all three faults were correct, indicating that separate Holocene earthquakes had occurred on the RCF and GMF, but that no Holocene events had ruptured the PF; (2) the dates of MREs on the RCF and GMF are correct, but evidence of the MRE on the PF was not exposed in the Wong et al. (1993) trenches, so there may have been a Holocene event on the PF that matches the MRE on either the RCF or GMF; or (3) the MREs on the RCF and GMF are actually the same event, poorly constrained by current dates. If so, then this MRE also may have ruptured the PF, but that rupture was not exposed in the Wong et al. (1993) trenches.

In order to test these three hypotheses a paleoseismic program was implemented to find the MRE on the PF. First, the PF scarp was mapped at a scale of 1:1200 (McCalpin, 1997). Based on the map, a structural model was developed for the PF scarp, showing that the scarp consisted of an articulated monocline (ca. 50% of its length), landslide blocks (ca. 30% of its length), or a simple high-angle normal fault (ca. 20% of its length). Given this structural configuration, three possible trenching strategies were envisioned (Table 1). The first was a megatrench through the ca. 50 m-thick colluvial wedge at the scarp base where the scarp was underlain by one or more high-angle normal fault. This option was given low priority due to logistical problems of megatrenching through the coarse colluvium. The second strategy consisted of seven trenches scattered along strike on the PF scarp, but on different structures. Although this strategy was logistically feasible, rupture events (including the MRE) might be missed due to the scattered locations

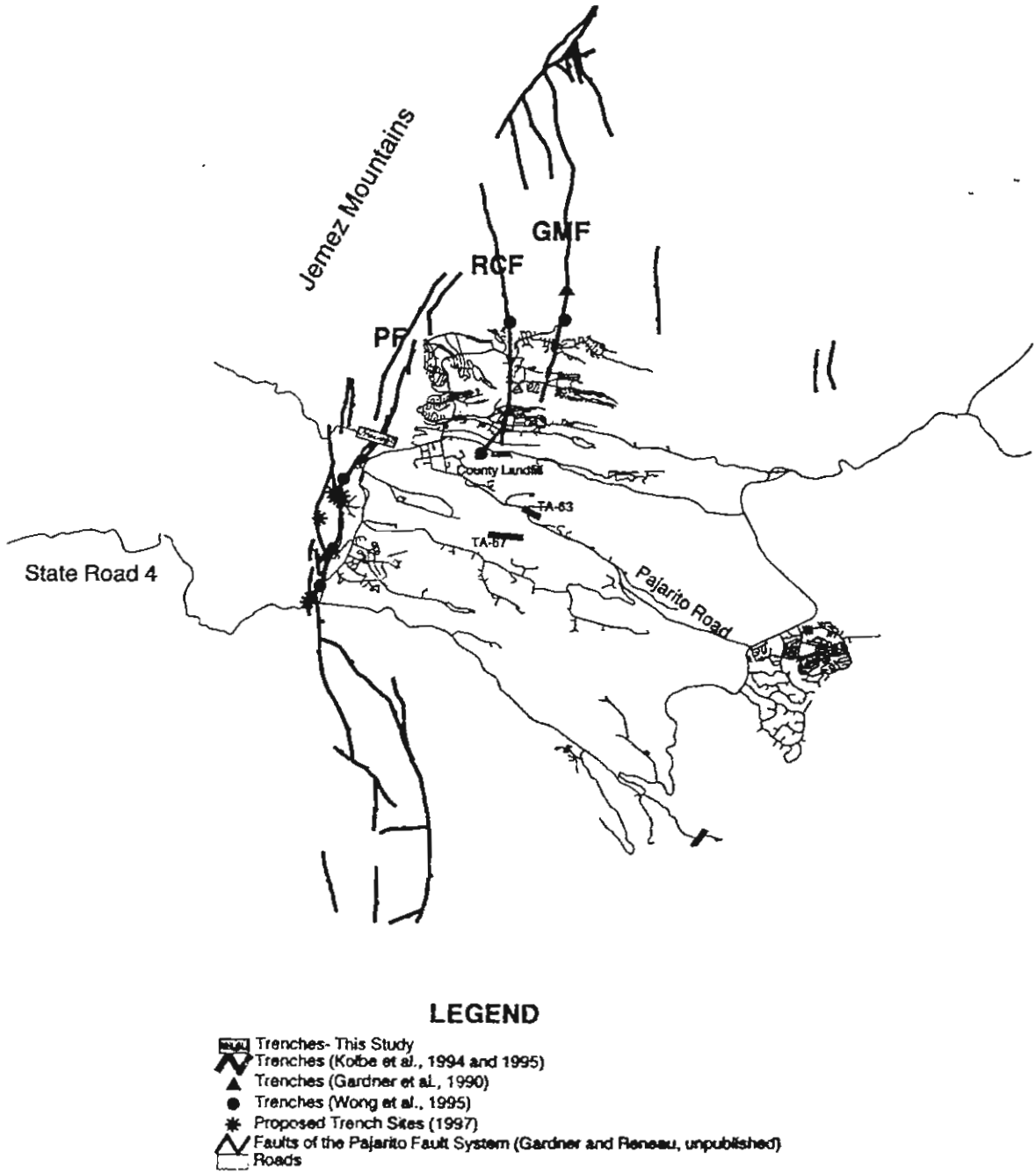

Fig. 1. Location map of Pajarito fault system, showing locations of 1992 trenches (Wong et al., 1993, 1995) and 1997 trenches. PF, Pajarito fault; RCF, Rendija Canyon fault; GMF, Guaje Mountain fault. Asterisks show locations to be trenched in summer of 1998.

of trenches. The third strategy, which we adopted, involved a transect of seven trenches across all major component scarps of the PF at a given latitude. This strategy was considered the best for capturing evidence of the MRE on the PF, and is described in detail in Sec. 2.2.

Table 1. Comparison of Trenching Approaches for Characterizing the Pajarito Fault

Trenching Approach	ADVANTAGES	DISADVANTAGES
1. The "Megatrench" [1]	1) if a large displacement fault underlies the scarp, it would be found 2) if every faulting event broke the main scarp, the entire paleoseismic history is potentially decipherable	1) excavation would be very expensive 2) trench would be environmentally damaging on such a steep slope, and nearly impossible to backfill 3) to expose the entire colluvial wedge, trench would have to be ca. 50 m deep 4) due to steep slope of the scarp face, evidence of paleoearthquakes may have been eroded off scarp 5) the MRE on the PF may not have ruptured the trenched fault traces
2. 8 Trenches on Scattered Smaller Scarps and Structures[2]	1) scarps are small enough to trench 2) small scarps may preserve a better record of young faulting events	1) it is difficult to correlate displacement events among trenches
3. 7 Trench Transect S. of Los Alamos Canyon[3] (This report)	1) scarps are small enough to trench 2) small scarps may preserve a better record of young faulting events 3) trenches cross every structure on which the MRE could have occurred	

[1] The "Megatrench" would be a single continuous trench across the entire Pajarito main fault scarp, excavated where the scarp is underlain by subhorizontal (nonrotated) tuff displaced by high-angle faults, such as north of Canyon de Valle.
[2] These localities include 7 identified by GEO-HAZ (1996) and 1 suggested by F.H. Swan and W. L-ttis (pers. Comm., 1997); see Fig. 1
[3] for location, see Figs. 4, 5

The secondary purpose of trenching was to refine existing estimates for displacement per event, slip rate, and recurrence intervals among pre-MRE faulting events on the PF. Values for these three seismic source parameters were poorly constrained based on the Wong et al (1993) trenches, because none of these trenches captured a complete

paleoearthquake sequence for the PF. This secondary goal resulted in deepening our seven trenches to 5 - 7 m deep, well beyond the depth range necessary to identify and date the MRE in each trench.

2.2 Trench Locations and Rationale

The adopted trenching strategy relied heavily on our understanding of the structural nature of the PF main scarp, so a brief summary of the mapping results (McCalpin, 1997) is given below. Over most of its length, the PF main scarp is underlain by forward-tilted blocks of Bandelier Tuff, such that the scarp face is essentially a dip slope. These tuff blocks dip 30 - 45° east and are separated from subhorizontal tuff above (west of) the scarp by large tension fissures (Fig. 2). The structural analogy is a rigid surface layer, such as the sidewalk slab in Fig. 3, that accommodates vertical movement by tilting toward the downthrown block. At the base of the main scarp there is typically a poorly-exposed zone of normal faults, termed the basal fault zone. In some areas this basal fault zone forms the western boundary of a graben, the eastern boundary of which is one or more west-facing fault scarps. The forward-tilted tuff blocks beneath the scarp face may also be broken by mid-scarp tension fissures.

To capture the MRE on the PF we either had to trench a single fault plane which we knew contained evidence for all paleoearthquake ruptures, or a series of fault planes that collectively contained evidence for all ruptures. The first option would require trenching the colluvial wedge far up on the slope of the PF main scarp, where the scarp was thought to be underlain by a single high-angle normal fault, such as north of the quarry in Canyon de Valle (Fig. 1). However, a depositional record of the MRE might not be preserved on the angle-of-repose slopes found on such mid-scarp positions, and getting a backhoe halfway up the 100+ m-high scarp would be a challenge. In addition, deciphering the pre-MRE chronology of paleoearthquakes would require deep trenching in this perilous location.

The second strategy, trenching a complete sequence of smaller parallel fault strands, was more technically feasible. Experience at trench sites worldwide has shown that individual paleoearthquakes can often be best recognized and dated at sites where deformation is widely distributed, rather than being concentrated on a single narrow plane (McCalpin, 1996). On dip-slip faults like the PFZ, distributed deformation creates grabens and uphill-facing scarps that trap post-faulting sediments, thus forming strata that contain well-expressed faulting event horizons.

The PF deformation zone reaches its widest extent (ca. 2 km) directly south of Los Alamos Canyon (Fig. 1). Here the main PF scarp is ca. 50 m high and is flanked by both synthetic and antithetic scarps trending N and NE (Fig. 4). Our seven trenches were placed on the six major faults in this zone. A seventh deformation zone, the mid-scarp tension fissure, had mainly been destroyed by construction of Ski Hill Road (Fig. 5).

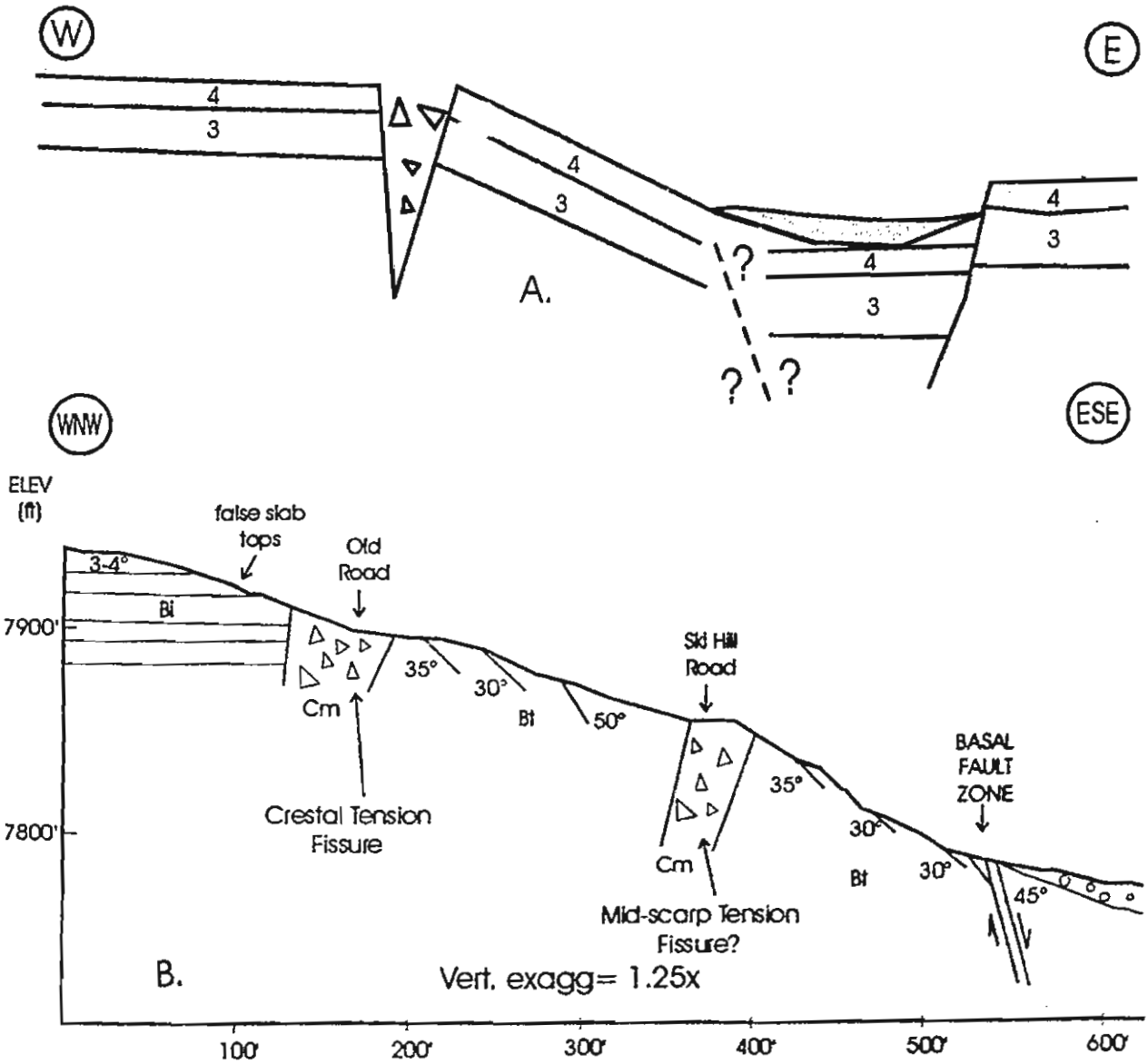

Fig. 2. Cross-sections through the Pajarito fault zone. A- schematic diagram showing the crestal tension fissure, east-tilted slab, basal fault zone, and graben. Units 4 and 3 are welded subunits of the Tsherige Member of the Bandelier Tuff, as defined by Broxton and Reneau (1995). Fault displacement is exaggerated compared to thickness of tuff subunits. Triangles indicate coarse crack fill, dots represent finer graben sediments; B- to-scale cross-section of the PF main scarp along Ski Hill Road. Dips are from field measurements. cm, megablock colluvium; Bt, tilted Bandelier Tuff; Bi, intact (untilted) Bandelier Tuff. Circles at far right indicate graben fill (alluvium and colluvium).

Fig. 3. Photograph of a sidewalk subjected to vertical displacement (down to right). Note tensional opening of the expansion joint at the head (left side) of the tilted slab. The right side (toe) of the tilted slab has also subsided slightly relative to the untilted slab on the right, due to soil compaction. This style of deformation is the proposed analogy for the "articulated monocline" model for the PF main scarp.

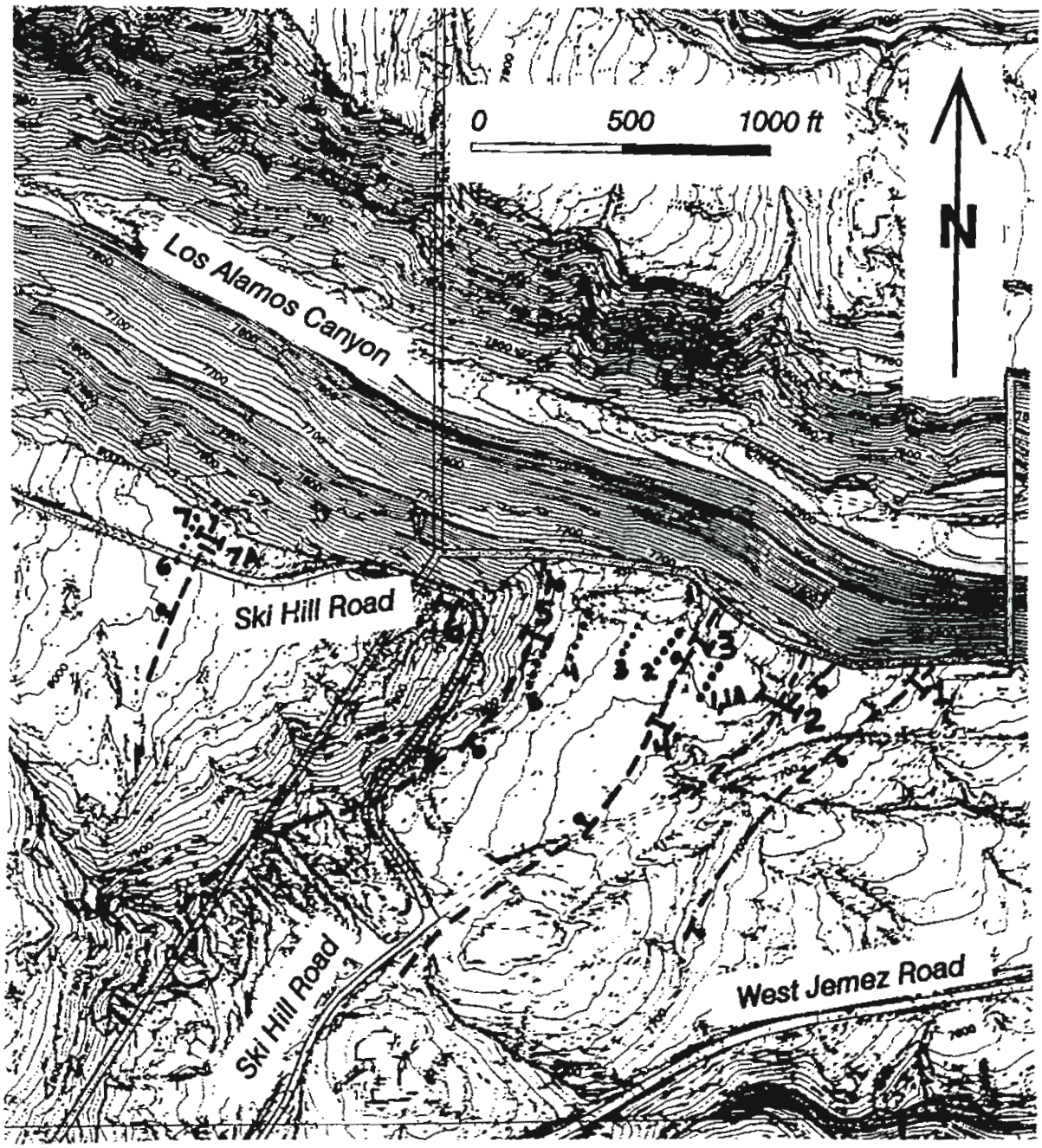

Fig. 4. Large- scale topographic map showing the seven 1997 trenches and trench 7A, plus major fault traces (dashed lines, bar-and-ball on downthrown side). Seismic refraction lines are shown by large dots.

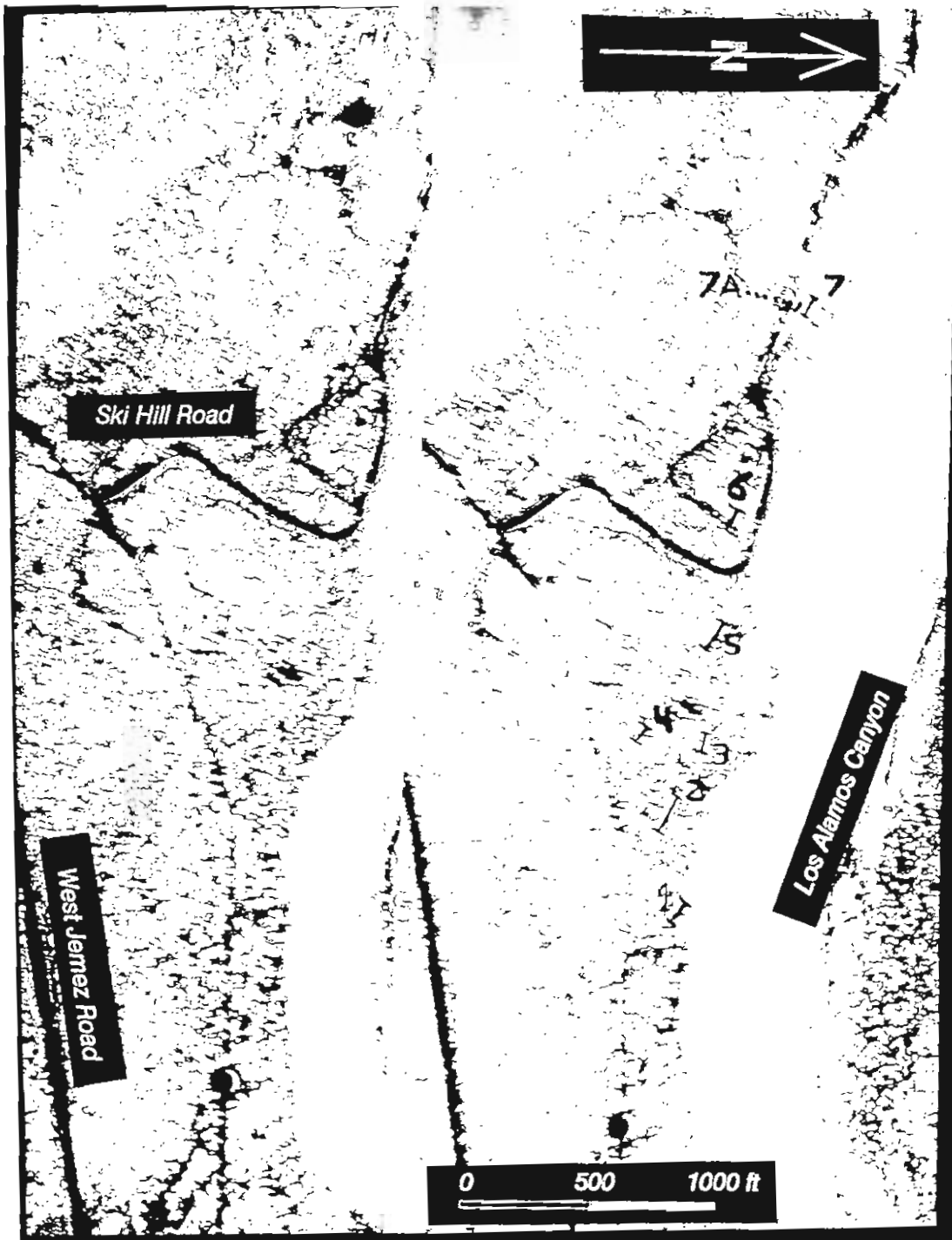

g. 5. Aerial stereopair showing the seven 1997 trenches and trench 7A.

2.3 Field Methods

Seismic Refraction Surveys: These surveys were performed by Craig V. Nelson of Dames and Moore, Salt Lake C. , UT assisted by J. P. McCalpin (GEO-HAZ) and Alexis Lavine (LANL), using a Geometronix ES-1225 engineering seismograph with a 12-lb sledgehammer source. Refraction lines were oriented parallel to fault scarps, to avoid possible complex signal returns caused by any buried steps in bedrock (Fig. 4). It was hoped that stratigraphic contacts would be more-or-less planar along lines parallel to fault scarps. Eight lines were shot, six of which were reversed, ranging from 24 m long (2 m geophone spacing, depth resolution ca. 1-2 m) to 60 m long (5 m geophone spacing, depth resolution ca. 2-3 m). Subsurface interpretation was based on P-wave first arrival times. Details of seismic line interpretation are given in Appendix A.

Trenching: Trenches 1 through 7 were excavated by Parker Construction, Los Alamos, with a Komatsu 200 track-mounted backhoe with a 20 ft-long arm and buckets ranging in width from 24" to 30". The time schedule for excavating, cleaning, and logging the trenches is shown in Table 2. Trench 7A was excavated by a Cat 416 backhoe. Parker Construction also shored the trenches with hydraulic aluminum shores from Plank, Inc., of various lengths up to 7 ft. Trench walls were cleaned by J. P. McCalpin, M.E. Berry, J. Amato, M. Bentley, J. Gardner, and A. Lavine. The softer, light colored Holocene sediments were best cleaned with scraping tools such as trowels or stirrup hoes. However, using these tools on hard, clay-rich Bt soil horizons resulted in smearing that obscured horizon contacts. Therefore, all hand cohesive materials were cleaned by plucking, usually using the claw end of a claw hammer. Horizontal string lines were attached to the trench walls at 1 m intervals, with every 1 m increment marked by labeled squares of duct tape. Contacts were scribed into the wall with trowels or knives. Logging contacts was done manually and the log was drawn on graph paper at a scale of 1 inch = 0.5 m (an approximate scale of 1:20). The definition and logging of units followed a mixed subjective- objective approach, as outlined in McCalpin (1996b).

Table 2. Time schedule of trench excavation and logging, summer 1997

Trench No.	Dug	Cleaned	Strung	Logged	Revised	Photographed & Sampled
1	July 8	July 9	July 10	July 11-12	Sept. 17, Oct 13	Oct 13, 14
2	July 9	Sept. 5	Sept. 6	Sept. 7-9	Oct. 14	Oct. 14
3	July 9	July 12	July 13	July 14-15		Oct. 13, 15
4	July 9	July 15	July 15	July 16-17		Oct. 15
5	July 10	July 21 25,26	July 27-29	Sept. 10	Oct. 16-17	Oct. 19
6	July 11	July 19	July 18	July 20-24	Sept. 19, Oct. 18	Oct. 18-19
7	July 11	July 22	July 22	July 23-26		Oct. 17, 19

In many trenches, the most obvious mappable contacts in unconsolidated deposits were soil horizon boundaries rather than stratigraphic contacts. For example, the thick colluvium in trenches 5 and 6 was composed of relatively uniform silty, gravelly sand (wash facies colluvium) which had been strongly affected by weathering and soil formation. In general, stone lines within the colluvium, and soil horizon boundaries, were parallel to each other and to the modern ground surface. This parallelism suggests that mappable buried soils are probably developed on discrete stratigraphic units, and that soil horizon contacts and stratigraphic contacts are parallel, in general. Thus, we use the same solid line map symbol for both lithologic contacts (where visible) and soil contacts. In all trenches except 5 and 6, both soil and stratigraphic units are consecutively numbered. In trenches 5 and 6 soil horizons are given horizon abbreviations, with parent material numbers (at front) decreasing with increasing age, and buried soil numbers (at end) increasing with increasing age. In both trenches, faulting has uplifted parent materials and their soils across faults, after which sediments/soils were stripped from the upthrown block, and then soil formation continued on the stripped surface, thus superimposing a soil across two parent materials. Thus, buried soil 2, which is typically developed on parent material 6 in trench 5, also is developed in older parent material 4 on the uplifted side of a fault. Conversely, when soils merge a single parent material can be affected by B horizon development from several distinct episodes of soil formation. For example, "8Bt3 + 4Bt3b2" means that the parent material mapped is unit 4, while the B horizon development is both a part of buried soil 2 (Bt3b2) and partly younger weathering contemporaneous with the surface soil (Bt3).

Soil Development Index: In addition to our definition of soil horizons, Eric McDonald (Desert Research Institute, Reno, NV) described vertical soil profiles at 11 locations on our logged trench walls. He also calculated Profile Development Index (PDI) and Soils Development Index (SDI) values for all soil horizons, after the methods of Harden (1982), Harden and Taylor (1983) and Taylor (1988). A preliminary version of McDonald's soil study is given in Appendix B.

IMPORTANT NOTE: MacDonald described his soil profiles after we had logged the trenches, so in many cases his soil horizon boundaries do not exactly correspond with the boundaries of our mapping units. There are several reasons for this. First, we had to define mapping units that could be traced for long distances along the trench walls, whereas MacDonald only had to define his soil horizons within a vertical strip about 20 cm wide. As a result, MacDonald defined many more soil horizons at a given stratigraphic level than we map on the trench logs. Second, MacDonald dug the trench wall back 15-20 cm when describing his soils. Soil contacts that are not horizontal thus shift slightly between his mapped position and our original mapping; usually these shifts are <5-10 cm. Most of MacDonald's contacts between his buried soils (b1, b2, b3, etc.) do correspond with our trench log mappping units.

Radiocarbon Sampling: Organic samples analyzed by radiocarbon dating methods consisted of one or more discrete charcoal fragments that were hand-picked from the

trench walls. Areas with discolored soil (suggesting the possibility of roots burned in place) or disrupted soil (such as due to animal burrows or the decay of large roots) were avoided, although the absence of distinct stratigraphy in the sampled units suggest some degree of mixing, and the possibility of bioturbation of younger charcoal into older deposits cannot be ruled out. In addition, the possibility of recycling older charcoal exists, potentially providing ages older than the sampled deposits. Where possible, multiple samples were collected from single units or single stratigraphic sections in order to provide internal checks on the analyses.

Luminescence sampling: Luminescence samples were collected from trench walls, in daylight conditions, by first scraping 5-10 cm of material from the trench wall at the sampling location. A 3-5 cm-diameter steel sampling tube was then quickly driven into the freshly-exposed trench wall. Upon extraction the open end of the tube was immediately sealed. In the laboratory the both ends of samples thus collected are discarded, and only the central part is used for luminescence analysis. Care was taken to avoid recognizable krotovinas.

Surveying: The locations of seismic refraction lines and trenches were surveyed by J.N. Gardner and A. Lavine (LANL) using a Geodimeter total station. All survey locations were tied to fixed reference points whose coordinates were determined from the Los Alamos Geographic Information System (FIMAD), in coordinates of the New Mexico Central Zone State Plane Coordinate System (in feet), 1983 North American Datum. Accuracy of the surveyed points is within about 3 feet in absolute 3-dimensional space.

2.4 Laboratory Methods

Luminescence Dating: Luminescence geochronometry has been used previously to determine ages of up to 100,000 yr and older for sediments that received sufficient solar radiation prior to deposition (e.g., Huntley et al., 1993). Usually, exposure of sediment to sunlight for at least 8 hours eliminates most of an inherited TL signal from mineral grains, thus resetting the TL clock. Luminescence geochronology usually measures the time-dependant dosimetric properties of quartz and feldspar minerals. Exposure of these minerals to ionizing radiation from the decay of naturally occurring radioisotopes in sediments imparts a luminescence signal that accumulates during burial, after the sediment is shielded from further light exposure. The intensity of the TL signal, if calibrated against a known radiation dose in the laboratory, can be used as a measure of sample age. The age is calculated by dividing the laboratory determined dose (equivalent dose, ED) by an estimate of the radioactivity the sample received during burial (dose rate, DR).

Thermoluminescence Dating Methods Used in This Study: The thermoluminescence signal was measured on the fine grained (4-11 um) polymineral fraction of sediments. All samples were analyzed by the total-bleach method, with the residual level defined as the TL remaining after an 8 hour exposure of a UV-dominated spectra from a 275-watt "sunlamp", which results in near total resetting of the TL signal. Dose rate estimates were

derived from U and Th concentrations, inferred from thick-source alpha counting and the ^{40}K content calculated from the total potassium concentration.

Table 3. SDI age estimates for trenches 3, 4, 5, 6, and 7. For supporting data, see Appendix B.

Trench no.	Fig. No.	Profile no.	Lowest Buried Soil Horizon	Lower Depth of Soil (cm)	Trench Unit	Soil PDI	SDI Age Estimate[a] Best Age (ka)	Lower Range (ka)	Upper Range (ka)
T3	3	p9.6	Bw	16	15	3	0.7	0.6	0.9
			Bt1b1	46	14	16	7.4	6.3	8.8
			Bt2b2	125	13	51	43	36	51
			BCb3	214	12a, 9, 7a	89	99	83	118
			Bt4b4	308	6	104	126	106	150
			CBb5	425	5, 4, 3	122	161	135	191
T3	4	P8.0	Bw2	22	15	4	0.8	0.6	0.9
			Bt2b1	77	14	31	20	17	24
			Bt2b2	113	13	47	38	32	45
			Bt4b3	205	12a, 9, 7a	78	81	68	97
			Bt2b4	284	6	99	117	98	139
T3	5	P5.4N	CB	49	15	7	2.2	1.9	2.7
T4	6	P7.4	BC	60	10e, 10b, 10c	11	4.5	3.7	5.3
			Bt3b1	97	9a, 9b, 9c	29	19	16	22
			Bt2b2	146	8a, 8b	54	46	39	55
			Bt3b3	243	6b, 4a	98	115	97	137
T4	7a	3.6N	Bw2	49	10e, 10c	7	2.3	1.9	2.7
T4	7b	P4.8	Bw1	43	10e, 10c	7	2.1	1.8	2.5
			Bt4b1	149	9d, 9a	58	52	44	62
T5	8	P16.6	Bt4	106	9A, 8Bt3	35	25	21	29
			Bt4b1	208	7Btb1-6Bt2b2	84	91	77	109
			Bt3b2	262	6Bt3b2, 6BC1b2	111	139	117	165
			Bt3b3	309	5Btb3, 5BCb3	131	177	149	211
			BCb4	379	4Btb4	159	238	200	282
			Bt5b5	507	3Btb5	209	362	305	431
			Bt5b6	623	2Btb5	256	492	414	585
T5	9	P6.2	Bt9	212	9A-8Bt3	79	83	70	99
			Bt4b1	329	7Btb1, 7BCb1	134	184	155	218
T6	10	P12.0	Bt	35	11	10	3.8	3.2	4.5
			Bt2b1	71	10	24	14	11	18
			Btb2	96	9–8	36	25	21	29
			Bt3b3	205	7	100	118	99	140
			Bt3b4	341	6	164	250	210	297
			Bt2b5	399	5	187	304	256	362
			Bt2b6	495	4	225	404	340	480
			Btb7	535	3	240	445	375	529
T7	11	P6.0	C	117	8, 7	23	13	11	15
			Bt5b1	211	4	59	53	45	63
			Bt2b2	277	3	72	72	61	86
T7	12	P8.5	C	144	10, 9, 6	24	13	11	16

[a] Age estimates based on no erosional loss between soils. See text for detailed discussion.

Blue TL emissions (which are considered a time sensitive luminescence signal; Balescu and Lamothe, 1992) were selected for measurement, by placing a Corning 5/58 filter in front of the photomultiplier tube. All samples were preheated at 124 degrees C for at least 48 hours, prior to analysis to remove a potential instability (anomalous fading) in the laboratory induced TL signal. E. sample, post heating was also tested for anomalous fading, by storing irradiated (100 to 450 Gy) material for at least 32 days and comparing to the TL signal of an unstored aliquot. The anomalous fading tests revealed no instability in the preheated TL signal.

The rate of TL growth was evaluated by applying progressively larger beta doses to the natural TL signal by a series of extended radiations with a calibrated 90Sr/90Y source. The highest radiation dose added to the natural TL signal was at least six times the calculated equivalent dose, which is sufficient to accurately interpolate an equivalent dose. The natural and additive dose data were fitted by a saturating double-exponential function to calculate an equivalent dose (cf. Huntley et al., 1988; Pierson, unpub. data). Equivalent dose values are calculated over a range of temperatures, usually between 250 to 350 degrees C or 250 to 400 degrees C which includes at least 90% of the measured TL signal and is also the temperature region that exhibits a pronounced plateau in equivalent dose values.

Radiocarbon Methods (contributed by S.L. Reneau, who collected and submitted most of the C-14 samples):

Before submission to the analytical laboratory, each charcoal sample was air-dried, examined under a binocular microscope, and cleaned to remove dirt and roots. All samples were analyzed by the accelerator mass spectometry (AMS) method, and were processed by Beta Analytic, Inc., of Miami, Florida. Sample pretreatment by Beta Analytic included standard hot acid (HCl) treatment to remove carbonates from the samples, followed by alkali (NaOH) treatment to remove secondary organic acids, followed by conversion to graphite (which constituted the actual accelerator target).
Using CALIB 3.0.3, the radiocarbon analysis were also converted to probability distributions in order to provide a better visual depiction of the most probable age of each sample and of stratigraphic units, and to allow easier comparison of the probable age ranges (Appendix B).

The radiocarbon analyses were calibrated to an absolute dendrochronological time scale using the computer program CALIB 3.0.3 developed by the Quaternary Isotope Laboratory of the University of Washington (Stuiver and Reimer, 1993). This calibration corrects for differences between radiocarbon years and calender years imparted by variations in the ^{14}C production rate in the atmosphere, and incorporates uncertainties both in the measurements of the radiocarbon content and in the calibration curves. The calibration can incorporate an "error multiplier" to account for sources of laboratory

Table 4: Thermoluminescence Age Estimates for Pajarito Fault Trench Studies, Los Alamos National Laboratory New Mexico

Field No.	Lab sample No.	Strat. Unit	Equivalent Dose Method[1]	Light Exposure[2]	Temperature (°C)[3]	Equivalent Dose (grays)[4] est.	TL age (ka)[4]
PF97-2	UIC-635	colluvium	TL-Total Bleach	16h sun	250-400	494.11+/-17.54	105.5+/-10.0
		TL-Total Bleach	8h UV	250-400	503.21+/-17.63	107.5+/-10.0	
PF97-3	UIC-633	colluvium	TL-Total Bleach	16h sun	250-350	445.32+/-15.25	69.5+/-6.0
		TL-Total Bleach	8h UV	250-350	449.43+/-15.28	68.5+/-6.0	
PF97-4	UIC-637	colluvium	TL-Total Bleach	16h sun	250-400	293.61+/-3.79	94.0+/-9.0
		TL-Total Bleach	8h UV	250-400	289.94+/-3.85	93.0+/-9.0	
PF97-5	UIC-634	colluvium	TL-Total Bleach	16h sun	250-400	206.41+/-10.31	43.0+/-4.5
		TL-Total Bleach	8h UV	250-400	206.11+/-10.41	43.0+/-4.5	
PF97-7	UIC-638	colluvium	TL-Total Bleach reset	thermal (close maximum estimate)	250-350	54.91+/-6.23	13.0+/-1.5*
PF97-8	UIC-639	colluvium	TL-Total Bleach reset	thermal (close maximum estimate)	250-350	30.99+/-3.31	7.0+/-0.8*
PF97-10	UIC-636	colluvium	TL-Total Bleach	16h sun	250-350	707.11+/-32.02	133.0+/-12.0
		TL-Total Bleach	8h UV	250-350	703.21+/-31.96	132.0+/-12.0	

[1]All TL measurements were made with a Corning 5/58 and HA-3 filters in front of the photomultiplier tube. Samples were preheated to 124 °C for 48 hrs prior to analysis.
[2]Hours of light exposure to define residual level. "Sun" is natural sunlight in Chicago, Illinois. UV is light exposure from 275 watt General Electric "sunlamp".
[3]Temperature range used to calculate equivalent dose.
[4] All errors are at one sigma and calculated by averaging the errors across the temperature range. A moisture content of 15 Ò 5% was assumed for all samples in the final age calculation.
* Preliminary age calculation.

uncertainty that are not encompassed by the reported analytical plus-or-minus (Stuiver and Reimer, 1993), and, following other researchers, we have previously used an error multiplier of 2.0 in work at Los Alamos (e.g., Reneau et al., 1995). Use of 2-sigma (2 standard deviation) uncertainties and an error multiplier of 2 provides a conservative estimate of the laboratory uncertainty assoicated with each radiocarbon analysis, although other uncertainties still exist (as discussed above).

2.5 Acknowledgments

This study would not have been possible without the support and cooperation of LANL personnel, in particular Douglas E. Volkman, Jamie N. Gardner, and Steven L. Reneau. Alexis Lavine also assisted in trench cleaning, logging and surveying. Our trenching crew of Margaret E. Berry, Molly Bentley, and Jason Amato persevered through rain, snow, hail, sleet, and mud to produce some fine trench logs. Eric McDonald described soils in our trenches and Steve Forman collected and analyzed luminescence samples, as well as assisting with trench interpretation. Trench reviewers William R. Lettis and Frank H. Swan provided many helpful observations during their field review. Susan S. Olig and Ivan G. Wong contributed information on the previous trenching by Woodward-Clyde Federal Services. Our day-to-day trench safety was ensured by Mr. Ron Riggins (Johnson Controls, Inc.). We also thank the efficient crew from Parker Construction for their artful trench shoring, particularly Mr. Brad Parker. This report benefitted from technical reviews by F.H. Swan, W.R. Lettis, J.N. Gardner, and A. Lavine.

Table 5. Summary Table of Radiocarbon Dates (all dates on charcoal)

Trench	Unit	Lab. No.	C-14 Age	Calendar Age[1]	Event Constraint
3	15b	B-108400	1300 +/- 80	1260 (920-1520)	Z3, minimum age
4	10c	B-108401	1690 +/- 40	1560 (1400-1800)	Z4, minimum age
4	10c	B-108402	22[illegible] +/- 40	2200, 2310 (2000-2360)	Z4, minimum age
7	8a	B-108398	3960 +/- 60	4410 (4000-4820)	Z7, far maximum age
7	7c	B-108399	4020 +/- 50	4450, 4510 (4160-4830)	Z7, far maximum age
7	7c	B-113029	1510 +/- 50	1360, 1390 (1260-1600)	Z7, close minimum age
7	6	B-113030	2580 +/- 40	2740 (2360-2840)	Y7, far minimum age
7	6	B-113031	2870 +/- 40	2960 (2780-3220)	Y7, far minimum age
7	6	B-113032	2200 +/- 50	2150, 2290 (1940-2360)	Y7, far minimum age
7A	8AC1	B-117083	modern	N/A	Z7A, far minimum age
7A	8D	B-117086	770 +/- 50	680 (650-755)	Z7A, far minimum age
7A	8Cox2	B-117084	1620 +/- 60	1520 (1360-1620)	Z7A, minimum age
7A	8Cox3	B-117082	1520 +/- 50	1390 (1305-1520)	Z7A, close minimum age
7A	8Cox3	B-117085	1450 +/- 60	1320 (1270-1420)	Z7A, close minimum age
7A	7A?	B-117081	1590 +/- 50	1500 (1350-1560)	Z7A, very close maximum age
7A	7e	B-117087	1870 +/- 70	1815 (1610-1945)	Z7A, close maximum age
7A	7b	B-117080	3430 +/- 80	3680 (3470-3870)	Z7A, far maximum age

3. RESULTS

3.1 Pre-Trenching Seismic Refraction Survey

Seismic refraction surveys were performed before trenching to give us an estimate of depth to bedrock in the 200 m-wide graben, and at trench site 7, because we anticipated that the trenches would not reach Bandelier Tuff on the downthrown fault block. This supposition proved to be correct at trench sites 3, 4, and 5 in the main graben; bedrock was reached at a depth of 2-3.5 m on the downthrown block at Trench 7. The estimated depth to tuff at Trenches 3 and 5 permits us to estimate the net vertical tectonic displacement in the past 1.2 Ma (see descriptions of individual trenches).

Four N-S seismic refraction lines were measured in the 200 m-wide graben, including one at the toe of Trench 5 and three more farther east in the graben, including line 2 at the toe of Trench 3 (Fig. 4). Seismic line 5 was measured in a N-S direction at about the 2mH mark on Trench 5, with the north end of the line at the trench. The north-source line yielded a three-layer interpretation with the upper layer (Vp= ca. 200m/sec) 0.7 m thick, an intermediate layer with Vp=ca. 400 m/sec, and the lowest layer with Vp=865 m/sec. The bottom of the lower layer was not detected. When the results of line 5 are combined with those from lines 2-4, we can make an interpretive subsurface cross-section across the northern part of the graben (Fig. 6). A thin upper layer with Vp=200-300 m/sec thickens eastward toward the antithetic scarp and represents Holocene deposits and the uppermost Pleistocene deposits. A 5-6 m-thick layer beneath that has Vp=375-415 m/sec, except up against the antithetic scarp where velocities are considerably higher and may reflect multiple buried step-faults in the higher-velocity Bandelier Tuff. This layer corresponds to mid- to -early Pleistocene colluvium and alluvium that contains well-developed soil B horizons. The basal layer has Vp=1000-1350 m/sec and is interpreted as Bandelier Tuff. Beneath seismic line 5 this basal contact rises and velocities in the 3rd layer are considerably lower than elsewhere. We interpret the 3rd layer beneath the westernmost part of the graben as a clast-rich wedge of colluvium or fissure fill shed from the main fault scarp. The top of Bandelier Tuff at line 5 is interpreted to be lower than 7745 ft, perhaps close to where a linear projection of the top of tuff in lines 2-4 would intersect the inferred fault plane at ca. 7735 ft elevation. Detailed seismic data are given in Appendix A.

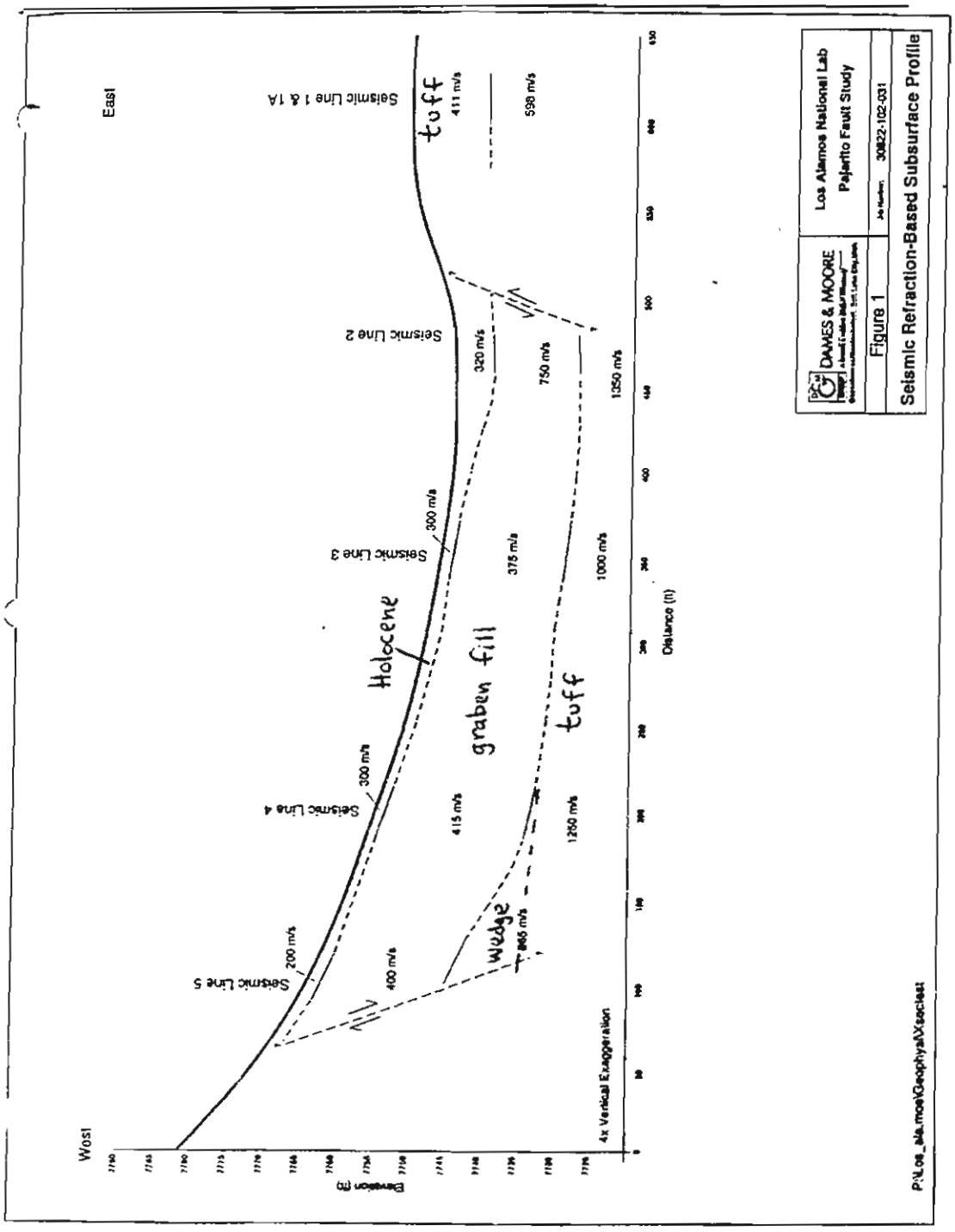

Fig. 6. Subsurface geophysical cross- section through the 200 m- wide graben east of the main scarp of the Pajarito fault. Detailed seismic data are given in Appendix A.

3.2 Trench 1

Trench 1 is located across the easternmost visible fault scarp of the PFZ between Los Alamos Canyon and West Jemez Road (Figs. 4 and 5). This southeast-facing scarp is roughly 2-3 m high and trends N 45° E. (Fig. 7). Trench 1 is located only about 15 m from the lip of Los Alamos Can. (Fig. 4)

3.2.1 Stratigraphy

Trench 1 exposes very few unconsolidated deposits, and most of the trench walls are composed of hard, white, welded Bandelier Tuff, probably equivalent to unit 4 of the Tsherige Tuff member (Broxton and Reneau, 1995) (Fig. 7, unit 1a). The shallow depth to Bandelier Tuff, especially at the toe of the scarp and beyond, was surprising. We expected a deposit of colluvium at the base of the scarp roughly half as thick as the scarp height (i.e., 1.25 - 1.5 m thick). Instead, scarp-base colluvium is either nonexistent, or is < 40 cm thick.

At the downhill (SE) end of the trench, the hard white tuff is oxidized to a light orange color (unit 1b), which may result from either surface-related weathering or fluid migration along fault B. In the southeasternmost 2 m of the trench, soft yellow, stratified surge beds of the Tuff (unit 1c) are found. Structural relations suggest that the surge beds overlie the orange oxidized Bandelier Tuff.

The southeasternmost 5 m of the trench also contains two beds of old alluvium (unit 2) that lie uncomformably on the surge beds and orange oxidized Tuff. The lower alluvium (unit 2a) comprises a channel cut into the soft surge beds, and contains subrounded dacite pebbles in a coarse sand matrix. The overlying alluvium (unit 2b) contains mainly sand and exhibits subhorizontal planar beds. Even before trenching, we expected this old alluvium would be present because old dacite-bearing gravels appear at the ground surface less than 20 m east of the trench toe (Reneau, unpub. mapping; McCalpin, 1997). We originally hoped that this old alluvium could be traced to the fault plane, where it would be faulted and overlain by a 1-1.5 m-thick colluvial wedge. Unfortunately, the alluvium pinches out about 5 m SE of the main fault zone (Fault Zone C), east of the scarp toe. The age of this alluvium is unknown, but dacite gravels could only have been deposited at this location by Los Alamos Creek, before the creek incised itself into the Plateau surface. At this site we are on the downthrown block of the main, 50 m-high scarp of the PF. Thus, during the initial incision of Los Alamos Canyon into the upthrown fault block of the PF, small stream terraces composed of dacite gravel were probably formed. Subsequently Los Alamos Creek also incised into the downthrown fault block, after which the creek could no longer deposit dacite gravels on the plateau surface.

Figs. 7. Ground- level photograph of Trench 1; view is northwest looking up the scarp from the toe.

Fig. 9. Photograph of the main deformation zone (fault zone C) exposed on the southwest wall of Trench 1; view is looking down at the logged wall from the

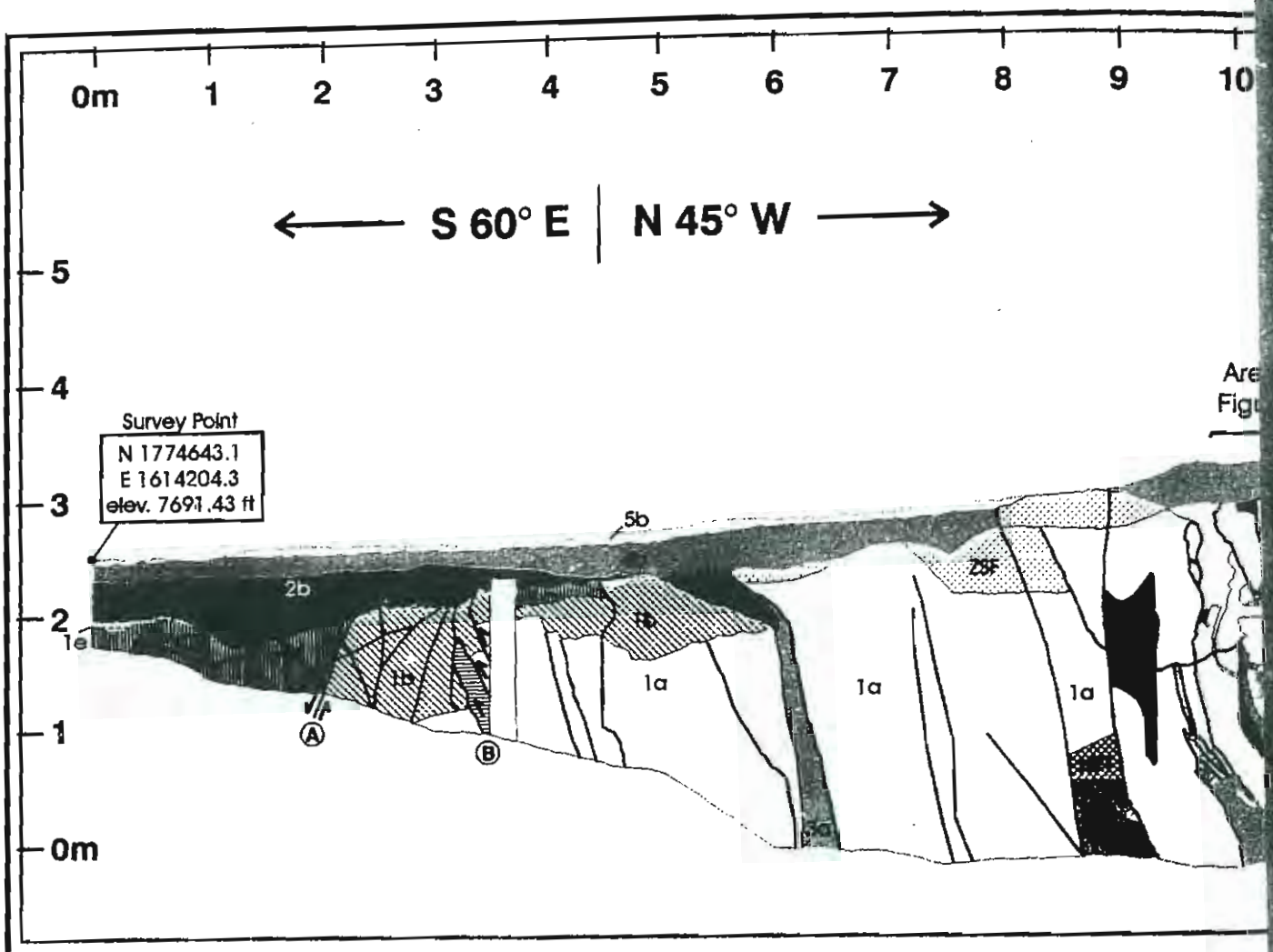

Explanation of Trench Units

Slope Colluvium (Holocene)	5b	Pale, stone-poor silt (distal colluvium)
	5a	Stony, loose, pale colluvium (Holocene)
Crack Fill	4b	Colluvium with strong Bt soil
	4a1	Crack fill containing Bt1 soil horizon
	4a2	Crack fill containing Bt2 soil horizon
	3c	Stratified sandy fissure infill
	3b	Clayey fissure fill (few clasts)
	3a	Blocks of tuff in fissures, clayey matrix
Old Alluvium	2b	Older alluvium, planar beds
	2a	Older alluvium (channel), contains dacite pebbles
Bandelier Tuff	1e	Transitional bed between surge beds and alluvium
	1d	Shear zone (oxidized) in tuff
	1c	Soft yellow, stratified surge beds
	1b	Light orange (oxidized) Bandelier Tuff
	1a	Intact white welded Bandelier Tuff

Symbo

Zone of Subhorizon Fractures (ZSF)

Void Space

Highly Fractured Tuff (HFT)

Dacite clasts

Tuff clasts

NOTE: Only shores cov the trench wall that c safety reason are mapp

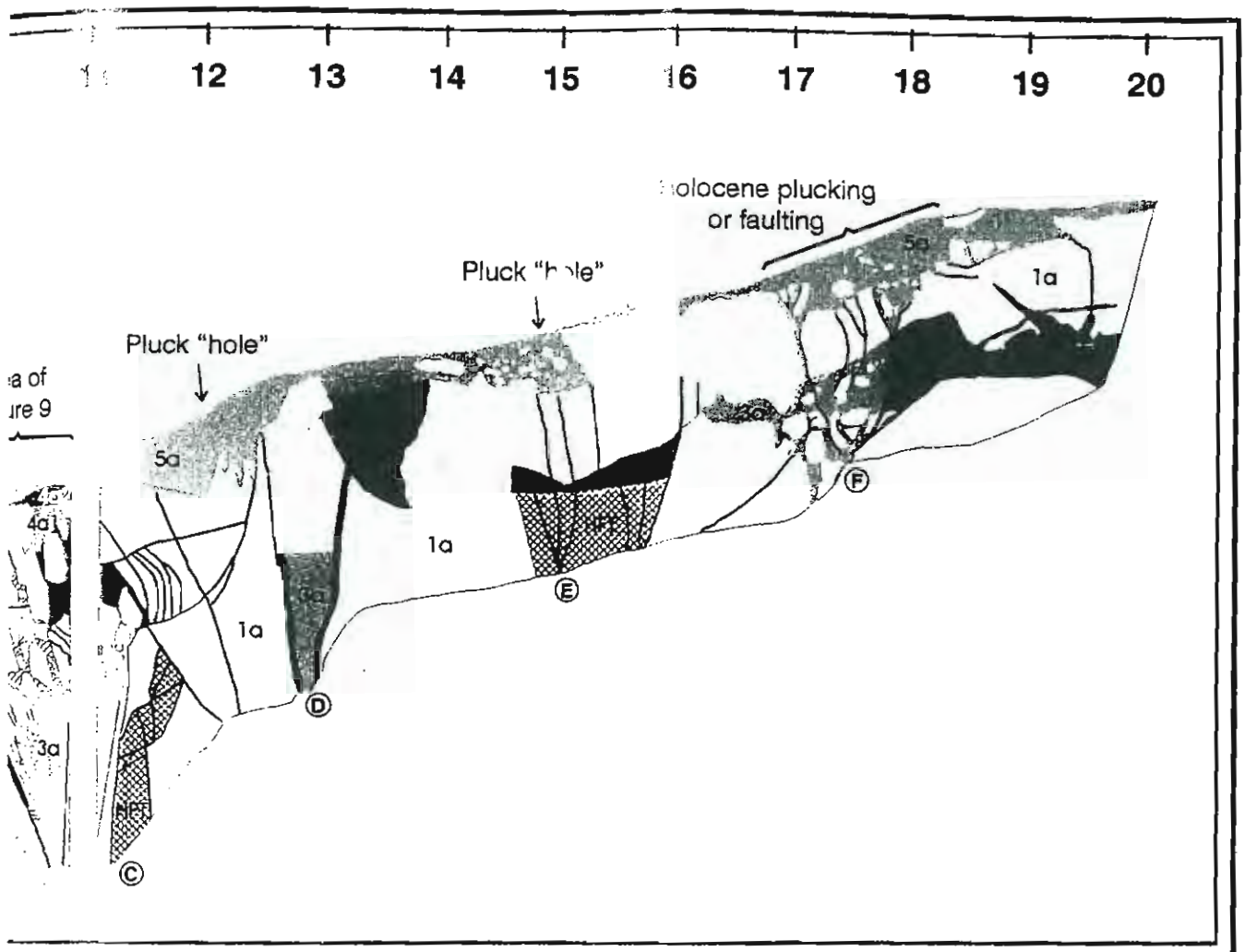

ls

al (A) ault or Fracture
ne Described in Text

ture

ault

a of wall covered
rench shore

ing important areas of
not be exposed for
d

NOTES:

1. Survey points refer to New Mexico Central State Zone Plane Coordinate System, NAD 1983; (in feet). Surveyed by J. N. Gardner and A. Lavine.
2. Trench excavated 9 July 1997.
3. Trench logged by M.E. Berry and Jason Amato, 10-12 July 1997. Revised by J.P. McCalpin in Sept. 1997.
4. Large areas of unit 3b (clayey crack fill) represent 5-10 cm-thick filled fissures which are nearly parallel to the trench wall. The apparent size of crack fill on the log is merely a function of how much clay was removed prior to logging.

SCALE

0 2 4 meters

GEO-HAZ Consulting, Inc.

PAJARITO FAULT, TRANSECT OF 7 TRENCHES, SUMMER 1997
LOS ALAMOS, NEW MEXICO

TRENCH 1-South Wall

DATE	MAY 1998	FIGURE 8
DWG. NO.	C:\GEOHAZ\LANL\LAMOS\TRENCH1.CDR	

Unit 3 contains fissure-filling material of various unknown ages. Some of this fissure fill (unit 3b) apparently underlies, and is thus older than, unit 4. Other units (unit 3a) represent fault breccia and rubble (unit 3a), void spaces, and small pockets of stratified inwash (unit 3c) that may range from very old (close to Bandelier Tuff age) to very young (historic). In the lower half of the trench wall rubble zones contain unfilled, interconnected void spaces, some of which are partially or totally filled with horizontally stratified silt and fine sand. From its stratified nature it appears that this material washed into rubble voids near the surface (either into open cracks or through decayed root holes) and infiltrated down the network of voids until it was trapped in a dead-end void. We call this stratified void-filling deposit "inwash", to differentiate it from normal fissure fill (or crack fill) deposits that accumulated by gravity fall processes into upward-flaring cracks open to the surface. Because fissures created by faulting commonly fill with deposits rapidly (within decades) after faulting, fissure fills can be used to define event horizons related to individual paleoearthquakes. (e.g., Sec. 3.3 of this report). Such an interpretation cannot be made for the inwash pockets and voids in brecciated, rubbilized bedrock, because they were both created and then filled entirely in the subsurface. The voids in the main deformation zone in Trench 1 (Fault Zone C) did not fill in any predictable sequence, such that at any depth below surface, there are both unfilled, partially filled, and completely filled void spaces at various positions on the trench wall.

Unit 4 contains both normal crack fill (unit 4a) and slope colluvium (unit 4b) with a well-developed textural B horizon. The crack fill occurs at the top of the zone of rubbilized bedrock in the center of the trench (Fault Zone C). Its poorly-sorted and poorly-stratified nature, and its location in a "pocket" atop shattered bedrock, suggest that it was deposited by gravity processes. The two B horizons in this deposit have comparable development to the pre-El Cajete soil of Reneau and McDonald (1996). Unit 4b carries a similar strong textural B horizon, but the location and the shape of the deposit suggest that it is distal (wash facies) colluvium derived from the fault scarp.

The youngest deposits in the trench (unit 5) are debris facies (unit 5a) and wash facies (unit 5b) colluvium of probable Holocene age. In contrast to all other unconsolidated deposits in the trench unit 5 is very loose, friable, and light in color (light gray to pinkish gray, Munsell 10YR7/2 to 7.5YR7/2); it shows little sign of B horizon development, and has only a thin incipient A horizon (not mapped). Unit 5a covers the scarp face, but is thickest in three pockets in the upper half of the scarp. At the scarp head the bottom of the colluvium tapers downward into tuff bedrock, contains subvertical oriented clasts, and thus resembles fissure fill. In the upper scarp face the colluvial pocket is rectangular, bounded by fractures that extend downward into tuff. At mid-scarp (9.5-12.5mH) the colluvial pocket has a downslope-tapering wedge shape. In each pocket the density and orientation of clasts suggests that the clasts were derived from tuff blocks at the upslope margin of the pocket.

Unit 5b is a thin, clast-free silt deposit that blankets the gentle area beyond the toe of the scarp. This area is evidently subject to modern sheetwash deposition from terrain

farther west, so we infer that this unit is a sheetwash/distal colluvial deposit transported by running water.

3.2.2 Structure

There are six major structures (or zones) in trench 1, lettered from A (toe) to F (head). Fault A is a SE-dipping normal fault with at least 0.7 m of vertical separation that places surge beds of the Bandelier Tuff (unit 1c) down against oxidized Bandelier Tuff (unit 1b). The net vertical displacement across this fault must be at least 0.7 m, because the base of unit 1c is not exposed on the downthrown side. Fault A continues up through unit 2 as a fracture with no displacement and terminates at the unit 2/4 contact. Almost all of the 0.7 m of displacement predates the deposition of unit 2, with possibly 1 cm of movement post-unit 2.

Fault B is a zone composed of three parallel NW-dipping reverse faults with a cumulative vertical displacement of 75 cm on the top of the white welded Bandelier Tuff (unit 1a). However, two NW-dipping normal faults 0.5 m to the NW of the reverse faults drop the top of unit 1a down 20 cm to the NW, leaving a net vertical separation of 55 cm down to the east. The reverse faults initially displaced unit 1b and 1c up on the hanging wall, after which those beds were partly removed by stream erosion associated with unit 2 alluvium. Later movement on the reverse faults displaced units 2a and 2b up 15 cm, after which unit 2b was stripped from the upthrown block. The faults terminate at the unit 2/4 contact. The previously-mentioned normal faults are older, and evidently do not displace the tuff surge beds (unit 1c).

Fault zone C is the main deformation zone in this trench (Fig. 9). It consists of a 2 m-wide zone of brecciated and rubbilized white tuff. The zone contains numerous fractures, fracture-bounded tuff blocks, open voids and voids partially to completely filled with crack fill and inwash. None of the fractures extend up into unit 5. Displacement across the fault zone cannot be measured due to lack of distinct stratigraphic markers in the white tuff. Because this is the strongest zone of fracturing in the trench, we infer that the majority of the 3 m of scarp height was created by vertical displacement across this zone.

The lower pocket of scarp-derived colluvium (unit 5a) overlies fault zone C and gives the impression of a tectonic colluvial wedge. However, the steep upslope edge of the colluvial pocket does not overlie the zone of strongest brecciation. Instead, the upslope edge overlies (and is apparently controlled by) a fracture that becomes subhorizontal with depth. This narrow fracture has no visible shear fabric that would indicate significant dip-slip movement, and its listric geometry precludes its being responsible for much net vertical displacement. Therefore we conclude that the pocket which is now filled with unit 5a must have been created by some nontectonic mechanism, probably by plucking a tuff block off the scarp face by tree throw.

Fault zone D is a relatively narrow zone defined by two clay-filled fractures with an intervening area of brecciated tuff and rubble. It is similar to several of the component

faults within Fault Zone C, but is defined as separate from C because: 1) it is separated from zone C by 1.5 m of relatively undeformed tuff, and 2) its bounding fractures underlie pockets filled with relatively young colluvium. Due to the lack of stratigraphic markers within the tuff, we cannot esrimate the net vertical displacement across zone D.

Fault E is a more weakly developed fracture zone overlain by a mid-scarp pocket of colluvium. This pocket is rectangular, bounded by subvertical and subhorizontal fractures that exhibit no shear fabric. The trench log implies that unit 4b is vertically displaced by the southeastern fracture trace. However, the shape of the colluvial pocket suggests that a fracture-bounded tuff block was plucked off the scarp face, after which the pluck hole was filled with Holocene debris-facies colluvium. My interpretation is that an earlier, shallower pluck hole was formed and then filled in with unit 4a colluvium. At some later time the upper part of this hole was plucked out to a deeper depth that removed all but the basal part of unit 4a, after which unit 5a was deposited in the hole. In this interpretation there has been no recent vertical displacement across the southeastern fracture in zone E, which is consistent with the lack of vertical displacement across unit 3b farther down on this same fracture.

Fault F lies near the head of the fault scarp and is overlain by an anomalously steep step in the scarp profile. Near the floor of the trench fault F exhibits multiple, anastomosing fractures that bound elliptical blocks of tuff. This appears to be a structural fabric created by shearing rather than by pure tensional fracturing. Subsidiary fractures diverge upward from fault F and are coincident with vertical steps in the top of tuff bedrock. The basal Holocene colluvium tapers downward into a fissure atop fault F. All of these lines of evidence provide circumstantial evidence that fault F has undergone some vertical displacement in the Holocene, although the amount cannot be measured due to the homogeneity of the tuff. If the increase of ground elevation across fault F is indicative of Holocene vertical uplift, then there may have been up to 65 cm of recent movement on this fault.

3.2.3 Geochronology

No numerical dates are available from Trench 1. The absence of dates stems from the sparse volume of unconsolidated deposits to begin with, and the absence of fine-grained deposits (aside from units 5b, which greatly postdates faulting, and unit 3b which has an unknown origin) suitable for TL dating. Indirect geochronologic controls include: (1) the rounded dacite clasts in unit 2; (2) the strong B horizons in unit 4; and (3) the lack of B horizons in unit 5. Dacite alluvium of unit 2 must have been deposited before the local incision of Los Alamos Canyon, which must have occurred at least several hundred ka to account for the ca. 80 m depth of the present canyon. Crack fills of unit 4 have Bt horizons similar to the pre-El Cajete soil, indicating an age of >50-60 ka. The lack of Bt horizons in unit 5 suggests that the unit is Holocene.

3.2.4 Paleoseismic Interpretation

There is evidence for at least three, and possibly five, displacement events in Trench 1. The oldest event (V_1) faulted units up through 1b but not 1c on normal faults NW of fault B. This event may have occurred during the emplacement of the Bandelier Tuff ca. 1.2 Ma, but as J. Gardner points out (pers. comm., 1998) the still-cooling tuff should have responded to vertical displacement by plastic, rather than brittle, deformation. The next event (W_1) faulted unit 1c along fault zones A (0.7 m) and B (0.75 m), but did not displace unit 2. Thus, the event occurred between 1.2 Ma and the time when Los Alamos Canyon began incising (several hundred ka.?). A later faulting event (X_1) on fault B displaced unit 2 by 15 cm but evidently occurred before unit 4b was deposited. This may be the same event (Y_1) that created the fissure that unit 4a filled in at Fault Zone C. Subsequent to these events, a strong soil formed, which is probably >50-60 ka. The last event (Z_1) may have occurred only on fault F at the head of the scarp, if the colluvial wedge represented by unit 5a is indeed tectonic. This event would have a vertical displacement of ca. 65 cm and must have occurred in the Holocene. However, the location of Fault Zone C beneath the center of the fault scarp suggests that most of the 3 m of the present scarp height must have been caused by vertical displacement on Fault Zone C. Due to the severely shattered nature of zone C, however, no discrete faulting events can be dated.

Due to the ambiguous evidence for events Y_1 and Z_1, and the poor dating control on all events, meaningful reccurence intervals cannot be calculated. Per-event displacements at this site, assuming that events W_1 and Y_1 were single events, were as large as 1.45 m, or as small as 15 cm. A great unknown in calculating slip per event is the unknown location of most of the 3.0 m of vertical displacement needed to create the present fault scarp. At most, only 65 cm (Fault F) of this 3.0 m can be attributed to a known fault beneath the present scarp (the 1.45 m of displacements on faults A and B have no surface expression, so do not contribute to modern scarp height). The remaining 2.35 m of vertical displacement must mainly be accommodated by fault zone C, but the number of contributing events cannot be determined in this zone.

3.3 Trench 2

Trench 2 is located across a complex southeast-facing (synthetic) fault scarp that bounds the eastern margin of a large horst. As shown in Fig. 4, this scarp is composed of two well-defined scarps north of Trench 2. Total scarp height at trench 2 is 8.3 m, the trench is 40 m long and averages [illegible] m deep (Figs. 10 and 11).

The trench is located at the intersection of the fault scarp and a NNW- trending zone mapped by McCalpin (1997) as a zone of fractured rock. This shear zone was inferred based on a lack of tuff outcrops along a NNW-trending band about 10 m wide. However, Swan (pers. comm., 1997) inferred that the lack of outcrops in the band may be caused by burial of tuff by a 10 m-wide shallow channel of gravels. This interpretation would also explain an anomalous NW trending scarp on the horst as a terrace riser cut by this channel. Thus, the sequence of events here would have been: 1) formation of a channel of Los Alamos Creek carrying dacite gravels across our site, 2) incision of Los Alamos Creek which cuts off the dacite supply, and 3) formation of the horst.

3.3.1 Stratigraphy

Like Trench 1, Trench 2 is almost entirely excavated in Bandelier Tuff, with only a thin veneer of young unconsolidated sediments. Most of the trench exposes hard white welded tuff (unit 1a), with only a thin surge bed (unit 1d) at the head of the trench. However, tuff at the foot of the trench (unit 1b) is infused with variable secondary coloring (light pink, violet, brown) that may be the result of hydrothermal alteration (J. N. Gardner, pers. comm., 1997). Similar staining occurs at 8-10 m H (between the 8 and 10 m marks on the horizontal scale of the log) and at 5-6 m H, but is restricted to joint surfaces at the latter location. Other tuff subunits include rubbilized tuff (unit 1f), tuff with subhorizontal fractures (unit 1g), and weathered (blocky) tuff directly below the surface (unit 1h). The first two of these units are equivalent to symbols HFT and ZSF in Trench 1. The unconsolidated deposits exposed in Trench 2 are subdivided into 6 major units and 17 subunits. In many cases the exact age relationship between major numbered units is unknown, because the units are not in physical contact with each other. For example, units 2a and 2b are stratified inwash surrounded by tuff and could be almost any age post-1.2 Ma. Unit 2c is the oldest fissure-fill colluvium in fault zone A, but it may older than some pockets of inwash and younger than others.

Unit 3 is old sandy alluvium containing rounded dacite pebbles and cobbles and occupies a channel-shaped cross-section beneath the toe of the scarp. The channel is cut into the relatively soft hydrothermally altered (?) tuff of unit 1b, and is probably correlative with unit 2 alluvium cut into surge beds in Trench 1. The channel trends roughly NW-SE, or at 45 degrees to the trench axis. The alluvial channel is cut on its downslope side by a complex filled fissure, the lower part of which (unit 4b) is occupied by crack fill composed of red clay mixed with unit 3 alluvium. Our interpretation is that unit 4b is merely a broken block of unit 3 and its overlying soil that became somewhat disaggregated when it fell into a fissure during faulting. Overlying unit 4b is a similar-looking but less dense and

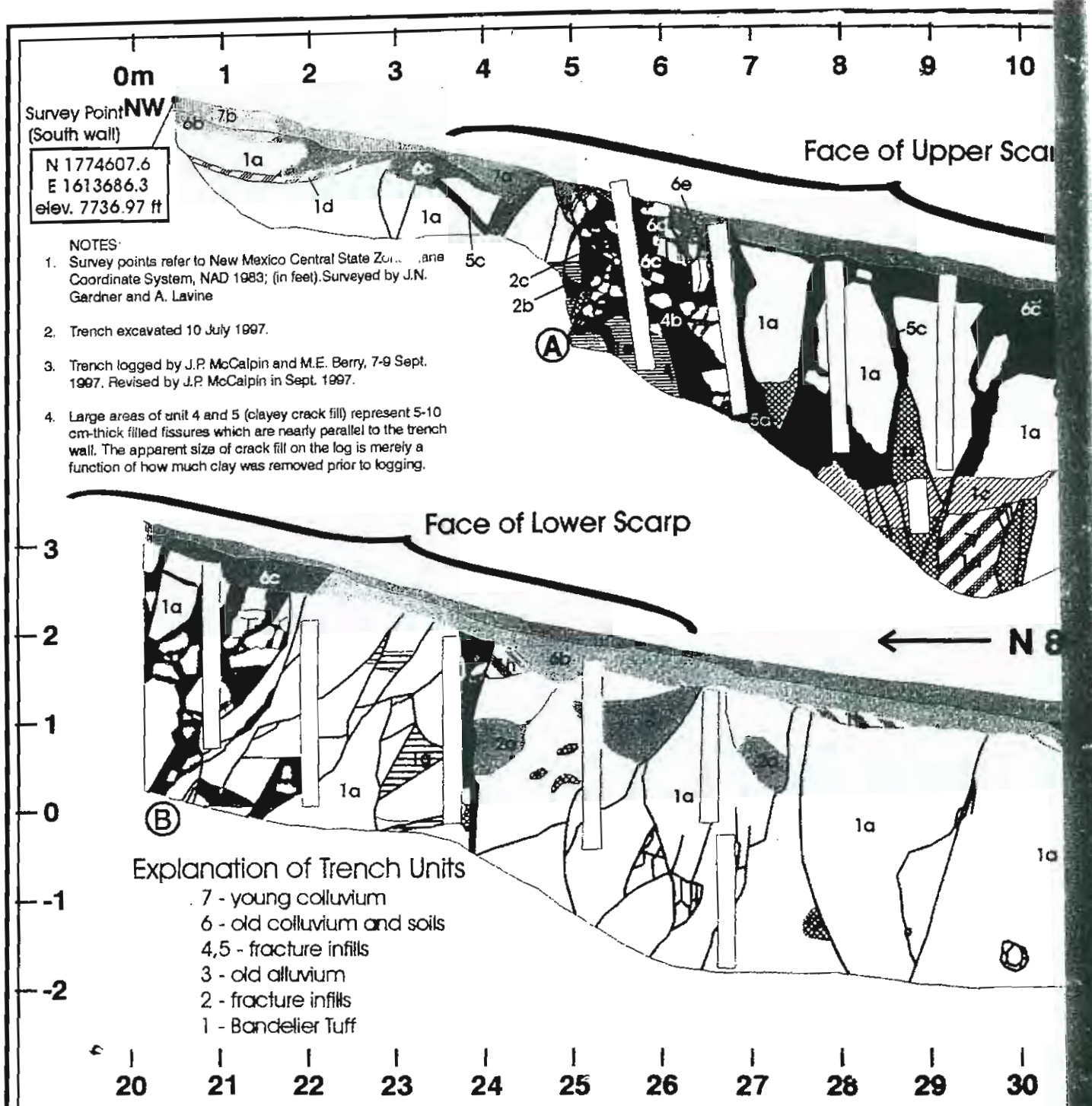

NOTES:

1. Survey points refer to New Mexico Central State Zo... ane Coordinate System, NAD 1983; (in feet). Surveyed by J.N. Gardner and A. Lavine
2. Trench excavated 10 July 1997.
3. Trench logged by J.P. McCalpin and M.E. Berry, 7-9 Sept. 1997. Revised by J.P. McCalpin in Sept. 1997.
4. Large areas of unit 4 and 5 (clayey crack fill) represent 5-10 cm-thick filled fissures which are nearly parallel to the trench wall. The apparent size of crack fill on the log is merely a function of how much clay was removed prior to logging.

Explanation of Trench Units

- 7 - young colluvium
- 6 - old colluvium and soils
- 4,5 - fracture infills
- 3 - old alluvium
- 2 - fracture infills
- 1 - Bandelier Tuff

7c	Crack fill in fault zone A	5c	Thin clay infill along fractures	2a	Stratified gravelly sand
7b	Same as 7a, but no clasts	5b	Intermediate-age crack fill, fault zone C	1h	Weathered tuff directly
7a	Pale brown, loose, stony Holocene colluvium	5a	Intermediate age crack fill with dacite clasts	1g	White tuff, close horizo
6e	Crack fill, hard pale red matrix	4b	Old crack fill, very red clay matrix	1f	Rubbilized white tuff, fo
6d	Same as 6c, but matrix is very loose	4a	Old crack fill, red matrix, dacite clasts	1e	White tuff, stained gray
6c	Bt horizon developed on unit 5	3	Old alluvium, contain dacite pebbles	1d	Surge bed in tuff
6b	Bt horizon developed on weathered tuff	2c	Sandy colluvium with hard orange matrix	1c	Same as 1b, 8-10m H
6a	Bt horizon developed on dacite gravels	2b	Stratified clay and silt, void infill	1b	Multi-colored, hydrothe

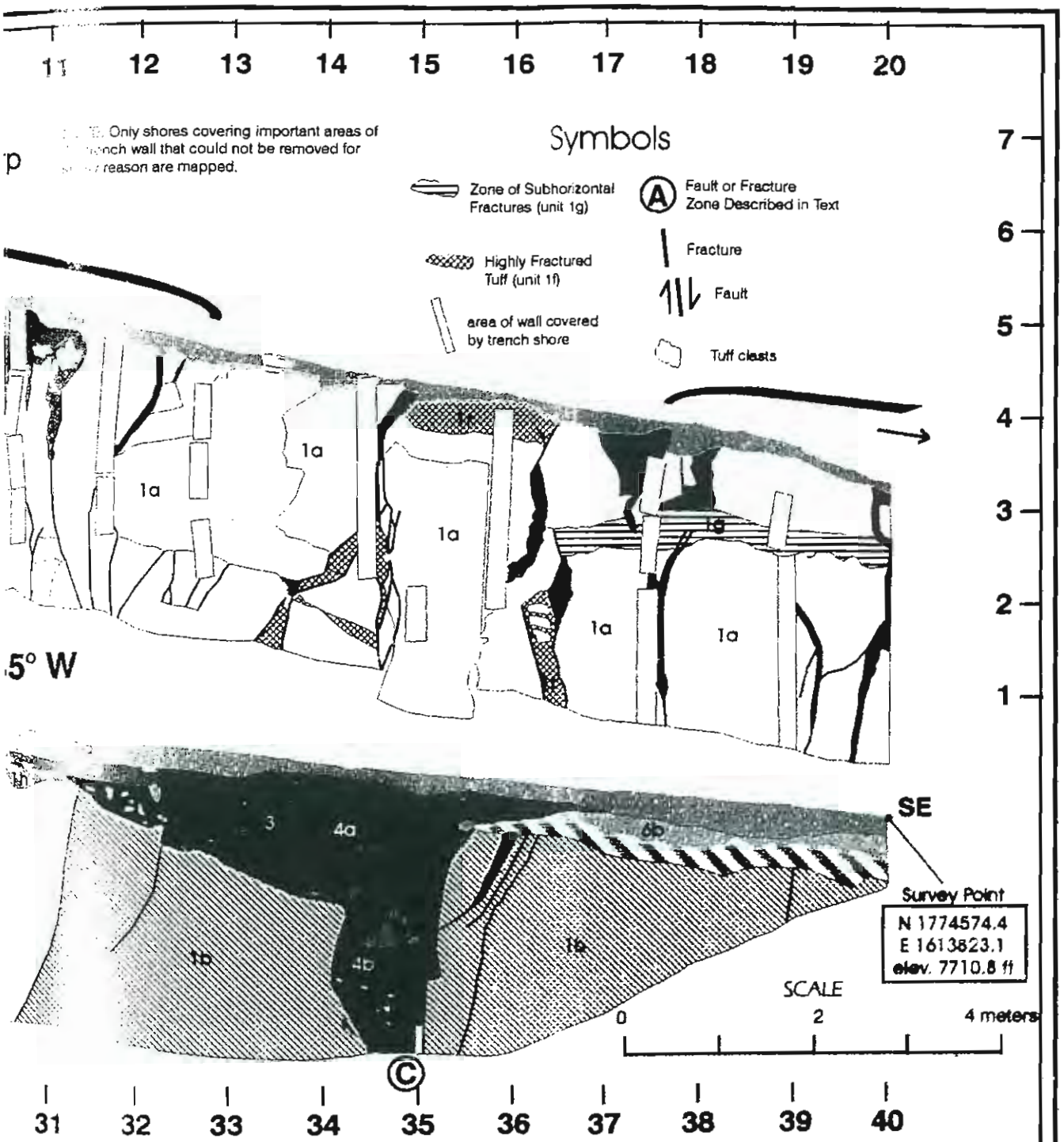

GEO-HAZ Consulting, Inc.

PAJARITO FAULT, TRANSECT OF 7 TRENCHES, SUMMER 1997
LOS ALAMOS, NEW MEXICO

TRENCH 2- North Wall

DATE	MAY 1998	FIGURE 10
DWG. NO.	C:\GEOHAZ\LANL\ALAMOS\TRENCH2..CDR	

Fig. 11. Photograph of Trench 2; view is northwest looking up the scarp from the toe.

less red fissure fill which also contains dacite clasts and must be derived from unit 3 alluvium. To the right of units 4a and 4b is slightly less dense, less red crack fill that also contains dacite clasts (unit 5b). The relative age sequence suggests that unit 3 has been fissured three times since its deposition, and all three episodes predate the Bt horizon of unit 6a. However, it is uncertain whether units 4a and 5b in this same area are contemporaneous with similar labeled units elsewhere in the trench.

In general, unit 4 is defined as old, very red, dense crack fill and unit 5 as intermediate-age, less red, less dense crack fill. In places (35 m H, 7-8 H) even unit 5 contains dacite clasts, which is more of an indication of where dacite clasts were available to fall into fissures, rather than an indication that unit 5 is old (i.e., nearly contemporaneous with unit 3). For example, dacite clasts are found in unit 5a crack fill beneath the face of the upper fault scarp, where no intact dacite gravel deposit is preserved on the present surface. Clearly at one time dacite gravels must have overlain the ground surface in the vicinity of 7-8 m H, but that alluvium was stripped off by subsequent erosion of the scarp-face as the fault scarp formed.

Unit 6 is a Bt soil horizon that is developed on a variety of parent materials (6a on dacite alluvium, 6b on weathered tuff, 6c on unit 5 crack fill). Generally these B horizons parallel the ground surface beneath the entire scarp, and beneath unit 7a. Unit 6e is a stratigraphic unit, rather than a soil unit, and represents red crack fill that by cross-cutting relations in fault zone A must be younger than unit 4b.

The youngest units in the trench are loose, pale brown to beige stony debris-facies colluvium with a silty matrix (unit 7a) and a similar clast-free deposit (unit 7b). These two units are correlative with units 5a and 5b in Trench 1 and are presumably Holocene, based on their lack of soil development. Unit 7a mantles the entire scarp but is rarely thicker than 20 cm except where it fills fissures in fault zone A.

3.3.2 Structure

Trench 2 contains three deformation zones. Zone A underlies most of the face of the upper scarp (between 5-11 m H) with the severity of fracturing and rubbilization increasing to the west. The only fault with clear shear fabric is the western boundary fault of zone A at 5 m H. This west-dipping fault is defined by a zone of crushed tuff roughly 10 cm wide that is coincident with a 1.5 m vertical step in the top of tuff bedrock. This is the largest step in the top of bedrock. In addition, the crack fill between 5 m and 7 m H is the thickest in the trench, extending 2.2 m from the ground surface to the floor of the trench. Fault zone A contains the only thick colluvial deposits that contain clasts and stratigraphic contacts that dip downslope, as if derived from a nearby free face. Further, zone A is the only site where unit 6e crack fill is recognized, and unit 6c is found at an abnormally low elevation compared to elsewhere in the trench, suggesting it was downfaulted here. Finally, above fault zone A is the only place where Holocene colluvium (unit 7a) thickens in downward-tapering wedges that look like young fissure fills (at 4 m,

5 m, and 6.5 m H). All of these lines of evidence suggest that the youngest deformation in the trench has occured on fault zone A.

Fault zone B underlies the face of the lower scarp between roughly 20-24 m H. This zone does not contain the thick fissure fills and slope colluvia such as found in zone A, but instead contains an anastomozing system of west-dipping fractures, fracture-bounded blocks, and intermediate-age crack fills. Zone B thus resembles the main deformation zone in trench 1 (fault zone C) except that it contains no open voids and fewer pockets of inwash (unit 2a). The fissure fill in zone B (unit 5b) is overlain by undeformed soil unit 6c, whereas unit 6c has been deformed by fissuring in zone A. Thus the latest deformation in zone B is presumably older than in zone A.

Fault zone C consists of the compound fissure fill complex described previously. The alluvial channel (unit 3) is not present east of the fissure, which either means: (1) the channel never extended east of the eastern margin of the fissure; or (2) the channel did extend farther east, but was uplifted and eroded sometime after deposition. We prefer the latter interpretation, which implies an up-to-the-east vertical displacement of at least 1 m across the fissure. Such a displacement would predate unit 6a, which overlies the fault zone and resembles the pre-El Cajete soil (older than 50-60 ka.).

On the three major deformation zones we can only directly infer 1.5 m of vertical displacement on the western boundary of zone A, compared to the scarp height of 8.3 m. Therefore, if the entire scarp height was created by vertical displacement along faults, we are unable to assign the remaining 6.8 m of vertical displacement to any particular structures. Much of this displacement must have occurred along the large fissures in fault zones A and B, but the lack of stratigraphic markers in the tuff prevents precise measurement. Displacement on fault zone C has no surface expression and does not contribute to the 8.3 m scarp height.

The fractures (faults?) bounding fissures in zones A, B, and C generally are not perpendicular to the strike of the trench (N85W) nor parallel to the fault scarp (N22E). Instead, almost all major fractures (with the exception of the western boundary fault of zone A, which strikes perpendicular to the trench wall) occur in two conjugate sets trending N65E and N55W, or roughly at a 30 degree angle to the trench walls. Some joints are nearly parallel to the trench walls. The regional joint sets in the tuff in this area trend N20-25W and N45-50E and are subvertical. Thus, the joints that bound the disjointed tuff blocks in Zones A and B are neither parallel to the scarp nor to the regional joint set, but are closer to the latter.

It appears that vertical displacement of the tuff beneath this fault scarp has mainly been accomplished by extensional dilation of the two conjugate joint sets, and incremental stepping-down of joint-bounded blocks to the east. This certainly appears to be true for most faults outside of fault zone A. For example, in zone B all major fractures dip 65-85 degrees west, as if they were reverse faults. However, I believe that the westward dip

represents eastward toppling accompanied by extension across joints, rather than true compressive reverse faulting. However, due to the lack of stratigraphic markers in the tuff this hypothesis of eastward toppling cannot be tested. The dilated nature of joints and cracks here (and in Trench 1) may explain why there are few structures that display shear fabric, since extension during vertical displacement would pull the bounding slip surfaces away from each other. Shear movement must be occurring in the clayey crack fills between blocks (to account for the >8.3 m vertical displacement needed to create the fault scarp), but subsequent wet-dry shrinking and swelling is presumably obscuring its evidence.

Fault zone A is bounded on the west by a west-dipping fault with shear fabric, and then contains east-dipping faults that displace the widest zone of fissure infills and colluvium. It appears that fault zone A is a major pull-apart that separates in-place tuff to the west from a domain of toppled and extended tuff blocks to the east. The only east-dipping normal faults in the trench occur in the colluvium deposited in this pull-apart zone. This coincidence suggests that east-dipping normal faults can only form where unconsolidated materials are in thick pockets on the fault scarp. Where tuff extends up nearly to the surface, the deformation occurs by toppling and extension along pre-existing colling joints in the tuff, rather than by the formation of "new" east-dipping notmal faults.

3.3.3 Geochronology

No numerical dates are available from Trench 2, for reasons similar to those outlined for Trench 1. Indirect age control includes: (1) the rounded dacite gravels in unit 3; (2) strong Bt horizon development on units 4, 5, and 6; and (3) lack of a Bt horizon in unit 7. MacDonald (Appendix B) suggests that roughly 40 ka is required to form a strong Bt horizon. The dacite alluvium must have been originally deposited before the local incision of Los Alamos Canyon (at least several hundred ka), but could have been locally reworked later. The presence of dacite gravel in crack fills of fault zone A implies that the gravels were deposited in a stream channel before formation of the fault scarp. The source area of the channel lies to the NW, but at present the large horst lies astride this path between Trench 2 and Los Alamos Canyon. It seems probable that unit 3 alluvium was deposited here before development of the horst or its companion 200 m-wide graben to the west.

It is difficult to estimate the true age of soil Bt horizons in Trench 2, since scarp-face erosion has led to an attenuated thickness of surficial deposits on the scarp, so a comparison with the more stable calibration sites of MacDonald (Appendix B) is not warranted. In fact, the lack of pre-Holocene colluvium atop tuff bedrock over some of the trench suggests that the entire scarp face is erosionally stripped from time to time. The lack of a Bt horizon in unit 7 implies that it is Holocene.

3.3.4 Paleoseismic Interpretation

A relative sequence of deformation events can be deduced for fault zones A and C, but it is difficult to correlate events between zones. In fault zone C three episodes of fissuring are suggested. The earlier event dropped a sliver of unit 3 dacite alluvium down into a fissure (unit 4b). Overlying unit 4a [illegible] be later disaggregated crack fill from this same event, or a separate fill from a younger event. Crack fill unit 5b clearly represents an even younger fissuring event. All of these events post-date deposition of dacite-bearing alluvium (several hundred ka) and predate formation of the unit 6a Bt horizon (at least 40 ka).

These same events could have created some of the older filled fissures in fault zone A, since dacite clasts are present in crack fill unit 5a. At least four colluvial deposits exist in zone A between 5-7 m H, the three lowest of which carry textural B horizons, and the youngest of which (unit 7a) does not. The three downward-tapering wedges of colluvium between 4-6.5 m H suggest that unit 7a is filling young (Holocene) fissures, but similar shaped wedges might be caused by tree throw. The three older colluvial deposits in fault zone A appear to be younger (less dense) than the three crack fill units in fault zone C, but the oldest colluvium in fault zone A might be correlative with the youngest crack fill in fault zone C. If the four events in zone A are different than the three events in zone C, there have been seven displacement events in the past 1.2 Ma. Most of these events also postdate the dacite-bearing gravels which are considerably younger than 1.2 Ma. However, it is likely that some of the older A and younger C events are the same, which would decrease the number of events to as few as five.

None of the events can be dated precisely, nor can displacement per event be reliably estimated, because the main paleoseismic evidence consists of filled fissures and the depth and width of fissures bears no consistent relation to free face hight (i.e., vertical displacement per event). Overall, if the 8.3 m of scarp height were created by a minimum of 5-7 events, average displacement per event on zones A plus B would range from 1.2-1.7 m.

3.4 Trench 3

Trench 3 is located across a 1.5 m-high west-facing fault scarp that bounds the western edge of the horst (Fig. 4) and the eastern edge of a 200 m-wide graben at the foot of the main Pajarito fault scarp. The trench is 19 m long and up to 5.5 m deep (Figs. 12 and 13).

3.4.1 Geophysics

Several seismic refraction lines were surveyed near Trench 3 before trenching to estimate the depth to Bandelier Tuff in the graben. Previous geologic mapping (McCalpin, 1997) documented discontinuous tuff outcrops on the valley wall of Los Alamos Canyon about 7 m below the ground surface of the graben. However, it was not known whether graben fill was uniform in depth, or whether buried horsts and grabens might exist within the 200 m-wide graben.

Seismic lines 1 and 1A were run in a N-S direction on the horst between Trenches 2 and 3, where Bandelier Tuff outcrops at the surface (Fig. 4). The purpose of these unreversed lines was to measure the P-wave velocity of Bandelier Tuff, so that it's signature beneath the graben floor could be recognized. Each line was 60 m long with 5 m geophone spacing, and thus sampled P-wave velocities down to a depth of ca. 15-20 m with a depth resolution of 2-3 m. Line 1 yielded a single-layer solution where Vp = 450 m/sec, whereas line 1A yielded a two-layer solution where Vp = 400 m/sec above ca. 3.2 m and 600 m/sec below that. These velocities are anomalously low for welded tuff, and may represent dilation and filling of joints in the near-surface due to surface weathering effects.

Line 2 was run N-S parallel to but about 2 m west of the toe of the antithetic fault scarp (about position 8-9 m H on the Trench 3 log; Fig. 13). This reversed line was 24 m long with a geophone spacing of 2 m, corresponding to depth penetration of ca. 8 m and depth resolution of ca. 0.5-1 m. The preferred subsurface interpretation is three layers, with Vp = 300-350 m/sec from the surface down to 1.5-1.8 m, Vp = 750-800 m/sec from 1.5-1.8 m to 5.7 m depth, and Vp = 1333-1382 m/sec below 5.7 m. The trench 3 log shows that the break at 1.5-1.8 m roughly corresponds to the contact between clayey Bt horizons on fine sediments, and coarser stratified alluvium in the lower half of the trench wall. The basal, high-velocity layer (ca. 0.7 m below the trench floor) is inferred to be Bandelier Tuff. For details on geophysical lines, see Appendix A.

3.4.2 Stratigraphy

Despite the small height of the fault scarp here, the unconsolidated graben sediments on the downthrown block are at least 5.5 m thick (Fig. 13). Bandelier Tuff could not be reached by the backhoe arm in the graben.

Bandelier Tuff is exposed only on the upthrown fault block at the head of the trench and is composed of hard white welded tuff (units 1a, 1e) separated by a 50 cm-thick surge

Figs. 12. Photograph of Trench 3, looking NE across the trench toward the lip of Los Alamos Canyon. Scarp height increases north of the trench (upper left center) due to stream incision along the scarp.

Fig. 14. Photograph of Holocene debris- facies colluvium (unit 15b, upper half of photo) overlying the main fault zone in Trench 3 (slightly to right of center). Red- brown material to right of main fault and beneath the white Holocene colluvium is strongly overprinted by Bt soil formation. To the left of the main fault Bandelier Tuff is highly fractured (lower left center). String lines are 1 m apart, rails of shores are 20 cm wide

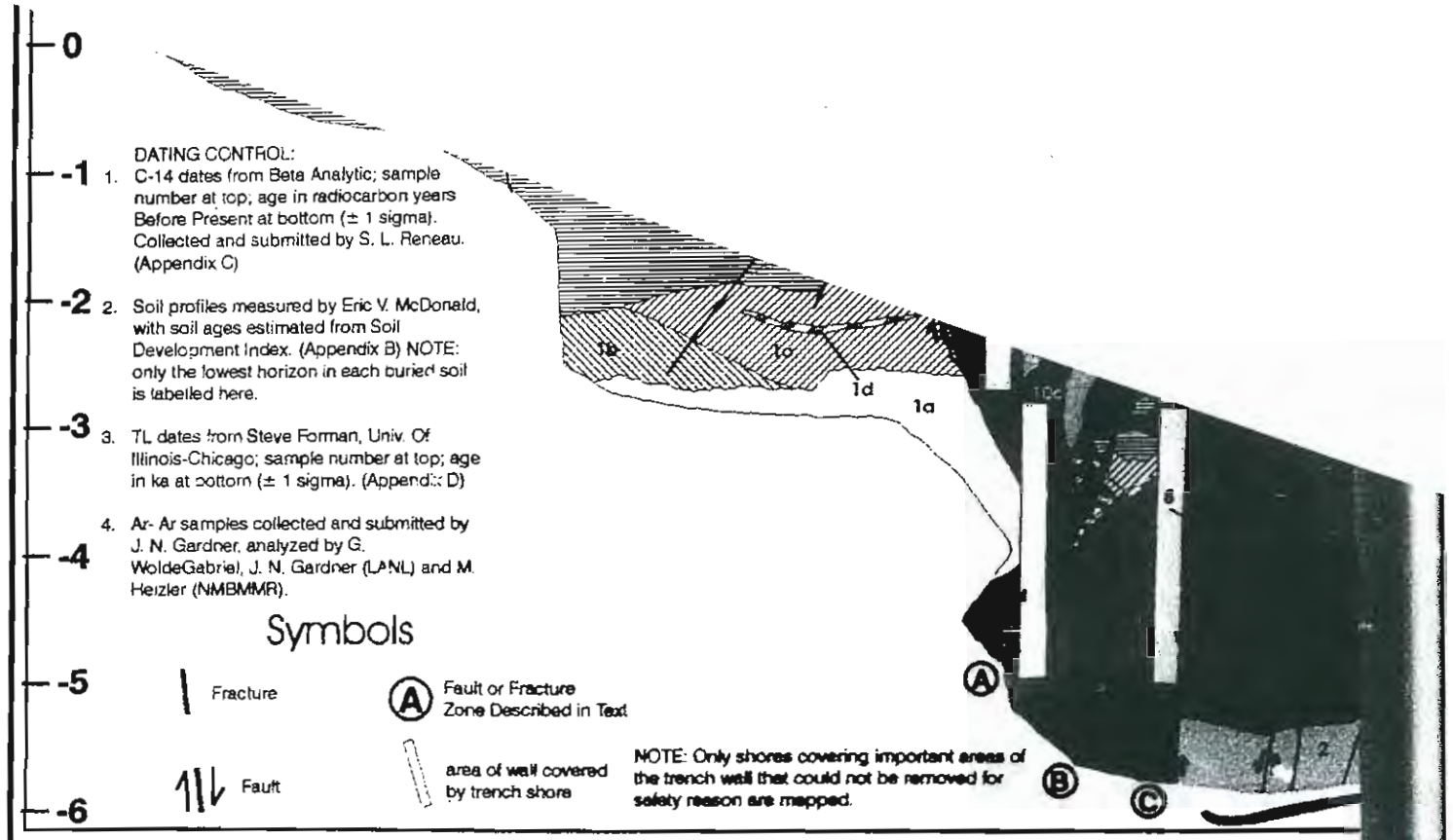

DATING CONTROL:

1. C-14 dates from Beta Analytic; sample number at top; age in radiocarbon years Before Present at bottom (± 1 sigma). Collected and submitted by S. L. Reneau. (Appendix C)
2. Soil profiles measured by Eric V. McDonald, with soil ages estimated from Soil Development Index. (Appendix B) NOTE: only the lowest horizon in each buried soil is labelled here.
3. TL dates from Steve Forman, Univ. Of Illinois-Chicago; sample number at top; age in ka at bottom (± 1 sigma). (Appendix D)
4. Ar- Ar samples collected and submitted by J. N. Gardner, analyzed by G. WoldeGabriel, J. N. Gardner (LANL) and M. Heizler (NMBMMR).

Symbols

Fracture

Fault or Fracture Zone Described in Text

Fault

area of wall covered by trench shore

NOTE: Only shores covering important areas of the trench wall that could not be removed for safety reason are mapped.

Explanation of Trench Units

15c	Modern A horizon (5- 10 cm thick; not mapped)
15b	White, loose, silty colluvium with tuff clasts
15a	Incipient Bt horizon (?), White
15	Distal silty colluvium, rare clasts
14	Red soil (contains several Bt horizons)
13	Red soil (contains several Bt horizons)
12c	Red Bt horizon developed on stony crack fill
12b	Red Bt horizon developed on stony crack fill
12a	Red Bt horizon developed on finer graben sediments
11	Stony crack fill
10d	Block of hard fine sand
10c	Stony crack fill
10b	Stony crack fill
10a	Stratified blocks in crack fill
9	Slope colluvium, few clasts
8b	Blocks of hard fine sand
8a	Stony crack fill and colluvium
8	Block of yellow gravel
7a	Slope colluvium, few clasts
6d	Transition zone to slope colluvium
6c	Transition zone to graben fill (buried A horizon)
6b	Pumice gravel, clean
6a	Pumice gravel with red clay matrix
6a-b	Pumice gravel, undivided
6	Pumice gravel, undiff.
5	Yellow sandy gravel, fluvial deposit
4f	Pumice gravel
4e	Stratified sand
4d	Pumice gravel
4c	Stratified sand

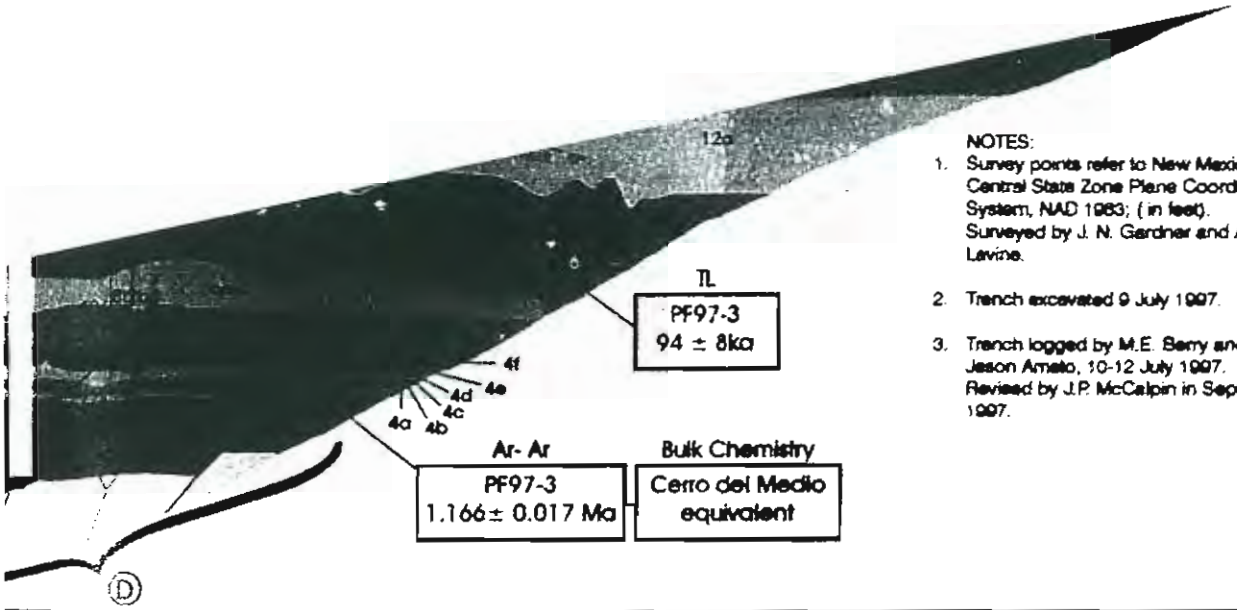

NOTES:

1. Survey points refer to New Mexico Central State Zone Plane Coordinate System, NAD 1983; (in feet). Surveyed by J. N. Gardner and A. Levine.
2. Trench excavated 9 July 1997.
3. Trench logged by M.E. Berry and Jason Amato, 10-12 July 1997. Revised by J.P. McCalpin in Sept. 1997.

4b ... gravel
4a ... volcanic ash
3 ... gravelly sandy silt, fluvial deposit
2 ... sands, fluvial deposit
1h ... Colluvium
1g ... tuff
1f ... cobble clasts of tuff
1e ...
1a ... beds
1c ... beds
1b ... beds
1a ... hard tuff
k ... Nacimiento

SCALE

0 2 4 meters

GEO-HAZ Consulting, Inc.

PAJARITO FAULT, TRANSECT OF 7 TRENCHES, SUMMER 1997
LOS ALAMOS, NEW MEXICO

TRENCH 3- South Wall

DATE	MAY 1998	FIGURE 13
DWG. NO.	C:\GEOHAZ\LANL\ALAMOS\TRENCH3..CDR	

bed (units 1b, 1c, 1d). The cross-bedding directions of units 1b and 1c cross-cut each other, indicating multiple surges. Tuff near the main fault (unit 1g) is intensely brecciated, in places so much so that the deposit resembles old colluvium (unit 1h) composed entirely of angular tuff fragments.

The overall graben stratigraphy can be subdivided into three major groups. The upper ca. 2 m (units 7a, 12a-15) is sandy to clayey, massive sheetwash and distal colluvial deposits, all of which except unit 15 have been strongly overprinted by multiple textural B horizons. The central 2 m (units 4a-6d) are dominantly pumiceous gravels and silty volcanic ashes and sands. The lower 1.5 m (units 2-3) are less well stratified, compact, pumice-poor alluvium and/or slopewash.

Units 2 and 3 are the oldest unconsolidated units in the trench, and are considerably denser (compacted) than younger units. Unit 2 contains moderately developed planar stratification in relatively clean medium-coarse gravelly sands, whereas unit 3 contains more silt and is more massive. These two units were probably deposited by intermittent streams flowing down the graben axis, for two reasons. First, Los Alamos creek today carries large cobbles and boulders, not medium-coarse sands. If these sands were deposited by Los Alamos Creek they should contain much coarser gravel. Second, no dacite clasts were observed in this unit, but Los Alamos Creek gravels are rich in dacite clasts. In contrast, a stream heading on the main fault scarp would have no access to dacite gravel. In addition, the grain size and bedding in this unit does not change close to the main fault, as would be expected if the stream was restricted to the graben such that a channel margin existed along the fault scarp; in this case we should see facies relationships between scarp-derived deposits and stream deposits. Thus, the retrodeformation analysis (Fig. 17) indicates that these units were probably also deposited on what is now the upthrown block at trench 3, indicating that, if the graben existed at that time, deposition filled up and overflowed the eastern graben margin.

Unit 4 is a sequence of thin, well stratified beds that alternate from pumice gravel (units 4b, 4d, 4f) to stratified medium-coarse sand (units 4c, 4e). The basal unit (unit 4a) is a dense, silty, nearly pure white volcanic ash. All subunits appear to have been deposited by running water, since their matrices are remarkably free of silt and clay. Overlying unit 5 is similar to unit 3, but is less dense, slightly better stratified, and more gravelly, indicating a slightly stronger intermittent stream.

Unit 6 is a thick deposit composed almost entirely of pea-size to marble-size rounded pumice clasts. In unit 6a the pumice clasts are coated and bonded by a matrix of red clay, whereas in unit 6b there is an absence of matrix and an openwork texture exists in places. This deposit evidently represents a blanketing of the local landscape by pumice fall, after which local streams eroded the pumice and redeposited it in the graben.

Unit 6 grades upward into a 2 m-thick section of finer-grained, massive deposits (units 12a-15) that contain progressively more clasts of tuff closer to the main fault. Units 12a,

13, and 14 are actually three buried soils, each composed of one or more textural B horizons (all horizons are not shown on the log; see Appendix B). The parent materials of these three soils is poorly-to non-stratified, but probably the original weak stratification has been abscured by the influx of pedogenic clay and the development of pervasive strong, angular blocky ped struct Within each soil unit the top is characterized by 5 YR colors and prismatic to strong angular blocky structure with abundant clay films on ped faces. B horizon color and structure weaken toward the bottom of each unit, with colors decreasing in hue (often to 7.5 YR) and structure decreasing to moderate subangular blocky. Because the stratification in the parent material has been obscured by pedogenesis, we cannot detect erosional unconformities within the parent material of each soil. The top of each soil must comprise at least a hiatus in deposition, but in addition some thickness of each soil top (e.g., the A horizon) may have been eroded before deposition of the overlying parent material. There are no stone lines either within or between the three soil units (12a, 13, 14), so if erosional unconformities exist in the section, they are too obscure to map.

Within 2 m of the main fault there is a sequence of three fissure-fill units (8a, 10, 11) with thin overlying scarp-derived colluviums (9, 12a). The gradual facies transition of these units with the graben deposits described above has been obscured by faulting and fissuring. Generally, the three fissure-fill units are downward-tapering wedges of poorly-sorted gravelly diamictons. Each wedge contains: (1) angular clasts of tuff; (2) slivers and blocks of stratified gravels (usually units 4-5); and (3) a clayey matrix with the color and structure of the B horizons previously described. Due to the chaotic nature of this fissured zone near the fault, it is difficult to know whether a block (such as 10a) forms the eastern boundary of one fissure fill unit or the western boundary of the adjacent unit. The three fissure fills described on the log were differentiated from one another on the following basis: (1) unit 11 (the closest to the main fault, the highest, and presumably the youngest) is considerably less dense (compacted) than the other two units; (2) unit 10 is harder than unit 11, contains many more blocks of stratified gravel, and its top (indeed the entire wedge) appears tilted west about 10 degrees; and (3) unit 8a contains at its base exclusively blocks of tuff surge beds (units 1b, 1c) that do not appear in the other fissure fills, and the entire wedge appears tilted to the west about 25 degrees. It might have been possible to subdivide this fissure zone into even more than three distinct units if individual blocks or groups of blocks were counted, but such a fine subdivision might result in overestimating the actual number of discrete fissure forming events. Unfortunately, the definition of adjacent fissure-fill units is inherently more ambiguous than the definition of superjacent colluvial wedges separated by buried soils. Applying the principle of parsimony to Trench 3, as few as three fissuring events could create the geometry shown in the trench wall.

The youngest deposits in Trench 3 (unit 15) generally do not contain any trace of Bt horizon development, and are similar to the youngest units exposed in Trenches 1 and 2. Unit 15 is the youngest graben unit and is relatively clast-free, light gray to pinkish gray, sandy silt with indistinct stratification. We infer that this deposit was laid down by

sheetwash, either descending westward from the scarp face or traveling eastward on the floor of the graben. Summer thunderstorms occured during our 1997 trench logging and formed thin (0.5-1 cm thick) sheetwash deposits in road tracks and other topographic low spots in the graben. These modern sediments are essentially identical to unit 15. By analogy, we also infer that the par material of units 12a, 13, 14 was originally light gray silt transported by sheetwash.

This distal silty colluvium/slopewash grades eastward into a stonier, thicker debris facies colluvium (unit 15b); the contact is arbitrarily placed behind a shore. Unit 15b reaches its maximum thickness atop the main fault zone (Fig. 13) and thins westward, thus having the shape and position of a typical scarp-derived proximal colluvial wedge. The matrix of unit 15b is very loose and friable, in strong contrast to the red clayey matrix of all the underlying fissure fills. Finally, unit 15a is a thin, insipient B horizon developed on white, moderately loose, silty gravel that veneers the upper scarp face. This parent material and soil are probably older than unit 15b (note the contact between them) and could represent material that was already on the scarp face prior to the latest faulting event.

3.4.3 Structure

Trench 3 exposes a discrete subvertical main fault plane (A) that abuts Bandelier Tuff (on the east) against more than 5 m of unconsolidated sediments. In the upper 2/3 of the trench fault A has a smooth, slightly concave shape in profile (Fig. 14). Small parallel splay faults in the tuff, and oriented clasts in the adjacent fissure fills, suggest there has been shearing movement on this plane. However, in the lower 1/3 of the trench fault A bends sharply and curves back to the east. It is not clear how dip-slip faulting could be accommodated on a fault with such shape. A possible solution to this dilemma is suggested by the fact that the strike of fault A is not parallel to the fault scarp, but trends 25-30 degrees more easterly (as pointed out by reviewer F.H. Swan III). This geometry suggests that fault A may be a preexisting joint surface that was used as a fault during dip-slip faulting that has a strong extensional componant. The downthrown block may be both dropped down and pulled away from the upthrown block during faulting. This mixed dip-slip and extensional movement would result in plucking of fracture-bounded tuff blocks off of the upthrown block, leaving a fault plane with an irregular profile. However, it is difficult to understand how such a mode of motion would produce the shear fabric seen along the fault at higher levels.

The area within about 2 m of fault A contains fissure fills bounded by reverse faults. These faults occur at the boundaries of the fissure fills and presumably represent the riginal margin of the fissure. Fissure fill units 8a and 10b appear to have been shoved up and westward by faulting subsequent to their emplacement. The same phenomenon also occurs in Trench 7, another small west-facing scarp underlain by a thick fine-grained graben fill. The geometry of these reverse faults should not be taken to indicate regional compressive tectonic stresses. The more likely explanation is that vertical downdropping

of unconsolidated material to the right of curving fault A "hangs up" the prism of sediments above the curved fault, preventing it from dropping down as far as its correlative strata farther west, and thus creating the "reverse" faults. These fissure margins were probably vertical when initially formed, but have been rotated westward along with their fissure fills by a topp[illegible] style of motion. Another effect of "hanging up" this prism of sediment is that a void space is opened beneath the overhang in fault A. This area is currently filled with pockets of sediment that do not correlate with any others in the trench.

The sequence of graben units 2-6b are downfaulted and tilted east along faults B and C. The units maintain similar thicknesses across fault C, suggesting that slip along that fault only began after deposition of unit 6b, but ended after the deposition of unit 6d . Farther west, fault zone D contains about 10 small normal faults that displace units 2-5,

Fig. 15. Close-up photograph of the main fault plane (fault A) in Trench 3 The level line at bottom is at - 3.0 mV; compare the two shores to those on Fig. 12. Sheer fabric is apparent in both units 10 and 11 (fissure fill to the right of the fault), expressed as microfractures and oriented clasts parallel to the fault plane. Unit left of fault plane is hard white tuff (unit 1a). Rails of shores are 20 cm wide

but die out in the thick pumice gravels of unit 6. Either movement on these faults predates unit 6, or later movement occurred but was generally absorbed by intergranular adjustments (note however, four faults extend into units 6a or 6a-b).

3.4.4 Geochronology

Radiocarbon (C-14), thermoluminescence (TL), and soil development index (SDI) age estimates are available in Trench 3. The single C-14 date of 1300± 80 C-14 yrs BP (on a small piece of charcoal) confirms the Holocene age of unit 15b. TL age estimates are 69± 6 ka for unit 14 (base), 106± 9 ka for unit 9, and 94± 8 ka for unit 7a. The two latter dates constitute a weak age reversal since unit 7a immediately underlies unit 9, but the two TL ages overlap at 1 sigma.

SDI age estimates were made from two vertical soil profiles at 8 mH and 9.6 mH. The techniques and assumptions of SDI age estimates are described in Appendix B.

Table 6. SDI Age Estimates of Soils in Trench 3[1]

Unit[2]	Position	Age @ 8 mH[3]	Position	Age @ 9.6 mH[3]
15	lower 1/3	0.8 ka	bottom	0.7 ka
14	bottom	20 ka	middle	7.4 ka
13	near bottom	43 ka	near bottom	38 ka
7a	middle	81 ka	bottom	99 ka
6	middle	[117 ka][4]	middle	[126 ka]
3			near bottom	[161 ka]

[1] For complete data see Appendix B.
[2] see Fig. 13.
[3] "best age"; for range see Appendix B.
[4] ages in brackets are from stratigraphic units not heavily affected by pedogenesis.

For unit 15, both the C-14 age (1300 yrs BP) and the SDI age estimates (0.7-0.8 ka) suggest a Holocene age. For unit 14, TL ages are considerably older than SDI ages. Near the bottom of unit 14 at 8 m H the TL age estimate is 69± 6 ka whereas an adjacent SDI estimate is 17-24 ka (mean 20 ka). The TL age may be older than true age if an inherited signal is present, or the SDI age may be younger than true age if the upper part of unit 14 was removed prior to deposition of unit 15. The unit 14/15 contact appears to be an erosional channel between 16-18 m H, raising the possibility that some unknown thickness of unit 14 was eroded at 8 m H and 9.6 m H. Thus, the age of the base of unit 14 is almost certainly older than 20 ka, and could be as old as 69 ka if silts were completely TL-zeroed at time of deposition.

For unit 13, SDI ages near the bottom contact are similar at 8 m H (43 ka) and 9.6 m H (38 ka). Unit 9 has a TL age estimate of 106± 9 ka. For unit 7a, TL ages are similar to SDI ages. The western part of unit 7a (12.3 m H) yields a TL age of 94± 8 ka, whereas

the SDI age from a slightly lower stratigraphic position in the unit 2.5 m away is 99 ka. At its far eastern end, the middle of unit 7a has an SDI age of 81 ka. This date is from a stratigraphic position only 15 cm lower than the TL sample from unit 9, dated at 106± 9 ka. Therefore, it appears reasonable that the base of unit 7a is about 100 ka, assuming that there was little erosion and silts were initially TL-zeroed.

SDI age estimates were made for units 6 and 3 (Appendix B), but those units are weakly affected by pedogenesis and the possibility of erosional loss in that part of the stratigraphic section is high. Therefore, the SDI age assumptions are probably not valid.

The final geochronologic control is the age of the fine volcanic ash of unit 4a. According to J.N. Gardner (pers. comm., 1998) this ash resembles ashes from the waning stages of the Bandelier Tuff eruptive sequence, and is ca. 1 Ma. If this correlation is correct, and the previously-cited SDI and TL age estimates are approximately correct, there must be major unconformities and/or hiatuses between the base of unit 7a (age approx. 100 ka) and unit 4a (age ca. 1 Ma). Of the 1.5 m of stratigraphic thickness between units 4a and 7a about half is contained in unit 6, the coarse pumice gravel. We originally surmised that unit 6, as well as the well-stratified beds of units 4 and 5, could have been deposited rapidly in a series of storm events. Thus, given the short amount of time required to deposit units 4-6, the 900 ka of missing time presents a mystery. One explanation is that sediment/soils similar to units 12a-15 accumulated above unit 4a between 1 Ma and 100 ka, but were removed by erosion prior to deposition of unit 7a. However, the 2+ m-thick sequence of units 12a-15 accumulated over only 100 ka, so in the "missing" 900 ka such sequences would have to be deposited and then removed in multiple cycles. Postulating multiple cycles of deposition followed by erosion based on an absence of evidence, is hard to justify.

In summary, the relative concordance of TL and SDI age estimates back to about 100 ka in Trench 3 suggests that there has been only minor erosion in the stratigraphic record composed of fine graben fill sediments (units 7a-15). The large age discordance between SDI ages and the correlated age of volcanic ash unit 4a indicates that large spans of time are missing from the stratigraphic record of alluvial units 4-6. In addition, if the correlated ash age of ca. 1 Ma is correct, then the 1.3+ m of units 2 and 3 were deposited in a very short time during the waning stages of the Bandelier Tuff eruption. Such rapid deposition may be possible, but has no analogs in other trenches.

3.3.5 Paleoseismic Interpretation

The complex sequence of depositional and faulting events in Trench 3 can only be reconstructed by rigorous vertical retrodeformation of the trench log (possible lateral components of fault displacement are not accounted for). During each retrodeformation step, all unfaulted beds are removed from the trench log, such as post-faulting colluvium and alluvium. Next, beds eroded from the upthrown block during deposition of the colluvium (either pre-faulting colluvium or alluvium) are replaced on the upthrown block.

Their thickness and shape are assumed to be less than or equal to that of their counterparts still preserved on the downthrown block. Finally, the upthrown block is moved downward to reverse the effect of the faulting event. The amount of movement is gauged by several requirements: (1) if clasts and blocks in scarp-derived colluvium come from a recognizable source bed on the upthrown block, that the bed must have been exposed in the fault free face; and (2) the top of reconstructed deposits on the upthrown block must be brought down to match the top of the equivalent deposit on the downthrown block. However, since the thickness of eroded material on the upthrown block is only estimated, there is an element of circular reasoning at this step. Thus, while cross-cutting relationships on the trench log typically demand a unique sequence of depositional and faulting events, there are many possibilities for displacement in each event that will satisfy the two requirements outlined above.

In this retrodeformation sequence we simplified the sequence of events in graben beds by assuming that deposition of parent material and then soil formation in that parent material occurred in a single step. This is equivalent to assuming that soil units 12a-14 are also stratigraphic units, although that assumption cannot be proven. If soil horizons cut across different parent materials with angular "unconformity" this assumption would induce errors in the reteodeformation, but generally such discordance does not occur in Trench 3.

Before creating the retrodeformation sequence, we envisioned a conceptual sequence-model of alternating dip-slip faulting, tectonic fissure creation, filling by scarp-derived debris, burial by graben aggradation equal to the scarp height, and surface stabilization and soil formation (Fig. 16). The subsequent faulting event would create a new fissure through the graben aggradation deposits, and the sequence would repeat. Thus, the three fissure fills (units 8a, 10, 11) were thought to correspond to graben-fill units 12a, 13, and 14, respectively.

This model appears to be too simplistic to account for the relationships exposed in the trench. First, after formation of the older two fissure fills, subsequent faulting events pushed them up and westward due to curvature of the main fault plane. Second, unit 12, the oldest of the three graben soil units, evidently overlaps and is thus younger than the youngest of the fissure fills (unit 11). Retrodeformation suggests that units 12a and 13 were not separated by a faulting event, whereas two faulting events (Y_3 and Z_3) postdate unit 13.

The retrodeformation sequence in Fig. 16 contains 8 displacement events, the first two of which ($S_3$and T_3) occurred before the deposition of unit 6. Event U_3 immediately preceded the deposition of colluvial unit 7a, which has an estimated age of ca. 100 ka. All five subsequent events (V_3-Z_3) can be approximately dated by SDI and TL ages. Based on the ages and the displacements required by the retrodeformation sequence, we can compile a slip history diagram (Fig. 17). The individual event displacements may be in error by ca. 25% in some cases, but the cumulative vertical displacement must total 7.9 m

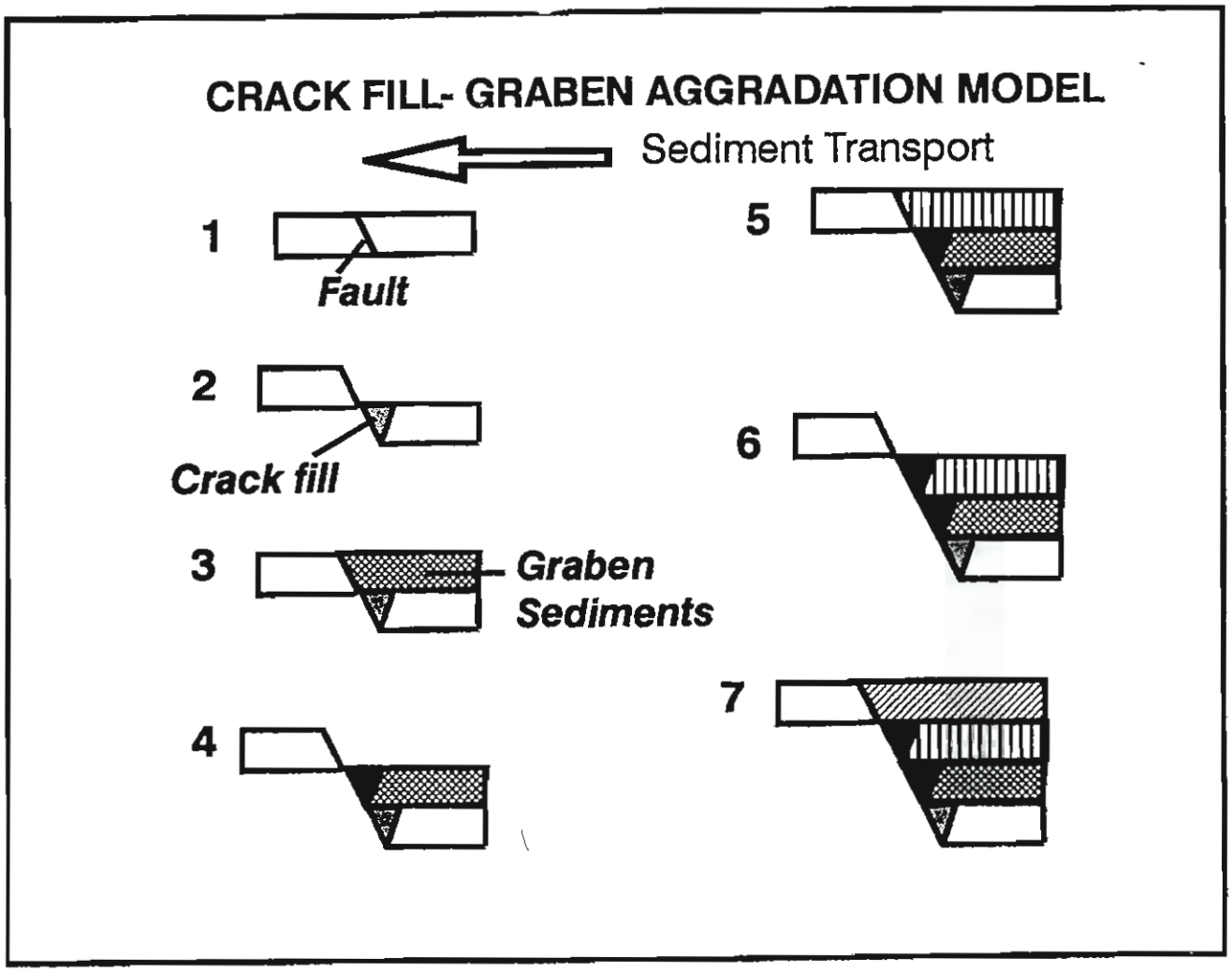

Fig. 16. Hypothetical model for faulting and deposition in a graben, where normal faulting is accompanied by the formation of large fissures at the scarp base

1

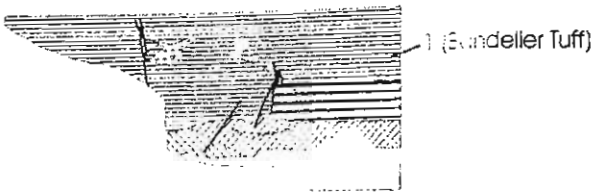

PRE-FAULTING GEOMETRY

2

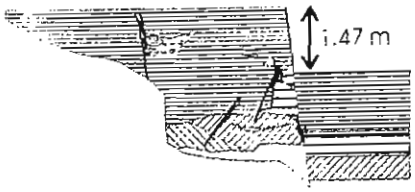

Faulting Event S3; displaces tuff and forms initial graben; may be more than one event.

3

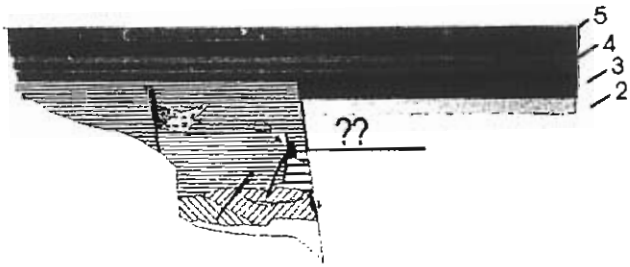

Initial graben fill is deposited (of unknown character) and is now beneath the trench floor; later stratified alluvium (units 2 and 3), ash and pumice gravel (unit 4), and more alluvium (unit 5) fill graben, then spill eastward and bury scarp.

4

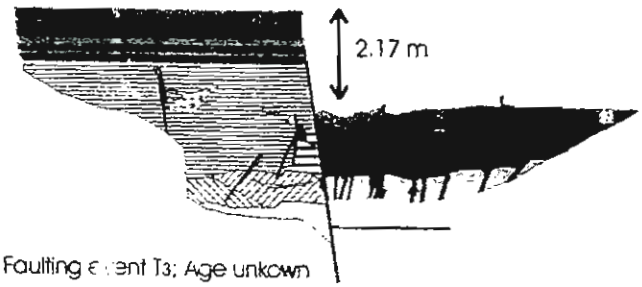

Faulting event T3; Age unkown

5

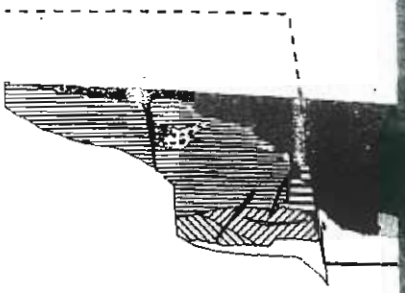

Scarp-derived chunks of stratified alluv
fall into proximal part of pumice grave
is deposited; Age ca. 117-126 ka (by s

6

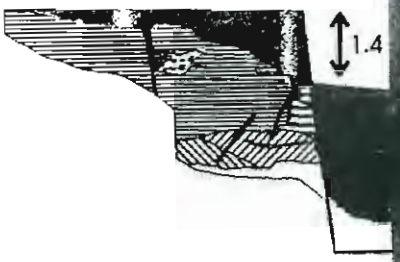

Faulting event U3; Age ca. 110 ka

7

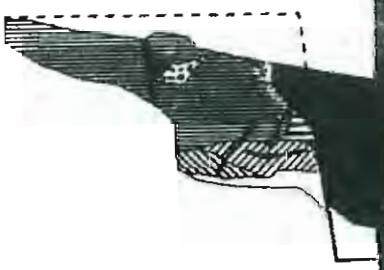

Scarp-derived colluvium (pink) bur

um (dark blue)
(purple) as ir
ɔil SDI) or cn.

Faulting event V3; First large fissure opens, pumice gravel backtilted; Age ca. 100 ka.

m

9

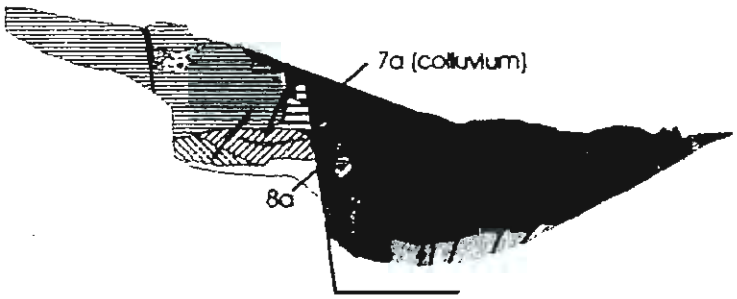

Fissure fills with chunks of tuff surge bed (8a); scarp-derived colluvium (7a) buries crack fill; Age ca. 94- 99 ka.

6d

es pum... ...avel

GEO-HAZ Consulting, Inc.	
PAJARITO FAULT, TRANSECT OF 7 TRENCHES LOS ALAMOS, NEW MEXICO TRENCH 3- South Wall	
DATE MAR. 1998	FIGURE 17
DWG. NO. C:\GEOHAZ\LANL\ALAMOS\RETRO3.CDR	

10

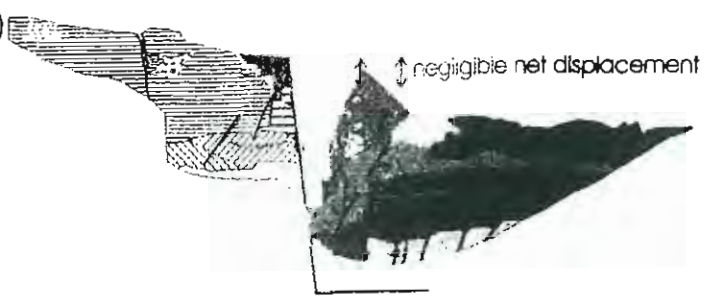

Faulting event W3; no net vertical displacement, fissuring only; Age 81 - 106 ka (mean 94ka)

11

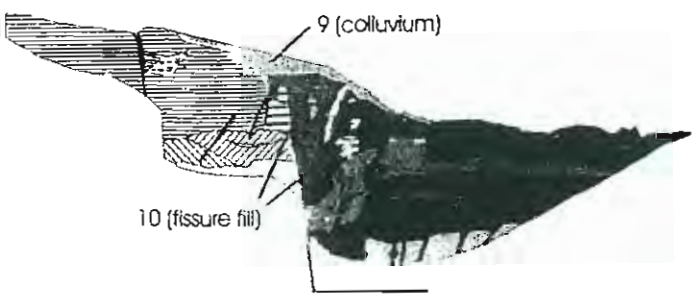

Fissure fills with recycled proximal colluvium (10); colluvium (unit 9) overlaps fissure

12

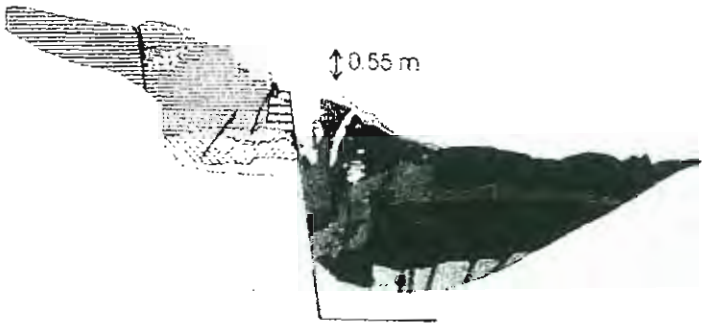

Faulting event X3; last large fissure opens; age ≤ 81 ka.

13

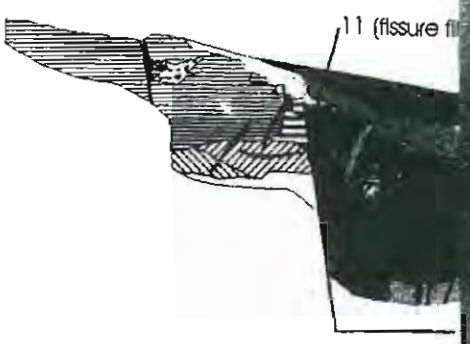

Fissure fills (unit 11) and is overlapped by co stratigraphic packages form at scarp base ca. 81 ka to ca. 20 ka.

14

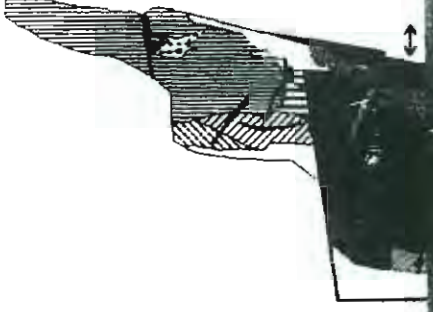

Faulting event Y3; 0.25 m vertical displ on subsidiary fault trace; Age ca. 20 ka

15

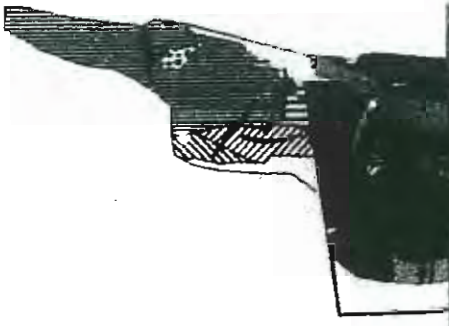

Scarp-base colluvium (14) accumulates o

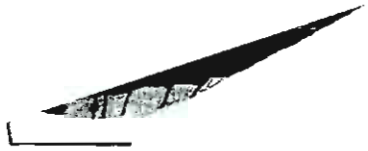

...ng event Z3; small free face created. Age ca. 4 ka.

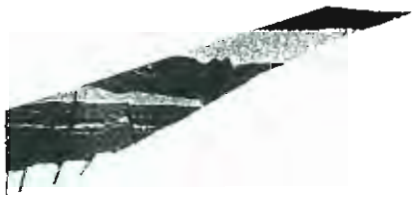

...cement. ...

17

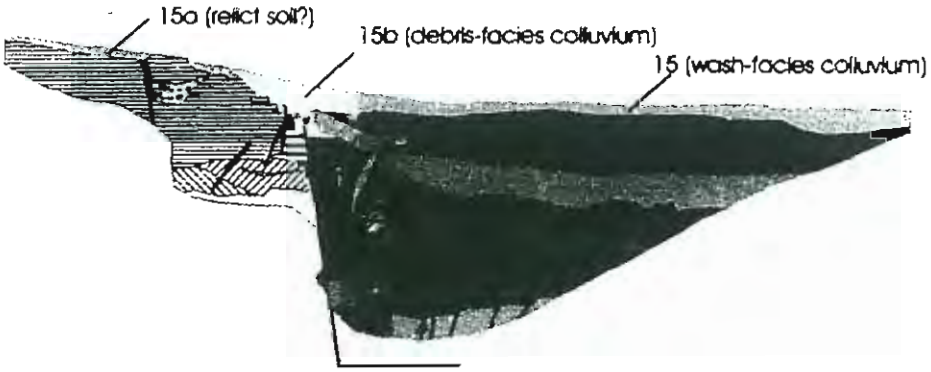

...vium and soil)

Latest colluvium deposited on scarp face (15b) and at base (15a); weak A/C soil profile develops (not shown).

...nd soil ...

GEO-HAZ Consulting, Inc.

PAJARITO FAULT, TRANSECT OF 7 TRENCHES
LOS ALAMOS, NEW MEXICO

TRENCH 3 Retrodeformation- South Wall

DATE MAY 1998	FIGURE 17
DWG. NO. C:\GEOHAZ\LANL\LAMOS\RETRO3.CDR	

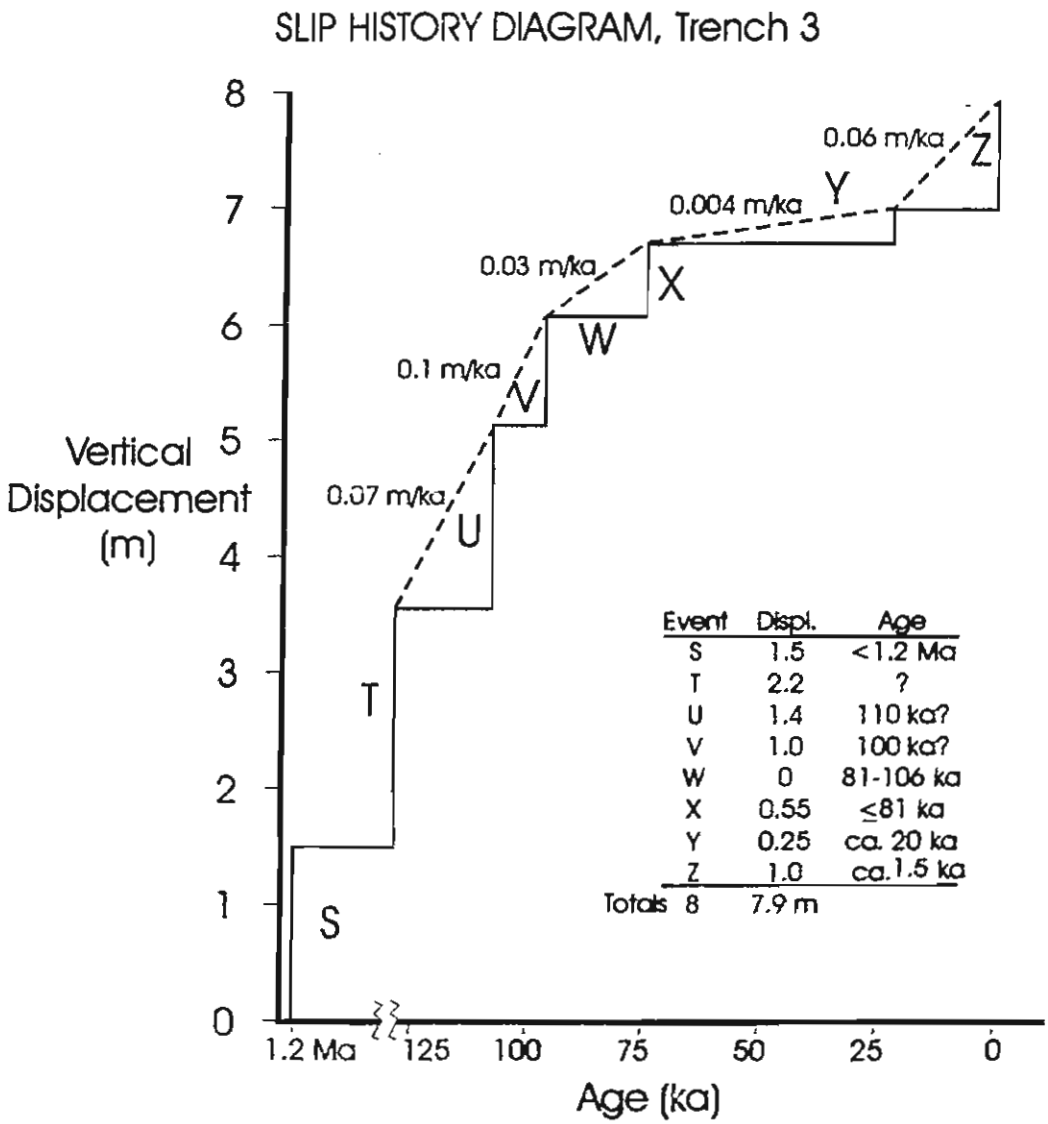

Event	Displ.	Age
S	1.5	<1.2 Ma
T	2.2	?
U	1.4	110 ka?
V	1.0	100 ka?
W	0	81-106 ka
X	0.55	≤81 ka
Y	0.25	ca. 20 ka
Z	1.0	ca.1.5 ka
Totals 8	7.9 m	

Fig. 18. Slip history diagram for Trench 3, based on the retrodeformation sequence

(distance from the top of the scarp to 5.7 m depth of tuff in the graben, based on seismic line 2). The overall slip rate (7.9 m/ 1200 ka) is 0.0066 m/ka. In contrast, slip rates during the past ca. 100 ka range from 0.004 to 0.10 m/ka over various seismic cycles (mean = 0.053 m/ka, sigma = 0.033 m/ka, COV = 0.62). This degree of slip rate variability through time is slightly less than that deduced for a set of 18 faults in the western USA (McCalpin, 1995). Vertical displacement per event ranged from 0 (event W_3) to 2.2 m (event T_3), with mean = 0.99 m and sigma =0.67 m, COV = 0.68. This degree of variation is larger than that found by Hecker and Schwartz (1994) in a larger (but currently unpublished) data set where COV was typically <0.3. However, the two data sets mentioned above were collected from primary fault traces, not secondary antithetic faults such as at Trench 3, so a rigorous comparison is not justified.

The major ambiguity in interpreting the long-term paleoseismic record at Trench 3 is the unknown ages of strata below unit 7a. However, even if those ages were known, the slip rates in the past 100 ka would still be an order of magnitude larger than the long-term (post- 1.2 Ma) slip rate at this site. One way to explain that discrepancy is if the graben began forming much later than 1.2 Ma. If this is true, then units 6 and older were deposited as widespread sheets rather than being confined in a graben. Such a depositional mode was required for units 2-5 by the retrodeformation analysis, in order to explain how blocks of unit 3 became incorporated into the proximal part of unit 6 (stages 3-5 in Fig. 16). Because this is the first deep exposure of graben sediments, and does not reach the base of graben fill, we do not know if a mid-Pleistocene origin for the graben is reasonable. Perhaps study of other graben exposures could shed light on this issue.

3.5 Trench 4.

Trench 4 is located across the same west-facing fault scarp as is trench 3, but 100 m farther south (Fig. 4). The scarp here is only 0.4 m high, compared to the trench depth of up to 3.2 m and length of 14 m (Fig. 18). Trench 4 was excavated in hopes of exposing a thicker section of Holocene deposits than was exposed at trench 3. Trench 4 lies on a lower, younger geomorphic surface in the graben that currently receives drainage and sediment from two gullies that incise the main fault scarp ca. 200 m to the west. In contrast, Trench 3 lies on an older graben-floor surface about 2 m higher than at Trench 4, and Holocene sediments are very thin. It was hoped that as much as 1 m of Holocene strata would abut the fault at trench 4, and thus it would be easier to bracket the most recent faulting event. Conversely, we had less interest in the long-term paleoseismic record at Trench 4, since the exposure at Trench 3 appeared sufficient to interpret that aspect.

3.4.1 Stratigraphy

In a general sense the deposits in trench 4 are similar to those in trench 3, i.e. fine-grained sediments and multiple buried soils in the graben, grading into coarser-grained fissure fill and colluvium near the fault (Fig. 19). However, the pumice gravels and other well-stratified beds observed in Trench 3 deeper than 2.5 m below the surface are never exposed in Trench 4, probably because most of Trench 4 is <2.5 m deep. No geophysics lines were surveyed near Trench 4.

Hard, white, welded Bandelier Tuff comprises the upthrown block. On the downthrown block similar, but more fractured blocks of tuff exist at the bottom of the trench. I believe that all these blocks except possibly the westernmost are in-situ fractured bedrock outcrops caught in a fault sliver, rather than loose colluvial boulders.

Units 2-5 are fissure fill deposits differentiated by their general hardness and by cross-cutting relationships. As in Trench 3, the loosest (and presumably youngest) unit abuts the main fault plane (A). Fine grained graben deposits and soils appear to lap up onto unit 4a, so they are inferred to be generally younger than the fissure fills, as was interpreted in Trench 3. However, unlike in Trench 3, the soils in Trench 4 are laterally discontinuous and have angular discordances. We did not attempt to reconstruct the chronology of older faulting events here because the stratigraphy (especially the soil stratigraphy) was more ambiguous than at Trench 3.

Holocene deposits were indeed thicker here (55 cm) than at Trench 3 (20-40 cm) and were subdivided into three subunits. The lowest unit (10b) overlies a red Bt horizon with well-developed prismatic structure (unit 9c) and is composed of a gravelly sand containing small pebbles. This unit maintains a relatively constant thickness of 7-15 cm, except for one small channel of pebble gravel eroded into unit 9c (unit 10a). Unit 10A has a light gray color and no signs of Bt horizon development. Most of the overlying Holocene section (20-30 cm) is composed of unit 10c, a massive, white to light gray sandy silt with

Fig. 19. Photograph of Trench 4, looking E toward the very low antithetic scarp.

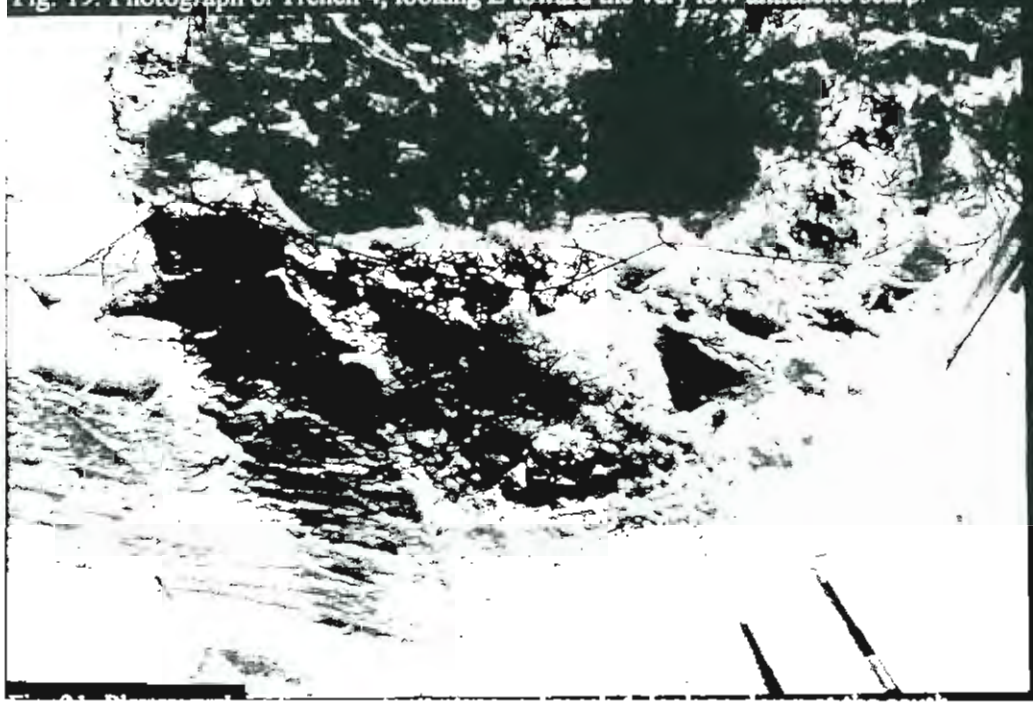

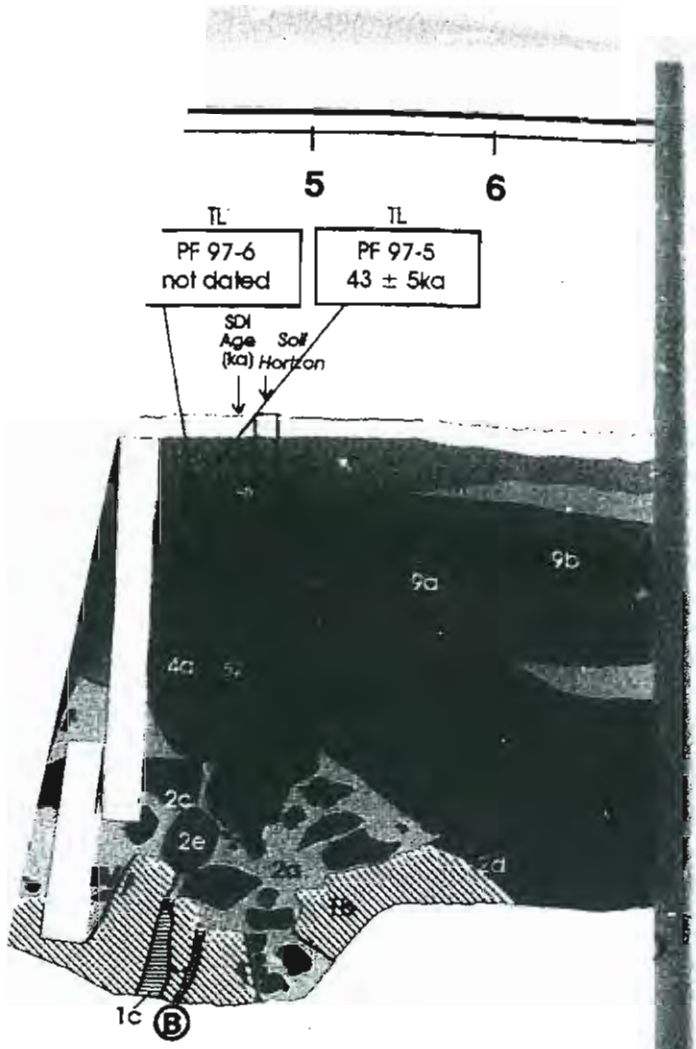

ination of Trench Units

	5a	Mottled red and white cl
	4c	Krotovina
ne)	4b	Clasts of tuff in unit 4
ne)	4a	Slope colluvium
	3b	Clasts of tuff in unit 3
	3a	Crack fill (smaller clasts o
	2e	Red and white mottled c
graben fill	2d	Sandy clay
nge to red	2c	Krotovina? - soft pocket c
graben fill	2b	Clasts of tuff in unit 2
	2a	Crack fill and scarp-deri
Bandelier Tuff	1c	Fractured tuff
	1b	In-situ blocks of tuff
on of 6a and 7b)	1a	In-situ tuff (upthrown bloc

Symbols

Fracture

Fault or Fracture Zone Described in Text

Fault

area of wall covered by trench shore

NOTE: Only shores covering important areas of the trench wall that could not be removed for safety reason are mapped.

DATING CONTROL:

1. C-14 dates from Beta Analytic, sample number at top; age in radiocarbon years Before Present at bottom (± 1 sigma). Collected and submitted by S.L. Reneau. (Appendix C)
2. Soil profiles measured by Eric V. McDonald, with soil ages estimated from Soil Development Index. (Appendix B) NOTE only the lowest horizon in each buried soil os labeled here.
3. TL dates from Steve Forman, Univ. Of Illinois-Chicago; sample number at top; age in ka at bottom (± 1 sigma). (Appendix D)

SCALE

0 — 2 meters

NOTES:

1. Survey points refer to New Mexico Central State Zone Plane Coordinate System, NAD 1983; (in feet). Surveyed by J.N. Gardner and A. Lavine.
2. Trench excavated 9 July 1997.
3. Trench logged by M.E. Berry and Jason Amato, 10-12 July 1997. Revised by J.P. McCalpin in Sept. 1997.

GEO-HAZ Consulting, Inc.

PAJARITO FAULT, TRANSECT OF 7 TRENCHES, SUMMER 1997
LOS ALAMOS, NEW MEXICO

TRENCH 4 - South Wall

DATE MAY 1998	FIGURE 20
DWG. NO. C:\GEOHAZ\LANL\ALAMOS\TRENCH4..CDR	

rare small clasts. This deposit is similar to unit 15 in Trench 3 and is inferred to be a sheetwash deposit. The upper 10-12 cm of this unit (unit 10e) is the modern A horizon.

3.4.2 Structure

The main fault (A) is defined by a sharply defined, subvertical contact that abuts sparsely-fractured Bandelier Tuff (on the east) against fissure fill units (Fig. 21). However the strike of the fault plane is more north-easterly (N30E) than the strike of the fault scarp (N05E), and on the north trench wall several more irregular fault traces abut the fissure fills. Thus, like the main fault in Trench 3, this fault appears to be a preexisting joint surface that accommodates both dip-slip (down to the west) and extensional (E-W) movement. The fault appears to continue as a fracture through soil unit 9c, but the top of the unit is not vertically offset.

The western boundary of fissure fill unit 3 is shown as a fault, to emphasize the tectonic nature of the structure, but it could just as well be thought of as a very steep depositional contact, i.e. a fissure wall. There is no direct evidence that this fissure margin was reactivated by later "reverse" faulting associated with toppling, as observed in Trench 3.

Fault zone B is exposed at the bottom of the trench where zones of highly fractured tuff lie between more intact tuff blocks. The separate tuff block at the west edge of this zone may be the top of a pillar of fracture-bounded tuff similar to that more deeply exposed at the head of Trench 5. If so, the tuff under the graben floor is probably faulted down an additional amount at 6 m H. On the western margin of the tuff blocks at the floor of the trench, unit 2d separates tuff from graben fill. Unit 2d is a 10 cm thick sandy clay that is more compact and less red than soils in the graben, and could be fault gouge (?) associated with this inferred fault.

On the north wall of the trench, structures and deposits near fault A are somewhat different than on the south wall (Fig. 22). The main fault plane is more undulatory and has slivers of fracture-bounded tuff that grades westward into fissure fill. Where Holocene sediments abut the main fault plane there is a tension fissure 10 cm wide, in which the prismatic B horizon (unit 9c) appears to be downdropped 15 cm. Overlying the B horizon is the basal gravelly sand unit (10b) of Holocene slopewash/alluvium. The upper contact of unit 10b continues horizontally to the main fault, whereas this gravelly sand is >20 cm thick in the fissure. The overlying Holocene sandy silt (unit 10c) abuts the tuff at the main fault along a curved plane along which there is no discernable shear fabric.

3.4.3 Geochronology

C-14 dates from Holocene unit 10c are a bit older (1690± 40 C-14 yrs BP, 2230± 40 C-14 yrs BP) than dates from Trench 3 (1300± 80 C-14 yrs BP), but still attest to a late Holocene age for the uppermost pale, loose deposits (unit 10). SDI age estimates for the

Fig. 22. Photograph of the main fault plane in Trench 4, looking down at the north wall. Note prominent 10 cm-wide fissure

base of the Holocene section range from 2.1 ka (at 5 mH) to 4.5 ka (at 7.4 mH). The latter age is somewhat discordant with the C-14 and other SDI ages, and coincides with a thickened Holocene section that includes unit 10b. In contrast, the TL age estimate for basal unit 10c is 43+/- 5ka. This age is much too old for the observed degree of soil development (an A/Cox profile) and [illegible] C-14 dates in unit 10. Perhaps the dated silt grains in unit 10c carried a large inherited TL component that evaded resetting during deposition.

SDI age estimates for the bases of units 9a, 8a, and 5a are 19 ka, 46 ka, and 115 ka respectively. This latter age is similar to SDI age estimates of 99 ka and TL ages of 94 - 106 ka from near the bottom of the fine-grained graben fill soils in Trench 3, and may indicate that the stratified part of the graben fill section is immediately beneath the trench floor.

3.5.4 Paleoseismic Interpretation

We did not construct a retrodeformation sequence for Trench 4 because only one of the graben fill deposits is in contact with the fissure fill sequence, so it would not be possible to relate the five graben soils to faulting events. If our subdivision of fissure fill units is valid, there have been four fissuring events (represented by units 2, 3, 4, and 5) all of which predate the prismatic red B horizon (unit 9a). However, none of these events can be dated precisely due to the lack of datable material in the coarse-grained fissure fills.

The most recent event fractured unit 9c on the south wall of the trench, and dropped unit 9c into a tension fissure on the north wall. The presence of overlying unit 10b in the fissure, and the undisturbed upper contact of that unit, means either: (1) the fissure was still open when unit 10b was deposited; or (2) the lower part of unit 10b had already been deposited atop the Bt horizon before faulting, it was then downdropped into the fissure, and unit 10b deposition continued. In the first scenario, the event horizon for the MRE is the basal contact of unit 10b, whereas in the second it is somewhere within unit 10b, which is ca. 10 cm thick. C-14 ages indicate that the base of unit 10b is older than 1.7 - 2.2 ka, and SDI ages from that contact are 2.3 - 4.5 ka. Thus, the MRE occurred somewhere after 2.1 - 4.5 ka, more likely after 2.1-2.3 ka.

3.6 Trench 5

Trench 5 is located at the base of the main, 50 m-high scarp of the Pajarito fault (Fig. 23a). This large trench is 30 m long and up to 6.5 m deep (Fig. 22b). The upslope end of the trench (8.8 m above the foot) coincides with the lowest outcrop of Bandelier Tuff on the scarp face (Fig. 24). This tuff outcrop exhibits east-dipping partings and is interpreted as the toe of the forward tilted slab that underlies the main scarp. Thus, Trench 5 begins at the basal fault zone described in Sec. 2.2., and occupies a similar structural and topographic setting to the Water Tanks and Pajarito Canyon trenches of WCFS (1996). Despite its large size, this trench only ascends 8.8 m vertically up the toe of the 50 m-high main fault scarp.

3.6.1 Stratigraphy

Except for the head of the trench, the entire length of Trench 5 is cut into a thick wedge of scarp-derived colluvium containing a surface soil and at least 7 buried soils (Fig. 25). Except for one prominent stone line in mid-trench, the parent materials are a homogenous gravelly silty sand throughout the entire 6.5 m. The only mappable units are the soil horizons, most of which parallel the modern ground surface. Because all the mapping units are soils, we use a mixed scheme of stratigraphic and soil horizon terminology for all map units. In this terminology, each unit abbreviation begins with a number that increases with decreasing age, as was done for the stratigraphic and soil units in Trenches 1 - 4. By strict soil survey rules these initial numbers would represent parent materials of different texture, but we use the numbering to represent parent materials of very similar texture but different age.

Upslope of 19 m H colluvial deposits begin to dip more steeply than the modern ground surface, and their upper ends have been eroded. Consequently soils that were physically separate in the thicker stratigraphic sections downslope of 19 m H, have been superimposed upon each other as their parent materials thinned, approached the ground surface, and/ or pinched out. Upslope of 21 m H parent materials were uplifted and eroded, such that quite young soils were superimposed on old colluvial deposits that already had old soils developed in them. We mapped these areas of superimposed soils as combination units, e.g. "8Bt3+4Bt3b2". This label indicates that parent material 4, in which soil horizon Bt3 had previously developed in the second-to-oldest buried soil (b2), had been brought up close enough to the surface to be overprinted with the Bt3 horizon of the surface soil. The leading number "8" has no meaning here, except to say that usually soil horizon Bt3 is developed on parent material 8 where no stripping or faulting has occurred.

a.

b.

Fig. 23. Overview photographs of Trench 5. a- base of main scarp of Pajarito fault, with graben to left and Trench 5 to right; b- looking up Trench 5 from the toe of the main scarp. Apparent crest of scarp at upper center is Ski Hill Road; true scarp crest is 15 m higher.

Fig. 24. Head of Trench 5 showing the lowest intact Tuff outcrop on the scarp face, and its subsurface extent (to right of ladder) that defines the head of the trench.

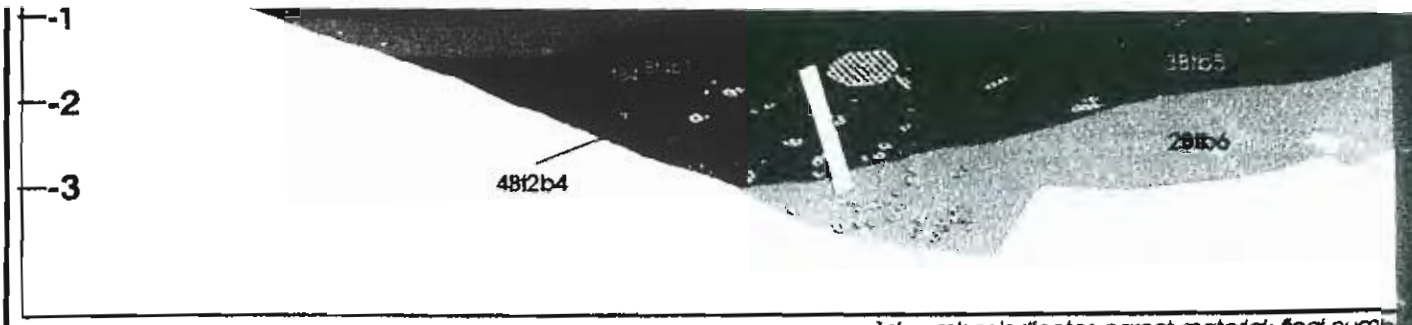

Explanation of Trench Units

1st number indicates parent material; final numb
intermediate letters and numbers are soil horizon

- 9A — A horizon
- 9AC — AC horizon
- 9EB — EB horizon
  - parent material is pale beige, loose stony colluvium with a silty matrix (Holocene)
- 9Bt1 — Bt1 horizon
- 8Bt1 — Bt1 horizon
- 8Bt2 — Bt2 horizon
- 8Bt3 — Bt3 horizon
  - parent material is inferred to be similar to that of unit 9, but is now overprinted by soils
  - surface soil
- 8Bt3 + 6Bt3b3 + 6BC1b2
- 8Bt3 + 4Bt3b2
- 9 + 8 + 7Bt
  - Several soils superimposed on multiple parent materials (deposits)
- 7Btb1 — Bt horizon- buried soil 1- on coarse colluvium
- 7BCb1 — BC horizon- buried soil 1- on coarse colluvium
- 6Bt1b2 — Bt1 horizon
- 6Bt2b2 — Bt2 horizon
  - parent material is wash facies colluvium
- 6Bt3b2 — Bt3 horizon
- 6BC1b2 — BC1 horizon
- 6BC2b2 — BC2 horizon
  - parent material is proximal (debris-facies) colluvium
  - buried soil
- 5Btb3 — Bt horizon
- 5BCb3 — BC horizon
  - parent material is wash- facies colluvium
  - buried soil
- 4Btb4 — Bt horizon
- 4Bt2b4 — Bt2 horizon
  - buried soil
- 4BCb2 — BC horizon of buried soil 2 developed on parent ma

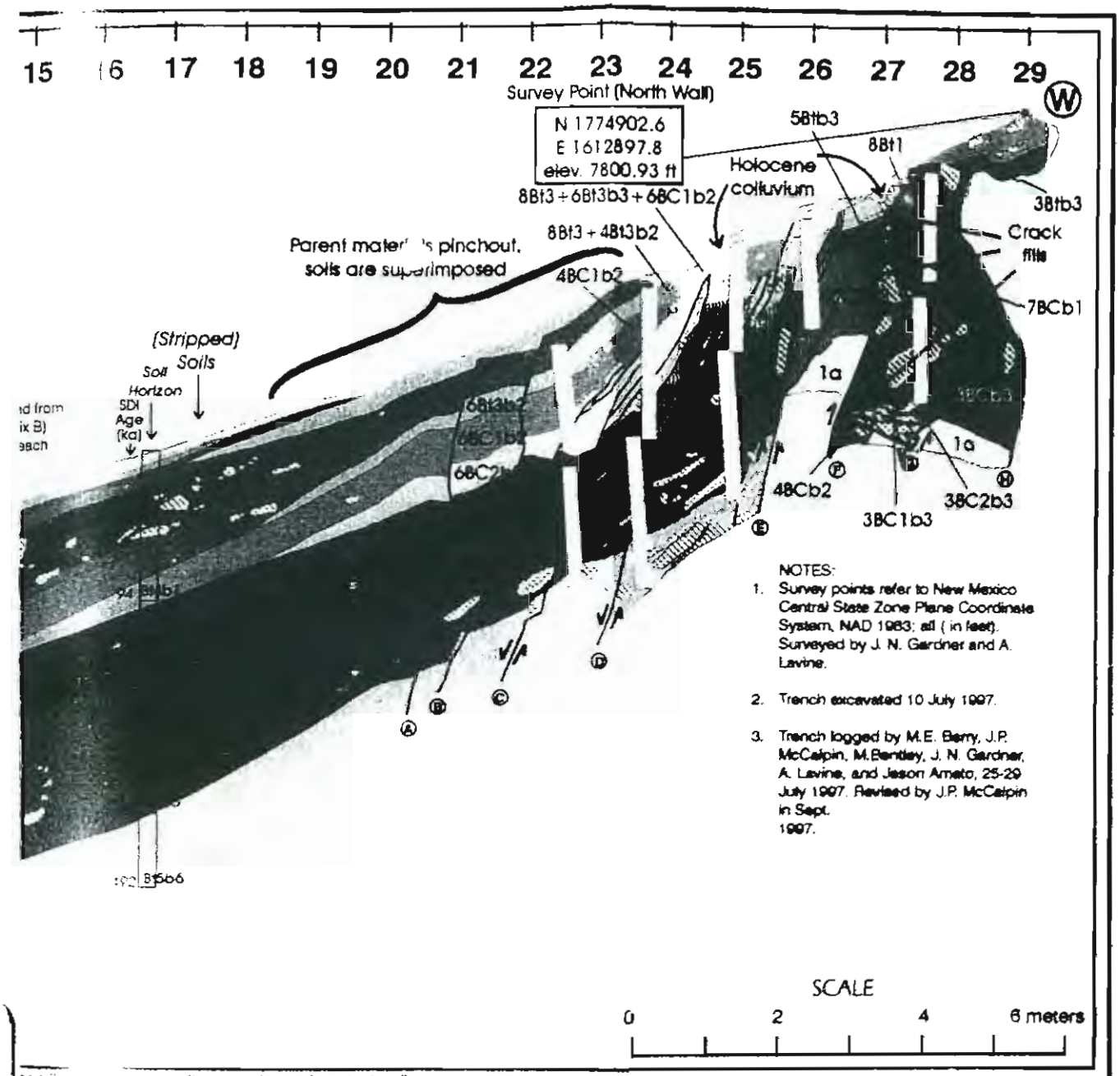

...otes the number of buried soil;
...after Soil Survey Staff (1975)

1BC2	BC1 horizon of buried soil 2 developed on parent material 4
1Bt2	BC2 horizon of buried soil 2 developed on parent material 4
2Bt3	Bt horizon of buried soil 3 developed on parent material 3.
2BC3	BC horizon (buried soil 3 developed on parent material 3)
2BC1b3	BC1 horizon (buried soil 3 developed on parent material 3)
2BC2b3	BC2 horizon (buried soil 3 developed on parent material 3)
3Btb5	Bt horizon on debris facies colluvium- buried soil 5
2Btb6	Bt horizon on debris facies colluvium- buried soil 6
1b	Clasts of white tuff
1a	Hard white tuff

GEO-HAZ Consulting, Inc.

PAJARITO FAULT, TRANSECT OF 7 TRENCHES, SUMMER 1997
LOS ALAMOS, NEW MEXICO

TRENCH 5-South Wall

DATE MAY 1998	FIGURE 25
DWG. NO. C:\GEOHAZ\LANL\LAMOS\TRENCH5.CDR	

As occurred in Trench 4, the 8 colluvial soils do not interfinger clearly with the fissure fill units at the head of the trench. The fissure fills are all upslope of a prominent fault-bounded pillar of tuff in the trench floor at 26 - 27 m H. We distinguished three relative ages of fissure fills based on cross-cutting relationships. The lowest fill (unit 3BCb3) occupies the very head of the trench beneath the tuff overhang. A younger fill (unit 4BCb2) bounds the eastern side of the "pocket" between the tuff pillar and the tuff overhang at the head of the trench. The youngest fill (unit 7BCb1) is a downward-tapering wedge overlain by colluvium bearing a Bt horizon of the modern surface soil (unit 8Bt1). All these fissure fill units are pre-Holocene.

Holocene deposits constitute an extremely thin (5 - 10 cm) surface layer on the scarp and are all contained in the A horizon of the surface soil (unit 9a). This thin layer pinches out on the scarp between 18 - 22 m H, as the slope steepens near the fault zone. However, the colluvium reappears with a thickness of up to 15 - 20 cm above the fault zone. The coincidence of this deposit with the fault zone, and the sharp downslope contact of the colluvium with older soils, suggests that a graben formed at the ground surface and trapped sediments moving downslope.

3.6.2 Structure

The downslope 2/3 of Trench 5 is composed of an east-dipping sequence of six buried soils, the horizons of which generally parallel the ground surface. Two exceptions are from 2 - 5 m H, where horizons 6Bt1b2 through 5BCb3 (buried soils 2and 3) flatten to nearly horizontal, and from 18 - 23 m H, where buried soils 1 and 2 converge with the ground surface. The break in dip for buried soils 2 and 3 may occur where the toe of the fault scarp was at that time. The toe of the modern scarp has prograded farther eastward, due to the deposition of units 7BCb1 through 9A. The convergence of buried soils 1 and 2 with the ground surface evidently results from the scarp surface being regraded to a lower angle than their dip from 18 - 23 m H. Part of the reason for the anomalously steep dips of horizons 6Bt2b2 through 7BCb1 is the existance of wedge-shaped units 6BC1b2, 6BC2b2, and 6BC3b2 which pinch out downslope at 14 m H, 18 m H, and 18 m H, respectively. These horizons are probably formed on a proximal colluvial wedge, the distal (wash facies) counterparts of which are the parent material for horizons 6Bt2b2 and 6Bt1b2. These latter two horizons have the reddest color and strongest prismatic structure of all horizons in the trench and are possibly correlative with the strongest soil (informally termed "Big Red") observed by Wong et al (1995) in the Water Tanks trenches. Unit 6 (buried soil 1) is overlain by the most prominent stone line in the trench, suggesting colluviation from tuff free faces upslope.

The fault zone in Trench 5 is composed of eight east-dipping normal faults between 20 m and 29 m H. Fault traces were recognized first by anomalously steep dips of clasts in the proximal colluvium, and alignment of those clasts (Fig. 26). A second criterion is

small offsets in soil horizons, but in many cases the horizon boundaries are so vague and the offsets so small, that applying these criteria becomes extremely subjective.

Faults A and B displace the soil horizons only a few cm up to the west, but faults C and D uplift unit 6BC2b2 and lower units from 2 m below the surface to only 30 cm below the surface, where the units are now affected by the modern surface soil. Fault E uplifts these units nearly to the ground surface. All the soil horizons overlying unit 6BC2b2 (11 horizons which reach an aggregate thickness of 2.5 m near the foot of the trench) were either never deposited upslope of fault C, or they have been uplifted and eroded.

Faults E and F bound either side of a pillar of hard white tuff that sticks up 1.5 - 2.2 m from the trench floor. Fault E has the best-developed shear fabric and fault gouge of any fault in the trench. In contrast, fault F may be primarily a tensional structure that comprises the eastern boundary of a deep "pocket" of colluvium at the head of the trench. The lack of well-defined soil horizons that dip downslope, and the random orientation of clasts, suggest that all the material west of fault F is fissure fill. At the bottom of this pocket in-situ (?) tuff is offset ca. 40 cm by fault G. Fault H forms the eastern boundary of the overhanging wall of tuff that makes up the head of the trench. There were no orientated clasts or shear fabric near this fault. That fact, and the curving irregular shape of the tuff/fissure fill contact, suggest that this structure has accommodated both extensional and shearing movement, possibly along a pre-existing joint surface, like the main faults in Trenches 3 and 4.

3.6.3 Geochronology

The thin Holocene deposits in Trench 5 yielded no charcoal, and TL dating was impractical due to the lack of fine slopewash parent materials that were relatively unaffected by B horizon pedogenic processes. Therefore, the only age control in Trench 5 is SDI-based age estimates. Eric McDonald measured detailed vertical soil profiles at 6.2 mH and 16 mH (Appendix B). At 6.2 mH he defined 3 soils (14 soil horizons) in the upper 3.2 m, compared to our 3 soils (11 horizons). At 16 mH he defined 7 soils (29 soil horizons) compared to our 7 soils (15 horizons). Thus, many of the soil horizons defined by McDonald were too vague to be traced continuously across the trench wall, but the major soils themselves were mapped by us.

Fig. 26. Photograph of fault E in the fault zone of Trench 5. The large pillar of tuff in the floor of the trench is barely visible at bottom center. Note steep clast orientations in trench wall.

At 6.2 mH the SDI age estimates are 83 ka at the bottom of unit 7BCb1 (i.e., the surface soil plus buried soil 1) and 184 ka at the bottom of unit 5BCb3 (the surface soil plus the top three buried soils). At 16 mH, the bottom of buried soil 1 dates at 25 ka, the base of buried soil 2 at 91 ka, base of buried soil 3 at 177 ka, base of buried soil 4 at 238 ka, base of buried soil 5 at 362 ka, and the lowest exposed part of buried soil 6 at 492 ka. SDI age estimates for the base of buried soil 3 are similar in both locations (184 ka vs. 177 ka). However, the base of buried soil 1 dates at 83 ka at the toe of the scarp, and only 25 ka 10 m farther up the scarp. Most of this age difference is attributed to stripping of the upper two soils upslope of 15 mH, and/or redeposition of stripped material at the scarp toe. For example, the thickness of the surface soil plus buried soil 1 is 1.97 m at 6.2 mH, whereas it has thinned to 1.06 m at 16 mH. In his first report (McDonald, 1997, p.2) McDonald suggested that the SDI age calculated at 6.2 mH was more "correct" than the one calculated at 16 mH since the latter site had been stripped, and that the difference in age (83 - 25 ka, or 58 ka) should be added to all the SDI ages in the 16 mH profile to account for the missing soil thickness. In more recent discussions McDonald (pers. comm., 1998) has stated that the SDI ages at 6.2 mH may be too old, due to depositional thickening of the profile and redeposition of pre-weathered material at the scarp footslope. Previous work on soil catenas of other fault scarps (e.g. McCalpin and Berry, 1996) showed that the SDI values of footslope soils could be 35% or more higher than that of identical-age soils on stable geomorphic surfaces (see also McCalpin, 1996, Ch. 3). So, the key question is whether the LANL PDI chronofunction developed by McDonald (Appendix B) is mainly based on soils from stable geomorphic surfaces, or from footslopes. If the former, then it is possible that SDI values at 6.2 mH are 35% or more larger then they would have been, had the soil developed on a stable geomorphic surface. In this case, the surface soil plus first buried soil would have a cumulative SDI = 65% of 79, or 51.3 if it had developed on a stable surface, which is equivalent to an SDI age of 45 ka. Note that this age is still 20 ka older than the SDI-based age of those same soils at the stripped profile at 16 m H.

Given the age differences between the upper two soils, it is surprising that the cumulative ages of the upper four soils at 6.2 mH (184 ka) and 16 mH (177 ka) are so similar (the upslope age total is actually younger). Why aren't these soils at 16 mH at least 23 ka older than those at 6.2 mH? There are two possible reasons. The first is that the difference merely represnts random, stochastic spatial variability in soil properties. The second reason may be the presence of the weakly-developed horizon 6BC1b2 at the 16 mH transect, which pinches out at ca. 13 m H. Horizon 6BC1b2 is developed of the toe of a proximal colluvial wedge that is replaced by finer wash facies colluvium by 6.2 mH. Due to the coarser grain size of parent material at 16 mH, soil structure is not as well developed as in horizon 6Bt2b2, which is developed on wash-facies colluvium. A secondary factor is the anomalous thinning of horizon 5Btb3 at 6.2 mH.

As at Trench 3, these SDI age estimates are only accurate if there has been no significant erosion in the colluvial section. We can recognize the effects of local erosion of soils at 15 - 22 mH from the thinning and pinching out of horizons such as 7BCb1 and 8Bt3. However, if the colluvial surface was at some time eroded down parallel to soil horizon boundaries, such erosion would be difficult to detect. There is no easy way to check the reliability of the SDI age estimates, since no TL ages were obtained, and neither the El Cajete pumice nor the ca. 1 Ma pumice seen in Trench 3 are present in Trench 5. The basal SDI age (492 ka) accounts for less than half of post-Bandelier Tuff time. However, the seismic refraction profile (Fig. 6) suggests that the top of tuff may be 8.5 m below the surface here, whereas the 492 ka age is only 6.2 m below the surface, so there may be another 2 - 2.5 m of sediments and soils beneath the bottom of Trench 5.

3.6.4 Paleoseismic Interpretation

At least two faulting events are suggested by stratigraphic units. The later event (Y_5) led to deposition of the large rubble clasts that lie atop buried soil 2. Faults A and B clearly displace buried soil 2, and may extend upward into the surface soil, but cannot be traced upward due to the high clay content and shrink- swell behavior in that soil. An earlier event is required by the colluvial wedge- shaped deposit that horizons 6Bt3b2, 6BC1b2 and 6B2b2 are developed in. This faulting event would have post- dated buried soil 3 and pre-dated development of buried soil 2.

No other stone lines or colluvial wedges are evident in Trench 5. However, the fissure fill at the head of the trench can be roughly divided into three relative- age units, all of which are older than the Bt horizon of the modern surface soil. The youngest fissure cuts buried soil 2 and thus may be contemporaneous with event Y_5. The intermediate fissure carries a soil similar to buried soil 3, suggesting that the event predates buried soil 3 and thus must be older than event X_5, which postdates buried soil 3. The oldest fissure fill represents an even older event (W_5) which cannot be related to buried soils 4-6 because it is not in contact with them.

There is indirect evidence for a young event (Z_5). The first line of evidence is an abnormally thick deposit of Holocene colluvium (i.e., colluvium without B horizon development) between 24- 27 mH. The abrupt downslope limit of this colluvium appears to be a buried uphill- facing free face above a splay fault coming off of fault C. In the absence of a tectonic cause, it is difficult to explain how this pocket of thickened colluvium came to form high on the scarp profile.

A second line of evidence is the pinchout of buried soil 1 and the Bt horizons of the surface soil between 18- 21 mH. Clearly this part of the scarp profile has been regraded to a lower slope angle since the formation of these soils. The trench log shows that the B horizons of the modern surface soil dip less steeply than horizons of buried soil 1, but they themselves are truncated by the Holocene colluvium of units 9A and EB. This type of angular unconformity in soils suggests that buried soil 1 was warped, then eroded, after

which the parent material of unit 8 was deposited across it. Later, unit 8 was warped, then eroded, and unit 9 was deposited across 8 in angular unconformity. This scenario requires two warping events younger than unit 7, ($Z_{5\text{-}1}$ and $Z_{5\text{-}2}$), the later of which would presumably be equivalent to the event creating the depression which Holocene colluvium filled between 24- 27 mH.

In summary, four or five displacement events can be inferred from angular unconformities, stone lines, and fissure fills in Trench 5. If every buried soil represents a faulting event (rather than a climatic response), there have been seven such events in 492 ka. The latest 3 to 4 events ($Z_{5\text{-}1}$, $Z_{5\text{-}2}$, Y_5, X_5) that post- date buried soil 3 have evidently occurred in the past ca. 177-184 ka (the SDI age for buried soil 3). By comparison, the retrodeformation sequence of Trench 3 on the opposite side of the graben requires six events (two of which had negligible net vertical displacement) in the past 110 ka. It seems reasonable that the main scarp (Trench 5) should record as many displacement events as the antithetic scarp (Trench 3), so we may have missed evidence of several events in Trench 5. For example, small- displacement events may not have formed stone lines because no free faces in tuff were created. Or, small- displacement events may have created only small fissures that were engulfed by later larger fissures and made unrecognizable.

3.7 Trench 6

Trench 6 is located between elevations 7887 ft and 7906 ft on the upper face of the main scarp of the Pajarito fault (Figs. 4 and 27). At this location, about 5m below the crest of the scarp, an old dirt road traverses the scarp face along a sloping bench that separates subhorizontal Bandelier Tuff (to the west) from tuff dipping 25 - 35 degrees east. The absence of tuff outcrops on this bench and the divergence of tuff dips on either side initially suggested that the bench overlay the crestal tension fissure. Excavation of the 16 m-long, 7.3 m-deep Trench 6 confirmed this supposition. The lower half of the trench was unknowingly cut in Bandelier Tuff which was so soft and shattered that it was initially assumed to be fissure fill. Later logging showed that the true fissure fill occupies only the upslope half of the trench (Fig. 28).

3.7.1 Stratigraphy

Although much of Trench 6 was excavated through Bandelier Tuff, the character of the tuff is quite different than in other trenches. The hard white or gray welded tuff (unit 1a in this and other trenches) is encountered only on the upslope wall of the trench. The backhoe scraped along the hard wall of the tuff/unconsolidated deposit contact from the head of the trench to the floor at 13 m H. Only a small area of unit 1a was cut into deeply enough to portray on the trench headwall. Most clasts in the colluvium are composed of hard gray tuff (unit 1a), hard white tuff (unit 1b), or softer weathered tuff (unit 1c).

Downslope of the large filled tension fissure the Bandelier Tuff has been highly shattered and brecciated (unit 1d). The broken tuff blocks resemble the hard white tuff, but fracture spacing is typically 10 - 15 cm here, as opposed to >50 cm in unit 1a. The upper part of the rubbilized tuff is a pale tan color and resembles a well-bedded sandstone (unit 1e), so is presumably a surge bed. Overlying this well-bedded unit is a more massive, yellow, moderately soft tuff (unit 1f) 15 - 20 cm thick.

The tuff layers of unit 1d, 1e, and 1f, are overlain by a distinctive set of fine-grained (very fine sand to silt) volcanic ashes. The lowest ash (unit 2a) is the same yellow color as the underlying but coarser-grained tuff and is 20 - 25 m thick. Next is a white ash 10 - 12 cm thick, overlain by a pink ash 10 - 12 cm thick. This set of fine ashes can be traced more-or-less continuously from the toe of the trench to the point where the top of the tuff goes below the trench floor at 12 mH.

Unconsolidated deposits in Trench 6 fall into three general catagories: (1) relatively thin colluvium and fissure fills in the downslope half of the trench, and in the huge crestal tension fissure; (2) fine-grained fissure fill with superimposed soils; and (3) coarser fissure fill and colluvial wedges. Because all unconsolidated deposits in Trench 6 are strongly affected by soil formation, we defined and labeled the mapping units based on soil horizon properties and nomenclature, as we did in Trench 5. The thickest soil-stratigraphic record (7.3 m thick) is found in the crestal tension fissure. The basal 1.5 - 2

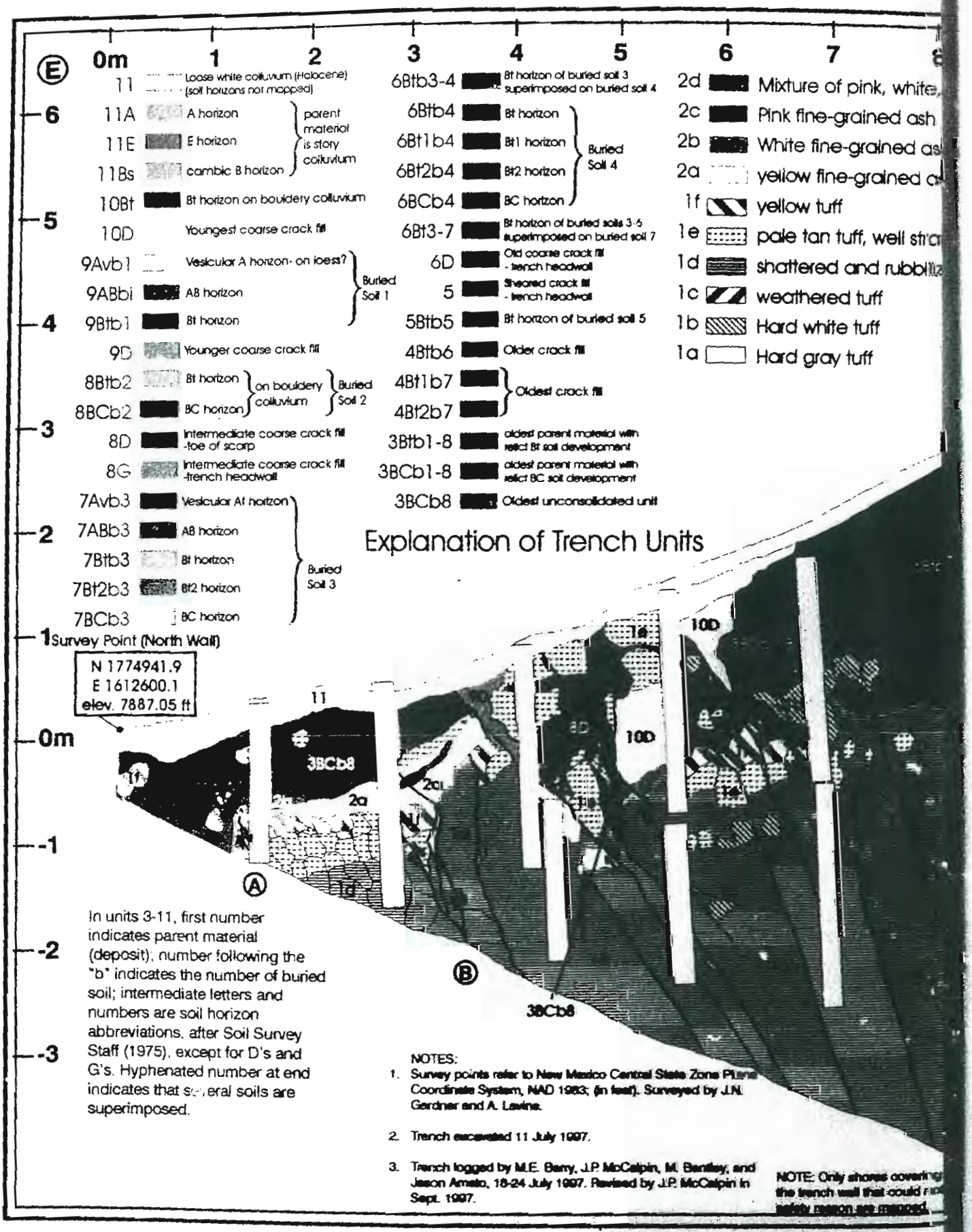
Explanation of Trench Units
0m
1
2
3
4
5
6
7
E
11 Loose white colluvium (Holocene) (soil horizons not mapped)
11A A horizon
11E E horizon
11Bs cambic B horizon
parent material is story colluvium
10Bt Bt horizon on bouldery colluvium
10D Youngest coarse crack fill
9Avb1 Vesicular A horizon- on loess?
9ABbi AB horizon
9Btb1 Bt horizon
Buried Soil 1
9D Younger coarse crack fill
8Btb2 Bt horizon
8BCb2 BC horizon
on bouldery colluvium
Buried Soil 2
8D Intermediate coarse crack fill -toe of scarp
8G Intermediate coarse crack fill -trench headwall
7Avb3 Vesicular At horizon
7ABb3 AB horizon
7Btb3 Bt horizon
7Bt2b3 Bt2 horizon
7BCb3 BC horizon
Buried Soil 3
Survey Point (North Wall)
N 1774941.9
E 1612600.1
elev. 7887.05 ft
6Btb3-4 Bt horizon of buried soil 3 superimposed on buried soil 4
6Btb4 Bt horizon
6Bt1b4 Bt1 horizon
6Bt2b4 Bt2 horizon
6BCb4 BC horizon
Buried Soil 4
6Bt3-7 Bt horizon of buried soils 3-6 superimposed on buried soil 7
6D Old coarse crack fill - trench headwall
5 Sheared crack fill - trench headwall
5Btb5 Bt horizon of buried soil 5
4Btb6 Older crack fill
4Bt1b7
4Bt2b7
Oldest crack fill
3Btb1-8 oldest parent material with relict Bt soil development
3BCb1-8 oldest parent material with relict BC soil development
3BCb8 Oldest unconsolidated unit
2d Mixture of pink, white,
2c Pink fine-grained ash
2b White fine-grained as
2a yellow fine-grained a
1f yellow tuff
1e pale tan tuff, well stra
1d shattered and rubbiliz
1c weathered tuff
1b Hard white tuff
1a Hard gray tuff
6
5
4
3
2
1
0m
-1
-2
-3
11
3BCb8
2a
10D
8D
A
B
In units 3-11, first number indicates parent material (deposit); number following the "b" indicates the number of buried soil; intermediate letters and numbers are soil horizon abbreviations, after Soil Survey Staff (1975), except for D's and G's. Hyphenated number at end indicates that several soils are superimposed.
NOTES:
1. Survey points refer to New Mexico Central State Zone Plane Coordinate System, NAD 1983; (in feet). Surveyed by J.N. Gardner and A. Lavine.
2. Trench excavated 11 July 1997.
3. Trench logged by M.E. Barry, J.P. McCalpin, M. Bentley, and Jason Amato, 18-24 July 1997. Revised by J.P. McCalpin in Sept. 1997.
NOTE: Only shows covering the trench wall that could safely person see mapped.

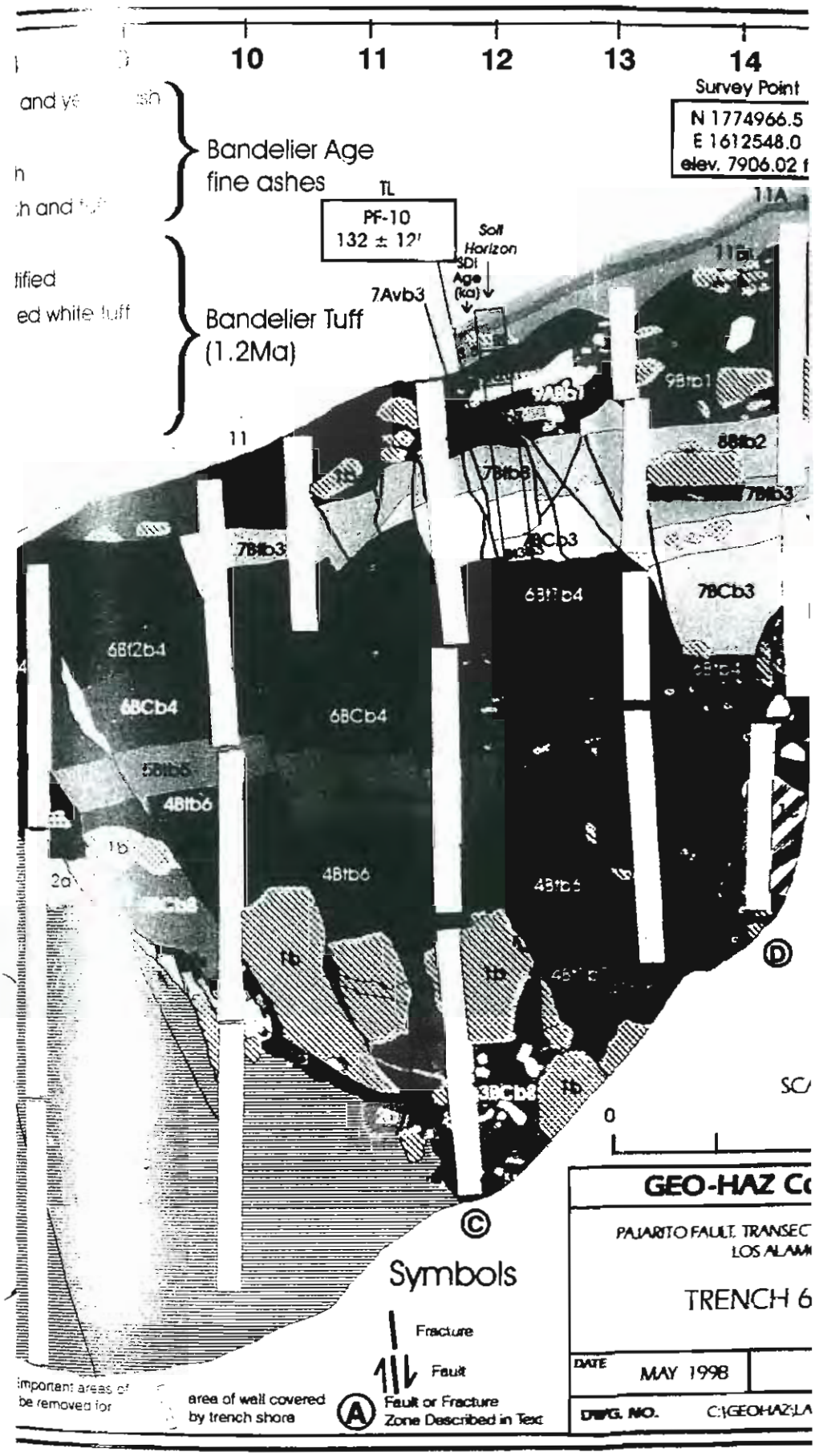
10
11
12
13
14
Survey Point
N 1774966.5
E 1612548.0
elev. 7906.02 f
Bandelier Age
fine ashes
Bandelier Tuff
(1.2Ma)
TL
PF-10
132 ± 12'
Soil
Horizon
SDI
Age
(ka)
7Avb3
11A
11B
9Bfb1
9ABt1
8Bfb2
7Bfb3
7BCb3
6Bf2b4
6BCb4
5Bfb5
4Bfb6
3BCb3
Fb
11
Symbols
Fracture
Fault
Important areas of
be removed for
area of wall covered
by trench shore
Fault or Fracture
Zone Described in Text
GEO-HAZ C
PAJARITO FAULT TRANSEC
LOS ALAM
TRENCH 6
DATE
MAY 1998
DWG. NO.
C:\GEOHAZ\LA

m of this fissure is filled with small blocks of unit 2 (often recognizably lying sideways or upside-down) and large blocks of white tuff in a matrix of hard orange sandy silt. Most of these clasts (even ones >1 m in size) are so weathered that the backhoe cut cleanly through them rather than plucking them from the walls. Above this relatively coarse-grained unit (3BCb8, i.e. parent soil horizon BC/ of the 8th buried soil below the surface soil) deposits and soils contain few clasts larger than 1 - 2 cm. The buried soils developed in the relatively clast-free fissure fill were identified from slight changes in soil color, consistence, or structure, based on hacking at the wall with hammers, knives, and picks and plucking out peds. At times the identification was quite subjective, and perhaps different workers might have identified a different grouping of soils. The vague soil horizon boundaries were difficult to trace laterally because subsidiary step faults kept displacing the east-dipping contacts up to the east. This ambiguity in contacts was particularly problematic in the lower half of the trench where the light was dim.

Difficulties notwithstanding, we identified 8 buried soils and the surface soil and were able to trace their boundaries across the width of the crestal tension fissure. The surface soil and uppermost buried soil (b1) are developed on a cobble-rich colluvial wedge and crack fill deposit that are much coarser-grained than underlying deposits. The colluvial wedge has a "heel" of fissure fill facies up against the fault zone (unit 9Btb1), such that the coarse deposit has a cross-section like a high-heeled shoe. Deposits beneath this "heel" also contain a high concentration of tuff clasts and are presumably older fissure fills similar to the youngest one. The boundary between material that fell into an open fissure, and material that was deposited on a colluvial slope is hard to pinpoint, but it is probably around fault D.

The downslope half of the trench contains colluvium and fissure fill 1 - 1.5 m thick that is coarser-grained and has a slightly denser and redder soil matrix than deposits at equivalent depth in the crestal tension fissure. We interpret these deposits as correlatives to the coarse colluvial units at the base of the crestal tension fissure (parent material 3). This early, coarse slope colluvium was beheaded from its source area (the upslope face of the tension fissure) by development of the fissure itself, and by normal slip movement on fault C. Because this colluvium was never buried like its counterparts in the crestal tension fissure, it has been within the pedogenic effect zone of the surface soil ever since deposition (i.e., it is a relict soil). Thus, the effects of soil formation that are spread out over 7.3 m of stratigraphic thickness in the deepest part of the crestal tension fissure are telescoped into only 1 -1.5 m of stratigraphic thickness at 2-3 mH. To signify that this is old parent material (3) affected by a long history of soil formation (equivalent to buried soils 1 - 8 in the fissure) we label this colluvium 3BCb1-8.

The old colluvium is disrupted by several younger fissure fills that lie above faults (units 8D, 9D, 10D). All three of these fissure fills have the Bt horizon of the surface soil developed across their tops, indicating that they are all pre-Holocene. All we know for certain is that these fissures are younger than unit 3 and older than unit 11, but we cannot

bracket ages any more closely because the fills are not in physical contact with the tension fissure soils b1 - b7.

3.7.2 Structure

The dominant structures in Trench 6 are west-dipping normal faults that displace both tuff and unconsolidated deposits. These faults represent a "domino" style of faulting that affects the entire trench except the westernmost 2 m. Fig. 29 shows a schematic representation of how this domino-style extension works with the concept of a crestal tension fissure. The "Back wall" of the crestal tension fissure (i.e., its western margin) is the breakaway plane between the stable subhorizontal tuff to the west of the fault scarp, and the east-tilted slab of tuff that comprises the monocline and the scarp face. In our model the stable tuff block does not move and the "back wall" maintains its steep (70-75 degree) dip between all faulting events. With every faulting event the block at the base of the main fault scarp (below Trench 5) drops relatively down, the slab underlying the scarp face tilts incrementally more steeply eastward, and the crestal tension fissure opens by another increment of width. However, if this were the only process acting we would see only a large V-shaped tension fissure in Trench 6 and no other faults.

The pervasive faulting in Trench 6 indicates that the upslope end of the east-tilted megaslab is splintering into separate blocks on a spacing of 0.5-1 m. These blocks are accommodating east-west extension by rotating counterclockwise (viewed to the south) along their bounding faults, like a series of toppling dominos. This domino-style of faulting has continued to operate as colluvium and crack fill have been deposited here, as evidenced by the domino faults that displace all unconsolidated units. This rather unique deformation mechanism creates the unusual situation where down-to-the-east normal faulting at depth is expressed near the surface as a local zone of down-to-the-west faults.

During surface faulting the down-to-the-west domino faults evidently create small scarplets that face upslope on the scarp face. This style of geomorphic expression creates small "backstops" that disrupt the normal downslope transport of colluvium on the scarp face. As a result, colluvial deposits higher on the scarp tend to terminate against one of these backstops, instead of continuing to thicken downslope as on a normal fault scarp. For example, the bouldery colluvial wedge of units 10Bt and 9Btb1 lies only beneath the upper half of the scarp and pinches out at mid-scarp. This is the opposite geometry to a typical colluvial wedge, which only underlies the lower half of a fault scarp and pinches out at the toe.

In addition to domino-style faulting, some faults must have an additional component of dip-slip movement beyond that induced by mere rotation. For example, fault C bounds the eastern edge of the crestal tension fissure but has 4.5 m of net dip slip, more than required by rotation. Actually fault C is a complex zone composed of individual normal faults that dip more steeply than the zone itself. These smaller faults progressively step unit 2 down to the west until the unit disappears beneath the trench floor. So, fault C is evidently

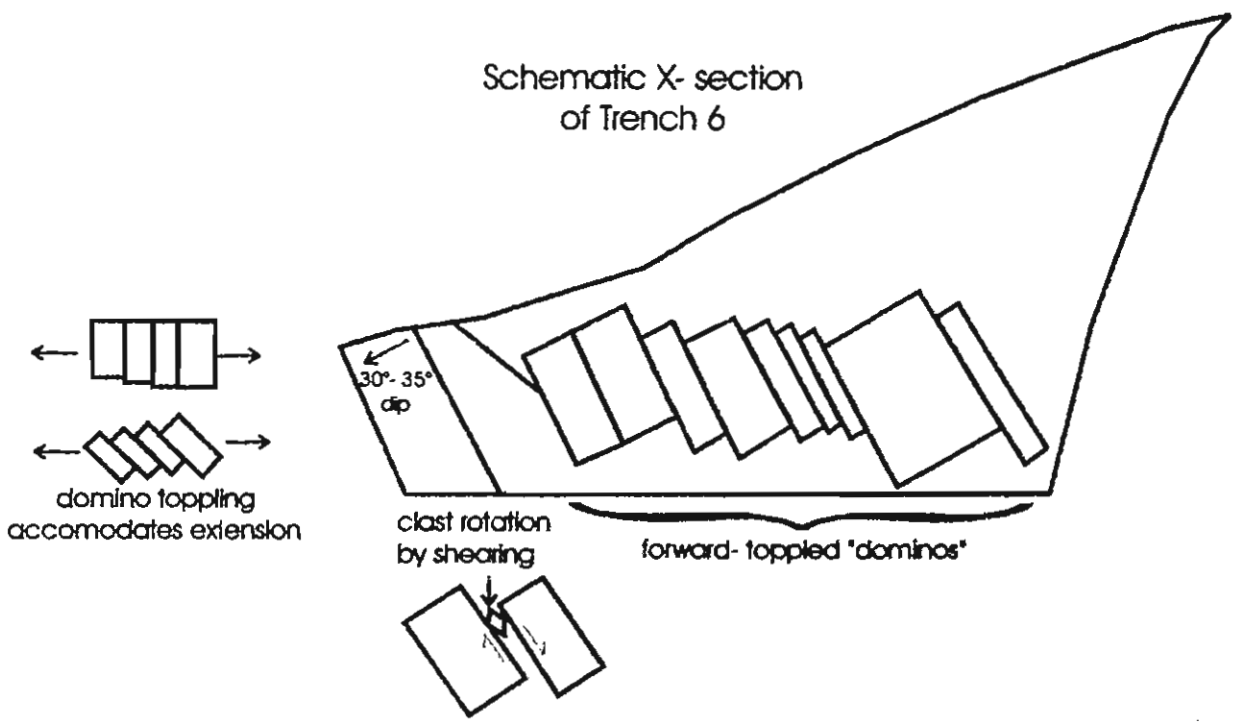

Fig. 29. Schematic diagram showing how domino-style faulting affects the downthrown block in Trench 6.

functioning both as a fissure boundary, a domino fault, and a normal fault.

The bouldery colluvial wedge of units 10Bt and 9Btb1 appears to have been derived from a fault free face in tuff that must have been at least as high as the thickness of the unit (2 m). Creating a free face this high would not occur as a normal consequence of merely tilting the megaslab forward by a few degrees. So, there must be occasions when there is dip-slip movement along the back wall of the tension fissure (fault D).

Finally, fault D is steeper than the domino-style faults to the east and does not appear to be favorably oriented to accommodate rotational movement. Instead, the fault separates coarser crack-fill facies (to the west) from finer fissure fill soils. The part of the crestal tension fissure between faults D and E thus resembles a steep-sided graben where the "heel" of the fissure fill is dropping down nearly vertically. The western part of this fault-bounded sliver is composed of angular blocks of tuff and pockets of stratified inwash, suggesting gravity fall of clasts into an open fissure. In contrast, most of the sediments east of fault D resemble wash-facies colluvium at the base of a typical normal fault scarp.

3.7.3 Geochronology

Our age estimates for deposition in trench 6 are based on one TL sample and the SDI age estimates (Appendix B). No charcoal for C-14 dating eas found in Trench 6. A TL sample was collected from unit 7Avb3 yielded an age estimate of 132± 12 ka. This age is much older than the SDI age estimate of 25 ka for the same stratigraphic level. Cumulative SDI age estimates from the bottom of buried soil 6 to the surface yield an estimated age for that contact as 445 ka (range 375 - 529 ka). However, there are about 1.5 m of fissure fill sediments beneath the level of that age estimate, so the inception of fissure opening must be considerably older than 445 ka. The age-depth trend defined by an age estimate of 445 ka at a depth of 535 cm is 0.83 ka/cm. This rate includes deposition of parent material, hiatuses in deposition, soil formation, and some periods of limited erosion. Extrapolating this rate down an additional 1.5 m below the 445 ka-level yeilds an additional 125 ka, implying that the fissure may have begun to open at roughly 570 ka. It is interesting to note that the sedimentation rate derived from Trench 5 (492 ka in 623 cm, or 0.79 ka/cm) is very similar, even though the structural and sedimentological setting is quite different (Trench 5 is at the base of the main scarp, while Trench 6 is nearly at the crest, albeit also on a slope). If these SDI-based age estimates are correct, they imply that the displacement at Trenches 5 and 6 did not begin until 550 ka after the deposition of the Bandelier Tuff.

3.7.4 Paleoseismic Interpretation

A complete retrodeformation sequence for Trench 6 was not attempted, primarily because we do not have sufficient confidence in the soil contacts logged in the fine-grained fissure fill. Although we believe that the number of soils shown in any fault slice (domino) is approximately correct, the exact offset of soil boundaries across faults is

highly ambiguous. A retrodeformation sequence is required to respect the soil boundaries as mapped and to treat them as stratigraphic units, and we are not confident (due to the lack of stratigraphy in fissure fill parent material) that soil units are also stratigraphic units. One difficulty easily foreseen in the retrodeformation of faults displacing units 4 through 7 is that displacement of higher soils is somewhat greater than that of lower soils, and such a pattern cannot be replicated by retrodeformation. If the constant- displacement- with-depth pattern is in fact correct, it implies that most domino faults experience only a single, late episode of movement, which we feel is unlikely given the inferred mechanics of domino movement.

However, the latest two displacement events (Z_6 and Y_6) were followed by the deposition of bouldery scarp- derived colluvial wedges that form distinct stratigraphic units. Each of these events requires movement on the back-wall of the fissure (fault J) to expose fractured tuff in a free face, and domino- style movement on one or more faults to create a backstop to prevent colluvium from being deposited lower on the scarp. For example, the partial retrodeformation sequence (Fig. 30) shows that event Z_6 was accompanied by down- to- the west movement of fault blocks EF, FG, and GH. Deposition of bouldery colluvium stops just downslope of fault E, suggesting that the backstop was an upslope- facing scarp on fault E. A similar argument can be made for event Y_6, which produced a deep "pocket" into which colluvial unit 9 was deposited. Unit 9 thickens and becomes considerably coarser grained west of fault I, suggesting that a fault I free face formed the backstop for this wedge. Directly underlying this wedge is unit 8, the A horizon of which yielded a TL age of 132± 12 ka and an SDI age estimate of 25 ka. Unless we have overlooked evidence for smaller displacement events, there have been only two faulting events post- 25 to 132 ka. If each buried soil represents a response to a faulting event, there have been eight faulting events cince 1.2 Ma, assuming that there has been no significant erosion of the fissure fill. Generally, the crestal tension fissure would be considered a local depocenter which would either receive inwashing sediments, or if filled to the brim between fissuring events, sediments would merely wash over the fissure top or perhaps a soil would form. The only way that material could be eroded from a fissure fill is if a stream became diverted to flow along the fissure, and that stream had an outlet to carry away the eroded material. Such a stream could locally erode the fissure fill in one location and redeposit the sediments in a deeper location within the fissure. This redistribution of material could lead to an ncomplete stratigraphic record in parts of the fissure fill. However, we see no channels or other evidence of erosion in the fissure fill in Trench 6.

Assuming that the fissure record is complete and that each soil formed after a fissuring event, the SDI ages of soil tops are 4, 14, 25, 118, 250, 304, 404, and 445 ka. There is a discrepency between the SDI age estimate for buried soil 2 (25± 4 ka) and the TL age (132± 12 ka). One way to interpret this discrepency is that the TL age is correct and that considerable material has been eroded from above buried soil 2 at this location. However, our retrodeformation sequence shows that subsequent to the formation of buried soil 2 in Trench 6, two colluvia have been deposited in a tectonic depression caused by domino-

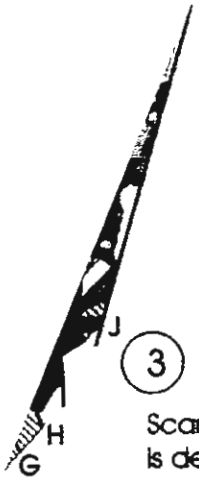

3

Scarp-derived bouldery colluvium
is deposited up against free face/
backstop formed by fault H

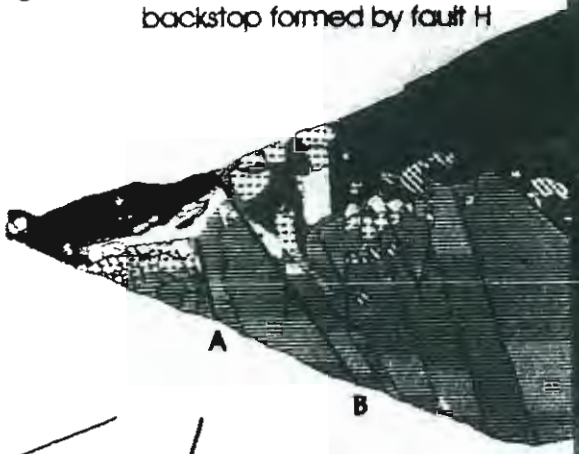

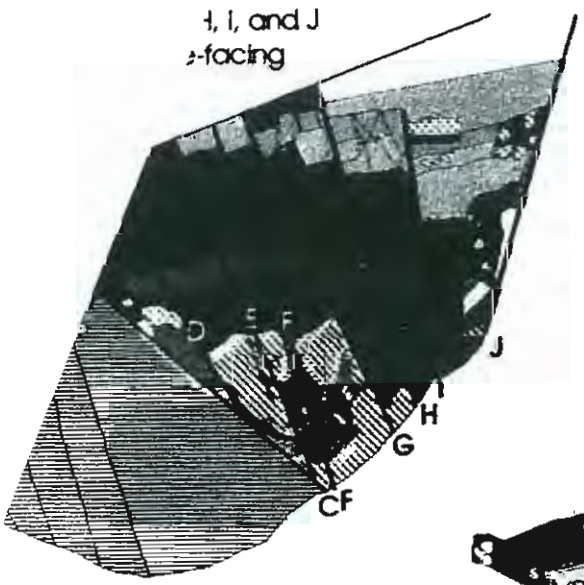

4

Faulting Event Z6; fau
to west; fissure forms
scarp face.

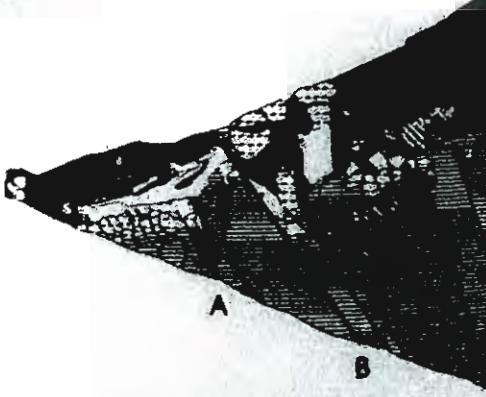

6

Holocene colluvium deposited as a thin blanket over scarp face; soil horizons A, E, and Bs form.

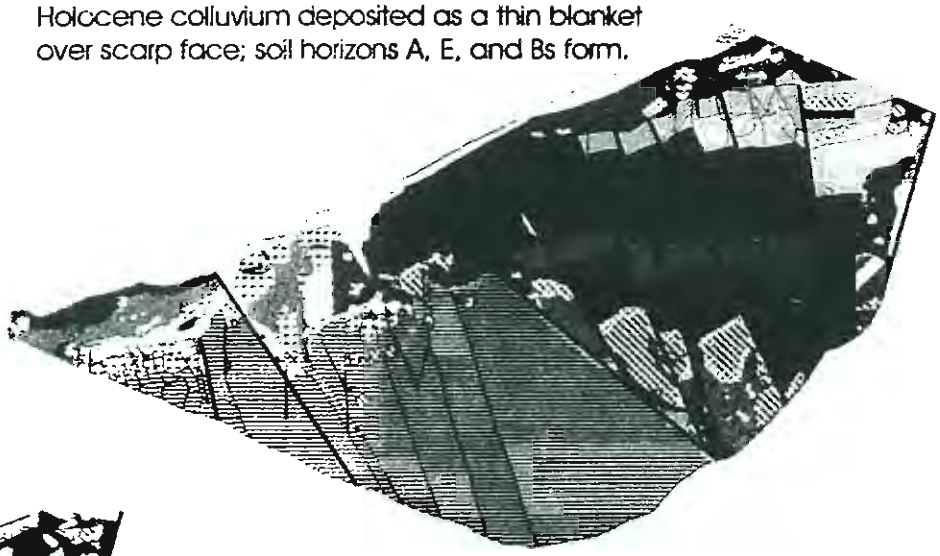

ts E slipdown
on

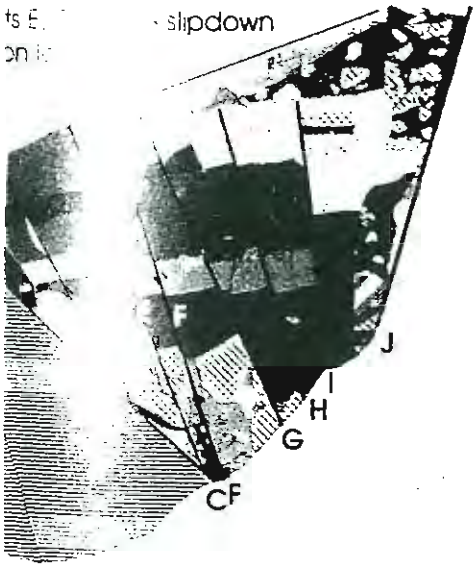

GEO-HAZ Consulting, Inc.

PAJARITO FAULT, TRANSECT OF 7 TRENCHES
LOS ALAMOS, NEW MEXICO

TRENCH 6 Retrodeformation- South Wall
[Latest Two Faulting Events Only]

DATE MAY 1998	FIGURE 30
DWG. NO. C:\GEOHAZ\LANL\ALAMOS\RETRO6.CDR	

style movement. Thus, the setting is not conducive to significant erosion, except on the tips of "back stop"- free faces that were overrun by the downslope edges of colluvial wedges.

Despite lack of positive evidence for erosion, the total SDI age of the fissure fill soils is only about 570 ka, compared to the 1.2 Ma age of the Bandelier Tuff. Therefore, either the SDI ages are correct and the crestal tension fissure did not begin to form until ca 570 ka, or the fissure began to form not too long after 1.2 Ma and the SDI ages are all underestimates by roughly a factor of 2.5. Our conceptual model for the articulated monocline requires that the crestal tension fissure begin to form as soon as significant vertical displacement accumulates. We do not know exactly when this displacement started, but the Trench 3 retrodeformation suggests that some faulting predates the 1.1 Ma Cerro del Medio- correlative ash and underlying sediments. Thus, we expect that the basal fissure fill should be on the order of 1 Ma rather than 570 ka, although the fill does not contain the 1.1 Ma ash or pumice exposed in Trench 3.

3.8 Trench 7

Trench 7 is located on a N-S-trending, west-facing scarp 200 m west of the crest of the main fault scarp (Figs. 4 and 31). This antithetic scarp is quite small (75 cm high), but the 16 m-long, 5 m-deep trench shows a much larger displacement in the subsurface (Fig. 32), as did the other west-facing sc: trenched (Trenches 3 and 4).

3.8.1 Geophysics

Seismic line 6 was located 2.5 m west of and parallel to the low (0.4 m-high) west-facing fault scarp. The north- source and south- source lines yield very different solutions. The north- source line shows a very thin (0.7 m) surface layer with low velocity (225 m/sec) overlying a higher- velocity layer (Vp= 681 m/sec). The south- source line shows a much thicker (2.7 m) low velocity zone (332 m/sec) overlying material with a velocity of 904 m/sec. Nelson (Appendix A) interpreted this pattern to represent a contact dipping south at 7 degrees. However, later excavation of Trench 7 revealed an intermediate step-fault block beneath the seismic line. Thus the 2.7 m-thick low velocity over high velocity solution matches the trench log west of the step- faulted block, suggesting that the south end of the line was underlain by 2.7 m of alluvium atop Bandelier Tuff. The north end of the line may have been underlain by the step- faulted block at a shallow depth, and the block may have narrowed or disappeared to the south.

3.8.2 Stratigraphy

The tuff and unconsolidated deposits exposed in Trench 7 bear some similarity to deposits observed in trenches 3 and 6. The Bandelier Tuff on the upthrown (eastern) block (unit 1a) is a hard white welded tuff with few fractures, and is thus similar to the hard white tuff mapped as unit 1a in Trenches 1 - 5. Unit 1b on the upthrown block is merely this same unit broken by tree throw and frost wedging near the surface. On the downthrown block the white tuff is considerably more fractured (unit 1d) than on the upthrown block, although not as badly rubbilized as unit 1d in Trench 6. This fractured white tuff is underlain by a fractured yellow (oxidized?) tuff in a fault-bounded block in the center of the trench.

Just as in Trench 6, the upper part of the white tuff on the downthrown block is a different color (tan here), is softer, and shows moderate subhorizontal stratification, all characteristics of surge beds. These surge beds are not present on either the intermediate fault block or the upthrown block, indicating they were either: (1) once present and subsequently stripped by erosion; or (2) they were deposited (buttressed) against a west-facing scarp and never existed on the intermediate fault block. I favor the former explanation, because unit 1e is visibly thinned by erosion beneath unit 2 even before it reaches the intermediate fault block. Overlying the surge beds is a sequence of fine-grained volcanic ashes (unit 2) remarkably similar to those observed in Trench 6. The basal ash (unit 2a) is pink, with overlying layers pink-white (unit 2c) and mottled orange and white (unit 2d). A slightly coarser but very thin tuff bed (unit 2e) overlies these fine ashes.

Fig. 31. Overview photograph of Trench 7, looking west from the head of the trench.

Fig. 33. Photograph of the main fault zone in Trench 7 (left center) where Holocene

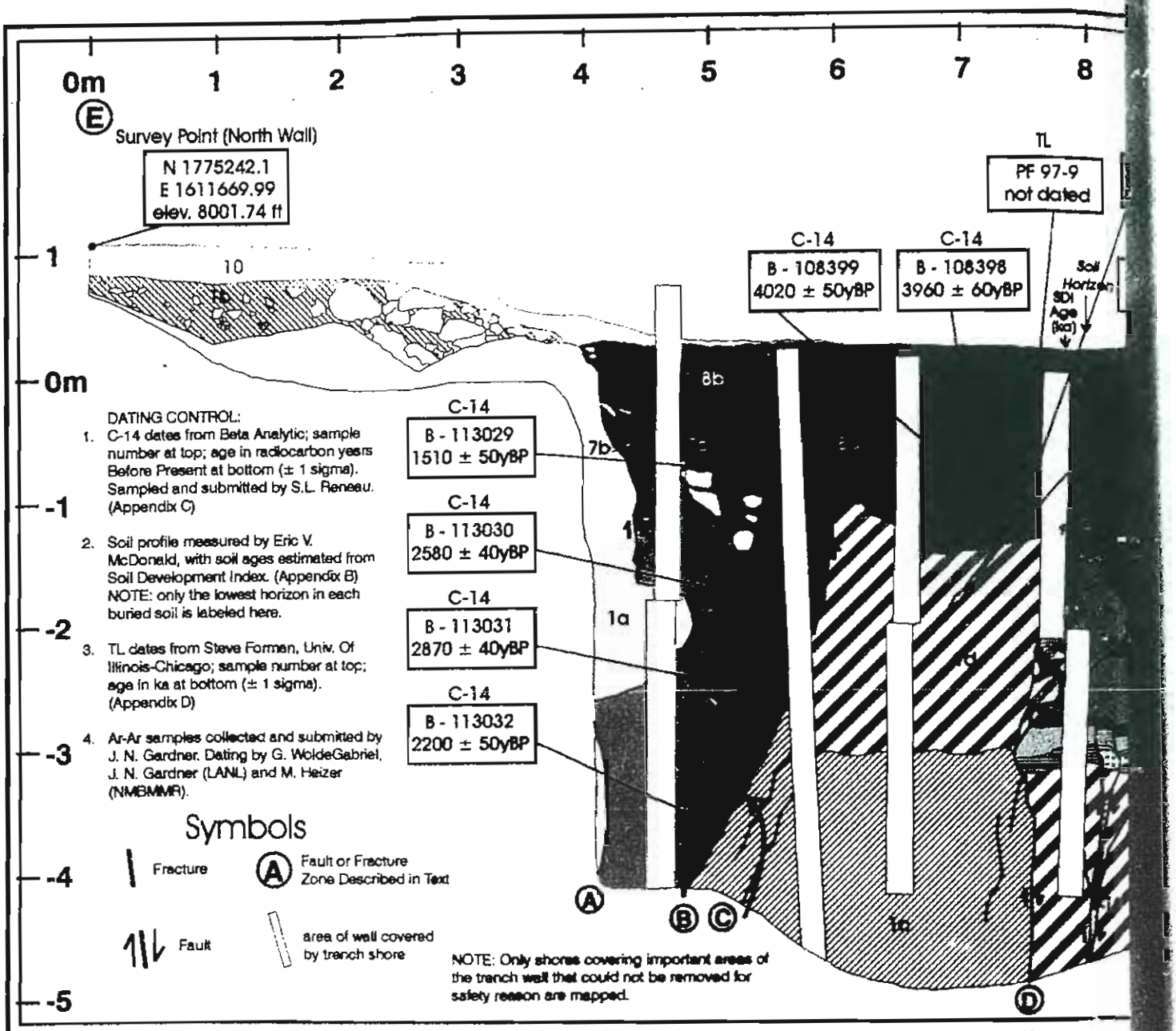

Explanation of Trench Units

- 10 Modern OA soil horizon
- 9 Laminated pale silt, historic?
- 8c Modern A horizon
- 8b Gray-brown soil AC horizon
- 8a Brown sandy silt, slopewash
- 7c Yellow-brown silty sand, gravel at base: W of 5.5mH, alluvium; E of 5.5mH, scarp-derived colluvium
- 7b Weak A horizon?
- 7a White tuffaceous colluvium
- 6 Tuff rubble with loose matrix and voids
- 5b Brecciated tuff with harder orange matrix
- 5a Crack fill
- 4c Red-brown sandy clay, Bt1 soil horizon
- 4b Red-brown gravelly sandy clay, Bt2 horizon
- 4a Red-brown sandy clay, Bt3 horizon
- 3b White clayey sand
- 3a Red-brown clayey sand, Bt horizon
- 2e Very weathered tuff
- 2d Mottled orange and white ash
- 2c Pink-white fine-grained ash
- 2b Red clay seam with angular clasts
- 2a Pink fine-grained ash
- 1g Pumice gravel
- 1f Tuff clasts in shear zones
- 1e Tan tuff

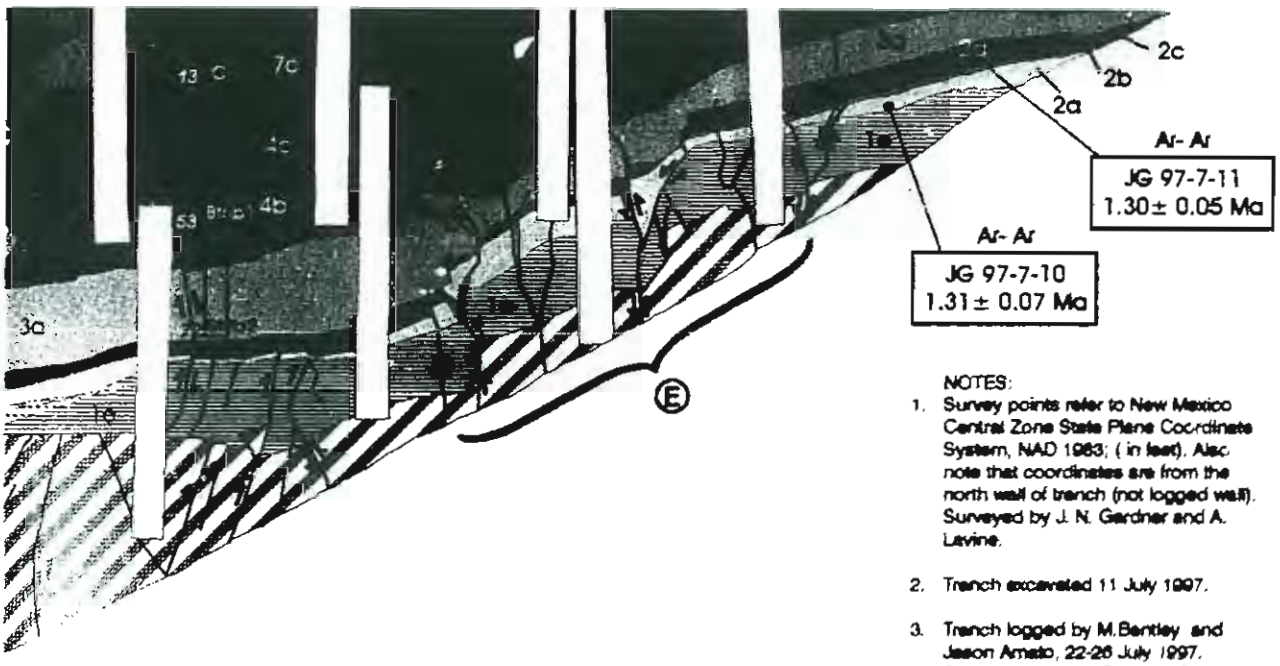

NOTES:

1. Survey points refer to New Mexico Central Zone State Plane Coordinate System, NAD 1983; (in feet). Also note that coordinates are from the north wall of trench (not logged wall). Surveyed by J. N. Gardner and A. Levine.
2. Trench excavated 11 July 1997.
3. Trench logged by M.Bentley and Jason Amato, 22-26 July 1997. Revised by J.P. McCalpin in Sept. 1997.

d [illegible] ctured white tuff
c [illegible] ctured yellow tuff
b [illegible] as and loose rubble in surface tuff
a [illegible] tact hard white tuff

SCALE

0 2 4 meters

GEO-HAZ Consulting, Inc.

PAJARITO FAULT TRANSECT OF 7 TRENCHES, SUMMER 1997
LOS ALAMOS, NEW MEXICO

TRENCH 7- South Wall

DATE	MAY 1998	FIGURE 32
DWG. NO.	C:\GEOHAZ\LANL\ALAMOS\TRENCH7.CDR	

Between the fine ashes and underlying tuffs there is one small channel of pumice gravel (unit 1g).

Overlying the fine ashes are relatively stone-free sandy and silty colluvium overprinted with Bt horizons, just as in Trench 6. Only two major soil-stratigraphic units can be defined, a lower one (unit 3) containing one thick Bt horizon, and an upper one (unit 4) in which three Bt horizons (4a, 4b, 4c) are developed. [Note: Our numbering system in Trench 7 is stratigraphically oriented (as in Trenches 1 - 4) rather than soil oriented (as in Trenches 5 and 6) because soil horizons comprise only four of the 10 defined units here].

At the main fault zone there are two fissure fill units, a larger one and a smaller one. The smaller (western) of these two units is a gravelly diamicton (unit 5b) with a matrix of compact, dense orange-brown silt. The color of the matrix suggests it was derived from Bt horizon material such as in units 3 and 4, and its compactness and density are more similar to those units than to others. The larger fissure fill (unit 6) abuts the main fault plane and is composed of loose angular clasts of hard white tuff with a very loose, pale, silty matrix. This matrix resembles the Holocene colluvium in Trenches 1 - 4 in consistency and color. This fissure also contains many large open voids, through which abundant tree roots penetrate.

Overlying the larger fissure fill near the main fault are two small deposits, the lower of which is a white gravelly silty sand (unit 7a) containing occasional clasts with a downslope (down to the west) fabric. This small deposit is probably scarp derived colluvium that prograded westward over the top of the filled fissure. The upper few cm of this deposit are slightly darker than the rest, as if there was an incipient soil A horizon (unit 7b) starting to develop.

The next four units cover the entire downthrown block and constitute the thickest sequence of Holocene deposits in any trench. The basal layer (unit 7c) is a yellow-brown silty sand, moderately compact, that contains small pebble gravel at its lowest basal contact. This unit is clearly eroded into underlying units, for example at 8 m H, and between 6.5 and 8 m H appears to form a stream channel that must have flowed nearly parallel to the fault scarp. The easternmost part of unit 7c (between 4 and 6 m H) has a similar color and grain size, but also contains clasts of Bandelier Tuff (unit 1a) with downslope fabric. This part of the unit may be partly debris-facies colluvium that interfingers with the alluvium near the base of the fault scarp.

Unit 8 composes the bulk of the Holocene section, with unit 8a being weakly oxidized parent material, unit 8b the soil AC horizon, and unit 8c the modern soil A horizon. Unit 8a is a massive brown sandy silt, the upper contact of which is horizontal, but the lower contact of which appears to be channeled into unit 7c between 5 and 8.5 m H.

The youngest stratigraphic unit on the downthrown block is unit 9, a thin lens of laminated pale silt with no evidence of soil formation. This deposit lies against the foot of

the fault scarp and probably represents historic slopewash, perhaps associated with disturbance of the surface when Ski Hill Road was built. On the upthrown block Bandelier Tuff is overlain by a peaty and rubbly OA soil horizon derived from the tuff.

3.8.3 Structure

Trench 7 contains two large fissures bounded by faults A, B, and C, an intermediate step- fault block bounded by faults C and D, and a zone of small faults and monoclinal warping (zone E). Faults A, B, and C are the boundaries of two large fissures, and are inferred to have accommodated both vertical and extensional movement. Fault A (Fig. 33) is very similar to fault A in Trench 3 in that: (1) the fault plane is very irregular in profile, containing bulges and overhangs; (2) the fault plane does not strike exactly parallel to the fault scarp; and (3) there is no obvious shear fabric (oriented clasts, anastomosing parallel sub-faults) near the fault plane. Given the width of the fissure (unit 6) and the abundance of open voids, there was clearly a major amount of E-W extension between faults A and B. Both faults B and C might be thought of as subvertical depositional contacts, but we cannot preclude the possibility that some small amount of dip- slip movement also occurred on them. This is particularly true if some of the tuff blocks in the fissured zones are in-situ fractured and rotated tuff, rather than loose colluvial blocks that fell into the fissure.

Fault D is a subvertical fault that bounds the western edge of a buried fault block; this block has no surface expression, despite its 1.8 m of vertical displacement on the top of Bandelier Tuff. This fault does contain a small fissure fill in its upper meter. A peculiar effect of fault D is that it spawns two reverse faults that displace units 3 and 4. These reverse faults connect to the main fault in the area of the fissure fault. Thus, the fault paradoxically displays an extensional feature (the fissure) connected to two faults that are normally considered compressional features. Our explanation for this anomaly is similar to that proposed for reverse faults in Trench 3, that is, the overhanging (east-dipping) shape of fault D creates some local space problems when the downthrown block subsides vertically during faulting. Above the fault tip strata are squeezed together, whereas below the overhang void space can be created. The displacements across these reverse faults, and across smaller- displacement faults farther west, are larger on the unit 3/4 contact that within unit 4. These differential displacements suggest that at least two episodes of faulting affected unit 3.

The western half of the trench is underlain by east-dipping Bandelier Tuff and overlying fine-grained ashes (unit 2) that are pervasively faulted (zone E). Unit 2 outlines a monoclinal flexure that has its center, and steepest dips, at about 12 mH. The subvertical small-displacement faults have both normal and reverse senses of slip. A series of reverse faults on the foot of the monocline (9- 10mH) may represent the local compression expected in such a position of a flexure. In contrast, fault geometries on the face and crest of the monocline are more erratic. Numerous faults displace the unit 2/3 contact but not the 3/4 contact, suggesting displacement before the deposition of unit 3. However, some faults (e.g. at 11 mH) displace beds as young as unit 4b. The dips of units 2, 3, and 4 tend

to decrease upward in any vertical transect, indicating a slight angular unconformity between those units. This unconformity suggests that the monocline has continued to develop through successive faulting events.

3.7.4 Geochronology

Trench 7 yielded the largest number of charcoal samples of any trench. We have six C-14 dates as well as two TL ages and four SDI age estimates. Unit 7c yielded C-14 dates of 1510± 50 and 4020± 50 C-14 yr BP, and overlying unit 8a dated at 3960± 60 C-14 yr BP. Fissure fill unit 6 yielded three charcoal samples with dates between 2200± 50 and 2870± 40 C-14 yrs BP, but the youngest sample was stratigraphically lowest and the oldest sample in the middle. TL samples collected in units 7c and 8a yielded much older ages than C-14 dates, with 7c dating at 13 ka (compared to the C-14 date of 4 ka) and 8a dating at 7 ka (compared to the C-14 date of 3.9 ka). Finally, SDI age estimates for the base of unit 7c at two locations are 13 ka, and the base of the two B horizon buried soils are 53 ka and 72 ka. The latter age estimate is also at the upper contact of fine-grained volcanic ashes that must have an age of ca. 1.0 - 1.2 Ma.

In summary, numerical dates from the three different methods often contradict each other for a given unit and suggest that, either the units are not correctly logged, and/or some assumptions of certain dating methods do not hold true at this site.

The key unit to understanding the chronology of deposits in Trench 7 is unit 7c. The C-14 age of 1.5 to 4.02 ka contrasts with the TL age of 13 ka and two SDI ages of 13 ka. This discrepancy is mirrored in unit 8c, where the C-14 age is 3.96 ka and the TL age is 7 ka. The C-14 ages and two TL ages are each older with depth, but the two series are discordant. Possible explanations for this discrepancy are: (1) the dated charcoal is intrusive (burned roots) and is thus younger than the host deposit; (2) the TL-dated silt was not completely zeroed at deposition, so included a component of inherited TL that yielded a TL age older than true age; or (3) the SDI value was inflated because this site is a site of Holocene fluvial deposition, and horizon thickness is thus much greater than would be found on the stable geomorphic surfaces where the SDI chronofunction was calibrated. These possible flaws suggest that the C-14 ages provide minimum age estimates at this site, and the TL and SDI age estimates could be maximums. Thus unit 7c is probably older than 1.5-4 ka but younger than 13 ka. Unit 8c is older than 4 ka but younger than 7 ka.

The next dating issue is why unit 6, which underlies unit 7, yields younger dates (2.2 - 2.8 ka) that themselves are not in stratigraphic order. There are three possibilities for these two younger ages: (1) the unit 6 fissure fill is actually younger than unit 7, and the contacts were incorrectly logged; (2) the contacts logged are correct, but the charcoal in unit 6 is intrusive; or (3) contacts are correctly logged and unit 7c is about 1.5 ka, with the older C-14 ages from units 7c and 8a being reworked older charcoal deposited fluvially. The unit 6 fissure fill contains many open voids, voids partially filled with soft inwash, and

some totally filled voids. Tree roots of all sizes descend throughout these voids and pockets of sort inwash. If surface charcoal could somehow get through units 7 and 8 to the top of the fissure fill, it would be easy for infiltrating water to drag that charcoal deeper into the subsurface along interconnected voids. No open cracks exist today between the top of unit 6 and the ground surface, but decaying roots that penetrated units 7and 8 would provide the necessary conduit. We did not log decayed root holes because at the time of logging we did not realize they had any geologic significance. Based on the distribution of void spaces and the inwash processes inferred here and at Trenches 1 and 2, I think that it is very likely that the dated charcoal in unit 6 is intrusive, and only provides a minimum age on fissure formation. However, to confirm this supposition we excavated a new trench on April 8, 1998 through this stratigraphic section (Sec. 3.9).

3.8.5 Paleoseismic Interpretation

According to the retrodeformation sequence (Fig. 34) a minimum of four faulting events are required to reproduce the geometric relations exposed in the trench wall. These four events are required by faults that terminate at the unit 2/3 contact, the unit 3/4 contact, and the two fissure-creating events. It is possible that additional small displacement faulting events occurred between the four events we interpret, but if they did occur they did not interrupt ongoing depositon on the downthrown block or create any unconformities.

The earliest faulting event (W_7) created 1 m of throw on fault D and created the beginning of the monoclinal flexure in zone E. This event created the initial west-facing scarp that began trapping sediment at this site. Slopewash alluvium (unit 3a) was deposited against the scarp, and later a small channel (unit 3b) was formed above fault D by a stream running subparallel to the scarp. A period of soil formation followed for several 10s of ka. The next faulting event (X_7) produced another increment of movement on fault D and more flexing of the monocline, reactivating some of the faults originally created in event W_7. Unit 3 was thrust- faulted along fault D due to the overhanging dip of the fracture-controlled fault plane.

Following event X_7 two channels of alluvium (units 4a, 4b) were deposited against the small scarp. The bulk of unit 4 alluvium was then deposited across the entire scarp, burying it. Another period of soil formation commenced lasting several 10s of ka, and a Bt horizon formed. Fault event Y_7 induced movement on three faults. A fissure opened between faults A and C, and renewed faulting on fault D uplifted unit 4 and created a 1 m-deep narrow fissure. Following this event, B horizon material fell into the large fissure, creating the present orange, compacted fissure fill, and the smaller fissure fill (unit 5a). This colluviation removed all of unit 4 on the upthrown block. Soon thereafter a stream was diverted along the rejuvenated scarp and alluvium of unit 7c was deposited. This stream eroded the remnants of unit 4 off of the intermediate fault block.

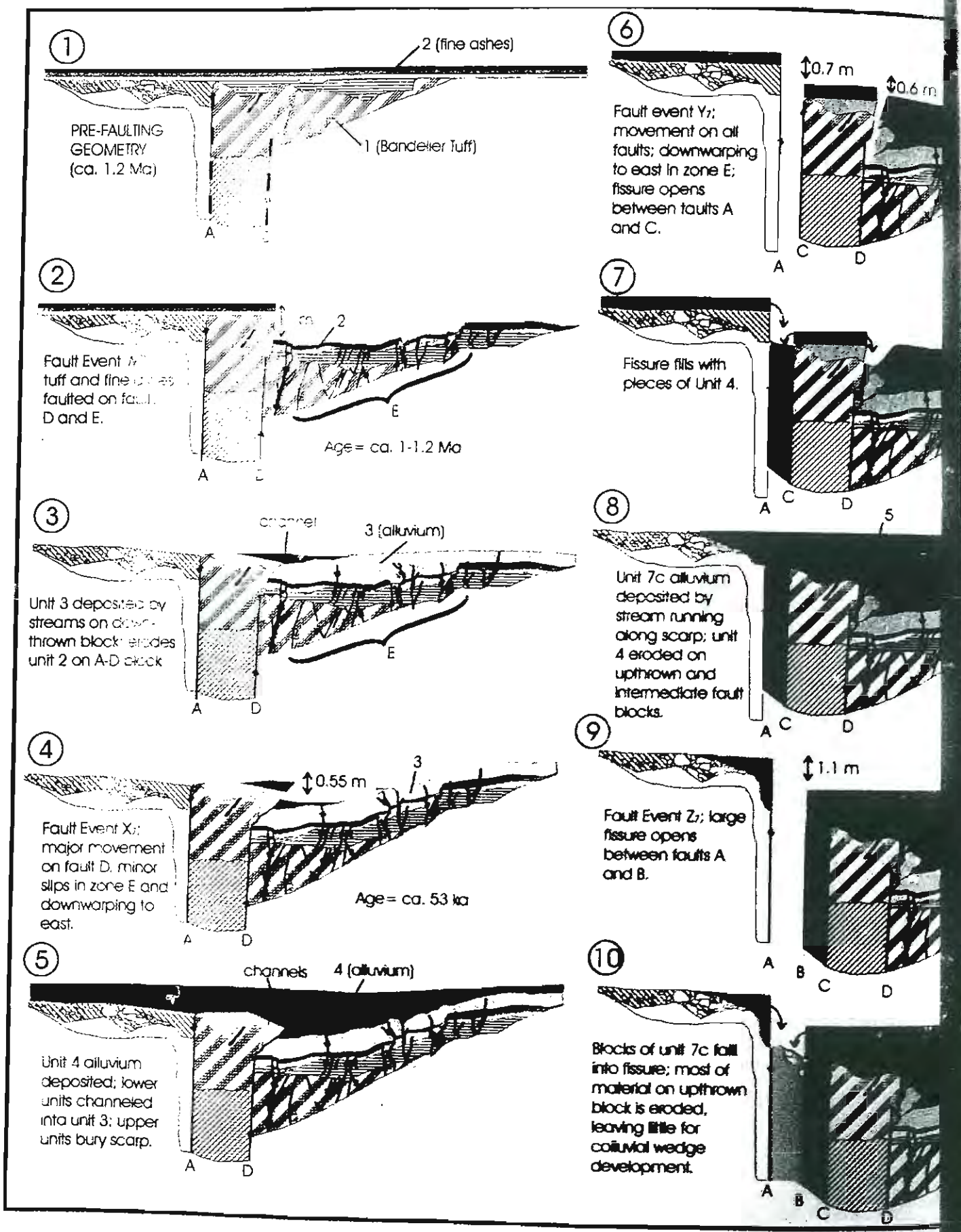
1
2 (fine ashes)
PRE-FAULTING GEOMETRY (ca. 1.2 Ma)
1 (Bandelier Tuff)
A
2
Fault Event
tuff and fine
faulted on fau
D and E.
2
E
Age = ca. 1-1.2 Ma
A
3
channel
3 (alluvium)
Unit 3 deposited by streams on down-thrown block erodes unit 2 on A-D block
E
A
D
4
0.55 m
3
Fault Event X7: major movement on fault D, minor slips in zone E and downwarping to east.
Age = ca. 53 ka
A
D
5
channels
4 (alluvium)
Unit 4 alluvium deposited; lower units channeled into unit 3; upper units bury scarp.
A
D
6
0.7 m
0.6 m
Fault event Y7: movement on all faults; downwarping to east in zone E; fissure opens between faults A and C.
A
C
D
7
Fissure fills with pieces of Unit 4.
A
C
D
8
5
Unit 7c alluvium deposited by stream running along scarp; unit 4 eroded on upthrown and intermediate fault blocks.
A
C
D
9
1.1 m
Fault Event Z7: large fissure opens between faults A and B.
A
B
C
D
10
Blocks of unit 7c fall into fissure; most of material on upthrown block is eroded, leaving little for colluvial wedge development.
A
B
C
D

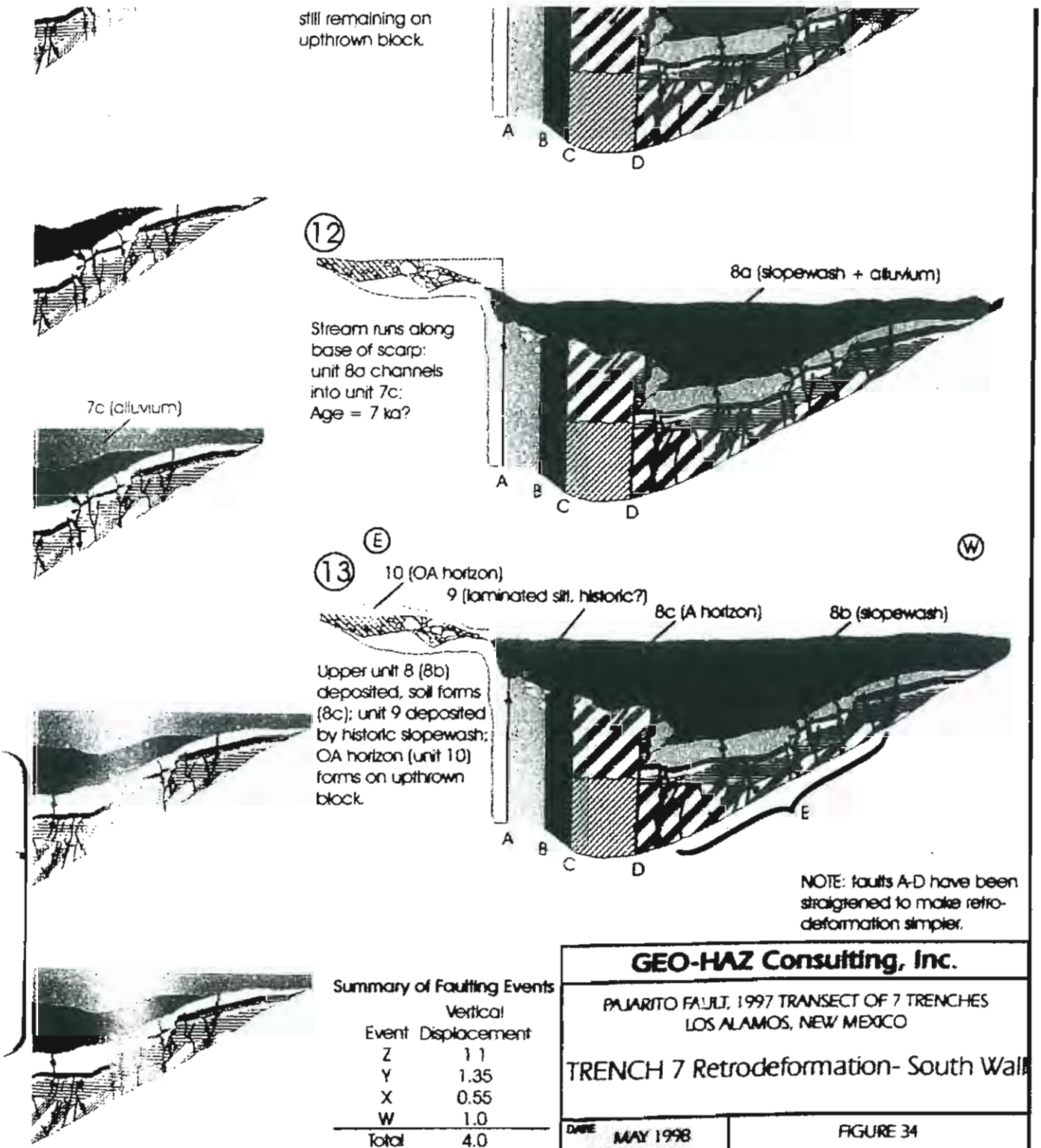

Summary of Faulting Events

Event	Vertical Displacement
Z	1.1
Y	1.35
X	0.55
W	1.0
Total	4.0
Average	1.0

GEO-HAZ Consulting, Inc.

PAJARITO FAULT, 1997 TRANSECT OF 7 TRENCHES
LOS ALAMOS, NEW MEXICO

TRENCH 7 Retrodeformation- South Wall

DATE	MAY 1998	FIGURE 34
DWG. NO.	C:\GEOHAZ\LANL\LALAMOS\RETRO7.CDR	

The final faulting event (Z_7) postdates the lower part of unit 7, if not the entire unit. No movement occurred on faults C or D, but a wide fissured zone was created between faults A and B. The reader should not imagine that this was an open fissure as shown in the retrodeformation sequence. Instead, the fissured zone is a pull-apart and shear zone composed of shattered and fract[illegible]l tuff interspersed with large open void spaces. The initial volume of actual open void space may be 50% or less than the volume of the whole fissure shown in the retrodeformation sequence. Thus, when we say that "blocks of unit 7c fall into fissure", what is actually happening is this: (1) chunks of unit 7c fall onto the fissure surface; (2) rain also washes exposed parts of unit 7c down onto the top of the fissure; (3) rain falling on chunks of unit 7c causes them to disaggregate; and (4) the infiltrating rainwater transports disaggregated sand and silt grains eroded from unit 7c down into the network of interconnecting voids, where it is eventually deposited as inwash.

After filling of the fissure, enough unit 7c still existed on the upthrown block to yield the small colluvial wedge of units 7a and 7b. Constinued colluviation deposited that part of unit 7c above units 7a and 7b. Thus, unit 7c as originally logged includes two deposits of different origin and age: (1) west of unit 6, unit 7c is alluvium ca. 4 ka, and (2) above unit 6, unit 7c is colluvium about 1.5 ka, derived from unit 7c that was faulted up by faulting event Z_7 (Fig. 34). Soon after faulting another stream was diverted along the scarp on the newly- downdropped block. This stream eroded into the top of unit 7c, and deposited unit 8a. Subsequent to that time units 8b, 8c, and 9 have formed.

The stratigraphic relations suggest that the MRE occurred after the deposition of some or all of unit 7c, and immediately before the deposition of the colluvial part of unit 7c. Thus, the MRE is dated between 1.5 and 4 ka by C-14, or after 7- 13 ka by TL and soils.

3.9 Trench 7A

Trench 7A was excavated on April 8, 1998 1 m south of the eastern part of Trench 7. This small trench (1.8 m deep, 4 m long; Fig. 35) was dug to re-expose the contacts between Holocene alluvium, Bandelier Tuff, and fissure fill that were the sources of some ambiguity in interpreting Trench 7. The logged (south) wall of Trench 7A is about 2 m south of the logged wall of Trench 7.

3.8.1 Stratigraphy

Trench 7A (Fig. 36) exposes the same general units as exposed in the upper part of Trench 7, i.e. Bandelier Tuff is unit 1, the basal Holocene alluvium is numbered unit 7, somewhat younger Holocene alluvium is numbered unit 8, and historic (?) slopewash with no soil formation is numbered unit 9, and the incipient soil developed on the upthrown block is unit 10. Because unit 8 in Trench 7A is thicker than in Trench 7, more soil horizons could be distinguished (six horizons in Trench 7A vs. two horizons in Trench 7). Hard white Bandelier Tuff (unit 1a) underlies the upthrown block. This tuff is rubbilized (unit 1b) near the surface and is overlain by an OA horizon (unit 10) composed of pine needle duff and very loose slightly organic sand. On the downthrown block the ground surface is underlain by laminated pale silt (unit 9).

The underlying fine slopewash/ alluvium can be divided into two broad units. The upper half is composed of a moderately compact, massive, silty sand with rare pea-size clasts. Near the fault six soil horizons (8A, 8AC1, 8AC2, 8Cox1, 8Cox2, 8Cox3) can be distinguished based on progressively lighter color tones with depth, but only the two darkest horizons (8A, 8AC1) can be traced toward the west end of the trench. At the fault zone this parent material contains a large block of white tuff which must have fallen from the upthrown block and an underlying disturbed pocket about 25 cm in diameter (unit 8D). This pocket contains anomalously large (for this deposit) clasts of white tuff with downslope (to the west) orientation, a "foliated" block of hard silt (foliated clast, or FC), embedded in a soft matrix. This pocket could be a krotovina, but krotovinas typically do not contain exotic clasts from upthrown block sources. The pocket could be a fissure fill, but no bounding fissure cracks can be traced downward to the trench floor. The pocket could also be a tree throw void, although it is suspicious that the only such void would occur right in the fault zone. Regardless of its origin, this pocket contains younger deposits than the surrounding area.

The lower half of the trench is composed of a slightly denser, massive silty sand (unit 7) very similar in grain size and color to that in the upper half of the trench. Two darkened and discolored zones (7A?, 7Av) define the top of this stratigraphic package, which we interpret as incipient soil A horizons. Another weaker discolored zone (unit 7b) which is finer-grained, more compact, and less gritty than typical, lies between units 7a and 7c. Unit 7 grades into a slightly coarser facies near the main fault. This facies (unit 7d) contains 10- 20 cm-diameter angular clasts of white Bandelier Tuff that have a subhorizontal to west-dipping orientation, suggesting they fell onto a west-sloping

Fig. 35. Photograph of Trench 7A.

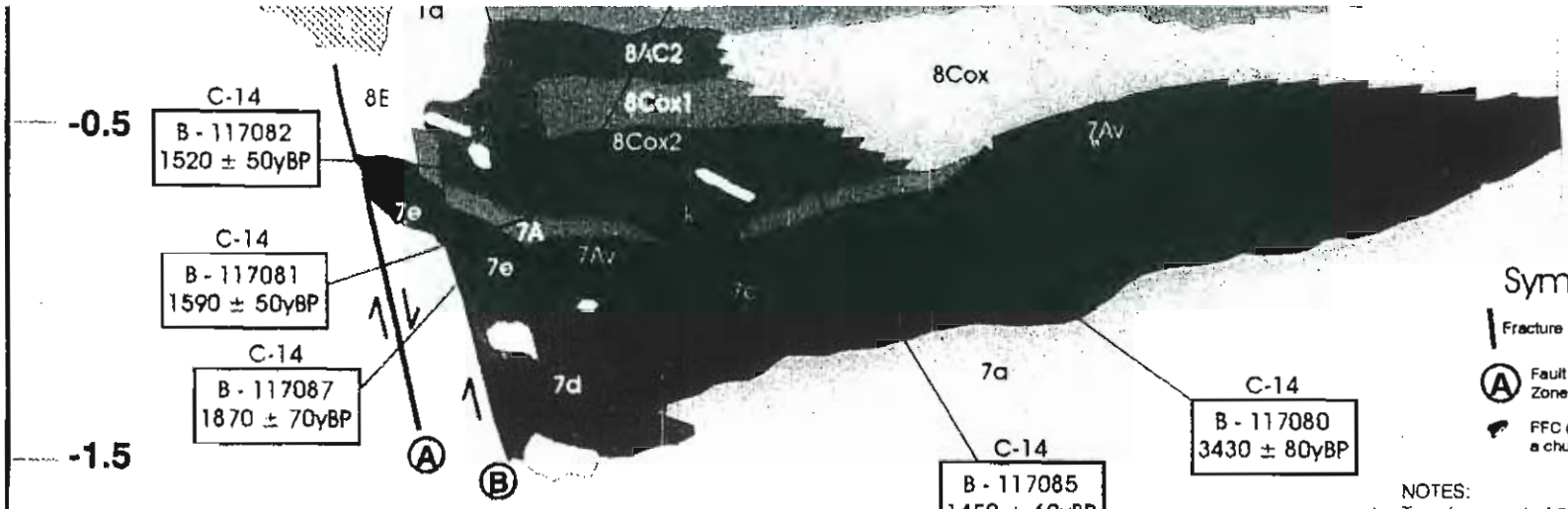

Symbols

- Fracture
- Fault
- Fault or Fracture Zone Described In Text
- FFC (funky clast, probably a chunk of unit 7)

NOTES:

1. Trench excavated 8 April 1998.
2. Trench logged by J.P. McCalpin and A. Lavine, 8-9 April, 1996.

SCALE

0 .5 1 meter

Explanation of Trench Units

10	Modern OA soil horizon	
9	Laminated pale silt, historic?	
8A	modern A horizon	parent material is massive silty sand
8AC1	modern AC horizon	parent material is massive silty sand
8AC2	lower AC horizon	parent material is massive silty sand
8Cox1	maximum oxidation horizon	parent material is massive silty sand
8Cox2	oxidized C horizon	parent material is massive silty sand
8Cox3	minimum oxidation horizon	parent material is massive silty sand
8Cox	undiff. Cox horizon	parent material is massive silty sand
8D	soft pocket containing exotic clasts	
8E	pocket of very soft silty sand (colluvium?)	
7A	weak discolored A horizon	parent material is dense, massive, silty sand
7Av	weakly discolored Av horizon	parent material is dense, massive, silty sand
7e	gravelly sand	parent material is dense, massive, silty sand
7d	coarser colluvium with clasts	parent material is dense, massive, silty sand
7c	upper part of unit 7, oxidized	parent material is dense, massive, silty sand
7b	clast-free zone	parent material is dense, massive, silty sand
7a	lower part of unit 7, oxidized	parent material is dense, massive, silty sand
1b	Voids and loose rubble in surface tuff	
1a	Intact hard white tuff	
k	Krotovina	
root	tree root	

GEO-HAZ Consulting, Inc.

PAJARITO FAULT, TRANSECT OF 7 TRENCHES
LOS ALAMOS, NEW MEXICO

TRENCH 7A- South Wall

DATE MAR. 1998	FIGURE 7A
DWG. NO. C:\GEOHAZ\LANL\LALAMOS\TRENCH7A.CDR	

colluvial slope. The upper 5-10 cm of this deposit is less dense and has more coarse sand and granules, and is defined as unit 7e. Unit 7d does not contain any void spaces or abundant angular tuff rubble, so it must overlie the fissure fill unit 6 exposed in Trench 7. We infer that the top of that fissure fill is about at the floor level of Trench 7A.

3.9.2 Structure

The structure exposed in Trench 7A is considerably different than that exposed in Trench 7. First, the lower part of the Holocene section (unit 7) dips eastward toward the fault at 15 degrees over most of its exposed length, only flattening out to subhorizontal within 75 cm of the fault. Second, units 7Av? and 7e at the top of this section are clearly displaced at the main fault. The fault plane at the bottom of the trench is planar, dips 75° west, and abuts Bandelier Tuff (on the east) against colluvium of unit 7d. About 65 cm above the floor of the trench the tuff/unconsolidated sediment contact abruptly flattens and swings to the east, forming a 20 cm-wide sloping bench before steepening again. Units 7Av? and 7e lie atop this bench, but they are clearly displaced 15 cm by two parallel faults that project upward from the 75°- dipping fault plane below. The fault zone is too disturbed, and unit 7A too weak, to confirm that unit 7A is also faulted. Instead, the uppermost material faulted could be either unit 7A, or unit 8Cox3 (these units are identical except for a slight color contrast). The steep contact on the left side of unit 8E could be either a fault or a depositional contact; there were no clasts to preserve a shear fabric.

3.9.3 Geochronology

Trench 7A contained small pieces of angular charcoal scattered throughout the stratigraphic section. Eight samples were dated by the AMS method by Beta Analytic, Inc. The dates are generally in correct stratigraphic order, ranging from "modern" (>100% modern level of C-14) at 35 cm below the surface to 3430± 80 C-14 yr BP at 1.2 m below the surface. However, there are some anomalies. The sample from unit 8D, the soft pocket containing clasts, dated at 770± 50 C-14 yr BP, or 800-900 years younger than adjacent soil- stratigraphic units. This large age departure suggest that unit 8D contains intrusive material that is much younger than adjacent strata.

Two samples from unit 8Cox3 yielded slightly different ages, 1450± 60 and 1520± 50 C-14 yr BP. However, these two ages overlap at 1 sigma. Unit 8Cox2 dated at 1620± 60 C-14 yr BP, which is 100-170 years older than the two dates from subjacent unit 8Cox3. However, all three dates overlap at 2 sigma.

In the tilted part of the stratigraphic section (unit 7) ages are slightly to considerably older than in unit 8. The buried A? horizon (unit 7A) yielded a date of 1590± 50 C-14 yr BP, which is statistically indistinguishable from the three dates in overlying units 8Cox2 and 8Cox3. Unit 7e dated at 1870± 70 C-14 yr BP, which does not overlap the cluster of younger dates at 1 sigma. Finally unit 7b dated at 3430± 80 C-14 yr BP at a depth of 1.2 m. This compares to a date of 3960± 60 C-14 yr BP at a depth of 1.05 m in Trench 7.

The MRE in Trench 7A appears to be tightly bracketed by C-14 dates at ca. 1500 C-14 yrs BP. This event timing can be reconciled with that in Trench 7, where unit 7c colluvium shed after the MRE dates at 1510± 50 C-14 yr BP. This correspondence between the MREs in Trenches 7 and 7A further suggests that the charcoal in the large fissure in Trench 7 (unit 6), which dated at 2200-2870 C-14 yrs BP, may be older charcoal washed into open voids.

A related issue is the non-correspondence between young C-14 dates and older TL and SDI dates in some trenches. For example, in Trench 7 the lower part of fluvial unit 7c has a C-14 age of ca. 4 ka and TL and SDI ages of 13 ka. However, in Trench 4 we have general agreement between C-14 dates (1690± 40, 2230± 40 C-14 yr BP) and SDI ages (2.1 ka, 2.3 ka), which are far younger than TL ages (43± 5 ka) for the same stratum.

Wong et al. (1995) also experienced discordance between C-14 and TL ages in their trenches. At the Water Tanks trenches, pre- El Cajete colluvium yielded C-14 dates of 19,070± 160 and 22,420± 690 C-14 yr BP, compared to TL ages of 45 ka and 73 ka. Wong et al (1995, p. 4-39) concluded that the C-14 samples were not intrusive into the host deposit, but instead had been contaminated during analysis. They thus explain the two finite dates listed above as resulting from lab contamination of C-14 dead charcoal with younger organics.

This explanation cannot be applied to our late Holocene charcoal samples, which all date at less than 4 ka. It would require large amounts of young carbon contamination to yield dates in the range 1.5- 4 ka from samples whose true age was 7-13 ka. In addition, it is unlikely that lab contamination would fortuitously result in C-14 ages in correct stratigraphic order, as is generally found in Trenches 7 and 7A. Finally, Beta Analytic periodically runs calibration standards in both its conventional and AMS dating lines, so significant lab contamination would be detected. Therefore, we tend to accept the young radiocarbon ages from Holocene colluvium and alluvium, and consider that much older TL age estimates are due to incomplete initial bleaching of TL at time of deposition.

3.9.4 Paleoseismic Interpretation

The sequence of events surrounding the MRE is simple enough that no formal retrodeformation sequence is required. Before the MRE, units 7a- 7c were deposited by slopewash against the scarp, and units 7d and 7e were deposited contemporaneously by colluviation. Unit 7B dates at 3430± 80 C-14 yr BP, and unit 7e at 1870± 70 C-14 yr BP. Then soil units 7A and 7Av formed atop units 7c and 7e. Unit 7A dates at 1590± 50 C-14 yr BP. It is unclear whether the parent material of soil unit 8Cox3 was deposited next, because it is difficult to see whether that parent material is folded (as is underlying unit 7A?) or merely deposited in a nonhorizontal manner atop a folded surface. Two ages from the upper part of unit 8Cox3 are 1450± 60 and 1520± 50 C-14 yr BP.

The MRE then occurred displacing unit 7A on fault B (and possibly the lower part of the parent material of 8Cox3) and tilting unit 7 eastward toward the fault. It is most likely that the top of unit 7A? was the ground surface at the time of the MRE, and that post-faulting sedimentation on the backtilted surface began with the parent material of unit 8Cox3. This is the typical response to creating a free face that faces upslope, and creates an event horizon at the top of a buried soil (e.g., see Pantosti et al., 1993).

Subsequent to the MRE all of unit 8 was deposited and the mapped soil formation developed. For example, unit 8Cox2 dates at 1620± 60 C-14 yr BP. The lower part of unit 8 was probably deposited more rapidly than soil forming processes, but as deposition rates slowed, soil formation started to keep pace with deposition, yielding the cumulic-style soil with thick AC horizons.

The 15 cm of vertical displacement on the top of unit 7Av? does not represent the entire displacement in the MRE, since additional displacement could have occurred on fault A, the evidence of which is now observed by scarp- derived colluviation. Based on retrodeformation of the Trench 7 wall only 2 m away, the MRE created ca. 1.1 m of vertical displacement.

Thus, the age of the preferred event horizon for the MRE (the 7A/ 8Cox3 contact) is bracketed by minimum ages of 1450± 60 and 1520± 50 C-14 yr BP, and a maximum age of 1590± 50 C-14 yr BP. This would seem to bracket the MRE tightly at around 1500 C-14 yr BP.

This age is somewhat younger than expected compared to the preferred interpretation of Trench 7. In that trench, the large fissure fill (unit 6) contains charcoal dated between 2200- 2870 C-14 yr BP, and the fissure is overlain by colluvium (colluvial part of unit 7c) dated at 1510± 50 C-14 yr BP. We thought that the large fissure opened sometime before 2.9 ka and the charcoal was washed into the fissure over the next 700 years. One difficulty with this scenerio was the 700- 1300 year time gap between the charcoal dates in the fissure and the 1510 yr age of colluvium that overlies the fissure. It should not have taken that long to fill the fissure (which was not a huge open void to begin with) and overtop it with colluvium.

Based on the dates from Trench 7A, it appears that the MRE occurred about 1500 C-14 yrs BP, which implies that the unit 7c colluvium in Trench 7 covered the fissure soon after the MRE. However, a fissure formed at 1500 yr BP could not have accepted charcoal inwash between 2200- 2870 yr BP, unless: (1) the fissured zone was initially created before the MRE, and was merely reactivated in the MRE; or (2) the fissure was initally created at 1500 yr BP, and old charcoal (700- 1300 years old) that was sitting around on the surface then washed into the fissure. I feel that option 2 is likely to be true, that surface charcoal could have been redeposited 700- 1300 years after its formation, because published reports (e.g. Blong and Gillespie, 1978) have documented charcoal as much as 1500 years old in active stream transport. On the other hand, the penultimate

faulting event almost surely induced some brecciation between faults A and B, since B forms the wall of the fissure fill from that event. Therefore, the 2.2- 2.9 ka C-14 ages from unit 6 in Trench 7 would be interpreted as very loose minimum age constraints on the penultimate event, rather than constraints on the MRE.

4. INTERPRETATION

4.1 Refinement of the Structural Model of the Pajarito Fault

The structural model of the PF (articulated monocline) was originally based on surface observations (McCalpin, 1997) plus limited subsurface exposures such as the Wong et al (1993) trenches and roadcuts along NM Highway 4. Our seven trenches excavated in 1997 provide additional subsurface information that bears on this model. The main uncertainty about structure in monoclinal sections of the scarp is where the underlying normal fault is located with respect to the east-tilted slab. Lettis and Swan (1997) proposed three possible geometries (Fig. 37). In Fig. 37a the subsurface normal fault would reach the surface at the toe of the slab. However, if this is true then the slab never would have developed in the first place, and only a deep tension fissure would be present. In Fig. 37b the subsurface normal fault lies beneath the middle of the tilted slab. This geometry requires: (1) an antithetic scarp at the head of the slab; (2) two tension fissures, one at the head of the slab, another in mid-slab above the subsurface fault; and (3) open spaces beneath the toe of the slab and mid-slab fissure. In Fig. 37c the subsurface fault daylights at the "back edge" of the crestal tension fissure. This geometry results in a large void space beneath the upper end of the slab.

The PFZ south of Los Alamos Canyon does contain an antithetic (west-facing) fault scarp at Trench 7, the mechanical function of which was not understood. Perhaps this scarp results from "lifting up" the back (west) edge of an east-tilted slab that has a fulcrum point atop a subsurface normal fault beneath the tilted slab. In Fig, 37b, however, such a scarp should occur on the eastern margin of the crestal tension fissure, not 200 m above the scarp crest as at Trench 7. Morever, Trench 7 does not expose a wide tension fissure as predicted by this model. However, the idea of creating a west-facing scarp by tilting (but not downfaulting) part of a thick tuff slab does have merit.

Both models b and c show large open spaces beneath the tilted slab directly downslope of large tension fissures. These spaces cannot remain as open voids and must therefore be "filled in" by some type of secondary faulting. Based on Trench 6, the area downslope of large fissures is chopped up into narrow domino-style blocks bounded by normal faults that dip toward the head of the slab. The domino blocks are both rotating, and the ones closest to the tension fissure are sliding down into some type of space.

Neither models b or c require a graben to form at the base of the tilted slab, so the 200 m-wide graben in our transect must have been created by complexities in the subsurface normal fault itself, rather than responses of a thin (50- 75 m) slab of hard tuff.

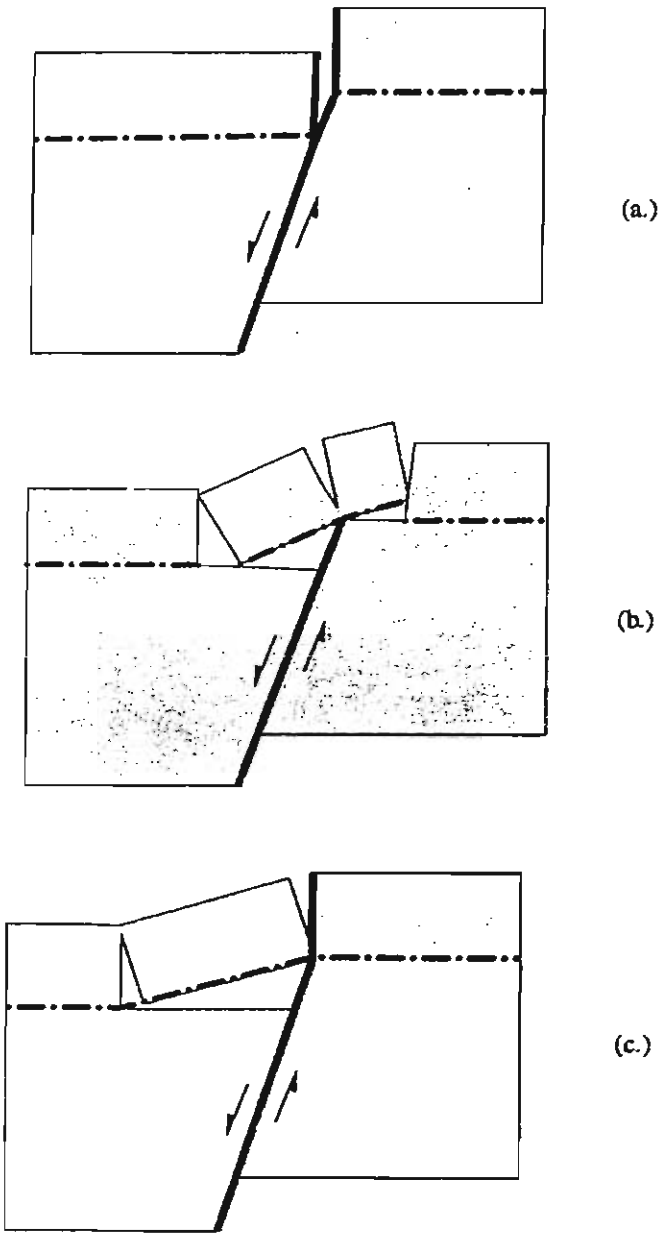

Fig. 37. Schematic diagrams showing how a subsurface normal fault would interact with a rigid surface slab of Tuff. No one diagram explains all the observed structures along the Ski Hill Road transect (see Fig. 2), so there may be more than one major fault beneath the fault scarp.

4.2 Timing of the Most Recent Faulting Event

A Holocene faulting event is required by logged relations in Trenches 3, 4, 7, and 7A, with suggestive evidence in Trenches 2 and 5. The timing of the MRE is mainly constrained by C-14 dates (Table 4), with a few SDI ages also relevant. In general, TL age estimates from within one meter or less from the ground surface are much older than either C-14 or SDI ages. The limiting ages for the MREs in Trenches 3, 4, 7, and 7A are shown graphically in Fig. 38.

Table 6. Summary Table of Radiocarbon Dates (all dates on charcoal)

Trench	Unit	Lab. No.	C-14 Age	Calendar Age[1]	Event Constraint
3	15b	B-108400	1300 +/- 80	1260 (920-1520)	Z3, minimum age
4	10c	B-108401	1690 +/- 40	1560 (1400-1800)	Z4, minimum age
4	10c	B-108402	2230 +/- 40	2200, 2310 (2000-2360)	Z4, minimum age
7	8a	B-108398	3960 +/- 60	4410 (4000-4820)	Z7, close minimum age
7	7c	B-108399	4020 +/- 50	4450, 4510 (4160-4830)	Z7, close maximum age
7	7c	B-113029	1510 +/- 50	1360, 1390 (1260-1600)	Z7A, close minimum age
7	6	B-113030	2580 +/- 40	2740 (2360-2840)	Z7, minimum age
7	6	B-113031	2870 +/- 40	2960 (2780-3220)	Z7, minimum age
7	6	B-113032	2200 +/- 50	2150, 2290 (1940-2360)	Z7, minimum age
7A	8AC1	B-117083	modern	N/A	Z7A, far minimum age
7A	8D	B-117086	770 +/- 50	680 (650-755)	Z7A, far minimum age
7A	8Cox2	B-117084	1620 +/- 60	1520 (1360-1620)	Z7A, minimum age
7A	8Cox3	B-117082	1520 +/- 50	1390 (1305-1520)	Z7A, close minimum age
7A	8Cox3	B-117085	1450 +/- 60	1320 (1270-1420)	Z7A, close minimum age
7A	7A?	B-117081	1590 +/- 50	1500 (1350-1560)	Z7A, very close maximum age
7A	7e	B-117087	1870 +/- 70	1815 (1610-1945)	Z7A, close maximum age
7A	7b	B-117080	3430 +/- 80	3680 (3470-3870)	Z7A, far maximum age

[1] in calendar years Before Present, with present taken as 1950 A.D. Calendar age is the intercept of the mean C-14 age with the calibration curve of Vogel et al., 1993. Ages in parentheses are the 2-sigma limits on the calibrated age.

In Trench 3 the MRE is bracketed by minimum constraints of 1300± 80 C-14 yr BP and 0.7- 0.8 ka (from SDI) and a maximum constraint of 20 ka (basal age of unit 14). In Trench 4 minimum constraints on the MRE are 1690± 40 and 2230± 40 C-14 yr BP. If the basal part of unit 10b was faulted, then SDI ages of 2.1- 4.5 ka form close maximum age constraints.

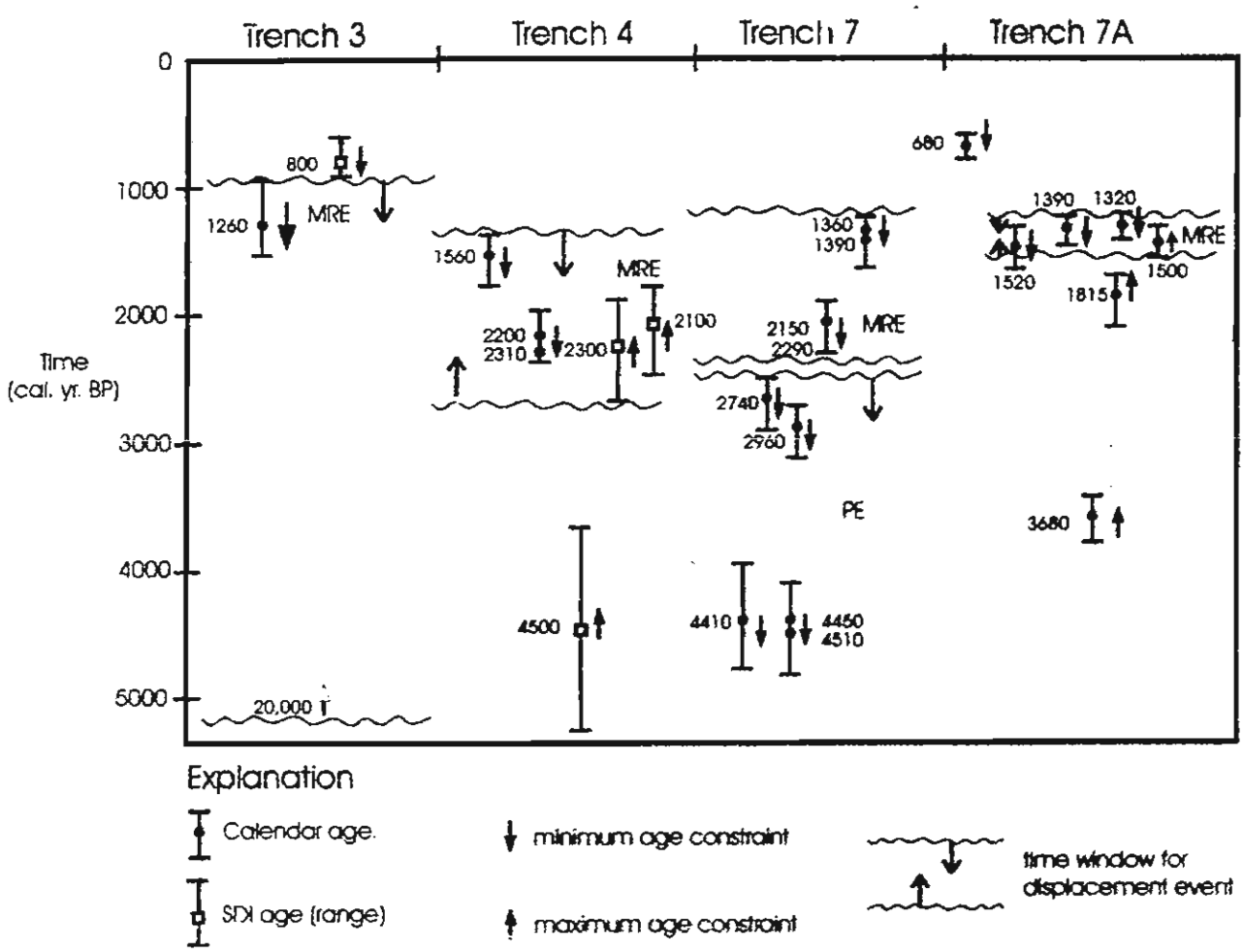

Fig. 38. Space-time diagram showing the limiting ages on the MREs in Trenches 3, 4, 7, and 7A.

In Trench 7, the minimum age constraint on the MRE is 1510 +/- 50 C-14 yr BP from the colluvial part of unit 7c, and the maximum age constraints are either 2200-2870 C-14 yr BP from subjacent unit 6, or, if they are old charcoal washed into a fissure, then the maximum constraint comes from in-situ ages of 3960±60 C-14 yr BP and 4020± 50 C-14 yr BP from units 7c and 8a.

The MRE is most tightly bracketed by six C-14 dates from Trench 7A. Minimum ages are (from farthest to closest constraint) 680, 1320, 1390, and 1520 calendar years BP, whereas maximum ages (from closest to farthest constraint) are 1500, 1815, and 3680 calendar years BP. These ages appear to tightly constrain the MRE to about 1500 calendar years BP. This age falls within the range of the MREs in Trenches 3 and 7, and comes close to the range of the MRE in Trench 4, depending on whether one considers the 2230 +/- 40 C-14 yr BP age from unit 10c as younger or older than faulting.

In summary, the MRE in Trenches 3, 4, 7, and 7A appears to fall in a relatively narrow age range between about 1260 and 2290 cal. yr BP, with the tightest bracketing coming from Trench 7A where the constraints are 1500 and 1520 cal. yr BP

4.3 Recurrence Intervals Between Paleoearthquakes on the Pajarito Fault

As displayed in the retrodeformation sequences for Trenches 3 and 7, we can roughly estimate the length of time intervals between paleoearthquakes that predate the MRE. In Trench 3 we have evidence for six events (five recurrence intervals) in the period from 1.5 ka to ca. 110 ka, which yields a long-term mean recurrence of 21.7 ka. However, recurrence is extremely variable, ranging from <10 ka to ca. 61 ka. The standard deviation of the recurrence series (values shown in Fig. 18) is 20.1 ka, which defines a coefficient of variation (COV, sigma/mean) of 0.95. This high degree of variability is rarely found in paleoseismic recurrence series elsewhere (Fig. 39; see also McCalpin and Slemmons, 1998), and suggests that either: (1) the dating of events here is inaccurate; (2) there are missing events in the series; or (3) not all earthquakes on the Pajarito fault are recorded in Trench 3. The three latest events in Trench 7 in the past 72 ka have a mean recurrence of 34 ka, sigma of 15 ka, and COV of 0.44. This COV is more typical of paleoearthquake sequences elsewhere, although Trench 7, being far west of the main fault scarp, is even less likely than Trench 3 to record all the surface-ruturing earthquake that have occurred on the Pajarito fault.

In Trenches 5 and 6 event horizons are insufficiently preserved to identify and date paleoearthquakes with confidence. Repeated episodes of colluvial deposition and subsequent soil formation can be definitely related to earthquake displacements in some, but not all cases. If we assume that most depositional episodes in our tectonic depressions are related to faulting, we can analyze the durations of soil-forming between these episodes as if they were recurrence intervals. In the center of Trench 5 soil ages are 25, 91, 139, 177, 238, 362, and 492 ka, yielding soil durations of 66, 48, 38, 61, 124, and 130 ka. This series has a mean of 77.8 ka, sigma of 35.9 ka, and COV of 0.46.

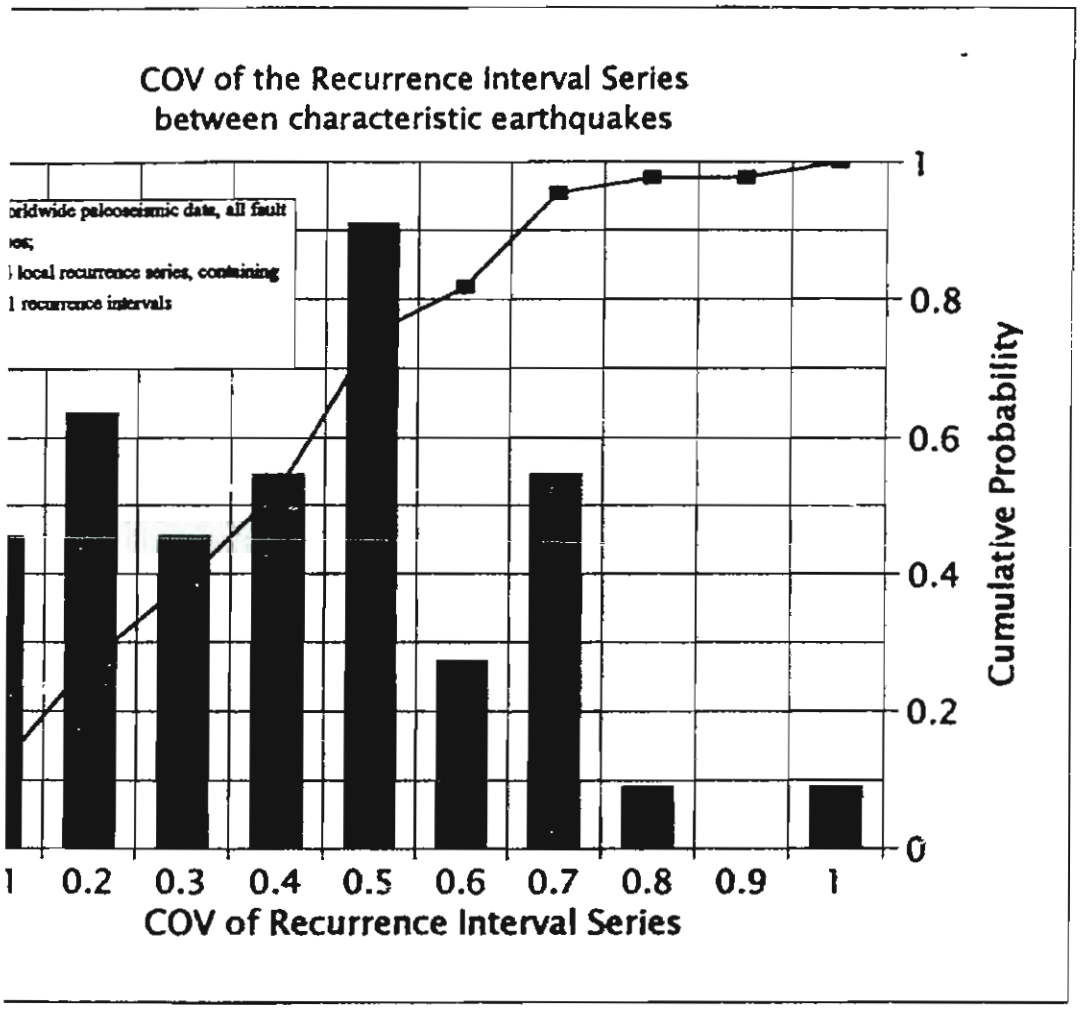

ıpirical probability distribution of the COV of recurrence interval series
aracteristic earthquakes, based on a worldwide paleoseismic data set. The
of local recurrence series is 0.36.

In Trench 6 soil ages are 4, 14, 25, 118, 250, 304, 404, and 445 ka, yielding soil durations of 10, 11, 93, 132, 54, 100, and 41 ka. This series has a mean of 63 ka, sigma of 43.3 ka, and COV of 0.69. It is interesting that the calculated recurrence intervals in the past 100 ka from the two small antithetic faults (Trench 3, 21 ka; Trench 7, 34 ka) are much shorter than the post-500 ka recurrence intervals from the two trenches on the main fault scarp (Trench 5, 78 ka; Trench 6, 63 ka). One would expect that a higher proportion of the total post-500 ka faulting events on the Pajarito fault would be recorded on the main fault trace, rather than on smaller antithetic faults. It seems reasonable that the main-scarp faults exposed in trenches 5 and 6 have moved at least as many times as those in trenches 3 and 7. Thus, my interpretation of the apparent longer recurrence times in Trenches 5 and 6 is that many faulting events occurred on those faults which we could not detect during logging, due mainly to the heavy overprinting of homogeneous colluvium with strong textural B horizons.

4.4 Displacement per Event on the Pajarito fault

It is difficult to provide estimates of displacement per event on the entire Pajarito fault, even for the MRE, from a transect of trenches across various fault strands. During the MRE estimated vertical displacement was 1.0 m at Trench 3 and 1.1 m at Trench 7, but both of these displacements are down-to-the-west (antithetic to the main fault). In Trench 6 the MRE (undated) formed a 0.8 m-high west-facing fault that backstopped the subsequent colluvial wedge, which must have been shed from an east-facing free face of at least equal height. No displacement measurements could be made for Holocene faulting in Trench 5. In summary, the MRE was evidently accompanied by at least 2.1 m of net down-to-the-west faulting on antithetic faults. Because the long-term style of the Pajarito fault is net down-to-the-east displacement, the MRE probably caused even more than 2.1 m of down-to-the-east displacement at trenches 1, 2, 5, and on untrenched structures. However, Holocene colluvium from the MRE was generally not well preserved on east-facing fault scarps, so this hypothesis cannot be rigorously tested.

It is tempting to conclude that the net vertical displacement in the MRE was equal to or greater than the combined antithetic displacements observed at Trenches 3 and 7. Pezzopane and Dawson (1996) analyzed 24 historic surface ruptures from the western US, of which 15 had rupture on secondary as well as primary faults. They found that within the range M=6-7, the maximum primary displacement ranged from 1.5 to 2.5 times as large as the maximum secondary displacement. Given a maximum secondary (albeit antithetic) displacement in the MRE of at least 2.1 m, the results of Pezzopane and Dawson (1996) suggest that the maximum primary displacement could have been in the range 3.1-5.2 m. From our logging of trenches across east-facing scarps (Trenches 1, 2, 5, and 6) we can conclusively state that Holocene vertical displacements of 3.1-5.2 m were not exposed in any one trench. However, a cumulative 3-5 m of down-to-the-east displacements could conceivably have been distributed among trenches 1, 2, 5, and 6 and possible untrenched structures in the middle of the main fault scarp. For example, Trench 1 contained a possible 0.7 m Holocene offset near its head, and Trench 5 contained evidence for a small Holocene offset event. Such a cumulative offset, however, would not

be comparable to the maximum primary displacement tabulated by Petropane and Dawson (1996), which occurred on a single fault trace.

In summary, due to the scattered nature of rupturing during the MRE and the non-preservation of Holocene colluvial wedges on east-facing scarps, we cannot five a precise estimate of the net vertical tectonic displacement on the Pajarito fault as a whole during the MRE, or during any earlier events.

5. CONCLUSIONS AND RECOMMENDATIONS

5.1 Conclusions

The Pajarito fault is a structurally complex feature that presents a challenge to the traditional methods of paleoseismology. Based on our first field season of work, it appears that a Holocene displacement event has ruptured the PF, but that evidence of such rupture is well preserved only where scarps face upslope. On east- facing scarps the evidence for Holocene rupture is much more ambiguous, and could be interpreted as the result of tree-throw.

A Holocene surface- faulting event was detected and dated in Trenches 3, 4, 7, and 7a. The event is most closely bracketed in Trench 7A by ages about 1500 calendar years BP, and somewhat more broadly bracketed in Trenches 3, 4, and 7 as between 1260 and 2290 cal. yr BP. This MRE does not overlap the time range of the MRE on the Guaje Mountain fault (4-6 ka; Gardner et al, 1990), nor the MRE on the Rendija Canyon fault (8 or 23 ka).

Vertical displacement during the MRE could be estimated most accurately at Trenches 3, 7, and 7A, all antithetic scarps, where the cumulative displacement was 2.1 m down-to-the-west. The MRE was presumably accompanied by an equal amount of down-to-the-east displacement, perhaps as much as 3.1-5.2 m, but due to erosion on steep east-facing scarps the evidence of such displacements was poorly preserved. Therefore, we cannot provide an estimate of Holocene displacement-per-event on the Pajarito fault as a whole.

5.2 Implications of the 1997 Trench Results on Quaternary Slip Rates for the Pajarito Fault

According to the Final Report of the Seismic Hazards Evaluation of the Los Alamos National Laboratory (WCFS, 1995), the net slip rate of the Pajarito fault is the most important input parameter in the PSHA. WCFS (1995) calculated a range of slip rates for the Pajarito fault, based on: (1) the average height of the fault scarp (81 m); (2) a spatially-averaged long-term vertical slip rate of 81m/1.2 Ma, or 0.07 mm/yr; and (3) net slip on a 70-degree rake of 123% of the vertical slip rate, or 0.086 mm/yr (WCFS, 1995, Table 7-1, footnote 9). To account for short-term variations in slip rate, McCalpin (1995) suggested a space-for-time substitution utilizing the variability of short- vs. long term slip rates on many faults in the Basin and Range and Rio Grande rift provinces. WCFS adapted this approach the the PF and calculated the following slip rates for the PF:

Table 1. Slip rates used for the PF in the WCFS 1995 Logic Tree

Net Slip Rate (mm/yr)	Probability[1]	Percentile[2]
0.01	0.1	5th
0.05	0.2	20th
0.09	0.4	50th
0.20	0.2	80th
0.95	0.1	95th

[1] Probability used on the PSHA logic tree
[2] Cumulative percentile assuming a space-for-time substitution; see WCFS (1995), Fig. 7-26

If the PF experienced an average secondary vertical displacement of 2.1 m down-to-the-west during the MRE, combined with an estimated 3.1-5.2 m "primary" vertical displacement down-to-the-east, the net vertical displacement would have been 1.0-3.1 m. Geochronology from the 1997 trenches indicates that the MRE occurred about 1.5 ka. The penultimate event is well-dated only at Trench 3, where it is about 20 ka. Therefore, in the latest seismic cycle which culminated in the MRE, 1.0-3.1 m of slip accumulated in 18.5 ka. The slip rate calculated from these parameters for the latest complete seismic cycle is thus 0.05-0.17 mm/yr This vertical slip rate can be increased by 123% to account for a possible 70-degree rake of the net slip vector, as was assumed by WCFS (1995, Table 7-1, footnote 9). Thus, the net slip rate for the last seismic cycle is 0.06-0.21 mm/yr. NOTE: slip rates should always be calculated on the basis of complete seismic cycles, not on time spans (such as the Holocene) where the time span boundary does not coincide with a seismic cycle boundary.

The above net slip rate can be compared with the slip rates used in the WCFS (1995) logic tree (Table 1, above). The lower of the two values cited above falls below the median slip rate value of 0.09 mm/yr assumed by WCFS. The higher slip rate, 0.21 mm/yr, is roughly the 86th %-ile value (see WCFS Fig. 7-26). Thus, even the fastest slip rate suggested by the 1997 trenching and geochronology data is already covered in the WCFS 1995 logic tree, at a probability of roughly 20%. **Therefore, if the 1.5-2 ka event in the 1997 trenches is the only Holocene event to have occurred on the Pajarito fault, then the equivalent slip rates are already covered in the WCFS 1995 logic tree.**

2) A separate issue is whether the 4-6 ka event on the Guaje Mountain fault, and the 8 (23?) ka event on the Rendija Canyon fault, also involved seismogenic rupture of the PF. The current age control on the MRE on the Rendija Canyon fault is insufficient to permit a correlation with events on the PF. For example, if the 8 ka date is correct, then this event did not rupture the PF, since we have strata of that age that do not record a faulting event (aside from the 2.2-4 ka one). Thus, it is very unlikely that a characteristic earthquake rupture could have occurred at ca. 8 ka on the PF and did not create evidence in any of our 7 trenches logged in 1997. Even a rupture as small as the 15 cm seen in Trench 7A would have been detected. However, if we assume that a 15-20 cm displacement event did

occur on the PF ca. 8 ka and was missed during logging, that would create a seismic cycle from 20 ka to 8 ka with 15-20 cm displacement, and a cycle from 8 to 2.2-4 ka of 0.58-1.02 m. The former cycle yields net slip rates of 0.015 to 0.021 mm/yr, and the latter 0.1 to 0.255 mm/yr. Note that all of the values are covered in the WCFS (1995) logic tree.

Alternatively, if the 23 ka TL date is correct, then the MRE on the RCF may be correlative with the penultimate event seen in Trench 3 and dated at ca. 20 ka. This event had "characteristic" displacement in Trench 3, which would match the large displacements seen in the Cemetery trenches. However, the slip rate of this seismic cycle (0.58-1.02 m of average displacement between 20-23 ka to 2.2-4 ka) only amounts to 0.034-0.078 mm/yr. These values are smaller than the median assumed by WCFS.

Thus, it appears that under either correlation scenario between the PF and RCF, the paleoseismic data suggest seismic-cycle-based net slip rates that are within the range in the existing WCFS logic tree.

3) It has been suggested that the occurrence of 3 or 4 characteristic earthquakes on the PF during the Holocene would imply slip rates larger than any contained in the WCFS 1995 logic tree. This is partly true. For example, characteristic (0.58-1.02 m vertical displacement) events at 8 ka, 2.2-4 ka, and 1.5 ka would define two complete seismic cycles with net slip of 0.58-1.02 m between 8 to 2.2-4 ka (0.1-0.255 mm/yr) and 0.58-1.02 m between 2.2-4 ka and 1.5 ka (0.28-1.79 mm/yr). Three of these four slip rates are within the range covered by WCFS, but the highest value (1.79 mm/yr) is 88% larger than the largest value used by WCFS.

However, the 1997 and 1998 trenching results do not support the existence of three characteristic earthquakes during the Holocene on the PF, given our geochronological results at this time.

5.3 Recommendations

Our first field season has resulted in a better understanding of the complex structural style, depositional patterns and soil formation on the Pajarito fault, but more work needs to be done to capture the Late Quaternary movement history of the fault.

Task #1 - Trench smaller fault scarps on younger landforms

The evidence of the most recent displacement event(s) are poorly preserved on large fault scarps, probably because: (1) relatively small surface offsets are occurring on steep pre-existing scarps; and (2) active slopewash transports scarp-derived colluvium far downslope to the scarp toe, so it can no longer be traced to the causative fault plane. Therefore, we need to trench smaller fault scarps with lower slope angles to detect the colluvial deposits associated with < 0.5 m displacements. An excellent place to try this is the intermediate- age (post- El Cajete?) alluvial fan complex south of Pajarito Canyon

traversed by several low scarplets or lineaments. These features were recommended for trenching by McCalpin (1997) and are scheduled for trenching in the summer of 1998.

Task #2 - Detailed Geochronology Studies

Much of the ambiguity in this first- year study arises from the discordance among C-14 dates, TL ages, and SDI- based age estimates. If charcoal in area sediments is mainly intrusive and much younger than host sediments, then we should not be using the C-14 dating method in any geologic investigations, including calibrating the SDI chronofunction with C-14 dates. Alternatively, if charcoal is detrital and contemporaneous with deposition, then the TL method is grossly overestimating ages (at least in the Holocene), although TL ages on the El Cajete pumice (50 -60 ka) are concordant with other age estimates. Therefore, future trenches should be more meticulously sampled for dating than past trenches. This would involve: (1) more samples, especially in Holocene or post- El Cajete sediments; (2) more extended tests of partial bleaching in the TL method; and (3) closer collaboration between the trench loggers and Eric McDonald to map finer soil details on the logs.

Task #3 - Where is the El Cajete?

Our 1997 trenches did not expose any primary or reworked El Cajete pumice, despite the fact that the pumice is 1.5 m thick in roadcuts on Ski Hill Road, only a few hundred feet from Trenches 5 and 6. We need to explain why this thick pumice is present in the roadcuts, and define where this pumice may be preserved in fault zone traps that could assist in dating events.

Task #4 - How Old is the Graben?

The 200 m-wide graben south of Los Alamos Canyon is the best surface expression of a structural feature that extends far to the south. This graben is evidently filled with deposits 1 Ma and older, suggesting that much of the structural relief on the Pajarito fault was formed within a few hundred ka of the Bandelier Tuff eruption. If this supposition could be proven by describing other sections of graben sediments, it would imply that slip rates from the mid- Pleistocene to the present have been much less than the mean computed over the past 1.2 Ma. One promising study site is an old quarry just east of West Jemez Road, where a thick sequence of graben sediments is exposed. This exposure should be subjected to careful logging and detailed age dating to confirm the age of most graben fill.

6. REFERENCES

Aitken, M. J., and Bowman, S. G. E. 1975, Thermoluminescent dating: Assessment of alpha particle contribution. Archaeometry, 17, 132-138.

Balescu, S. and Lamothe M., 1992, e blue emissions of K-feldspar coarse grains and its potential for overcoming TL age underestimates: Quaternary Science Reviews, v. 11, p. 45-51.

Blong, R.J. and Gillespie, R., 1978, Fluvially transported charcoal gives erroneous 14-C ages for recent deposits: Nature, v. 271, p. 739-741.

Broxton, D.E. and Reneau, S.L., 1995, Stratigraphic nomenclature of the Bandelier Tuff for environmental restoration project at Los Alamos National Laboratory: Los Alamos National Laboratory Report LA-13010-MS, Los Alamos, NM, 21 p.

Gardner, J.N., Baldridge, W.S., Gribble, R., Manley, K., Tanaka, K., Geissman, J.W., Gonzalez, M. and Baron, G., 1990, Results from seismic hazards trench #1 (SHT-1), Los Alamos Seismic Hazards Investigations, Los Alamos National Laboratory Report No. EES1-SH90-19, 57 p.

Godfrey-Smith, D. I., Huntley, D. J. and Chen, W.-H., 1988, Optical dating studies of quartz and feldspar sediment extracts: Quaternary Science Reviews v. 7, p. 373-380.

Harden, J.W., 1982, A quantitative index of soil development from field descriptions--Examples from a chronosequence in central California: Geoderma, 28:1-28.

Harden, J.W. and Taylor, E.M., 1983, A quantitative comparison of soil development in four climatic regimes: Quaternary Research, v. 20, p. 342-359.

Hecker, S. and Schwartz, D.P., 1994, The characteristic earthquake revisited; geological evidence of the size and location of successive earthquakes on large faults: U.S. Geological Survey Open-File Report 94-568, p. 79-80.

Huntley, D. J., and Wintle, A. G., 1981,The use of alpha scintillation counting for measuring Th-230 and Pa-231 contents of ocean sediments. Canadian Journal of Earth Sciences, 18, 419- 432.

Huntley, D. J., Hutton, J. T. and Prescott, J. R., 1993, The stranded beach-dune sequence of south-east sout Australia: A test of thermoluminescence dating, 0-800 ka: Quaternary Science Reviews v. 12, p. 1-20.

Kelson, K.I., Hemphill-Haley, M.A., Olig, S.S., Simpson, G.D., Gardner, J.N., Reneau, S.L., Kolbe, T.K., Forman, S.L. and Wong, I.G., 1996, Late Pleistocene and possibly Holocene displacement along the Rendija Canyon fault, Los Alamos County, New

Mexico, in New Mexico Geological Society Guidebook, 47th Field Conference, Jemez Mountains Region, p.

Lettis, W.R. and Swan, F.H. III, 1997, Review of paleoseismic trenches (No. 1 through 7) along a transect across the Pajarito f zone south of Los Alamos Canyon, September 17, 18, and 19, 1997: unpublished letter report submitted by Wm. Lettis & Associates and Geomatrix Consultants, Inc. to Los Alamos National Laboratory, Oct. 15, 1997, 8 p.

McCalpin, J.P., 1995, Frequency distribution of geologically-determined slip rates for normal faults in the western USA: Bulletin of the Seismological Society of America, v. 85, no. 6, p. 1867-1872.

McCalpin, J.P. (ed.), 1996a, Paleoseismology: Academic Press, New York, 583 pp.

McCalpin, J.P., 1996b, Field Techniques in Paleoseismology, Chapter 2 in McCalpin, J.P. (ed.), Paleoseismology: Academic Press, New York, p. 33-84.

McCalpin, J.P., 1997, Geomorphology and structure of the Pajarito fault zone west of Los Alamos National Laboratory, New Mexico: unpublished report submitted to Los Alamos National Laboratory, Los Alamos, NM, by GEO-HAZ Consulting, Inc., Estes Park, CO, April 9, 1997, 54 p.

McCalpin, J.P. and Slemmons, D.B., 1998, Statistics of paleoseismic data: unpublished Final Technical Report submitted to U.S. Geological Survey, Reston, VA by GEO-HAZ Consulting, Inc., Estes Park, CO, Contract 1434-HQ-96-GR-02752, March 20, 1998, 62 p.

Olig, S.S., Kelson, K.I., Gardner, J.N., Reneau, S.L. and Hemphill-Haley, M.A., 1996, The earthquake potential of the Pajarito fault system, New Mexico, in New Mexico Geological Society Guidebook, 47th Field Conference, Jemez Mountains Region, p. 143-152.

Pantosti, D., Schwartz, D.P. and Valensise, G., 1993, Paleoseismology along the 1980 surface rupture of the Irpina fault; implications for earthquake recurrence in the southern Appennines, Italy: Journal of Geophysical Rserach, v. 98, p. 6561-6577.

Pezzopane, S.K. and Dawson, T.E., 1996, fault displacement hazard; a summary of issues and information, in Whitney, J.E. (ed.), Seismotectonic framework and characterization of faulting at Yucca Mountain, Nevada: report by U.S. Geol. Survey, Denver, CO submitted to US Dept. of Energy, Contract DE-AC04-94AL85000, 3 vols.

Reneau, S.L., 1996, West Jemez geomorphology: unpublished map produced by S.L. Reneau for Los Alamos National Laboratory, FIMAD Plot ID g105108, scale 1:5,686.

Reneau, S.L. and McDonald, E.V., 1996, Landscape history and processes on the Pajarito Plateau, northern New Mexico: Fieldtrip Guidebook, Rocky Mountain cell, Friends of the Pleistocene, 12-15 Sept. 1996, Los Alamos, NM, 179 pp.

Rogers, M.A., 1995, Geologic map of the Los Alamos National Laboratory Reservation: New Mexico Environment Department, Santa Fe, NM.

Taylor, E.M., 1988, Instructions for the soil development index template- Lotus 1-2-3: U.S. Geological Survey Open-File Report 233A.

Vogel, J.C., Fuls, A., Visser, E. and Becker, B., 1993, Praetoria calibration curve for short lived samples: Radiocarbon, v. 35, p. 73-8

Wong, I. and 16 others, 1993, Seismic hazards evaluation of the Los Alamos National Laboratory, Draft Final Report: submitted to Los Alamos National Laboratory by Woodward Clyde Federal Services, June 1, 1993, 3 vols.

Wong, I. and 16 others, 1995, Seismic hazards evaluation of the Los Alamos National Laboratory, Final Report: submitted to Los Alamos National Laboratory by Woodward Clyde Federal Services, 25 Feb. 1995, 3 vols.

APPENDIX A

Report by Dames and Moore Consultants on seismic refraction surveys.

DAMES & MOORE
A DAMES & MOORE GROUP COMPANY

127 South 500 East, Suite 300
Salt Lake City, Utah 84102-1959
801 521 9255 Tel
801 521 0380 Fax
800 432 6375 Tel

September 8, 1997

Mr. Doug Volkman, P.E.
Los Alamos National Lab
3400 Arizona
Los Alamos, NM 87544

Subject: Geophysical Exploration Data and Interpretation
Pajarito Fault Zone Study
Los Alamos National Laboratory (LANL)
Los Alamos, New Mexico

Dear Doug:

Attached are the results of the geophysical exploration conducted for the Pajarito Fault Zone Study. This submittal was prepared pursuant to your request and our proposal dated June 3, 1997. The results are presented in seismic refraction worksheets for each line and a subsurface profile interpretation of the data.

I hope these results prove useful in Jim McCalpin's study. It has been a pleasure working with you, Jamie Gardner, and the staff at LANL. If you have any questions regarding this work please call.

Respectfully submitted,

DAMES & MOORE

Craig V Nelson, C.E.G.
Geoscience Manager

Attachments:
Seismic Line 1 Refraction Worksheet
Seismic Line 1A Refraction Worksheet
Seismic Line 2 Refraction Worksheet
Seismic Line 3 Refraction Worksheet
Seismic Line 4 Refraction Worksheet
Seismic Line 5 Refraction Worksheet
Seismic Line 6 Refraction Worksheet
Figure 1 - Seismic Refraction-Based Subsurface Profile

P:\LOS_ALAM.OS\GEOPHYS\LANL_GEO.RPT

SEISMIC LINE 1

Project	LANL Pajarito Fault Study		
Location	N-S on horst		
Seismograph	EG&G ES-1225		
Channels	12	Spacing (m)	5
Date			
Operator(s)	C. Nelson & J. McCalpin		

North Line

Second Layer Solution

NXC_1	n/a	NXC_2	n/a
NTC_1	n/a	NTC_2	n/a
Calculated NV_1			n/a
Calculated NV_2			n/a
Depth to 2nd layer (m)			n/a

Third Layer Solution

NXC_2	n/a	NXC_3	n/a
NTC_2	n/a	NTC_3	n/a
Calculated NV_3			n/a
Calculated P value			n/a
Depth to 3rd layer (m)			n/a

South Line

Second Layer Solution

SXC_1	5.0	SXC_2	60.0
STC_1	11.3	STC_2	133.8
Calculated SV_1			442
Calculated SV_2			449
Depth to 2nd layer (m)			0.2

Third Layer Solution

SXC_2	60.0	SXC_3	n/a
STC_2	133.8	STC_3	n/a
Calculated SV_3			n/a
Calculated P value			n/a
Depth to 3rd layer (m)			n/a

North Energy Source

	Dist. (m)	Time (ms)	Vel. (m/s)
	0	0	0
1	5	n/a	n/a
2	10	n/a	n/a
3	15	n/a	n/a
4	20	n/a	n/a
5	25	n/a	n/a
6	30	n/a	n/a
7	35	n/a	n/a
8	40	n/a	n/a
9	45	n/a	n/a
10	50	n/a	n/a
11	55	n/a	n/a
12	60	n/a	n/a

South Energy Source

	Dist. (m)	Time (ms)	Vel. (m/s)
	0	0	0
1	5	11.3	442
2	10	23.8	400
3	15	35.0	446
4	20	41.3	794
5	25	48.0	746
6	30	58.8	463
7	35	67.5	575
8	40	79.3	424
9	45	95.5	309
10	50	105.5	500
11	55	121.3	316
12	60	133.8	400

Comments/Interpretation: 1 layer
The scatter of points about the line is likely related to either inhomogeneities within the bedrock. Only one layer, with a velocity of about 450 m/s is resolved from the data from this line.

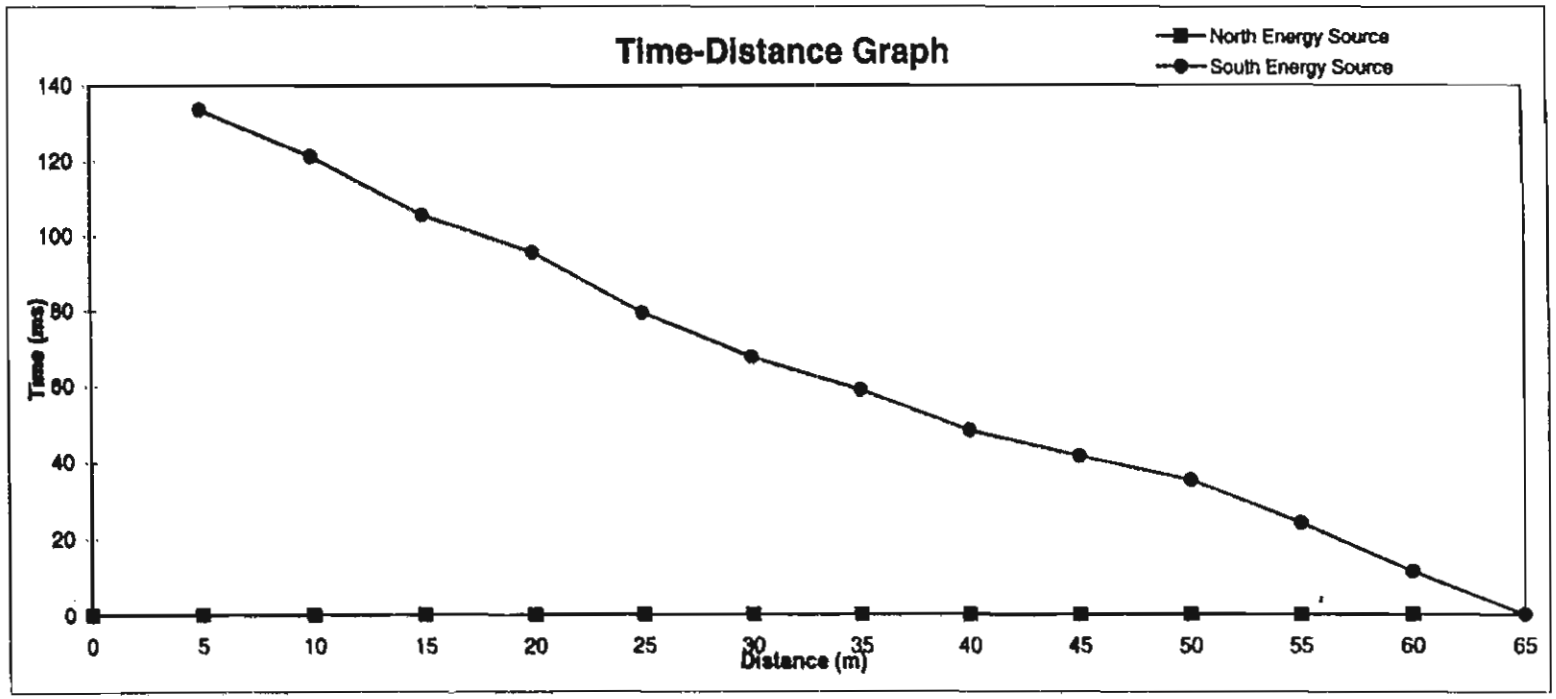

SEISMIC LINE 1A

Project	LANL Pajarito Fault Study		
Location	N-S on horst		
Seismograph	EG&G ES-1225		
Channels	12	Spacing (m)	5
Date			
Operator(s)	C. Nelson & J. McCalpin		

North Line

Second Layer Solution

NXC_1	n/a	NXC_2	n/a
NTC_1	n/a	NTC_2	n/a
Calculated NV_1			n/a
Calculated NV_2			n/a
Depth to 2nd layer (m)			n/a

Third Layer Solution

NXC_2	n/a	NXC_3	n/a
NTC_2	n/a	NTC_3	n/a
Calculated NV_3			n/a
Calculated P value			n/a
Depth to 3rd layer (m)			n/a

South Line

Second Layer Solution

SXC_1	15.0	SXC_2	45.0
STC_1	36.5	STC_2	86.7
Calculated SV_1			411
Calculated SV_2			598
Depth to 2nd layer (m)			3.2

Third Layer Solution

SXC_2	45.0	SXC_3	n/a
STC_2	86.7	STC_3	n/a
Calculated SV_3			n/a
Calculated P value			n/a
Depth to 3rd layer (m)			n/a

North Energy Source

	Dist. (m)	Time (ms)	Vel. (m/s)
	0	0	0
1	5	n/a	n/a
2	10	n/a	n/a
3	15	n/a	n/a
4	20	n/a	n/a
5	25	n/a	n/a
6	30	n/a	n/a
7	35	n/a	n/a
8	40	n/a	n/a
9	45	n/a	n/a
10	50	n/a	n/a
11	55	n/a	n/a
12	60	n/a	n/a

South Energy Source

	Dist. (m)	Time (ms)	Vel. (m/s)
	0	0	0
1	5	12.0	417
2	10	22.0	500
3	15	36.5	345
4	20	42.5	833
5	25	50.7	610
6	30	57.0	794
7	35	65.2	610
8	40	74.7	526
9	45	86.7	417
10	50	n/a	n/a
11	55	n/a	n/a
12	60	n/a	n/a

Comments/Interpretation: 2 Layers

The scatter of points about the straight lines is likely related to either inhomogeneities within the layers, roughness in the contacts between the layers, or both. The data suggest 2 layers with slightly increasing velocity contrast. The surface layer has a velocity of about 400 m/s. The top of the second layer is about 3.2 m in depth with a velocity of about 600 m/s.

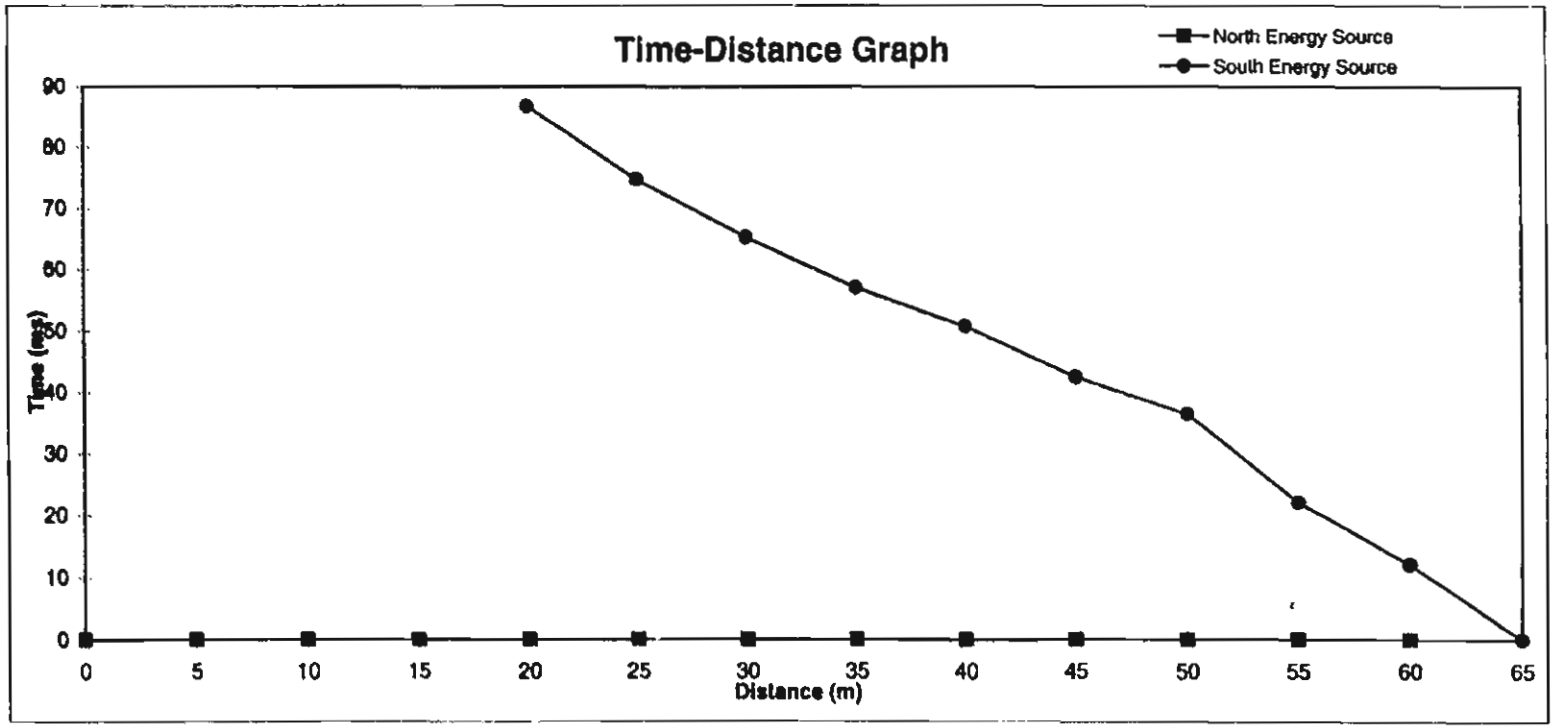

SEISMIC LINE 2

Project	LANL Pajarito Fault Study		
Location	N-S @ E Margin of Graben		
Seismograph	EG&G ES-1225		
Channels	12	Spacing (m)	2
Date	7/11/97		
Operator(s)	C. Nelson		

North Line

Second Layer Solution

NXC_1	6.0	NXC_2	16.4
NTC_1	17.6	NTC_2	31.5
Calculated NV_1			341
Calculated NV_2			748
Depth to 2nd layer (m)			1.8

Third Layer Solution

NXC_2	16.4	NXC_3	24.0
NTC_2	31.5	NTC_3	37.0
Calculated NV_3			1382
Calculated P value			0.6
Depth to 3rd layer (m)			5.7

South Line

Second Layer Solution

SXC_1	4.5	SXC_2	18.0
STC_1	15.0	STC_2	32.5
Calculated SV_1			300
Calculated SV_2			771
Depth to 2nd layer (m)			1.5

Third Layer Solution

SXC_2	18.0	SXC_3	24.0
STC_2	32.5	STC_3	37.0
Calculated SV_3			1333
Calculated P value			0.7
Depth to 3rd layer (m)			5.7

North Energy Source

	Dist. (m)	Time (ms)	Vel. (m/s)
	0	0	0
1	2	6.2	323
2	4	11.7	364
3	6	17.6	339
4	8	21.2	556
5	10	22.2	2000
6	12	24.7	800
7	14	28.1	588
8	16	30.6	800
9	18	32.4	1111
10	20	34.0	1250
11	22	35.8	1111
12	24	36.7	2222

South Energy Source

	Dist. (m)	Time (ms)	Vel. (m/s)
	0	0	0
1	2	6.2	323
2	4	12.5	317
3	6	16.1	556
4	8	18.1	1000
5	10	20.9	714
6	12	24.8	513
7	14	26.7	1053
8	16	29.3	769
9	18	32.2	690
10	20	33.2	2000
11	22	35.1	1053
12	24	36.5	1429

Comments/Interpretation: 3 Layers - horizontal contact
The scatter of points about the straight lines is likely related to either inhomogeneities within the layers, roughness in the contacts between the layers, or both. Calculations suggest that 3 layers of significant increasing velocity contrast are seen. The surface layer has a velocity of 300-350 m/s. The top of the second layer is about 1.7 m in depth with velocity of 750-800 m/s. The top of the third layer is about 5.7 m in depth with a velocity of about 1300-1400 m/s.

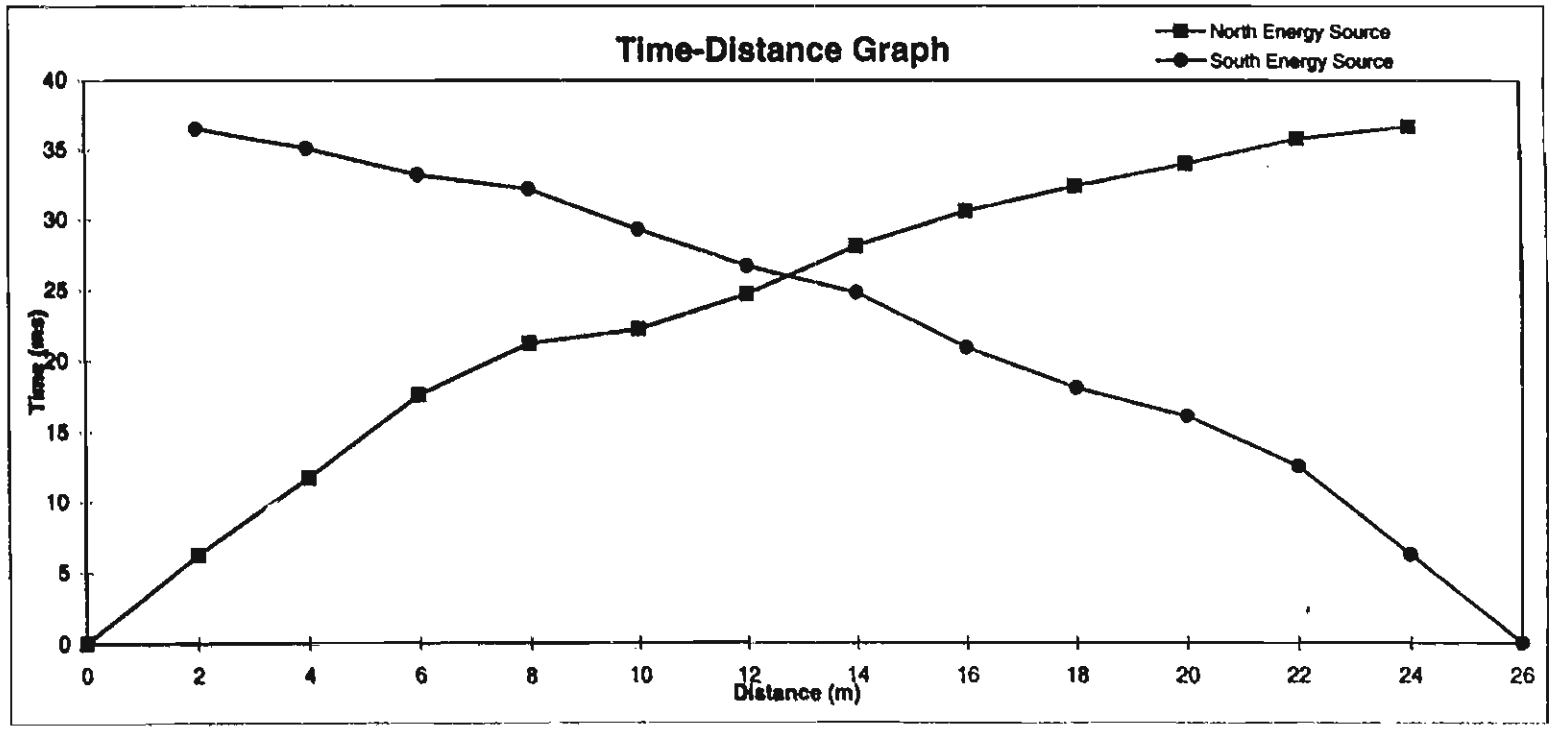

SEISMIC LINE 2A

Project	LANL Pajarito Fault Study		
Location	N-S @ E Margin of Graben		
Seismograph	EG&G ES-1225		
Channels	12	Spacing (m)	2
Date	7/11/97		
Operator(s)	C. Nelson		

North Line

Second Layer Solution

NXC_1	6.0	NXC_2	16.4
NTC_1	17.6	NTC_2	31.5
Calculated NV_1			341
Calculated NV_2			748
Depth to 2nd layer (m)			1.8

Third Layer Solution

NXC_2	16.4	NXC_3	24.0
NTC_2	31.5	NTC_3	37.0
Calculated NV_3			1382
Calculated P value			0.6
Depth to 3rd layer (m)			5.7

South Line

Second Layer Solution

SXC_1	4.5	SXC_2	18.0
STC_1	15.0	STC_2	32.5
Calculated SV_1			300
Calculated SV_2			771
Depth to 2nd layer (m)			1.5

Third Layer Solution

SXC_2	18.0	SXC_3	24.0
STC_2	32.5	STC_3	37.0
Calculated SV_3			1333
Calculated P value			0.7
Depth to 3rd layer (m)			5.7

North Energy Source

	Dist. (m)	Time (ms)	Vel. (m/s)
	0	0	0
1	2	6.2	323
2	4	11.7	364
3	6	17.6	339
4	8	21.2	556
5	10	22.2	2000
6	12	24.7	800
7	14	28.1	588
8	16	30.6	800
9	18	32.4	1111
10	20	34.0	1250
11	22	35.8	1111
12	24	36.7	2222

South Energy Source

	Dist. (m)	Time (ms)	Vel. (m/s)
	0	0	0
1	2	6.2	323
2	4	12.5	317
3	6	16.1	556
4	8	18.1	1000
5	10	20.9	714
6	12	24.8	513
7	14	26.7	1053
8	16	29.3	769
9	18	32.2	690
10	20	33.2	2000
11	22	35.1	1053
12	24	36.5	1429

Comments/Interpretation:
The scatter of points about the straight lines is likely related to either inhomogeneities within the layers, roughness in the contacts between the layers, or both. Calculations suggest that 3 layers of significant increasing velocity contrast are seen. The surface layer has a velocity of about 320 m/s. The top of the second layer is about 1.7 m in depth with a velocity of about 760 m/s. The top of the third layer is about 5.7 m in depth with a velocity of about 1350 m/s.

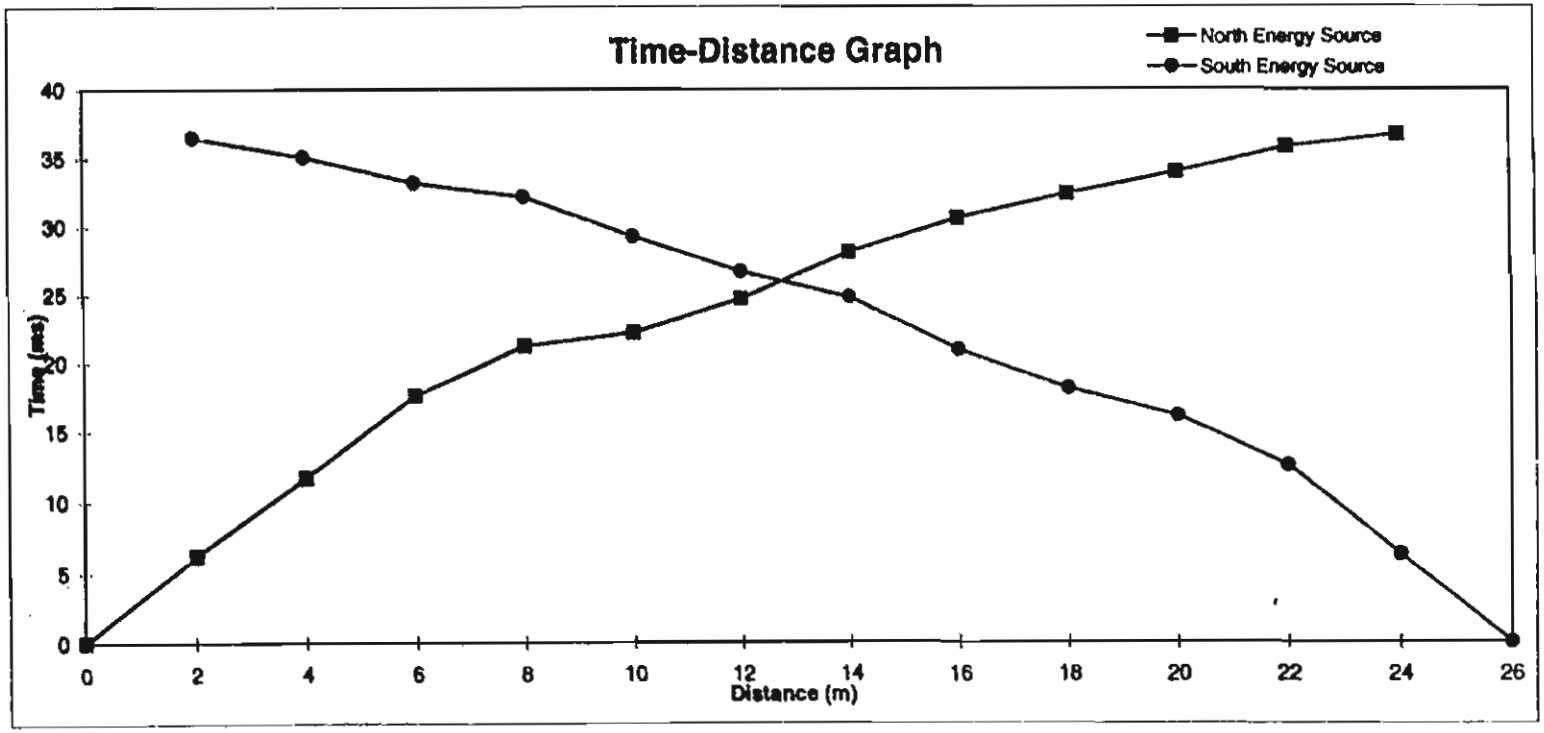

SEISMIC LINE 3

Project	LANL Pajarito Fault Study		
Location	N-S @ East Mid-Graben		
Seismograph	EG&G ES-1225		
Channels	12	Spacing (m)	2
Date	7/11/97		
Operator(s)	C. Nelson		

North Line

Second Layer Solution

NXC_1	4.0	NXC_2	14.0
NTC_1	12.2	NTC_2	37.9
Calculated NV_1			328
Calculated NV_2			389
Depth to 2nd layer (m)			0.6

Third Layer Solution

NXC_2	14.0	NXC_3	24.0
NTC_2	37.9	NTC_3	47.8
Calculated NV_3			1010
Calculated P value			0.3
Depth to 3rd layer (m)			4.9

South Line

Second Layer Solution

SXC_1	4.0	SXC_2	12.0
STC_1	14.9	STC_2	37.0
Calculated SV_1			268
Calculated SV_2			362
Depth to 2nd layer (m)			0.8

Third Layer Solution

SXC_2	12.0	SXC_3	24.0
STC_2	37.0	STC_3	47.2
Calculated SV_3			1176
Calculated P value			0.5
Depth to 3rd layer (m)			4.7

North Energy Source

	Dist. (m)	Time (ms)	Vel. (m/s)
	0	0	0
1	2	6.1	328
2	4	12.2	328
3	6	16.4	476
4	8	20.6	476
5	10	25.5	408
6	12	34.4	225
7	14	37.9	571
8	16	39.3	1429
9	18	40.7	1429
10	20	42.6	1053
11	22	45.3	741
12	24	47.8	800

South Energy Source

	Dist. (m)	Time (ms)	Vel. (m/s)
	0	0	0
1	2	8.8	227
2	4	14.9	328
3	6	20.1	385
4	8	26.0	339
5	10	32.0	333
6	12	37.0	400
7	14	38.1	1818
8	16	40.0	1053
9	18	41.8	1111
10	20	43.1	1538
11	22	45.4	870
12	24	47.2	1111

Comments/Interpretation: 3 Layers - near horizontal contact
The scatter of points about the straight lines is likely related to either inhomogeneities within the layers, roughness in the contacts between the layers, or both. Calculations suggest that 3 layers of significant increasing velocity contrast are seen. The surface la r has a velocity of 250-350 m/s. The top of the second layer is 0.6-0.8 m in depth with a veloc y of 350-400 m/s. The top of the third layer is 4.7-4.9 m in depth with a velocity of about 1000-1200 m/s.

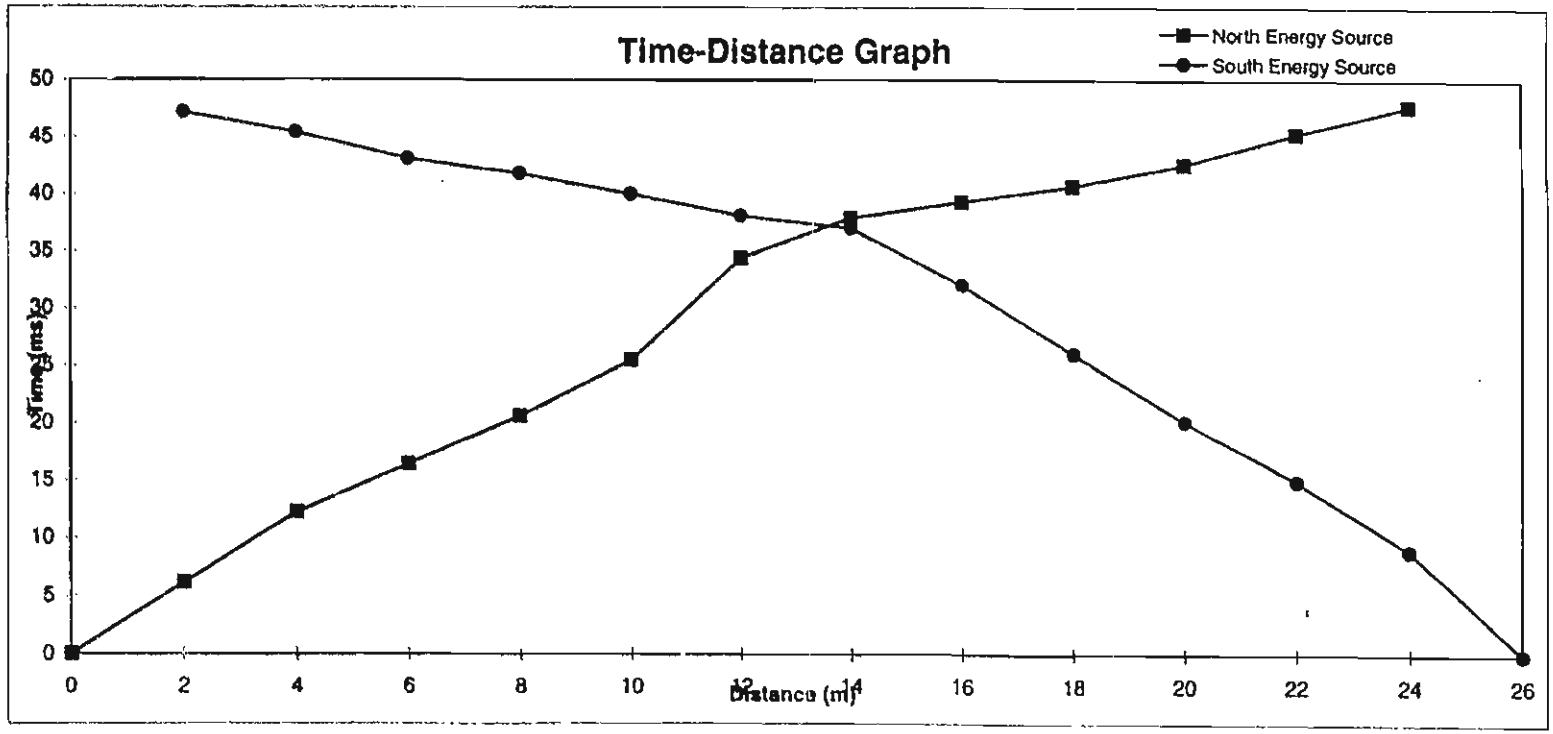

SEISMIC LINE 4

Project	LANL Pajarito Fault Study		
Location	N-S @ West Mid-Graben		
Seismograph	EG&G ES-1225		
Channels	12	Spacing (m)	2
Date			
Operator(s)	C. Nelson & J. McCalpin		

North Line

Second Layer Solution

NXC_1	2.0	NXC_2	18.0
NTC_1	5.7	NTC_2	45.1
Calculated NV_1			351
Calculated NV_2			406
Depth to 2nd layer (m)			0.3

Third Layer Solution

NXC_2	18.0	NXC_3	24.0
NTC_2	45.1	NTC_3	49.1
Calculated NV_3			1500
Calculated P value			0.4
Depth to 3rd layer (m)			6.9

South Line

Second Layer Solution

SXC_1	2.0	SXC_2	16.0
STC_1	6.9	STC_2	44.7
Calculated SV_1			290
Calculated SV_2			423
Depth to 2nd layer (m)			0.4

Third Layer Solution

SXC_2	18.0	SXC_3	24.0
STC_2	44.7	STC_3	50.7
Calculated SV_3			1000
Calculated P value			0.5
Depth to 3rd layer (m)			5.9

North Energy Source

	Dist. (m)	Time (ms)	Vel. (m/s)
	0	0	0
1	2	5.7	351
2	4	8.6	690
3	6	12.7	488
4	8	16.6	513
5	10	20.2	556
6	12	29.8	208
7	14	34.5	426
8	16	38.2	541
9	18	45.1	290
10	20	46.8	1176
11	22	47.3	4000
12	24	49.1	1111

South Energy Source

	Dist. (m)	Time (ms)	Vel. (m/s)
	0	0	0
1	2	6.9	290
2	4	12.8	339
3	6	18.5	351
4	8	24.2	351
5	10	30.0	345
6	12	34.8	417
7	14	37.9	645
8	16	41.7	526
9	18	44.7	667
10	20	46.0	1538
11	22	48.1	952
12	24	50.7	769

Comments/Interpretation: 3 Layers - horitontal to slightly dipping contact
The scatter of points about the straight lines is likely related to either inhomogeneities within the layers, roughness in the contacts between the layers, or both. Calculations suggest that 3 layers of significant increasing velocity contrast are seen. The surface layer has a velocity of 300-350 m/s. The top of the second layer is about 0.3-0.4 m in depth w a velocity of 400-450 m/s. The top of the third layer is 6-7 m in depth with a velocity of 1[illegible]-1500 m/s.

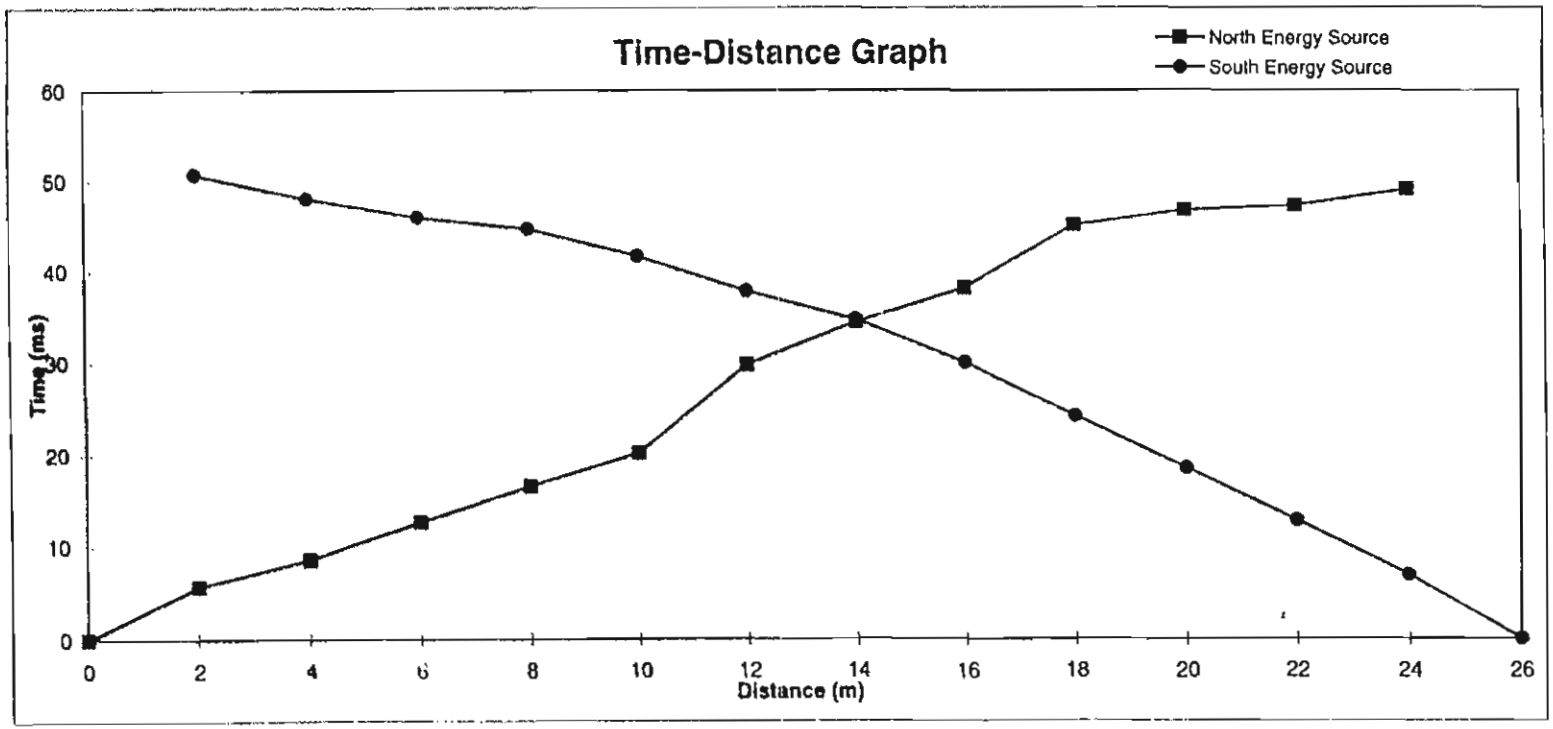

SEISMIC LINE 5

Project	LANL Pajarito Fault Study		
Location	N-S @ West Mid-Graben		
Seismograph	EG&G ES-1225		
Channels	12	Spacing (m)	3
Date			
Operator(s)	C. Nelson & J. McCalpin; C. Nelson & A. Levine		

North Line

Second Layer Solution

NXC_1	3.0	NXC_2	15.0
NTC_1	10.7	NTC_2	42.3
Calculated NV_1			280
Calculated NV_2			380
Depth to 2nd layer (m)			0.6

Third Layer Solution

NXC_2	15.0	NXC_3	36.0
NTC_2	42.3	NTC_3	70.6
Calculated NV_3			742
Calculated P value			0.4
Depth to 3rd layer (m)			4.5

South Line

Second Layer Solution

SXC_1	3.0	SXC_2	18.0
STC_1	16.1	STC_2	52.5
Calculated SV_1			186
Calculated SV_2			412
Depth to 2nd layer (m)			0.9

Third Layer Solution

SXC_2	18.0	SXC_3	36.0
STC_2	52.5	STC_3	70.7
Calculated SV_3			989
Calculated P value			0.7
Depth to 3rd layer (m)			6.4

North Energy Source

	Dist. (m)	Time (ms)	Vel. (m/s)
	0	0	0
1	3	10.7	280
2	6	18.0	411
3	9	25.6	395
4	12	33.0	405
5	15	42.3	323
6	18	45.2	1034
7	21	47.7	1200
8	24	51.5	789
9	27	57.3	517
10	30	62.5	577
11	33	66.8	698
12	36	70.6	789

South Energy Source

	Dist. (m)	Time (ms)	Vel. (m/s)
	0	0	0
1	3	16.1	186
2	6	22.9	441
3	9	28.9	500
4	12	40.7	254
5	15	45.3	652
6	18	52.5	417
7	21	57.0	667
8	24	59.7	1111
9	27	62.8	968
10	30	65.5	1111
11	33	68.1	1154
12	36	70.7	1154

Comments/Interpretation: 3 Layers - contact dipping to South
The scatter of points about the straight lines is likely related to either inhomogeneities within the layers, roughness in the contacts between the layers, or both. Calculations suggest that 3 layers of significant increasing velocity contrast are seen. The surfac layer has a velocity of 150-300 m/s. The top of the second layer is about 0.6-0.9 m in depth with a velocity of 350-450 m/s. The top of the third layer is 4.5-6.4 m in depth with a velocity of 750-1000 m/s.

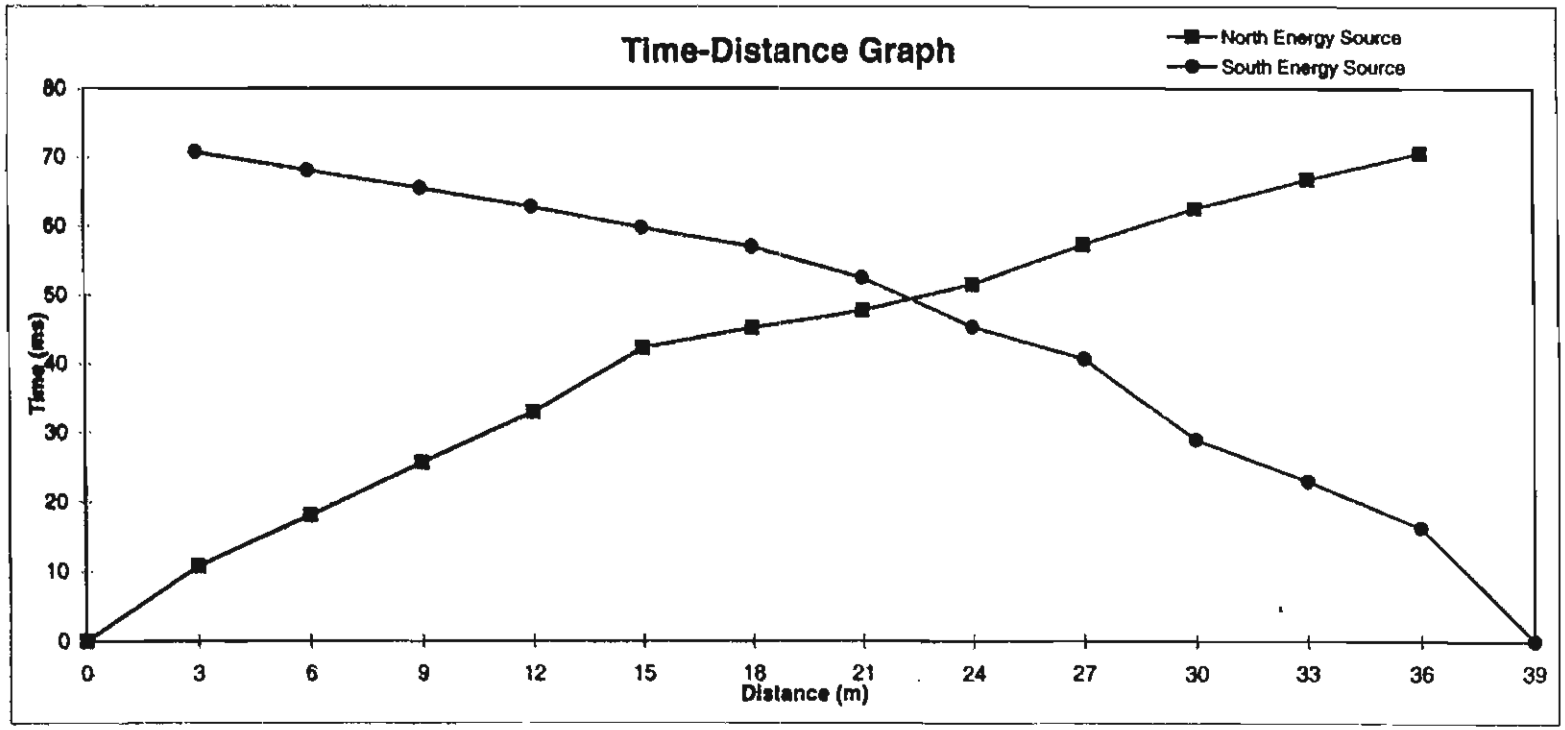

SEISMIC LINE 6

Project	LANL Pajarito Fault Study		
Location	N-S @ Toe perpendicular to Trench SH-5		
Seismograph	EG&G ES-1225		
Channels	12	Spacing (m)	2
Date	7/11/97		
Operator(s)	C. Nelson & A. Levine		

North Line

Second Layer Solution

NXC_1	2.0	NXC_2	24.0
NTC_1	8.9	NTC_2	41.2
Calculated NV_1			225
Calculated NV_2			881
Depth to 2nd layer (m)			0.7

Third Layer Solution

NXC_2	24.0	NXC_3	n/a
NTC_2	41.2	NTC_3	n/a
Calculated NV_3			n/a
Calculated P value			n/a
Depth to 3rd layer (m)			n/a

South Line

Second Layer Solution

SXC_1	8.0	SXC_2	24.0
STC_1	24.1	STC_2	41.8
Calculated SV_1			332
Calculated SV_2			904
Depth to 2nd layer (m)			2.7

Third Layer Solution

SXC_2	24.0	SXC_3	n/a
STC_2	41.8	STC_3	n/a
Calculated SV_3			n/a
Calculated P value			n/a
Depth to 3rd layer (m)			n/a

North Energy Source

	Dist. (m)	Time (ms)	Vel. (m/s)
	0	0	0
1	2	8.9	225
2	4	12.3	588
3	6	14.8	800
4	8	16.6	1111
5	10	19.8	625
6	12	24.8	400
7	14	26.9	952
8	16	30.5	556
9	18	33.8	645
10	20	36.4	714
11	22	39.0	769
12	24	41.2	909

South Energy Source

	Dist. (m)	Time (ms)	Vel. (m/s)
	0	0	0
1	2	6.5	308
2	4	12.8	317
3	6	18.8	333
4	8	24.1	377
5	10	27.7	556
6	12	29.7	1000
7	14	31.7	1000
8	16	32.5	2500
9	18	33.9	1429
10	20	36.6	741
11	22	39.4	714
12	24	[illegible]	833

Comments/Interpretation: 2 Layers - contact dipping to south
The scatter of points about the straight lines is likely related to either inhomogeneities within the layers, roughness in the contacts between the layers, or both. A 2-layer solution indicates that surface layer has velocities in the range of 200 to 350 m/s and the deeper layer has velocities in the range of 600 to 900 m/s. The calculations indicate the contact between the layers is 0.7 (north) to 2.7 m (south) below the surface and dips to the south at 7 degrees.

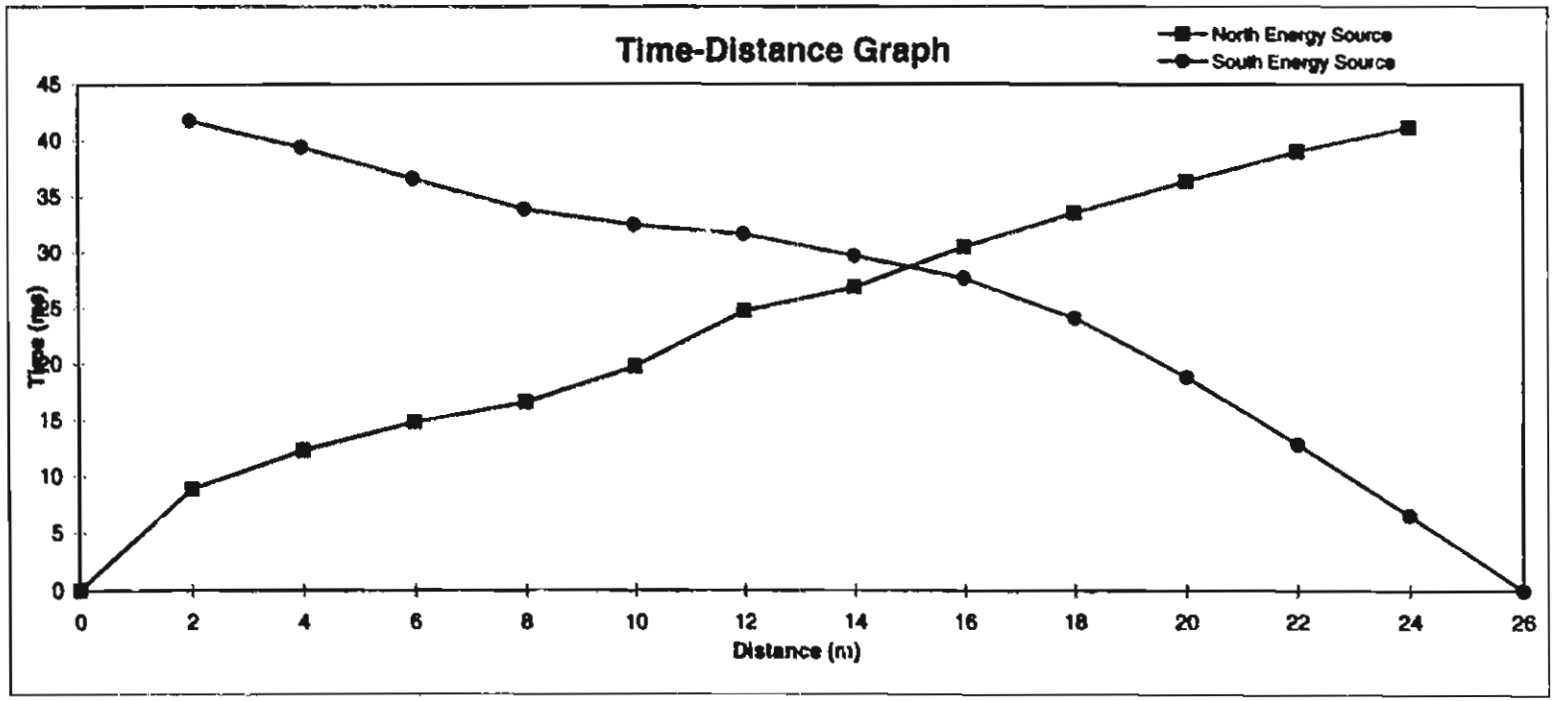

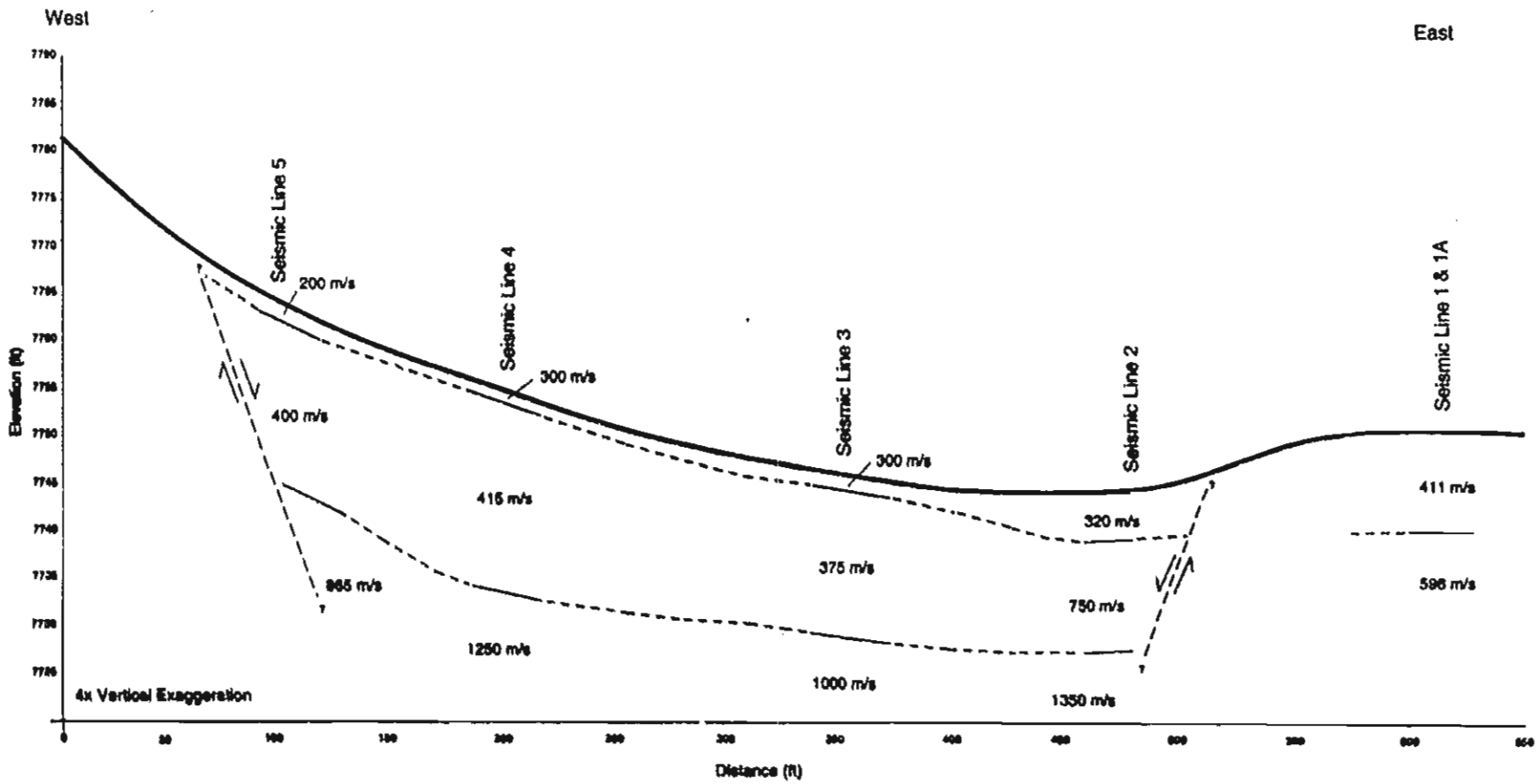

DAMES & MOORE	Los Alamos National Lab Pajarito Fault Study
Figure 1	Job Number: 30822-102-031
Seismic Refraction-Based Subsurface Profile	

P:\Los_ala.mos\Geophysl\Xsectest

APPENDIX B

**Report by Eric McDonald, Desert Research Institute,
on detailed soil profile descriptions and
Soil Development Index (SDI) calculations.**

SOIL STRATIGRAPHY AND PEDOLOGIC AGE ESTIMATES FOR SEISMIC HAZARD TRENCH INVESTIGATIONS FY 1997

DRAFT REPORT

Prepared by
Dr. Eric McDonald
Quaternary Sciences Center
Desert Research Institute
Reno, NV 89512

4/98

EXECUTIVE SUMMARY

This report summarizes the technical approach, soil stratigraphy, and age estimations for surface and buried soils exposed in Seismic Hazards Investigation Trenches 3, 4, 5, 6, and 7 excavated near Los Alamos National Laboratory (LANL) during July 1997. Morphologic information and radiometric ages for soils formed in the vicinity of LANL were used to develop and refine a soil chronofunction using a soil development index approach. Application of this soil chronofunction to surface and buried soils exposed within each trench provides reasonable age estimations for soil stratigraphy and related structural and geomorphic features exposed in these trenches. Soil ages calculated here are generally consistent with ages derived from radiocarbon and thermoluminescence dating of material sampled from these trenches.

INTRODUCTION

This report provides final age estimates for soil stratigraphy exposed in the 1997 Seismic Hazard Investigation Trenches 3, 4, 5, 6 and 7, documentation regarding the overall approach used for calculating Profile Development Index (PDI) age estimates, and detailed descriptions and discussion of the soil stratigraphy for each trench. Results of soil age estimates and the interpretation of soil stratigraphy for each trench are based on detailed regional studies of soils, geomorphic processes, and late Quaternary geology that was conducted during the last four years around Los Alamos National Laboratory (hereafter the Laboratory) in support of the Seismic Hazard Investigations program at the Laboratory.

The basic premise of using soils to provide age estimates for soils and associated stratigraphy is that soils generally develop in a systematic and progressive pattern over time. The rate and trends in soil formation can be determined by examining a sequence of soils on well dated surfaces. For this study, multiple soils develop in dated surface surfaces in the vicinity of the Laboratory (discussed below) are used to develop a soil chronofunction. A soil chronofunction is a simple linear equation that relates the degree of soil development with time. The soil chronofunction developed exclusively for application to soils around the Laboratory was used to calculate ages of surface and buried soils exposed in the trenches excavated in FY 1997 in support of Seismic Hazard Investigations at the Laboratory.

METHODS

Soil morphology was described according to the standard methods and nomenclature of the Soil Survey Staff (1981). Two or three soil-stratigraphic sections were described in each trench. The location of each profile was chosen based upon vertical soil sections that provided (1) key soil-stratigraphic information regarding any critical structural features and/or (2) the most complete, vertical record of deposition and soil formation. Soil profiles are identified by the trench number and the location a' g the horizontal grid (i.e. T3 P8.0 is a soil profile described in trench 3 at the 8.0 m mark). Descriptions reflect soil morphology exposed within about 0.5 m to either side of the horizontal position.

Soil morphology was quantified using the Soil Development Index (SDI) procedures according to Harden (1982), Harden and Taylor (1983), and Taylor (1988). Calculation of SDI values is based on a conversion of soil morphology (i.e. color, structure) into numerical data to enable semiquantitative comparisons of the degree of soil development. Points are assigned to each property based on the difference between the described soil property and the parent material. Points for each property are normalized to a percentage scale of maximum property development based on comparison of each property to a published or conceptual maximum value of development for each particular property. Maximum soil property values from Taylor (1988) were used to normalize soil property values in this study. Normalized property values are summed for each horizon and averaged yielding a Horizon Development Index (HDI) value that provides an estimate of overall horizon development relative to a conceptual idea of maximum possible horizon development. HDI values are multiplied by horizon thickness and summed for each profile yielding a Profile Development Index (PDI) value for that profile. PDI values provide a means of relative comparison among soils within a given sequence and can be used to develop a soil chronofunction. The chronofunction can be inverted to provide soil age estimates based on calculated PDI values.

PDI values for trench soils were calculated for all described soils using morphologic properties of rubification, texture, structure, dry and moist consistence, and argillans (clay skins). An important consideration in applying the SDI is determining the soil parent material values. Parent material values for each profile were adjusted to reflect vertical changes in texture, consistence, and color of the inferred parent material that correspond to vertical stratification associated with colluvial deposition. For most of the buried soils in this study, the weakly- to non-altered colluvium common to the surface of many of the trenches was used as a starting point for assessing parent material (discussed in more detail below). PDI values were calculated to the base of each recognized soil, with the summed PDI of the entire overlying soil column (if more than one soil) used to calculate soil age. The PDI based soil age therefore reflects the total time required to develop the overlying soil stratigraphy (i.e. the overlying stack of buried soils) down to a specific depth (the base of each buried soil). This assumes that there is no missing soil between the surface and the base of each soil. This is probably not realistic because it is possible that some soils are either partially truncated or completely either missing from within any trench section. In essence these PDI based ages should be considered minimum ages if any soil might have been eroded or truncated within the total stack of soils exposed within each trench.

DEVELOPMENT OF A SOIL CHRONOFUNCTION FOR DETERMINING PEDOLOGIC AGES

Soil ages can be estimated based on a systematic increase in soil profile morphology using simple linear regression analysis of logarithmic relationships between PDI values and soil ages (Fig.1; Table 1). Several different methods of linear statistical analysis have been employed for evaluating rates of soil development based on SDI values and to account for poor age control of studied soil surfaces (Swezer et al., 1988; Harden 1990; Harden et al., 1991). For the purpose of this study, simple linear regression was used to develop a soil chronofunction based on time related increases in PDI values and to provide age estimates for non-dated surfaces. Justification for a straightforward application of linear regression is the fact that the chronosequence used in this study is extremely well dated to the extent that each soil used in the chronofunction is directly dated as opposed to being based on correlative ages (soil dates based on correlation to dated soils or deposits in other areas).

Soils Used in Chronofunction

PDI values from 20 soils were used to develop the soil chronofunction (Table 1; Figure 1). These included soils formed on the Qt8, Qt7, Qt6, and Qt2 terraces in Rendija Canyon and soils formed in colluvium overlying the El Cajete pumice near the northwest corner of the Laboratory (just west of S-Site, TA-16). Between 3 and 5 soils are included from each surface (Table 1).

Soils used in the chronofunction represent the best combination of dated soils and lack of variation in the profiles due to factors such as erosion. Soils formed on the Qt8, Qt7, and Qt6 terraces are directly dated by radiocarbon analyses on charcoal from underlying sediments (Table 1). The soils formed in a layer of colluvium overlying the El Cajete pumice were originally thought to represent soil formation that has occurred within the last 50 to 60 ka (McDonald et al., 1996; Reneau and McDonald, 1996). A new radiocarbon date of about 40.5 $\pm$ 1.2 ka (sample WJR-10, Reneau unpublished) and a ^{21}Ne cosmogenic depth profile through this soil that yielded an exposure age of 44 $\pm$ 11 ka (Phillips et al., 1998). These ages suggest that this soil could be as young as about 40 ka, indicating a possible soil age range of 40 to 60 ka;, An average age of 50 ka therefore was used in the chronofunction for soils formed in the post-El Cajete colluvium.

An age of 144 $\pm$ 17 ka was estimated for a Qt2 terrace soil using a cosmogenic ^{21}Ne depth profile (Phillips, et al., 1998) and this dated terrace was used in the soil chronofunction. Because dating soil surfaces using ^{21}Ne is considered an experimental technique, there is some concern in using these dates as part of the soil chronofunction. The use of these dates can be justified in two ways. First, the quality of the ^{21}Ne depth profile indicates that this may be a reasonable date for this soil. Specifically, the ^{21}Ne results exhibited a near-uniform, exponentially decreasing profile pattern is consistent with expected trends for a soil-depth function. A near-uniform depth profile indicates that there was not excessive soil mixing due to bioturbation and that the resulting ^{21}Ne depth profile provides a reasonable numerical age for the Qt2 surface. Second, a 21Ne age range of 144 $\pm$ 17 ka for the Qt2 overlaps and agrees with a PDI age of 124 $\pm$ 24 ka for the Qt2 soils based on a soil chronofunction developed using only dated Qt8, Qt7, Qt6, and post-El Cajete soils (i.e. same chronofunction but without inclusion of the Qt2 soils). In other words, the PDI and ^{21}Ne dates are within reasonable agreement justifying the use of the ^{21}Ne dated soils in the chronofunction. Inclusion of the Qt2 soils

provides a better 'anchor' for the chronofunction for estimating the age of older soils. By comparison, excluding the Qt2 soil data favors younger soils (i.e. Holocene soils).

Previous versions of the chronofunction developed from Rendija Canyon soils (McDonald et al., 1996; Reneau and McDonald, 1996) included PDI values from soils developed in the colluvial cap that overlies the Qt4 and Qt2 soils. These soils were excluded in this data set because it is not clear when soil formation may have started. Radiocarbon ages and soil-stratigraphy suggests that soil formation in these colluvial deposits may have started between about 12.8 ka to 7.7 ka (age of oldest Qt6 not covered by colluvium of similar character).

Testing the Precision and Accuracy of the Soil Chronofunction

The soil chronofunction can be used to calculate approximate ages for other soils if environmental conditions are generally similar (i.e. parent material, climate, vegetation, topography). The soils exposed in the trenches have formed under similar environmental conditions as those used to construct the chronofunction. The one major exception is that the trench soils have formed primarily from colluvium whereas most of the chronofunction soils have formed primarily from fluvial deposits, although the post-El Cajete soil and the upper part of the Qt2 soils have formed from colluvium. Poorly weathered material within the surface soil of each trench was generally used as a starting point for parent material values. Basically, soil properties used in PDI calculations (consistence, structure, argillans)will represent soil formation following colluviation because these properties will not survive colluviation. Color and texture could conceivably be influenced by colluviation, especially if colluvial sediment is derived from the erosion of older, well developed soils just upslope of trench sites and without significant winnowing of clay and fine silt by surface runoff. Examination of soils formed in colluvium and/or alluvium at other areas on the Pajarito Plateau that are downslope of older, well developed soils, however, does not indicate that much, if any, of the character of the eroded soils is preserved within the colluvium (Reneau and McDonald, 1996). Not accounting for the reworking of older soils may result in inflation of PDI values, although it can be argued that the magnitude of inflated PDI values will be minimal. This is because the PDI values are based on an averaging of all soil changes and will tend to lessen potential impacts of inherited contributions to soil properties.

Given this variation in parent material and the general uncertainties in the application of a soil chronofunction for providing age estimates, it is desirable to have some means of determining the accuracy and precision of age estimates generated by a soil chronofunction. Confidence intervals for PDI age estimates were calculated based on linear relations between PDI values and best age estimates for chronosequence soils. At a 95% confidence level variation in age estimates is +/- 0.07 of the log of the estimated soil age. This represents an estimated error of -16% and +19% of the age calculated using the soil chronofunction. A means to test this confidence level is available given the abundance of relatively well dated soils within the Laboratory. Soil ages based on the soil chronofunction average within $\pm$ 18% of the 'true' soil age for soils dated radiometrically (^{14}C and ^{21}Ne) and formed in both colluvium and alluvium (n=23 soils; McDonald unpublished; Reneau and McDonald, 1997; Table 2). In other words, testing PDI-based age estimates with ages for dated soils (soils not used in the chronofunction) indicates that the PDI-based ages are within about 18 % of the dated soil age. This agrees well with the confidence interval estimates above suggesting that

the soil ages for buried soils with the trenches are likely to be within 20% of the actual soil age (except where trench soils have been truncated or stripped by erosion).

PDI AGE ESTIMATES FOR TRENCHES 3, 4, 5, AND 7

PDI-based age estimates (incl[illegible]g lower and upper range for each age) for soils exposed in trenches 3, 4, 5, 6, and 7 are presented in Table 3. The current age estimates are generally older than the preliminary PDI age estimates presented prior to the trench review in September 1997. The difference in ages primarily reflects redevelopment of the soil chronofunction using recent radiocarbon and cosmogenic nuclide dates for soils used in the soil chronofunction (Fig 1).

DESCRIPTION OF SOIL STRATIGRAPHY EXPOSED IN TRENCHES

The following text provides a general overview of the soil stratigraphy described in trenches 3, 4, 5, 6, and 7. Schematic diagrams showing representative morphology for each profile are shown in Figures 3 through 12 and a summary of soil morphology is presented in Table 4. Soil horizon designations (labeled 'Horizon' in Fig. 3 – 12; Table 4) vary from soil designations displayed on the trench logs. This partially reflects different opinions regarding interpretation of soil features and soil-geomorphic processes and the fact the trench unit designations combine soil, sedimentologic, and structural features. Soil horizon designations used in this report reflect interpretation of soil features and processes based on Laboratory-wide studies of soils and soil forming processes.

Vertically stacked sequences of multiple buried soils are exposed in each trench (designated by the numbered 'b' at the end of each horizon designation). Buried soils are former surface soils that have been buried by subsequent periods of colluvial deposition. In most cares, the top of each buried soil is recognized as an increase in B horizon properties, especially an increase (relative to the overlying horizon) in argillans (vertically translocated clay, also called clay skins), soil redness, and the strength of soil structure. In other words, the top a buried soil is often recognized as the top of the strongest B horizon of each buried soil. When soils form at the land surface, B horizons normally lie below the surface and are usually overlain by A and AB transitional horizons. In many cases, these former surface horizons are preserved within the base of the overlying soil, but the original morphology of these soils has been considerably altered by subsequent soil forming processes. As a result, the overlying soil is pedogenetically 'welded' to the underlying soil.

Most of the soils exposed in these trenches contain a similar range of genetic horizons. A horizons are horizons at the top of the soil profile and usually contain slightly higher concentrations of disseminated organic matter that imparts a slightly darker coloration (i.e. lower soil chroma and value). BA and AB horizons are transistional horizons that have dominant properties that are similar to both A and underlying B horizons. Bw horizons are weakly developed B horizons that have either redder soil color (higher value and chroma) due to the accumulation of iron (oxy)hydroxides relative to the parent material and/or development of soil structure. Bt horizons are horizons that are (1) usually better developed relative to Bw horizons and (2) have noticeable accumulation of translocated clay (argillans). In these soils argillians are commonly developed as coatings on pedfaces or lining pores. BE horizons are former E horizons that have had B horizon properties overprinted on them from subsequent soil

formation related to burial. The E horizon is usually very light colored (chroma ≤ 2) due to the lack of appreciable accumulation of either organic matter of iron (oxy)hydroxides on minerla particles. Skeletans, bleached quartz or feldspar grains) are common along pedfaces in E horizons. BC or CB horizons are transistional horizons that have dominant properties that are similar to both B and C horizons. C horizons are poorly altered to unaltered horizpns that may represent the the properties of the original soil parent material.

Trench 3

Three profiles where described at Trench 3. Profile 9.6 represents the most complete section of soils exposed in this trench. Profile 8.0 and Profile 5.4 were described to supplement soil stratigraphy identified in Profile 9.0 and to provide direct soil-stratigraphic information for interpretation of possible fault related structures exposed in the trench.

Profile 9.6: Soil characteristics were described to a depth of 450 cm (Fig. 3). At least 5 buried soils are recognized in addition to the surface soil.

Surface Soil: The surface soils is thin (16 cm), light colored (10YR 7/2), and is weakly developed (all colors are dry matrix colors). This soil has formed in poorly altered colluvium. This soil coincides with the unit 15 on the trench 3 log. Soil structure is largely moderate to weak subangular blocky. Soil color is 10YR 5/3. A PDI age of 1.0 to 1.4 ka was estimated for the base of this soil.

Buried Soil b1: The first buried soil is a thin (23-59 cm) well developed soil. This soil coincides with the unit 14 on the trench 3 log. The top of the soil in denoted by a noticeable increase in red color (7.5YR 6/3), structure, and development of argillans relative to the surface soil. The Btb1 horizon appears to have been partially altered in association with formation of the surface soil. Dry soil color ranges from 7.5YR 6/3 to 7/2. Soil structure largely consist of moderate and weak prismatic that parts to moderate and weak angular and subangular blocky. Argillan development is strong consisting of nearly continuous to many coatings along pedfaces (best along prismatic pedfaces) and lining pores. Skeletans occur along prismatic pedfaces in the BEtb1. A PDI age of 6.3 to 8.8 ka was estimated for the base of this soil. A TL date of 69 $\pm$ 6 ka (PF97-4) was obtained from the base of this soil unit near profile 8.0. Based on the overall degree of soil formation, this TL date appears to be too old.

Buried Soil b2: The second buried soil is a well developed soil that is lies between 46 to 125 cm below the surface. This soil coincides with unit 13 on the trench 3 log. The top of the soil in denoted by the presence of two BE horizons (BEt1b2, Bet2b2). Dry soil color ranges from 7.5YR 6/4 to 6/6. Soil structure largely consist of moderate and weak prismatic that parts to moderate and weak angular and subangular blocky. Argillan development is strong ranging from nearly continuous to common coatings along pedfaces (best along prismatic pedfaces) and lining pores. Skeletans occur on prismatic pedfaces in both BE horizons. The presence of the two BE horizons suggests that the top of this soil is largely intact. BE horizons have been interpreted as the tops of buried soil examined elsewhere around the Laboratory. A PDI age of 36 to 51 ka was estimated for the base of this soil.

Buried Soil b3: The third buried soil is a moderately developed soil that is lies between 125 to 214 cm below the surface. This soil coincides with units 12a, 9, and 7a on the trench 3 log. The soils is largely formed in colluvium. The top of the soil is denoted by the presence of a moderately developed Bt horizon that has slightly better development of argillans and redder color relative to the overlying horizon. The true top of this soil may be within the lower zone of the soil b2, but any features of former A and near-surface horizons have been overprinted by subsequent soil development. Dry soil color ranges from 7.5YR 5/4 to 10YR 7/3. Soil structure largely consist of moderate and weak subangular blocky. Argillan development is strong ranging from nearly continuous to common coatings along pedfaces (best along prismatic pedfaces) and lining pores. Fragments of tuff and pumice are scattered throughout the soil. A PDI age of 83 to 118 ka was estimated for the base of this soil. Two TL dates of 106 $\pm$ 9 ka (PF97-2) and 94 $\pm$ 9 ka (PF97-3) were obtained from the base of this soil. These dates are from location on either side of profile 9.6. The TL dates are generally consistent with the PDI age for the base of this soil.

Buried Soil b4: The fourth buried soil is a moderately developed soil that is lies between 214 to 308 cm below the surface. This soil coincides with unit 6 on the trench 3 log. Soil b4 has largely formed in pumice that retains primary depositional features. The top of the soil is denoted by the presence of a weakly to moderately developed Bt horizon that has formed in the top of a pumice layer. The top of the original b4 soil appears to have been partially stripped by erosion before formation of soil b3. Evidence for this is the abundance of pumice is considerably higher in the Bt1b4 (70-80% volume) relative to the BCb3 (5-15% volume). Bioturbation would likely result in the mixing of pumice into the soil overlying the pumice. Further, cross-cutting relations between unit 6 and overlying units indicates that pedogenesis in unit 6 probably pre-dates overlying units. Dry soil color ranges from 7.5YR 6/4 to 6.5/4. The soil is largely structureless (massive). Argillan development ranges from nearly continuous to common coatings on pumice and gravel and bridges. Clay lamallae occur in the Bt3b4 horizon. A PDI age of 106 to 150 ka was estimated for the base of this soil. This age should be considered a minimum because the top of the soil, and any overlying soil, may have been removed from erosion.

Buried Soil b5: The fifth buried soil is a weakly developed soil that is lies between 308 to 450 cm below the surface. This soil coincides with units 5, 4, and 3 on the trench 3 log. Soil b5 has formed in sandy-pebble stratified alluvium. The top of the soil is denoted by the contact between the pumice and underlying stratified alluvium. Pedogenic alteration may be genetically related to soil b4, rather than representing a separate period of soil formation. Dry soil color ranges from 7.5YR 54 to 5/4. The soil is largely structureless (massive, single grain in places). Argillan development ranges from nearly continuous to few coatings on gravel, pumice, and along fractures, and bridges. The base of this unit was note exposed at the trench bottom. A PDI age of 135 to 191 ka was estimated for the base of this soil. This age should be considered a minimum because the top of the soil, and any overlying soil, may have been removed from erosion.

Profile 8.C: Soil characteristics were described to a depth of 284 cm (Fig. 4). At least 4 buried soils are recognized in addition to the surface soil.

Surface Soil: The surface soils is thin (22 cm deep), light colored (10YR 7/3), and is weakly developed. This soil has formed in poorly altered colluvium. This soil coincides with unit 15 on the trench 3 log. Soil structure is weak subangular blocky and argillans were not present.. Soil structure is largely moderate to weak subangular blocky. Soil color ranges from 10YR 5/2 to 7.5YR 7/3. A PDI age of 0.6 to 0.9 ka was estimated for the base of this soil.

Buried Soil b1: The first buried soil is a thin (22-77 cm) well developed soil. This soil coincides with the unit 14 on the trench 3 log. The top of the soil in denoted by a noticeable increase in red color (7.5YR 6/3), structure, and development of argillans relative to the surface soil. The Btb1 horizon appears to have been partially altered in association with formation of the surface soil. Dry soil color ranges from 7.5YR 5/4 to 6/4. Soil structure largely consist of strong and moderate prismatic that parts to moderate and weak angular and subangular blocky. Argillan development is strong consisting of nearly continuous to many coatings along pedfaces (best along prismatic pedfaces) and lining pores. Skeletans occur along prismatic pedfaces in the BEtb1. A PDI age of 17 to 24 ka was estimated for the base of this soil. A TL date of 69 $\pm$ 6 ka (PF97-4) was obtained from colluvium near the base of this soil. This TL date appears to be too old based on the degree of soil formation in soil b1 and the surface soil.

Buried Soil b2: The second buried soil is a thin (36 cm) well developed soil that is lies between 77 to 113 cm below the surface. This soil coincides with unit 13 on the trench 3 log. Unlike soil b2 in profile 9.6, the top of soil b2 in this profile does not have BE horizons; however, soil b2 can be clearly traced between the two profiles. Dry soil color ranges from 7.5YR 6/4 to 6/6. Soil structure largely consist of weak prismatic that parts to moderate and weak subangular blocky. Argillan development is strong ranging from nearly continuous to common coatings along pedfaces (best along prismatic pedfaces) and lining pores. A PDI age of 32 to 45 ka was estimated for the base of this soil.

Buried Soil b3: The third buried soil is a moderately developed soil that is lies between 113 to 205 cm below the surface. This soil coincides with units 12a, 9, and 7a on the trench 3 log. The top of the soil is denoted by the presence of a moderately developed Bt horizon that has slightly better development of argillans relative to the overlying horizon. The true top of this soil may be within the lower zone of the soil b2, but any features of former A and near-surface horizons have been overprinted by subsequent soil development. Dry soil color ranges from 7.5YR 5.5/4 to 6/4. Soil structure largely consist of moderate and weak subangular blocky. Argillan development is strong ranging from nearly continuous to common coatings along pedfaces (best along prismatic pedfaces) and lining pores. A PDI age of 68 to 97 ka was estimated for the base of this soil. Two TL dates of 106 $\pm$ 9 ka (PF97-2) and 94 $\pm$ 9 ka (PF97-3) were obtained from the base of this soil. The first date is near the 8.0 profile. The TL dates are generally consistent with the PDI age for the base of this soil.

Buried Soil b4: The fourth buried soil is a moderately developed soil that is lies between 205 to 284 cm below the surface. This soil coincides with unit 6 on the trench 3 log. The top of the soil is denoted by the presence of a weakly to moderately developed Bt horizon that is has formed in the top of a pumice layer. Soil b4 has largely formed in pumice

that retains primary depositional features. The top of the soil is denoted by the presence of a weakly to moderately developed Bt horizon that has formed in the top of a pumice layer. The top of the original b4 soil appears to have been partially stripped by erosion before formation of soil b3. Evidence for this is the abundance of pumice is considerably higher in the Bt1b4 (70-80% volume) relative to the Bt3b3 (20-30 % volume). Bioturbation would likely result in the mixing of pumice into the soil overlying the pumice. Further, cross-cutting relations between unit 6 and overlying units indicates that pedogenesis in unit 6 probably pre-dates overlying units. Evidence for this is the abundance of pumice is considerably higher in the Bt1b4 (70-80% volume) relative to the Bt3b3 (20-30 % volume). Bioturbation would likely result in the mixing of pumice into the soil overlying the pumice. Dry soil color is 7.5YR 6/4. . Soil structure largely consist of weak subangular blocky. Argillan development ranges from nearly continuous to common coatings on pumice and gravel and bridges. Abundant to scattered fragments of tuff occur throughout soil b4, but generally increase in abundance toward the base of the soil. A PDI age of 98 to 139 ka was estimated for the base of this soil. This age should be considered a minimum because the top of the soil, and any overlying soil, may have been removed from erosion.

Profile 5.4: Only the surface soil was described at this trench location (Fig. 5). The description is from the north side of the trench. This site was chosen to enhance interpretation of possible fault related features exposed in the eastern third of the trench. Soil characteristics were described to a depth of 79 cm

Surface Soil: The surface soil is thin (49 cm deep) and weakly developed. This soil coincides with unit 15b on the trench 3 log. This soil has formed in poorly altered colluvium. Dry soil color ranges from 10YR 7/2 to 8/2. Soil structure is largely weak subangular blocky. Argillans are not present. A PDI age of 1.9 to 2.7 ka was estimated for the base of this soil.

Summary of Trench 3 Soil Stratigraphy: The PDI age for the surface soil ranges from 0.6 to 2.7 ka. PDI ages for this soil are consistent with a radiocarbon date of 1.3 ± .08 ka from trench 3 (WJR-18; Beta-108400). The PDI age for soil b1 ranges from 6 to 24 ka. The range in age partially reflects the differences in total soil thickness (77 vs. 46 cm) which may be due to truncation of the upper part of the soil and/or pedogenic overlap with the underlying soil.

The morphology and stratigraphic position of soil b1 (and b2?) is somewhat similar to the pre-El Cajete soil (a distinct soil that underlies the El Cajete pumice) described elsewhere across the Laboratory (McDonald, et al., 1997; Reneau and McDonald, 1997). The overall character of the morphology of soil b1, however, does not strongly support a possible correlation. If true, then the TL age of about 69 ka is too old for this soil. Support for this interpretation is a TL date of 43 ka for a near surface soil in Trench 4 which also appears to be to old (described below). Alternately, the lack of El Cajete pumice in either of the bI or b2 soil in trench 3 and the TL age of about 69 ka from the base of soil b1 would be consistent with this soil being correlative with the pre-El Cajete soil. If true, then the PDI ages for these soils are at least 50 to 60 kyrs too young. The interpretation that the TL age is too old is the preferred one. The PDI age for soil b2 ranges from 32 to 51 ka. The PDI age for soil b3 ranges from 68 to 118 ka. Two TL dates of 106 ± 9 ka (PF97-2) and 94 ± 9 ka (PF97-3) were obtained from the base of this soil. The TL dates are consistent with the PDI age for the base of this soil

suggesting that this soil is about 100 ka. Further, these ages suggest that soil b1 is not correlative with the pre-El Cajete soil.

The PDI range for soil b4 ranges from 98 to 150 ka. The PDI age for this soil should be considered a minimum because it is likely that the top of the pumice was truncated prior to formation of overlying soil. The PDI age for soil b5 ranges from 135 to 191 ka.

Trench 4

Three profiles where described at Trench 4. Profile 7.4 represents the most complete section of soils exposed in this trench. Profile 4.8 and Profile 3.6 were described to supplement soil stratigraphy identified in Profile 7.4 and to provide direct soil-stratigraphic information for interpretation of possible fault related structures exposed in the trench.

Profile 7.4: Soil characteristics were described to a depth of 243 cm (Fig. 6). At least 3 buried soils are recognized in addition to the surface soil.

Surface Soil: The surface soils is thin (60 cm deep), light colored (10YR 5/2), and is weakly developed. This soil coincides with units 10e, 10c, and 10 b on the trench 4 log. Soil structure is largely moderate to weak subangular blocky that parts to weak crumb. Soil color ranges from 10YR 5/2 to 8.75YR 5/3. A PDI age of 3.7 to 5.3 ka was estimated for this soil.

Buried Soil b1: The first buried soil is a thin (60-97 cm) well developed soil. The top of the soil in denoted by a noticeable increase in red color (7.5YR 6/4) relative to the surface soil. Dry soil color is from 7.5YR 6/4 to 6/3. This soil coincides with units 9a, 9b, and 9d on the trench 4 log. Soil structure largely consist of moderate prismatic that parts to moderate and weak angular and subangular blocky. Argillan development is strong consisting of many to common coatings along pedfaces (best along prismatic pedfaces) and lining pores. The top of this soil appears to have been truncated because the Bt1b1 horizon is the top of the soil and the original overlying A horizon does not appear to be part of the overlying soil. A PDI age of 16 to 22 ka was estimated for the base of this soil. Because of possible erosion to this soil, this may be a minimum age.

Buried Soil b2: The second buried soil is a well developed soil that is lies between 97 to 146 cm below the surface. This soil coincides with units 8a and 8b on the trench 4 log. The top of the soil is denoted by the presence of a moderately developed Bt horizon (Bt1b2) that is better developed relative to the overlying horizon. The true top of this soil may be within the lower zone of the soil b1, but any features of former A and near-surface horizons have been overprinted by subsequent soil development. The soil is missing east of the 5 m mark, however, suggesting that the top of this soil has been eroded. Dry soil color ranges from 7.5YR 6/4 to 6/3. Soil structure largely consist of moderate and weak prismatic that parts to moderate and weak angular and subangular blocky. Argillan development is strong to moderate ranging from many to common coatings along pedfaces (best along prismatic pedfaces) and lining pores. A PDI age of 39 to 55 ka was estimated for the base of this soil. Because of possible erosion to this soil, this is probably a minimum age.

Buried Soil b3: The third buried soil is a moderately developed soil that is lies between 146 to 243 cm below the surface. This soil coincides with units 6b and 4b on the trench 4 log. The top of the soil is denoted by the presence of a well developed Bt horizon that is better developed relative to the overlying horizon. The true top of this soil may be within the lower zone of the soil b3, but any features of former A and near-surface horizons have been overprinted by subsequent soil development. The soil is missing east of the 5 m mark, however, suggesting that the top of this soil has been eroded. Dry soil color ranges from 7.5YR 6/4 to 8.75YR 6/3. Soil structure largely consist of strong and weak prismatic that parts to moderate and weak subangular blocky. Argillan development is strong to moderate ranging from nearly continuous to few coatings along pedfaces (best along prismatic pedfaces) and lining pores. Abundant skeletans and small, poorly weathered fragments of tuff in the Bt2b2 horizon give this horizon a mottled appearance. A PDI age of 97 to 137 ka was estimated for the base of this soil. Because of possible erosion to overlying soils, this is probably a minimum age.

Profile 4.8: Soil characteristics were described to a depth of 149 cm (Fig. 7). At least 1 buried soil is recognized in addition to the surface soil.

Surface Soil: The surface soils is thin (47 cm deep) and is weakly developed. This soil coincides with units 10e and 10c on the trench 4 log. Soil structure is largely moderate to weak subangular blocky. Soil color ranges from 10YR 4/2 to 7.5YR 3/3. A PDI age of 1.8 to 2.5 ka was estimated for this soil

Buried Soil b1: The buried soil is a moderately developed soil that is lies between 47 to 149 cm below the surface. The base of this soil coincides with units 9d and 9a on the trench 4 log. The top of the soil is denoted by the presence of a well developed Bt horizon that is better developed relative to the overlying horizon. The top of this soil appears to have been truncated because the Bt1b1 horizon is the top of the soil and the original overlying A horizon does not appear to be part of the overlying soil. The base of the b1 soil profile appears to correlate with the b3 soil at profile 7.4. If so, then the b2 have either been removed from erosion (most likely) or did not form. Alternately, the top of soil b1 at profile 4.8 (Bt1b1, Bt2b1) is correlative to parts of b1 and b2 at profile 7.4. Dry soil color ranges from 7.5YR 6/4 to 8.75YR 6/3. Soil structure largely consist of moderate and weak prismatic that parts to moderate and weak subangular blocky. Argillan development is strong to moderate ranging from nearly continuos to common coatings along pedfaces (best along prismatic pedfaces) and lining pores. Skeletans occur in all horizons (best in the BEtb1). Skeletans combined with abundant small and poorly weathered fragments of tuff in the Bt3b1 and Bt4b1 horizons given these horizons a mottled appearance. The soil overlies fractured and poorly weathered tuff. A PDI age of 43 to 62 ka was estimated for the base of this soil. Because of possible erosion to overlying soils, this is probably a minimum age.

Profile 5.4: Only the surface soil was described at this trench location. The description is from the north side of the trench. This site was chosen to enhance interpretation of possible fault related features exposed in the eastern third of the trench. Soil characteristics were described to a depth of 49 cm

Surface Soil: The surface soils is thin (49 cm deep) and is weakly developed. This soil coincides with units 10e and 10c on the trench 4 log. Soil structure is largely moderate to weak subangular blocky. Soil color ranges from 10YR 4/2 to 7.5YR 5/3. A PDI age of 1.9 to 2.7 ka was estimated for this soil.

Summary of Trench 4 Soil Stratigraphy: The PDI age for the surface soil ranges from 1.8 to 5.3 ka. PDI ages for this soil partially overlap with two radiocarbon dates of 1.7 ± .04 (WJR-20; Beta-108401) and 1.3 ± .08 ka (WJR-21; Beta-108402) from trench 4. Variation between radiocarbon and PDI ages may reflect an overestimation of development of surface soils or introduction of charcoal in to the soil that is younger than the true age of the surface soil. A TL date of 43 ± 5 ka was also obtained from the base of surface soil. Based on the radiocarbon dates and the degree of soil development in the surface soil, the TL date appears to old. The PDI age for soil b1 ranges from 15.6 to 62.0 ka based on the soil exposed in profiles 7.4 and 4.8. The range in age partially reflects the differences in soil thickness (37 vs. 106 cm) but is probably largely because the base of soil b1 in profile 4.8 appears to be correlative with the b3 soil in profile 7.4. Excluding profile 4.8, the PDI age for soil b1 in profile 7.4 is 16 to 22.0 ka. The PDI age for soil b2 (profile 7.4) ranges from 39 to 55 ka. The PDI age for soil b3 (excluding b1, profile 4.8) ranges from 97 to 137 ka. The PDI ages for all buried soils in trench 4 may be minimum ages because it is likely that the top of the upper most buried soils have been truncated.

Trench 5

Two profiles where described at Trench 5. Profile 16.0 represents the most complete section of soils exposed in this trench. Profile 6.2 was described to supplement soil stratigraphy of the surface identified in Profile 16.0 because the surface soil at profile 16.0 appears to have been partially stripped from erosion.

Profile 16.0: Soil characteristics were described to a depth of 623 cm (Fig. 8) At least 6 buried soils are recognized in addition to the surface soil.

Surface Soil: The surface soils is 106 cm deep and is moderately developed. This soil pinches out just upslope of profile 16.0 suggesting that at least part of this soil has been stripped and removed from erosion. This soil coincides with units 9A through 8Bt3 on the trench 5 log. Dry soil color ranges from 10YR 6/3 to 7.5YR 6/4. Soil structure ranges from moderate to weak subangular blocky. Argillans range from many to very few coatings along pores and pedfaces. A PDI age of 21 to 29 ka was estimated for the base of this soil. Because of the possibility that this soil has been partially removed from erosion, the PDI age for this soil is probably a minimum age. Likewise, the PDI ages of all underlying soils may also be minimum ages.

Buried Soil b1: The first buried soil is a well developed soil that lies between 106 to 208 cm below the surface. This soil coincides with units 7Btb1 through 6Bt2b2 on trench log 5. The top of the soil in denoted by a noticeable increase in structure and argillans relative to the surface soil. The true top of this soil may be within the lower zone of the surface soil, but any features of former A and near-surface horizons have been overprinted by subsequent soil development. Dry soil color is 7.5YR 6/4. Soil structure largely consist of moderate

and weak prismatic that parts to strong to weak angular and subangular blocky. Argillan development is strong consisting of nearly continuous to many coatings along pedfaces (best along prismatic pedfaces) and lining pores. A PDI age of 77 to 109 ka was estimated for the base of this soil.

Buried Soil b2: The second buried soil is a well developed soil that is lies between 208 to 262 cm below the surface. This soil coincides with units 6Bt3b2 and 6BC1b2 on the trench 5 log. The top of the soil is denoted by a noticeable increase in Bt horizon development. The true top of this soil may be within the lower zone of the surface soil, but any features of former A and near-surface horizons have been overprinted by subsequent soil development. Alternately, this soil does not extend into the eastern half of the trench suggesting that the part of this soil has been removed from hillslope erosion. Dry soil color is 7.5YR 6/4. Soil structure largely consist of strong to weak prismatic that parts to moderate and weak angular and subangular blocky. Argillan development is strong ranging from nearly continuous to common coatings along pedfaces (best along prismatic pedfaces) and lining pores. A PDI age of 117 to 165 ka was estimated for the base of this soil.

Buried Soil b3: The third buried soil is a well developed soil that is lies between 262 to 309 cm below the surface. This soil coincides with units 5Btb3 and 5BCb3 on the trench 5 log. The top of the soil is denoted by a noticeable increase in Bt horizon development. The true top of this soil may be within the lower zone of soil b2, but any features of former A and near-surface horizons have been overprinted by subsequent soil development. Dry soil color ranges from 7.5YR 6/4 to 6/3. Soil structure largely consist of moderate and weak prismatic that parts to moderate and weak subangular blocky. Argillan development is strong to moderate ranging from many to few coatings along pedfaces (best along prismatic pedfaces) and lining pores. A PDI age of 149 to 211 ka was estimated for the base of this soil.

Buried Soil b4: The fourth buried soil is a well developed soil that is lies between 309 to 379 cm below the surface. This soil coincides with unit 4Btb4 on the trench 5 log. The top of the soil is denoted by a noticeable increase in Bt horizon development, an increase in clasts, indicating a possible stone line, and platy structure. The true top of this soil may be within the lower zone of soil b3, but any features of former A and near-surface horizons have been overprinted by subsequent soil development. Dry soil color ranges from 7.5YR 6/4 to 6/3. Soil structure largely consist of weak platy or prismatic that parts to moderate and weak subangular blocky. Argillan development is strong to moderate ranging from nearly continuous to few coatings along pedfaces (best along prismatic pedfaces) and lining pores. A PDI age of 200 to 282 ka was estimated for the base of this soil.

Buried Soil b5: The fifth buried soil is a well developed soil that is lies between 379 to 507 cm below the surface. This soil coincides with unit 3Btb5 on the trench 5 log. The top of the soil is denoted by a noticeable increase in Bt horizon development, an increase in clasts, indicating a possible stone line, and platy structure. The true top of this soil may be within the lower zone of soil b4, but any features of former A and near-surface horizons have been overprinted by subsequent soil development. Dry soil color ranges from 7.5YR 6/4 to 5/3. Soil structure largely consist of moderate and weak subangular blocky. Argillan development is strong to moderate ranging from many to common coatings along pedfaces and lining pores. A PDI age of 305 to 431 ka was estimated for the base of this soil.

Buried Soil b6: The sixth buried soil is a well developed soil that is lies between 507 to 623 cm below the surface. This soil coincides with unit 2Btb6 on the trench 5 log. The top of this soil is denoted by a noticeable decrease in Bt horizon development, a decrease in clast abundance, and an increase in evidence of insect burrowing. These relations suggest that the top of the soil is the Bt1b6 horizon, with development of argillans occurring subsequent to burial and formation of soil b5. Dry soil color is 7.5YR 6/4. Soil structure largely consist of weak prismatic that parts to subangular blocky. Argillan development is strong to moderate ranging from nearly continuous to few coatings along pedfaces and lining pores. A PDI age of 414 to 585 ka was estimated for the base of this soil.

Profile 6.2: Soil characteristics were described to a depth of 623 cm (Fig. 9). At least 1 buried soil was described in addition to the surface soil.

Surface Soil: The surface soil is 212 cm deep and is moderately to well developed. This soil coincides with units 9A through 8Bt3 on the trench 5 log. Dry soil color ranges from 10YR 6/3 to 7.5YR 6/4. Soil structure includes weak prismatic and strong to weak subangular blocky. Argillans range from nearly continuous to very few coatings along pores and pedfaces and bridging grains. Crude lamallae have developed in horizons Bt5 through Bt8. A PDI age of 70 to 99 ka was estimated for the base of this soil.

Buried Soil b1: The first buried soil is a well developed soil that lies between 212 to 329 cm below the surface. This soil coincides with units 7Btb1 and 7BCb1 on the trench log 5. The top of the soil in denoted by a noticeable increase in structure and argillans relative to the surface soil. The true top of this soil may be within the lower zone of the surface soil, but any features of former A and near-surface horizons have been overprinted by subsequent soil development. Dry soil color is 7.5YR 6/4. Soil structure largely consist of moderate and weak prismatic that parts to strong to weak angular and subangular blocky. Argillan development is strong consisting of nearly continuous to many coatings along pedfaces (best along prismatic pedfaces) and lining pores. A PDI age of 155 to 218 ka was estimated for the base of this soil.

Summary of Trench 5 Soil Stratigraphy: The PDI age for the surface soil ranges from 21 to 99 ka. Variation in PDI ages may largely reflects the differences in soil thickness (106 vs. 212 cm). The surface soil at profile 6.0 appears to be thicker because the surface soil at profile 16.0 has probably been partially removed from erosion. Further, colluviation and formation of a cumulic profile may have also enhanced the thickness of the soil at profile at 6.0 m relative to soil at profile 16.0 m. This would result in an overestimation of the age of the surface soil at profile 6.0 (due to over thickening of the soil), but it is difficult to estimate the magnitude of any possible overestimation. The PDI ages for profile 16.0, therefore, should be considered as minimum ages.

The PDI age for soil b1 ranges from 77 to 218 ka, reflecting differences in the thickness of the surface soil. The thickness of soil b1 is similar in both profiles as is the soil morphology. The PDI age for soil b1 ranges from 77 to 218 ka. The PDI age range for soil b2 is 117 to 165 ka. The PDI age range for soil b3 is 150 to 211 ka. The PDI age range for soil b4 is 200 to 282 ka. The PDI age range for soil b5 is 305 to 431 ka. The PDI age range for soil b6 is 414 to 585 ka. The PDI best age estimate (Table 3) indicates that each buried soil represents about 40 to

130 kyrs of development. This is compatible with the overall degree of soil development for each buried soil when compared with the range of development in soils of comparable age across the Pajarito Plateau.

Trench 6

Only one profile was described at Trench 6. Profile 12.0 represents the most complete section of soils exposed in this trench. Soil stratigraphy for this trench was not described in the field at the trench exposure. Soil horizon intervals were selected by J. McCalpin and M. Berry, with samples collected for each interval. Soils were described (by McDonald) based on sample morphology that could be determined from samples and interpreted from the trench 6 log. All PDI ages for this trench should be considered as general estimates.

Additional problems were encountered for these soils because of the highly fragmented and offset nature of the soil stratigraphy. PDI estimates for some horizons are also based on the average horizon thickness rather than the exact thickness of horizon at profile 12. This was done because the profile line only passes fragments of some soil horizons that clearly under represent soil horizon thickness. Soil horizon thickness in some cases in based on the average thickness of the horizon within about 1-2 m of the profile. The soil-stratigraphy (Fig. 10) also includes soil horizons associated with unit 3Bt2b7 which was not exactly located along the profile 12.0 transect.

Profile 12.0: Soil characteristics were described to a depth of 623 cm. At least 6 buried soils are recognized in addition to the surface soil.

Surface Soil: The surface soil is 35 cm deep and is weakly developed. This soil has a variable thickness and overlies several eroded units of different ages suggesting that this is a soil formed in young colluvium. This soil coincides with unit 11 on the trench 6 log. Dry soil color ranges from 10YR 4/2 to 8.75YR 6/4. Soil structure ranges from moderate to weak subangular blocky. Argillans occur in the Bt horizon as nearly continuous coatings along pores. The Bt horizon may actually be locally disturbed (bioturbation?) fragments of the underlying buried soil and not genetically related to the surface soil. A PDI age of 3.2 to 4.5 ka was estimated for the base of this soil.

Buried Soil b1: The first buried soil is a moderately developed soil that lies between 35 to 71 cm below the surface. This soil coincides with unit 10 on trench log 6. The top of the soil in denoted by a noticeable increase in structure and argillans relative to the surface soil. The soil is discontinuous along the trench indicating that this soil has probably been partially stripped from erosion. Dry soil color is 7.5YR 6/4. Soil structure largely consist of moderate and weak prismatic that parts to moderate and weak angular and subangular blocky. Argillan development is strong to moderate consisting of nearly continuous to common coatings along pedfaces and lining pores. A PDI age of 11 to 16 ka was estimated for the base of this soil. Because it is likely that this soil has been partially stripped, the PDI age is probably a minimum age estimate.

Buried Soil b2: The second buried soil is a thin (25 cm) moderately to strongly developed soil that lies between 71 to 96 cm below the surface. This soil coincides with units 9-8 on

trench log 6. The soil is discontinuous along the trench and is highly fragmented indicating that this soil has probably been partially stripped from erosion. Dry soil color ranges from 7.5YR 6/4 to 7/3. Soil structure largely consist of weak prismatic that parts to moderate and weak angular and subangular blocky. Argillan development is strong consisting of nearly continuous to many coatings along pedfaces and lining pores. A PDI age of 21 to 29 ka was estimated for the base of this soil. Because this soil has been partially stripped, the PDI age is a minimum age estimate.

Buried Soil b3: The third buried soil is a strongly developed soil that lies between 96 to 205 cm below the surface. This soil coincides with units 7 on trench log 6. The upper 20 40 cm of the soil highly fragmented and largely absent throughout most of the trench indicating that this soil has been partially stripped from erosion. Dry soil color ranges from 7.5YR 5/4 to 7/4. Soil structure largely consist of moderate to weak prismatic that parts to moderate and weak angular and subangular blocky. Argillan development is strong to moderate consisting of nearly continuous to common coatings along pedfaces and lining pores. A PDI age of 99 to 140 ka was estimated for the base of this soil. A TL date (PF-10) from the top of this soil yielded a date of 132 $\pm$ 12 ka. The location of this TL sample is near the top of the soil suggesting that this date may be related to burial of the soil rather the age of soil formation. Alternately, if the TL date is deep enough within the profile (such that bioturbation will not have provided adequate exposure to sunlight during soil formation) to reflect the deposition age of the colluvium the soil formed in. Because this soil has been partially stripped, however, and if the PDI age is a minimum age because of post-soil erosion, then the TL date probably dates burial of this soil.

Buried Soil b4: The fourth buried soil is a strongly to moderately developed soil that lies between 205 to 341 cm below the surface. This soil coincides with units 6 on trench log 6. The top of the soil is denoted by a noticeable increase in Bt horizon development. The true top of this soil may be within the lower zone of soil b3, but any features of former A and near-surface horizons have been overprinted by subsequent soil development. Dry soil color ranges from 7.5YR 5/4 to 6.5/4. Soil structure largely consist of moderate prismatic that parts to moderate and weak angular and subangular blocky. Argillan development is strong to moderate consisting of nearly continuous to few coatings along pedfaces and lining pores. A PDI age of 210 to 297 ka was estimated for the base of this soil. Because overlying soils have been partially stripped, this PDI age is a minimum age estimate.

Buried Soil b5: The fifth buried soil is a strongly to moderately developed soil that lies between 341 to 399 cm below the surface. This soil coincides with units 5 on trench log 6. The top of the soil is denoted by a noticeable increase in Bt horizon development. The true top of this soil may be within the lower zone of soil b3, but any features of former A and near-surface horizons have been overprinted by subsequent soil development. Dry soil color is 7.5YR 5/4. Soil structure largely consist of moderate and weak prismatic that parts to moderate and weak angular and subangular blocky. Argillan development is strong consisting of nearly continuous to common coatings along pedfaces and lining pores. A PDI age of 256 to 362 ka was estimated for the base of this soil. Because overlying soils have been partially stripped, this PDI age is a minimum age estimate.

Buried Soil b6: The sixth buried soil is a strongly to moderately developed soil that lies between 399 to 495 cm below the surface. This soil coincides with units 4 on trench log 6. The top of the soil is denoted by a noticeable increase in Bt horizon development. Dry soil color ranges from 7.5YR 6.55/4 to 5/4. Soil structure largely consist of moderate and weak subangular blocky. Argillan development is strong to moderate consisting of nearly continuous to common coatings along pedfaces and lining pores. A PDI age of 340 to 480 ka was estimated for the base of this soil. Because overlying soils have been partially stripped, this PDI age is a minimum age estimate.

Buried Soil b7: The seventh buried soil is moderately developed soil that lies between 495 to 535 cm below the surface. This soil coincides with units 3 on trench log 6. The soil lies to the west of profile 12.0, but stratigraphically underlies soil b6. Dry soil color is 7.5YR 4/4. Soil structure largely consist of moderate and weak subangular blocky. Argillan development is moderate consisting of common coatings along pedfaces and lining pores. A PDI age of 375 to 529 ka was estimated for the base of this soil. Because overlying soils have been partially stripped, this PDI age is a minimum age estimate.

Summary of Trench 6 Soil Stratigraphy: The soil stratigraphy exposed in trench 6 is highly fragmented due to multiple fractures that have resulted in faulted offsets in all of the buried soils. Horizon thickness varies considerably as a result of this fracturing. Further, PDI age estimates are based on incomplete soil morphology. PDI ages, are at best, general approximations for these soils. In addition, PDI ages should be considered minimum ages for most of the soils because of possible truncation of several of the buried soils.

The PDI age for the surface soil is 3.2 to 4.5 ka. The PDI age for soil b1 is 11 to 16 ka. The PDI age range for soil b2 is 21 to 29 ka. The PDI age range for soil b3 is 99 to 140 ka. A TL date (PF-10) from the top of this soil yielded a date of 132 ± 12 ka. The location of this TL sample is near the top of the soil suggesting that this date may be related to burial of the soil rather the age of soil formation. Alternately, if the TL date is deep enough within the profile to reflect the deposition age of the colluvium the soil formed in. Because this soil has been partially stripped, however, the PDI age is probably a minimum age. Likewise, the PDI age for soil b1 is also probably a minimum age. The PDI age range for soil b4 is 210 to 297 ka. The PDI age range for soil b5 is 256 to 362 ka. The PDI age range for soil b6 is 340 to 480 ka. The PDI age range for soil b7 is 375 to 529 ka. The PDI best age estimates (Table 3) indicate that each buried soil represents about 10 to 130 kyrs of development. Although the PDI values were calculated with incomplete soil information, these estimated ages for development of each soils are compatible with the overall degree of soil development for each buried soil when compared with the range of development in soils of comparable age across the Pajarito Plateau.

Trench 7

Two profiles where described at Trench 7. Profile 8.5 represents the most complete section of soils exposed in this trench. Profile 6.0 was described to supplement surface soil.

Profile 8.5: Soil characteristics were described to a depth of 277 cm (Fig. 11). At least 2 buried soils are recognized in addition to the surface soil.

Surface Soil: The surface soils is 117 cm deep and is weakly developed. This soil coincides with units 8c through 7C on the trench 7 log. Dry soil color ranges from 10YR 6/3 to 7.5YR 6/3. Soil structure ranges from moderate platy in the surface horizon to moderate and weak subangular blocky in lower horizons. Argillans are not present in this soil. A PDI age of 11 to 15 ka was estimated for the base of this soil.

Buried Soil b1: The first buried soil is a moderately developed soil that lies between 117 to 211 cm below the surface. This soil coincides with units 4c through 4a on trench log 7. The top of the soil in denoted by a noticeable increase in structure and argillans relative to the surface soil. The top of this soil appears to have been previously stripped by erosion. The soil pinches out to the east across the trench exposure. Dry soil color ranges from 7.5YR 7/4 to 6/4. Soil structure largely consist of moderate and weak prismatic that parts to moderate and weak angular and subangular blocky. Argillan development is strong to moderate consisting of nearly continuous to few coatings along pedfaces (best along prismatic pedfaces) and lining pores and bridging grains. A PDI age of 45 to 63 ka was estimated for the base of this soil. Because of partial stripping of this soil, this age should be considered a minimum age range.

Buried Soil b2: The second buried soil is a well developed soil that is lies between 211 to 277 cm below the surface. This soil coincides with units 3b and 3a on the trench 7 log. The top of the soil is denoted by a noticeable decrease in color, resulting in a white or pinkish grey color. The character of this horizon is similar to buried albic E horizons found elsewhere in buried soils on the Pajarito Plateau (McDonald et al., 1996). This soil horizon pinches out to the west suggesting that this soil has also been partially stripped from erosion. Dry soil color ranges from 7.5YR 8/1 to 6/4. Soil structure largely is massive. Argillan development is moderate ranging from nearly continuous to very few coatings lining pores and bridging grains. Lamallae occur in the EBtb2 horizon. The soil overlies pumice and fractured tuff (unit 1). A PDI age of 61 to 86 ka was estimated for the base of this soil.

Profile 6.0: Soil characteristics were described to a depth of 144 cm (Fig. 12).

Surface Soil: The surface soils is 144 cm deep and is weakly developed. This soil coincides with units 10 through 7c on the trench 7 log. The top of the soil has been recently (historic) disturbed (Ap1, Ap2). Dry soil color ranges from 10YR 6/3 to 7.5YR 5/3. Soil structure ranges from moderate platy in the surface horizon to moderate and weak subangular blocky in lower horizons. Argillans are not present in this soil. A PDI age of 11 to 16 ka was estimated for the base of this soil.

Summary of Trench 7 Soil Stratigraphy: The PDI age for the surface soil ranges from 11 to 16 ka. By comparison, radiocarbon dates of 4.0 (Beta 108399) and 4.0 ka (Beta 108398) near the base of the profile suggest that this soil is considerably younger. The overall degree of soil development is at least comparable with soils formed on the ca. 6 to 7 ka Qt6 surface in Rendija Canyon suggesting that the surface soil is older than the radiocarbon dates, but less than the estimated PDI age. The PDI age of the soil b1 is 45 to 63 ka. This should be

considered a minimum age because at least part of this soil has been removed from erosion. The PDI age of soil b2 is 61 to 86 ka. This is should also be considered a minimum age.

SUMMARY AND CONCLUSIONS

PDI ages for buried soils exposed in trenches 3, 4, 5, 6, and 7 were determined using a soil development index that has been calibrated for use around the Laboratory based on radiometric dating of local soils and deposits. Although several assumptions are required for providing age estimates using this type of method, comparison with radiocarbon and thermoluminescence dates from several of the same trenches indicates that the use of a soil development index probably provides reasonable age estimates that can be used for interpretation of the geomorphic and seismic history associated with each trench.

Confidence in PDI age estimates would be enhanced by comparing a thick sequence of soils within datable strata. One possible location for this type of test is the deep burrow pit that is just outside of S-Site at TA-16. The combination of interstratified pumice and magnetostratigraphy would provide datable stratum in which to compare a PDI ages for multiple buried soils within a thick sequence of colluvium that lies along the main fault scarp. Further, stratigraphic information from this site will enhance evaluation of possible long-term fault activity along this scarp.

REFERENCES

Harden, J.W., 1982, A quantitative index of soil development from field descriptions: examples from a soil chronosequence in central California: Geoderma, v. 28, p. 1-28.

Harden. J. W., 1990, Soil development of stable landforms and implications for landscape studies: *in* Knuepper, P.L.K., and McFadden, L.D., eds., Soils and landscape evolution: Geomorphology, v. 3, p. 391-398.

Harden, J.W., and Taylor, E.M., 1983, A quantitative comparison of soil development in four climatic regimes: Quaternary Research, v. 20, p. 342-359.

Harden, J.W., Taylor, E.M., Hill, C., Mark, R.L., McFadden, L.D., Reheis, M.C., Sowers, J.M., and Wells, S.G., 1991, Rates of soil development from four soil chronosequences in the southern Great Basin: Quaternary Research, v. 35, p. 383-399.

McDonald, E. V., Reneau, S. L., and Gardner, J. N., 1996, Soil-forming processes on the Pajarito Plateau: Investigation of a soil chronosequence in Rendija Canyon, In Goff, F., Kues, B.S., Rogers, M.A., McFadden, L.D., and Gardner, J.N. (eds.), The Jemez Mountains region: New Mexico Geological Society Forty-Seventh Annual Field Conference Guidebook, p. 367-374.

Phillips, W.M., McDonald, E.V., Reneau, S.L., and Poths, J., 1998, Dating soils and alluvium with cosmogenic 21Ne depth profiles: case studies from the Pajarito Plateau, New Mexico, USA: Earth and Planetary Science Letters (in press).

Reneau, S.L., and McDonald, E.V, 1996, Landscape history and processes on the Pajarito Plateau, Northern New Mexico: Rocky Mountains Friends of the Pleistocene, Fieldtrip Guidebook, Los Alamos National Laboratory report LA-UR-96_3035, 195 p.

Soil Survey Staff, 1981, Examination and description of soils in the field: *in* Soil Survey Manual (USDA-ARS): U.S government Printing Office, Washington D.C.

Switzer, P.S., Harden, J.W., and Mark, R.K., 1988, A statistical method for estimating rates of soil development and ages of geologic deposits: A design for soil-chronosequence studies: Mathematical Geology, v. 20, p. 49-61.

Taylor, E.M., 1988, Instructions for the soil development index template-Lotus 1-2-3: U.S. Geological Survey Open-File report, 233A.

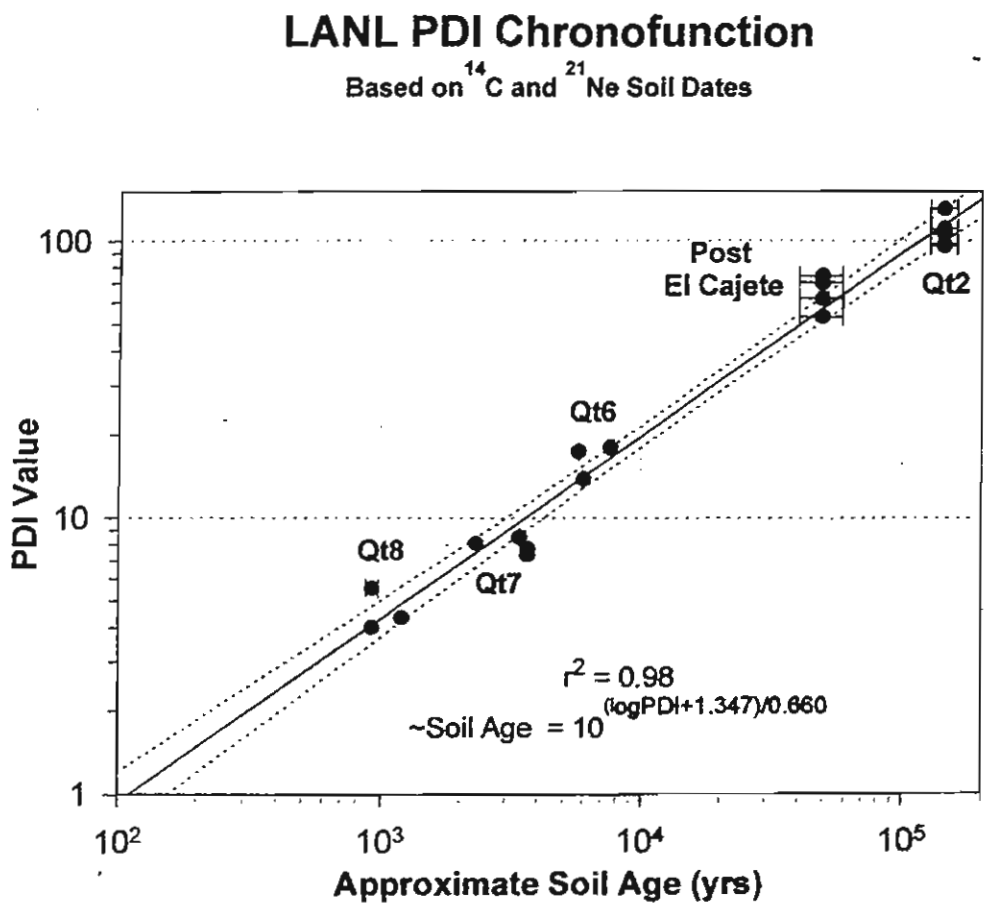

Figure 1. Soil chronofunction for calculating PDI ages. Error bars represent 1 sigma error on radiometric ages. Dotted line is 95% confidence interval.

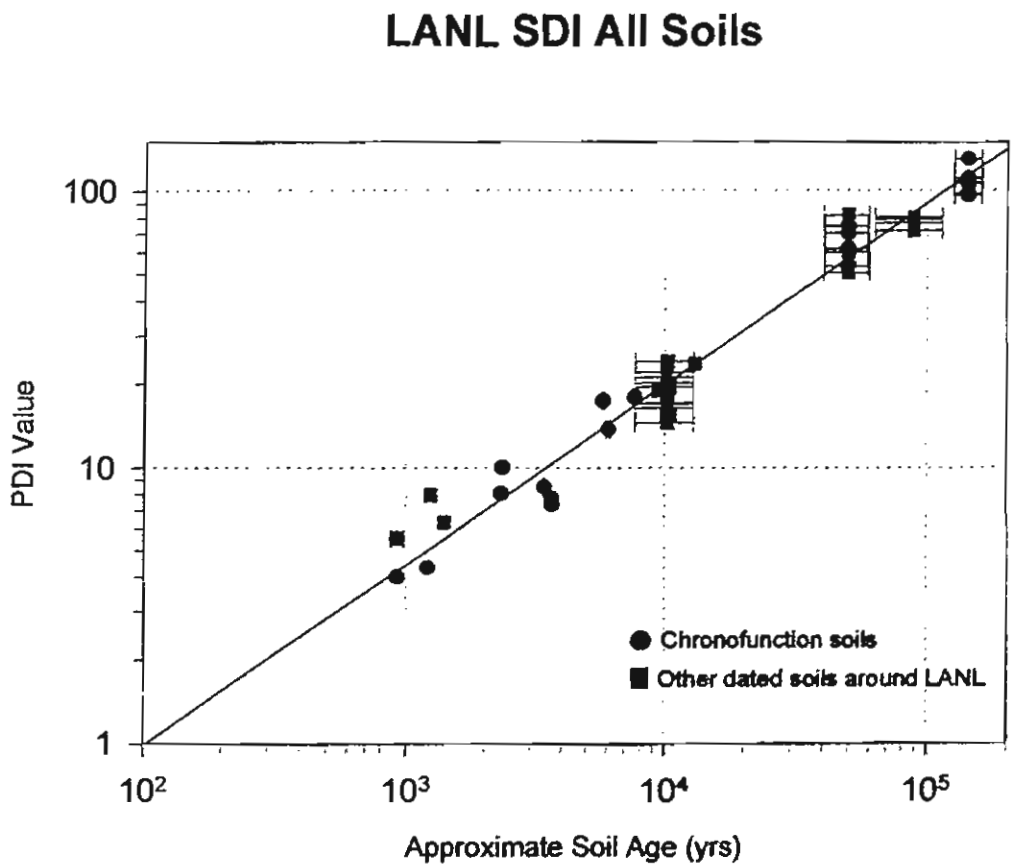

Figure 2. Soil chronofunction (regression line and soils) as compared to all dated soils (^{14}C, ^{21}Ne, and age of El Cajete Pumice) shown in Table 2.

T 3, P 9.6

Trench 3 Profile at 9.6 m mark

E. McDonald 9/

Log Descriptions

white soft colluvium

Reddish yellow

Red silty clay #1

-2m line

Red silty clay #2

Transition zone

-3m line

Red clayey matrix pumice gravel

-4m line

Hard yellow gravel sandy unit

-5m line

Depth (cm)

100

200

300

400

Estimated Age* (ka)

0.7

24

43

99

126

161

argillans on ca

argillans on ca

Horizon	Notes
Ap	Disturbed layer
Bw	
Bt	
BEtb1	Skeletal development along
Btb1	
BEtb2	Skeletons along pr pf
BEt2b2	skeletons along pr pf
Btb2	
Bt2b2	Several large root + clo lined pores → vc pr
Bt1b3	
Bt2b3	Scattered tuff fragment
Bt3b3	Scattered lenses of pumi (yellow
Bt4b3	" "
Bcb3	
Bt1b4	~75% pumice + ~25%
Bt2b4	~95% pumice - fall, in p L possible SiO2 coat in upper 5cm
Bt3b4	L weakly developed lam
Bt4b4	- maximum clay accum - thick clay linings along
CBt1b5	- massive, mod. stratified alluvium
CBt2b5	- massive, well stratified alluvium - thick masses sandy-pebble seds - clay-lined fractures (from oxi
CBb5	

Fig. 3

* PDI age

T3 P 8.0

Trench 3 Profile at 8.0 m mark

E. McDonald
9/97

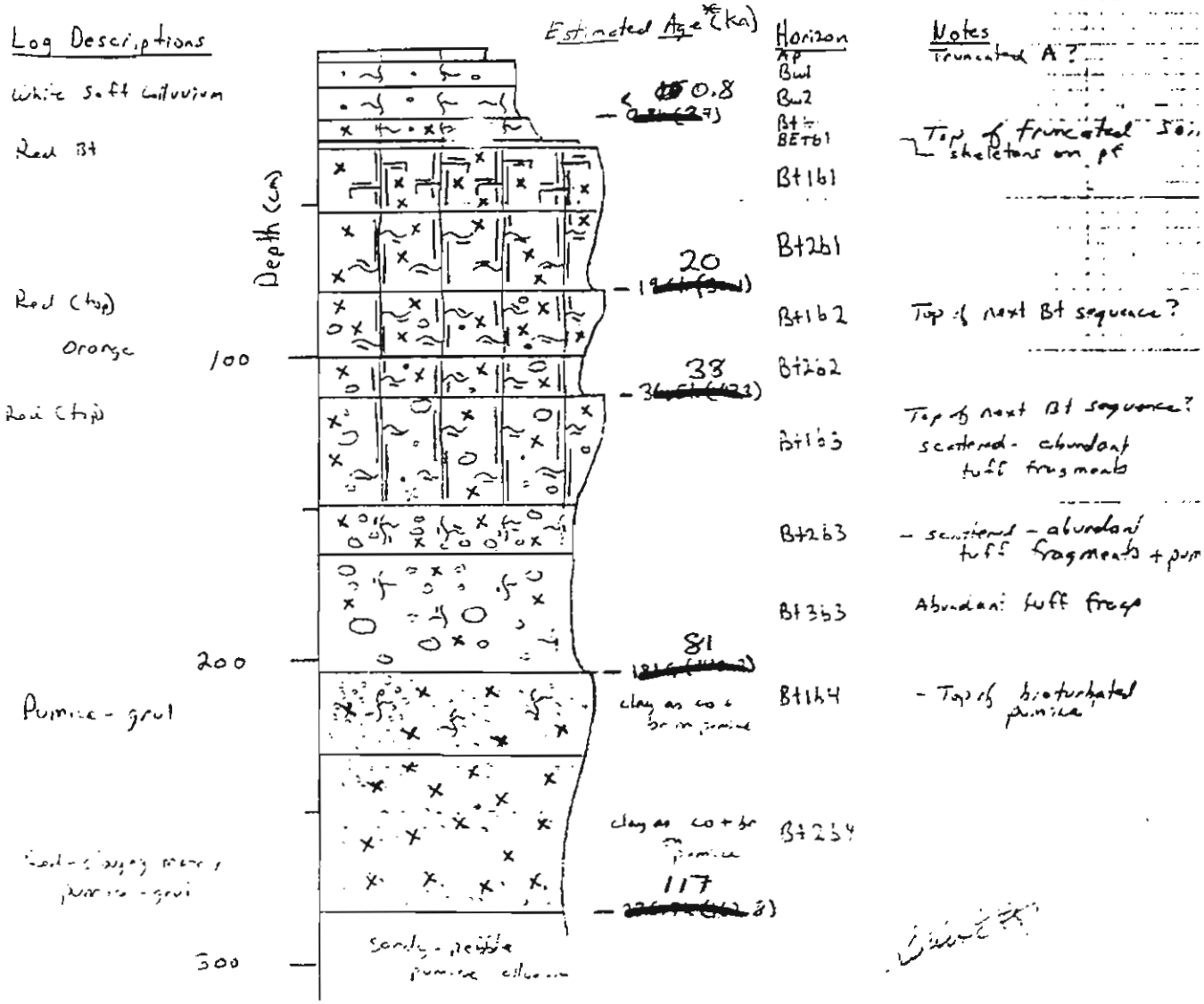

* PDJ age

Fig. 4

T3 P 5.4N

Trench 3 Profile at 5.4 m Mark
N side of trench

E. McDonald
9/97

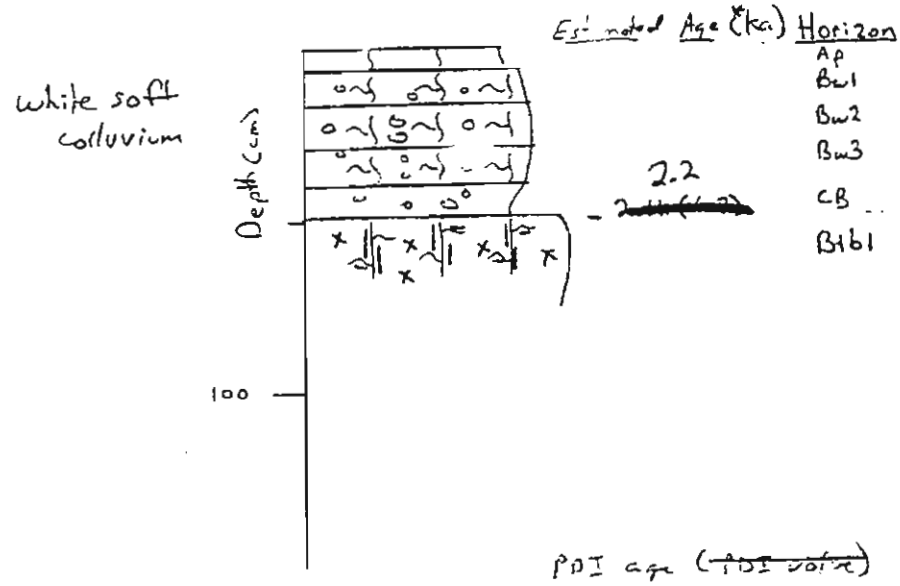

Fig. 5

T4 P 7.4

Trench 4 Profile at 7.4 m Mark

E. McDonald
9/97

Log Descriptions

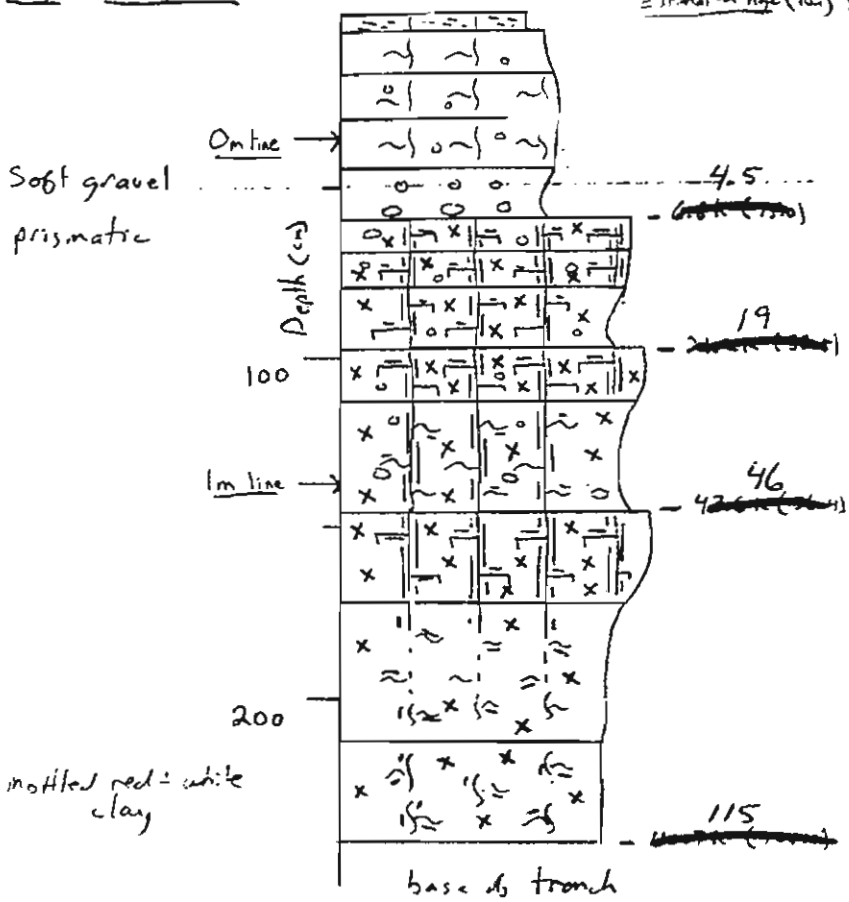

* POT derived age (POT site)

Fig. 6

T 4 P 4.8

Trench 4 Profile at 4.8m mark

Log Descriptions

Silt

Mottled red + white clay

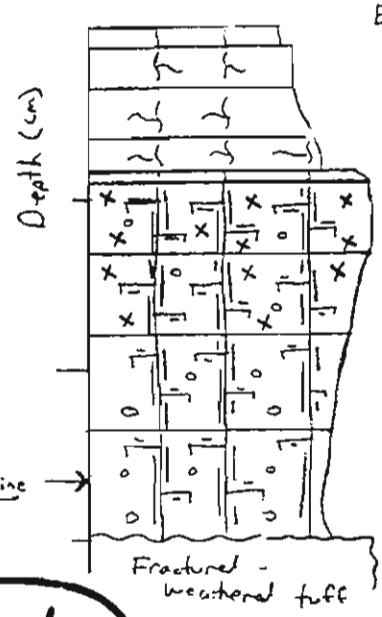

Estimated Age* (ka)	Horizon	Notes
	Ap	
	A1	
	Bw1	weak str.
2.1	Bw2	
~~3.6k (?)~~	BEtb1	- Skeletons along pf - Top of truncated Bt
	Bt1b1	
	Bt2b1	
	Bt3b1	- scattered to abundant skeletal development pad-interiors " "
	Bt4b1	
52 ~~51.8k (?)~~	tuff contact	irregular - unsure

Fig. 7b

T4 P 3.6N

Trench 4 Profile at 3.6m in on N side of trench

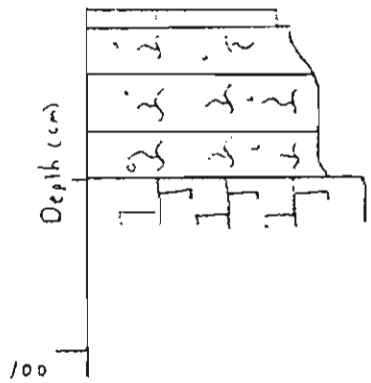

	Ap
	A1
	Bw1
2.3	Bw2
~~4.3k (?)~~	Bt1b1

* PDI based age. PDI solve.

Fig. 7a

switch

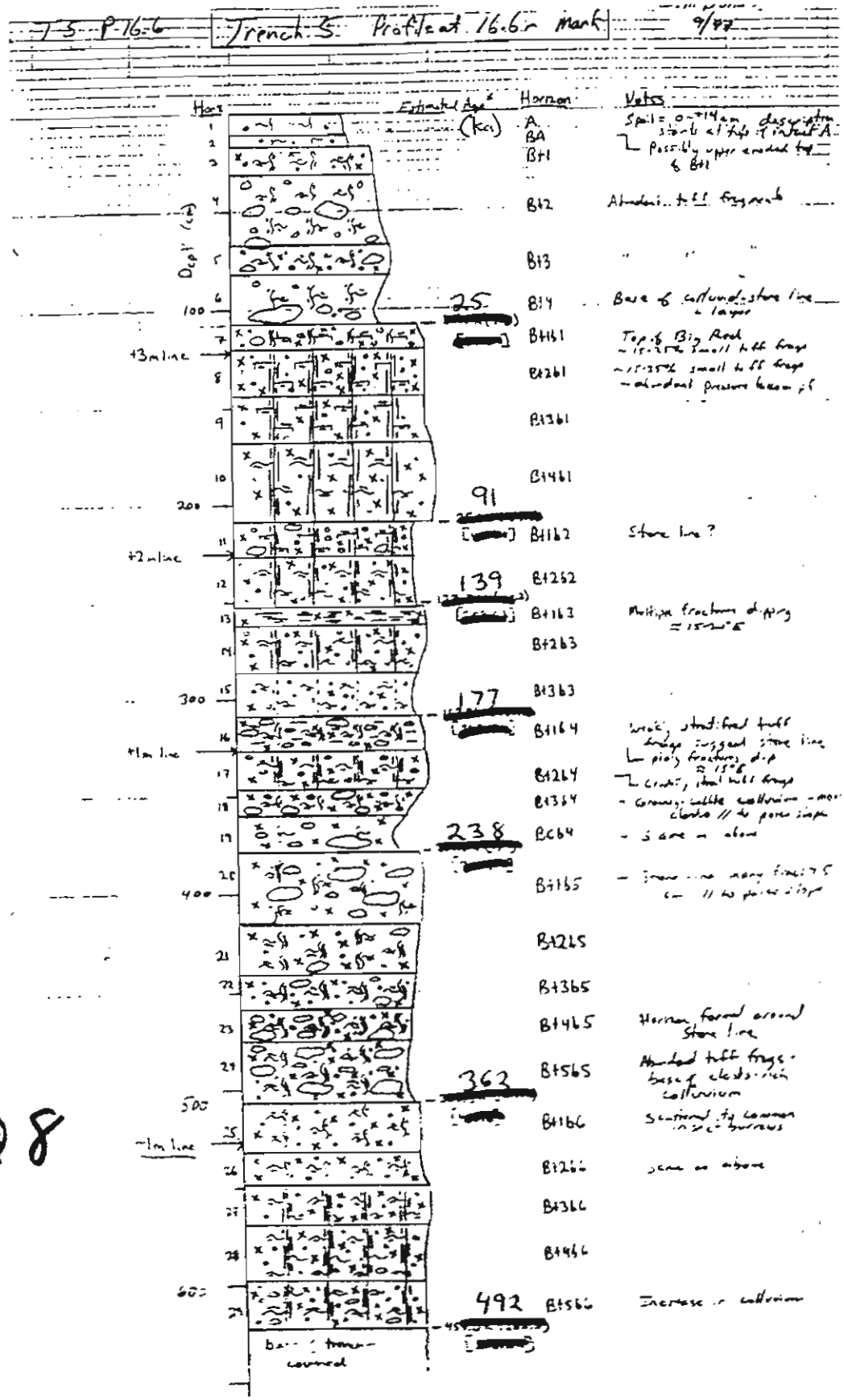
Trench 5
Horizon
Estimated Age (ka)
Horizon
Notes
Depth (cm)
+3m line
+2m line
+1m line
-1m line
25
91
139
177
238
363
492
A
BA
Bt1
Bt2
Bt3
Bt4
Bt161
Bt261
Bt361
Bt461
Bt162
Bt262
Bt163
Bt263
Bt363
Bt164
Bt264
Bt364
Bc64
Bt165
Bt265
Bt365
Bt465
Bt565
Bt166
Bt266
Bt366
Bt466
Bt566
Spill = 0-14cm, description starts at top of inset A
Possibly upper eroded top of Bt1
Abundant tuff fragments
Base of colluvial stone line layer
Top of Big Rock
small tuff frags
small tuff frags
abundant pressure beam pit
Stone line?
Multiple fractures dipping
Weakly stratified tuff frags suggest stone line
poly fractures dip
crushed tuff frags
Growing colluvium
clods // to pore slope
Horizon formed around stone line
Abundant tuff frags
base of clods-rich colluvium
Sediment fly common in rodent burrows
Increase in colluvium
bottom covered

Fig. 8

T5 P 6.4

Trench 5 Profile at 6.4 m mark

E. McD. Oman 9/97

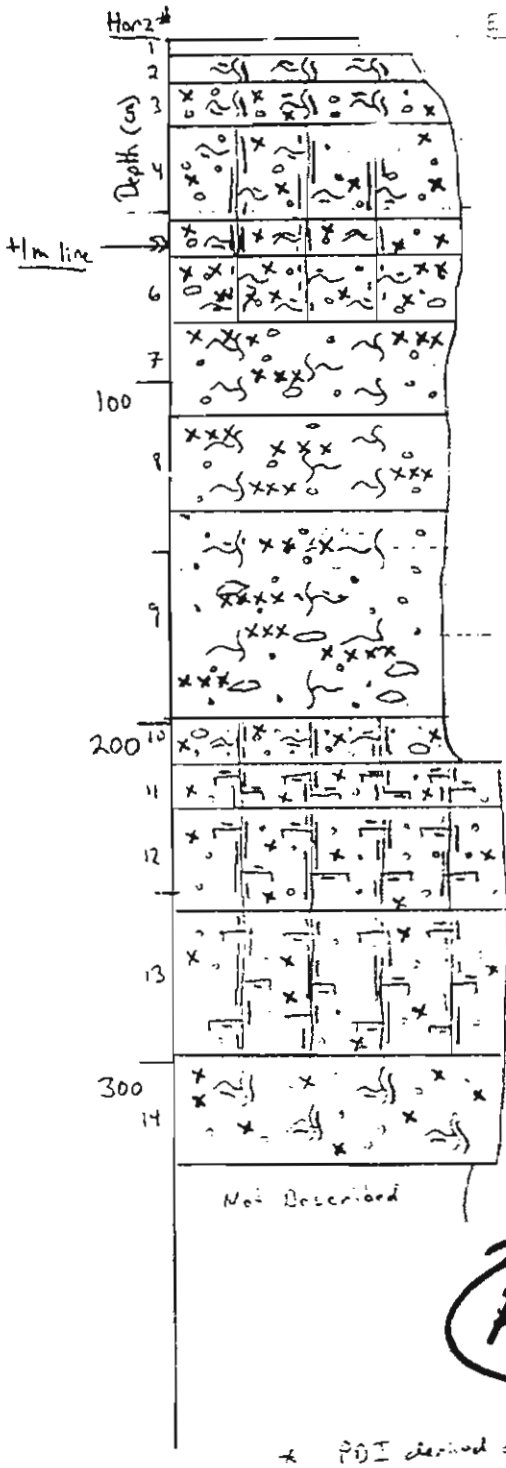

Estimated Age* (ka)	Horizon	Notes
	Ap	
	Bt1	
	Bt2	Truncated pre-EC soil No EC pumice
	Bt3	
	Bt4	
	Bt5	Lamallae (crude)
	Bt6	Crude lamallae
	Bt7	Lamallae
	Bt8	Crude lamallae
79	Bt9	may be top of Big Red;
	Bt1b1	"Big Red" many pressure faces in pt (Cl/silic
	Bt2b1	Many pressure faces
	Bt3b1	
134	Bt4b1	
	Bt1b2	

Fig. 9

* PDI derived age (PDI value) → specific soil depth

Trench 6

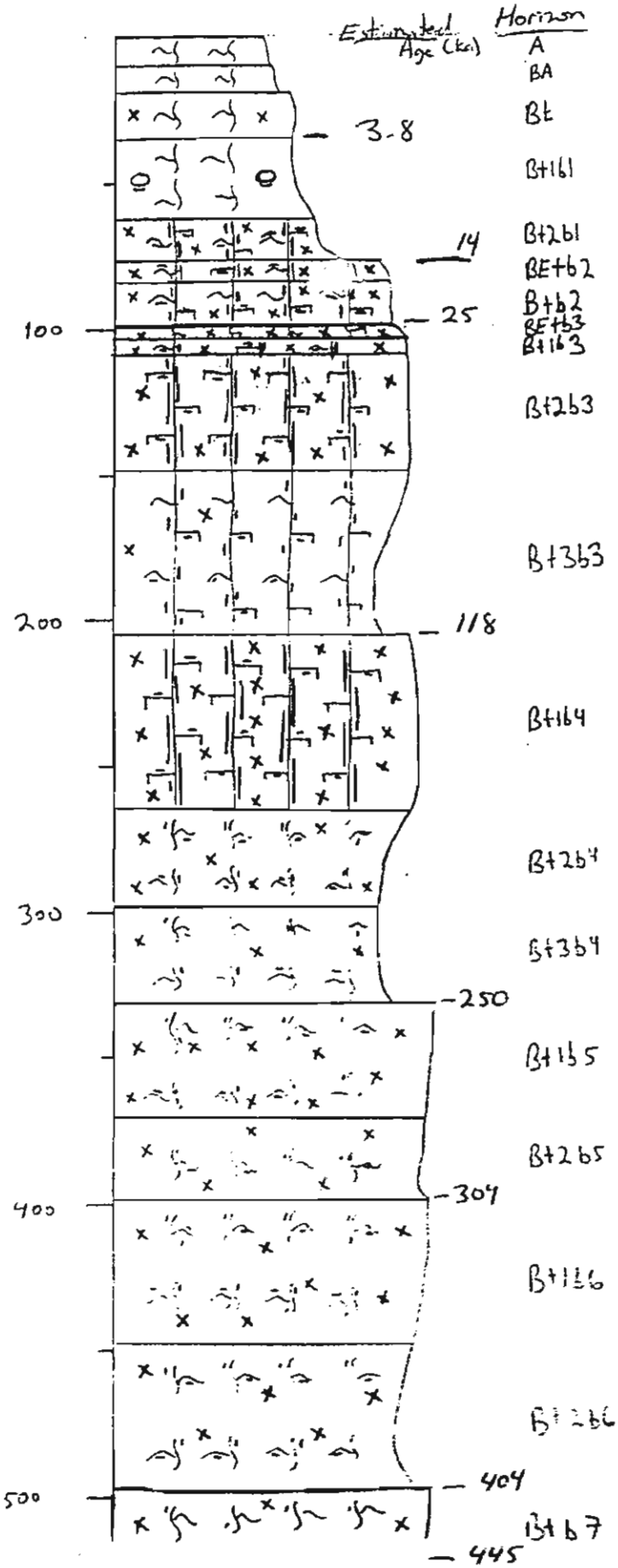

Notes

Fragmented horizons

Fig. 10

Not part 6 p 12.0

T7, P6.0

Trench 7, Profile at 6.0 m mark

E. McDonald 9/97

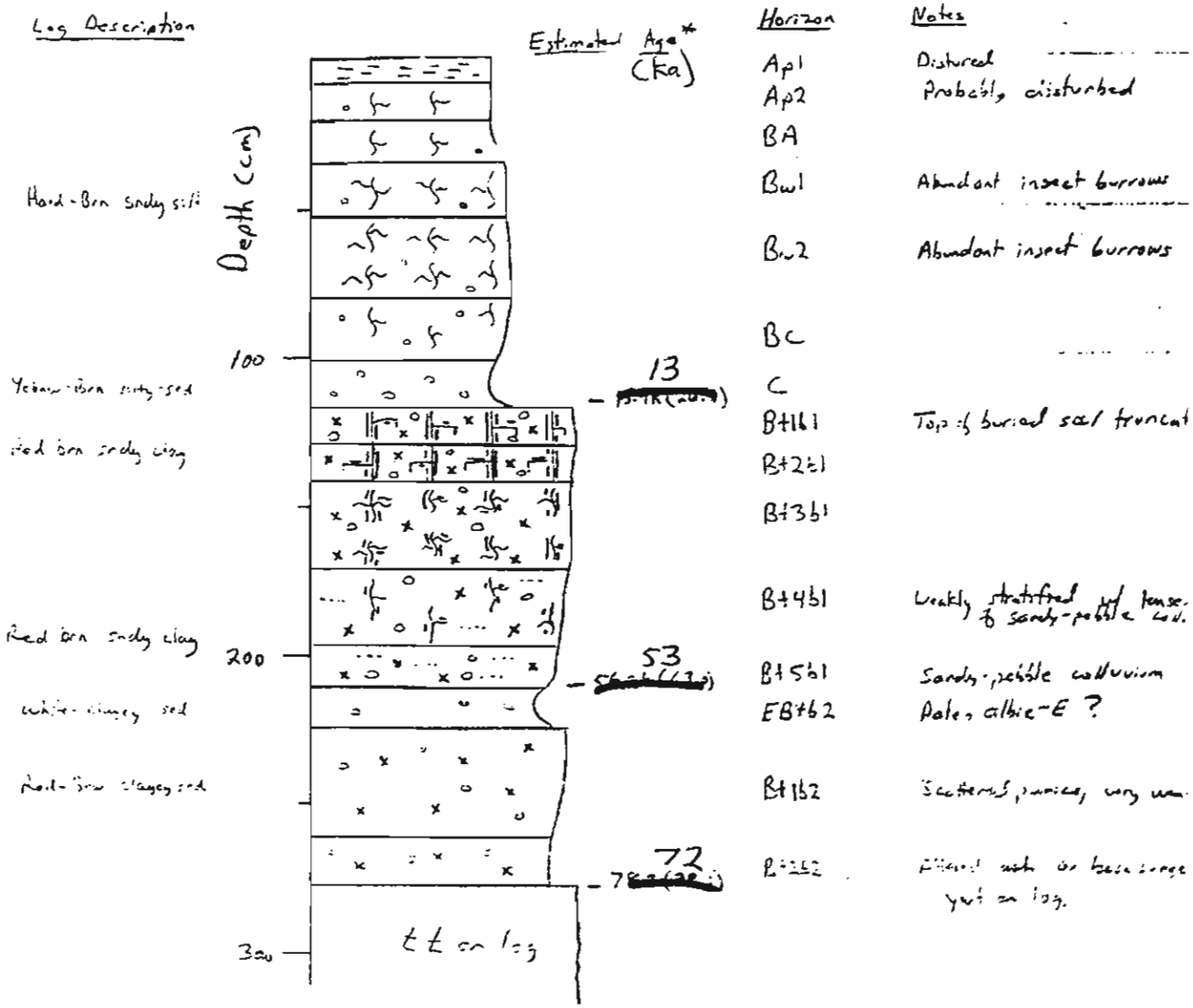

* PDI = [illegible] (PDI value)

Fig. 11

T7, P.8.5

Trench 7 Profile at 8.5 m Mark

E. McDonald
9/97

Log Description	Estimated Age*	Horizon	Notes
Gray brn		A1	
		A2	
		BA	
Brn-sandy silt		Bw1	weakly developed Bw
		Bw2	" "
		BC	
Yellow-brn silty-sand	13 ~~11.7K (95%)~~	C	Unweathered colluvium
fractured wt			

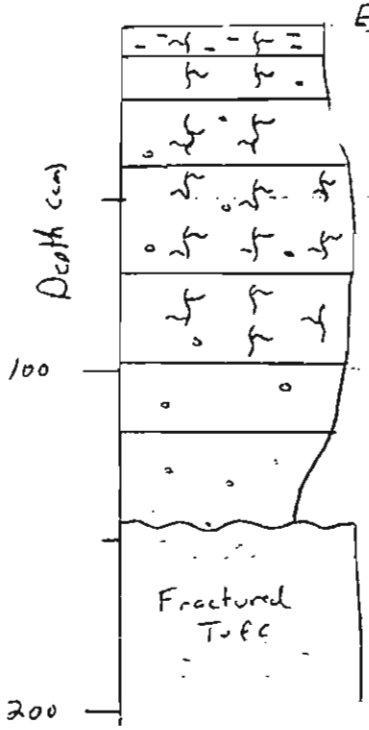

* POI age (POI value)

Fig. 12

Table 1. Summary of Soil Development Index results.

Soil	Soil Field #	PDI	Average PDI	^{14}C Age[b] / *^{21}Ne Profile Age*[c]
Qt8	RCT8-1	4.01		930 ± 0
	RCT8-3	5.54		930 ± 50
	RCT8-5	4.35	4.6 ± 0.8	1210 ± 0
Qt7	RCT7-1	8.52		3430 ± 20
	RCT7-4	8.07		2330 ± 0
	RCT7-7	7.74		3680 ± 0
	RCT7-8	7.35	7.9 ± 0.5	3680 ± 0
Qt6	RCT6-1	18		7710 ± 0
	RCT6-2	13.8		6080 ± 165
	RCT6-3	17.38	16.4 ± 2.3	5800 ± 80
Post EC[a]	WJR-5	74.28		50000 ± 9500
	WJR-9	53.26		50000 ± 9500
	WJR-10	70.33		50000 ± 9500
	WJR-11	61.76	64.9 ± 9.4	50000 ± 9500
Qt2	RCT2-1	95.49		*144000 ± 17000*
	RCT2-2	130.14		*144000 ± 17000*
	RCT2-3	110.55		*144000 ± 17000*
	RCT2-4	105.62		*144000 ± 17000*
	RCT2-5	96.93	107.7 ± 14.0	*144000 ± 17000*

[a]Soil formed in colluvium and loess overlying the ca. 50-60 ka El Cajete tephra.

[b]Calibrated ^{14}C ages.

[c]Ages (italics) for the Qt2 from Phillips et al. (1998).

Table 2. Comparison of PDI soil ages with radiometric dates for soils.

Parent Material[a]	Soil	PDI	PDI Age (yrs)	Radiometric Age (yrs)	Dating Method[b]	% Error
C	SC-1	50.15	37630	55000	EC	0.18
A	SC-2	6.32	1679	1400	14C	0.22
C	FC-1A	59.51	48644	55000	EC	0.06
A	AC-1	6.77	1859	1240	14C	0.53
A	WJR-8	19.75	9288	10470	14C	0.06
C	FRR-1	13.00	4958	9500	14C	0.46
C	FRR-1	67.06	58199	55000	EC	0.28
C	EG&G	11.21	3968	3970	14C	0.04
C	EG&G	16.75	7251	8050	14C	0.05
						0.20 ± 0.19
C/A	RCT4-1	76.03	70275	89000	21Ne	0.13
C/A	RCT4-2	71.44	64003	89000	21Ne	0.21
C/A	RCT4-3	78.63	73919	89000	21Ne	0.09
C/A	RCT4-4	78.86	74238	89000	21Ne	0.08
C/A	RCT4-5	79.88	75685	89000	21Ne	0.06
						0.18 ± 0.11
C	RCT4-1H	22.07	10972	10250.00	14C	0.13
C	RCT4-2H	24.21	12605	10250.00	14C	0.31
C	RCT4-3H	14.55	5870	10250.00	14C	0.40
C	RCT4-4H	19.48	9094	10250.00	14C	0.06
C	RCT4-5H	21.19	10323	10250.00	14C	0.07
C	RCT2-1H	16.92	7362	10250.00	14C	0.24
C	RCT2-2H	16.35	6990	10250.00	14C	0.28
C	RCT2-4H	20.17	9584	10250.00	14C	0.01
C	RCT2-5H	17.05	7444	10250.00	14C	0.24
						0.19 ± 0.13
					ALL	***0.18 ± 0.14***

Notes:

[a] Soils formed in colluvium (C); in alluvium (A); and in colluvium over alluvium (C/A).

[b] Dating control: radiocarbon (14C); El cajete Pumice (EC); and cosmogenic 21Ne (21Ne). Soil data from McDonald (unpublished; Reneau and McDonald, 1997). Radiocarbon dates from Reneau (unpublished; Reneau et al. (1995) and McDonald (1997)

Table 3. SDI age estimates for trenches 3, 4, 5, 6, and 7.

Trench no.	Fig. No.	Profile no.	Lowest Buried Soil Horizon	Lower Depth of Soil (cm)	Trench Unit	Soil PDI	SDI Age Estimate[a] Best Age (ka)	Lower Range (ka)	Upper Range (ka)
T3	3	p9.6	Bw	16	15	3	0.7	0.6	0.9
			Bt1b1	46	14	16	7.4	6.3	8.8
			Bt2b2	125	13	51	43	36	51
			BCb3	214	12a, 9, 7a	89	99	83	118
			Bt4b4	308	6	104	126	106	150
			CBb5	425	5, 4, 3	122	161	135	191
T3	4	P8.0	Bw2	22	15	4	0.8	0.6	0.9
			Bt2b1	77	14	31	20	17	24
			Bt2b2	113	13	47	38	32	45
			Bt4b3	205	12a, 9, 7a	78	81	68	97
			Bt2b4	284	6	99	117	98	139
T3	5	P5.4N	CB	49	15	7	2.2	1.9	2.7
T4	6	P7.4	BC	60	10e, 10b, 10c	11	4.5	3.7	5.3
			Bt3b1	97	9a, 9b, 9c	29	19	16	22
			Bt2b2	146	8a, 8b	54	46	39	55
			Bt3b3	243	6b, 4a	98	115	97	137
T4	7a	3.6N	Bw2	43	10e, 10c	7	2.3	1.9	2.7
T4	7b	P4.8	Bw1	43	10e, 10c	7	2.1	1.8	2.5
			Bt4b1	149	9d, 9a	58	52	44	62
T5	8	P16.6	Bt4	106	9A, 8Bt3	35	25	21	29
			Bt4b1	208	7Btb1-6Bt2b2	84	91	77	109
			Bt3b2	262	6Bt3b2, 6BC1b2	111	139	117	165
			Bt3b3	309	5Btb3, 5BCb3	131	177	149	211
			BCb4	379	4Btb4	159	238	200	282
			Bt5b5	507	3Btb5	209	362	305	431
			Bt5b6	623	2Btb5	256	492	414	585
T5	9	P6.2	Bt9	212	9A-8Bt3	79	83	70	99
			Bt4b1	329	7Btb1, 7BCb1	134	184	155	218
T6	10	P12.0	Bt	35	11	10	3.8	3.2	4.5
			Bt2b1	71	10	24	14	11	16
			Btb2	96	9–8	36	25	21	29
			Bt3b3	205	7	100	118	99	140
			Bt3b4	341	6	164	250	210	297
			Bt2b5	399	5	187	304	256	362
			Bt2b6	495	4	225	404	340	480
			Btb7	535	3	240	445	375	529
T7	11	P6.0	C	117	8, 7	23	13	11	15
			Bt5b1	211	4	59	53	45	63
			Bt2b2	277	3	72	72	61	86
T7	12	P8.5	C	144	10, 9, 8	24	13	11	16

[a] Age estimates based on no erosional loss between soils. See text for detailed discussion.

Table 4. Summary of soil morphology for trenches 3, 4, 5, 6, and 7.

Trench (Profile #)	Horizon	Depth (cm)	Gravel	Dry Color (Matrix)	Moist Color (Matrix)	TxL[a]	Structure	Consistence Dry	Consistence Moist	Consistence Wet	Argillans	Bdy[b]	Other Cutans	Notes
T3 (9.6)	Ap	5	4--8	10YR 7/2	10YR 5/3	l	1-2msbk:1m+fcrb	so	vfr	ss, ps		cs		
	Bw	16	2--6	10YR 7/2	10YR 5/3	l	1-2msbk	so-sh	vfr	ss, ps		cs		
	Bt1b1	23	2--6	10YR 7/2	10YR 5/3.5	sil	1-2msbk:1m+fcrb	sh-v	vfr	ss, ps		as		
	BEtb1	27	2--6	7.5YR 7/2	7.5YR 4.5/4	sicl	2mpr:2msbk+sbk	h	fr	ss, p	5n-mkpo; 4nfn-mkpf	as	3npr:pf skel	
	Bt2b1	46	2--6	7.5YR 6/3	7.5YR 4/3	sicl	1-2mpr: 1-2c+msbk+sbk	vh-h	fr	ss, p	5n-mkpr:pf;4n-mkbk:pf; 4n-mkpo	cs	1n-mkpo man	
	BEt1b2	59	4--8	7.5YR 6/4	7.5YR 5/4	sil	1-2cpr:2-1c+msbk: 2fpl	h	fr	ss, ps	5n-mkpr:pf;3npo; 2nbk:pf	cs	2fpf skel	
	BEt2b2	73	2--6	7.5YR 6/4	7.5YR 5/4	sil	2vcpr:1mpr: 2c+msbk	h	fi	ss, ps	5mkvc-pr:pf; 4npo; 3nm-kpr:pf+bk:pf	cs	2fpf skel	
	Bt1b2	95	4--8	7.5YR 6/4	7.5YR 4.5/4	sil	1mpr:2msbk+abk	h	fi-fr	ss, ps	4n-mkpr:pf; 4n-mkpo; 3nbk:pf	cs-cw		
	Bt2b2	125	4--8	7.5YR 6/6	7.5YR 4/4	sil	1vcpr:1msbk	dh	fr	ss, ps	4n-mkpr:pf; 4n-mkpo; 3nbk:pf	cs-cw		
	Bt1b3	159	5--15	7.5YR 5/4	7.5YR 4/4	sicl	1-2c+mpr:2msbk	h	fr	ss, p	4n-mkpr:pf; 4n-mkbk:pf; 4n-mkpo	cs	2npr:pf man	
	Bt2b3	160	10--20	7.5YR 5.5/4	7.5YR 4/4	sicl	1-2msbk	f	fr	ss, p	4n-mkpo; 3n-mkpf	cs-cw	1npo man	
	Bt3b3	190	20--30	7.5YR 6/4	7.5YR 4/4	sil	1c+msbk	vh-h	fr	ss, ps	4n-mkpo; 3n-mkpf	cs-cw	1npo man	Mixed pumice colluvium
	Bt4b3	202	15--30	7.5YR 6/4	7.5YR 4/4	sil	1c+msbk	h-sh	fr-vfr	ss, ps	4n-mkpo; 3nco; 2npf	as-aw		
	BCb3	214	5--15	10YR 7/3	10YR 5/4	l-sl	1c+msbk	sh-h	fr-vfr	vs, ps	1npf	as-cs		
	Bt1b4	236	70+	7.5YR 6/4	7.5YR 4/4	ls	1msbk: m in places	sh	vfr	so, vps		as-cs		top of pumice
	Bt2b4	263	95+	7.5YR 6/4	7.5YR 4/4	s	m-sg	lo	lo	so, po	3nco; 2mkbr	cs		
	Bt3b4	287	95+	7.5YR 6.5/4	7.5YR 5/4	s	m-sg	lo	lo	so, po	Lam: 5nco;4n-mkbr; Non-lam:2nco+br	cs		Lamallae
	Bt4b4	308	80+	7.5YR 6/4	7.5YR 4/4	sscl	m-sg	sh-lo	vfr	ss, vps	5kco,br	as		
	CBt1b5	326	25--35	7.5YR 6/4	7.5YR 5/4	ls	m-sg	h-sh	fr-vfr	so, vps	2mkbr	cs		Top of statified alluvium
	CBt2b5	375	15--25	7.5YR 6/4	7.5YR 4/4	s-ls	m-sg	sh	vfr	so, vps	3n-mkbr+co	cs		
	CBb5	425	5--20	7.5YR 7/4	7.5YR 5/4	sl	m-sg	sh	vfr	vs, vps	5mkco along fractures			
T3 (5.4N)	Ap	6	2--6	10YR 5/1	10YR 3/1	l	1mpl:1msbk:1mcrb	sh-so	vfr	vs, ps		as-aw		
	Bw1	16	10--20	10YR 7/2	10YR 5/3	l	1c+msbk	sh	vfr	vs, ps		cs		
	Bw2	29	5--25	7.5YR 7/2	7.5YR 5/3	l	1c+msbk	sh	vfr	vs, ps		cs		
	Bw3	40	5--15	7.5YR 7/2	7.5YR 5/3	sl	1c+msbk	sh	vfr	vs, ps		cw		
	CB	49	5--15	7.5YR 8/2	7.5YR 5/3	sil	1msbk in places	so	vfr	vs, ps		ai-aw		
	Btb1	79+	5--20	7.5YR 6/4	7.5YR 5/4	sicl-cl	1-2mpr: 2-3c+msbk	vh-h	fi-fr	ss, p		ai-aw		Truncated Bt, abundant tuff fragments

Table 4. Summary of soil morphology for trenches 3, 4, 5, 6, and 7.

Trench (Profile #)	Horizon	Depth (cm)	Gravel	Dry Color (Matrix)	Moist Color (Matrix)	Txt.[a]	Structure	Consistence Dry	Consistence Moist	Consistence Wet	Argillans	Bdy[a]	Other Cutans	Notes
	Bt5b1	211	5--15	7.5YR 7/4	7.5YR 5/4	l-secl	m	h-sh	fr	ss, ps	3nbr+po	ns		
	Eb2	215	5--10	7.5YR 8/1, 8/2	7.5YR 7/3	l	m	sh-so	vfr	vss, vps	lam: 5mkbr+co; non lam: 1nbr	as-aw		large (4-14 mm) lamallae
	Bt1b2	216	5--10	7.5YR 6/4	7.5YR 4/4	l	m	sh-so	vfr	ss, vps	4n-mkbr	as		
	Bt2b2	277	5--10	7.5YR 8/4	7.5YR 4/4	ls	m	sh-so	vfr	vss, po	3nbr+po	as	2npo man	
T7 P8.5	A1	9	2--5	10YR 4/2	10YR 3/1	sil	1-2c+msbk:1mpl	so	vfr	ss, ps		cs-aw		
	A2	22	2--5	10YR 5/2	10YR 3/2	sil-l	1 c+msbk	so	vfr	ss, ps		cs		
	BA	41	2--5	10YR 5/3	10YR 3/2	sil	1c+msbk	so	vfr	ss, ps		cs		
	Bw1	72	4--8	8.75YR 5/3	7.5YR 3/2	sil	1-2c+msbk	sh	fr-vfr	ss, ps		cs-cw		
	Bw2	98	4--8	7.5YR 5/3	7.5YR 3/2	sil	1c+msbk+m	sh	fr-vfr	ss, ps		cs		
	BC	119	5--15	8.75YR 5.5/3	8.75YR 4/3	l	m	sh	vfr	vss, vps		cs		
	C	144	5--15	10YR 6/3	10YR 4/3	l	m	sh	vfr	vss, ps		aw		

[a] txt = field texture; bdy = lower horizon boundary.
Morphology from trench 6 profile 12.0 dscribed from bag samples.
b Percent gravel not described.

APPENDIX C

Report by Steven L. Reneau, Los Alamos National Laboratory, on radiocarbon sampling and dating results, as of Feb. 11, 1998.

Radiocarbon Analyses From The 1997 Pajarito Fault Zone Trenches

Steven Reneau, EES-1

February 11, 1998

Summary

Nine radiocarbon analyses were obtained from isolated charcoal fragments collected in 1997 from trenches 3, 4, and 7 across two traces of the Pajarito fault zone along Camp May Road (Table 1). Six of the samples were collected from units that were inferred to post-date the most recent surface rupture event (MRE) in these trenches, presumably representing minimum-limiting age control for faulting. Three samples were collected from loose tuff rubble within a fissure fill along one fault trace in trench 7, and, presuming the fissure became isolated from the surface soon after faulting, the charcoal would provide maximum-limiting age constraints for faulting.

The radiocarbon analyses suggest two possible ages for the MRE along this part of the Pajarito fault zone, under the assumption that the same fault event is recorded in all three trenches (Figure 1). First, if the trench 7 fissure became isolated from the surface soon after faulting, the combined analyses suggest an age of ca. 2.2 ^{14}C ka (thousands of radiocarbon years before present) for the MRE (equivalent to about 2.2-2.3 calibrated (cal) ka, calibrated to an absolute dendrochronological time scale). However, this alternative would require the presence of an erosional unconformity between the fissure and sample sites 2 m to the west that was not recognized in the field. Second, if charcoal was introduced into the trench 7 fissure long after faulting and no unconformity exists at that location, then the analyses indicate an age of ≥ ca. 4.0 ^{14}C ka (≥ ca. 4.4 cal ka) for the MRE. Other possibilities exist if the MRE on the different fault traces were not contemporaneous.

Methods

Samples analyzed in this study consisted of one or more discrete charcoal fragments that were hand-picked from the trench walls. Areas with discolored soil (suggesting the possibility of roots burned in place) or disrupted soil (such as due to animal burrows or the decay of large roots) were avoided, although the absence of distinct stratigraphy in the sampled units suggests some degree of mixing, and the possibility of bioturbation of younger charcoal into older deposits cannot be ruled out. In addition, the possibility of the recycling of older charcoal exists, potentially providing ages older than the sampled deposits. Where possible, multiple samples were collected from single units or single stratigraphic sections in order to provide internal checks on the analyses.

Before submission to the analytical laboratory, each charcoal sample was air-dried, examined under a binocular microscope, and cleaned to remove dirt and roots. All samples were analyzed by the accelerator mass spectrometry (AMS) method, and were processed by Beta Analytic, Inc., of Miami, Florida. Sample pretreatment by Beta Analytic included standard hot acid (HCl) treatment to remove carbonates from the samples, followed by an alkali (NaOH) treatment to remove secondary organic acids, followed by conversion to graphite (which constituted the actual accelerator target).

The radiocarbon analyses were calibrated to an absolute dendrochronological time scale using the computer program CALIB 3.0.3 developed by the Quaternary Isotope Laboratory of the University of Washington (Stuiver and Reimer, 1993). This calibration corrects for differences between radiocarbon years and calendar years that are imparted by variations in the ^{14}C production rate in the atmosphere, and incorporates uncertainties both in the measurement of the radiocarbon content and in the calibration curves. The calibration can incorporate an "error multiplier" to account for sources of laboratory uncertainty that are not encompassed by the reported analytical plus-or-minus (Stuiver and Reimer, 1993), and, following other researchers, we have previously used an error multiplier of 2.0 in work at Los Alamos (e.g., Reneau et al., 1995). Use of 2-sigma

(2 standard deviation) uncertainties and an error multiplier of 2 provides a conservative estimate of the laboratory uncertainty associated with each radiocarbon analysis, although other uncertainties still exist (as discussed above).

Using CALIB 3.0.3, the radiocarbon analyses were also converted to probability distributions in order to provide a better visual depiction of the most probable age of each sample and of stratigraphic units, and to allow easier comparison of the probable age ranges (Fig. 1).

Results and Interpretation

The charcoal samples from trenches 3 and 4, along a west-facing fault trace east of the main Pajarito fault escarpment, are all from units that are believed to post-date the MRE. The oldest analysis, 2230 ^{14}C yr BP (years before present), is close to the fault in trench 4, and may provide the best minimum-limiting age for the MRE on this trace. The other analyses from trenches 3 and 4 are younger, 1300 and 1690 ^{14}C yr BP, and might record younger depositional events or the bioturbation of younger charcoal into the deposits. None of these samples are from the base of the post-faulting (Holocene) sediments, and thus may not closely define the initiation of deposition.

The charcoal samples from trench 7, along a west-facing fault trace east of the main Pajarito fault escarpment, are partially from units that were inferred to post-date the MRE, and partially from a fissure fill along the fault. The latter samples could presumably represent charcoal that was present on the surface or in the soil prior to faulting, which would have dropped into the fissure before it was buried by post-faulting colluvium. In this case, the samples could be similar in age to or pre-date faulting.

The trench 7 analyses display internal consistency in individual stratigraphic sections, but are inconsistent when two sampled sections, roughly 2 m apart, are compared. The western section, 2 m west of the fault, yielded statistically identical dates of 3960 and 4020 ^{14}C yr BP separated by 45 cm of colluvium, suggesting a well-constrained depositional event at ca. 4.0 ^{14}C ka, inferred from the stratigraphy to post-date the MRE. The eastern section at the fault, however, provided a date of 1510 ^{14}C yr BP from a unit directly overlying the fault and dates of 2200, 2590, and 2870 ^{14}C yr BP over a vertical range of about 2 m within the fissure fill. If the fissure became closed at the surface soon after faulting, then the dates at the eastern section suggest the MRE occurred between ca. 2.2 and 1.5 ^{14}C ka. This would require that an unrecognized erosional unconformity exist between the two sampled sections in trench 7.

The available radiocarbon analyses thus suggest two possibilities for the timing of the MRE along this part of the Pajarito fault zone. First, if the trench 7 fissure fill became isolated from the surface soon after the MRE, and if the same MRE is recorded on both sampled fault traces, then the best estimate of the MRE would be ca. 2.22 ^{14}C ka, equivalent to 2.16-2.3 cal ka or 210-350 cal BC (with 2σ range of 2.05-2.35 cal ka, or 100-400 cal BC, using an average of samples WJR-21 and WJR-29). Second, if the fissure fill samples were emplaced significantly after faulting, and no erosional unconformity exists between the two sampled trench 7 sections, then the MRE would be $\geq$ ca. 4.0 ^{14}C ka, equivalent to $\geq$ ca. 4.44 cal ka.

An age of ca. 2.2 ^{14}C ka is much younger than the MRE as previously estimated for either the Guaje Mountain fault zone (GMFZ) or the Rendija Canyon fault zone (RMFZ) (Gardner et al., 1990; Wong et al., 1995; Kelson et al., 1996), and would thus suggest that these three faults have moved independently in the Holocene. Alternatively, if the fissure fill samples are discounted, then the MRE on the trench 7 fault trace could be equivalent to the MRE on the GMFZ (ca. 4-6 ^{14}C ka) or perhaps the older MRE on the RCFZ (ca. 7.3 ^{14}C ka or ca. 23 TL ka).

References

Gardner, J. N., Baldridge, W. S., Gribble, R., Manley, K., Tanaka, K., Geissman, J. W., Gonzalez, M., and Baron, G., 1990, Results from Seismic Hazards Trench #1 (SHT-1) Los Alamos Seismic Hazards Investigations: unpublished report, Memorandum EES1-SH90-19, Los Alamos National Laboratory, Los Alamos, New Mexico.

Kelson, K. I., Hemphill-Haley, M. A., Olig, S. S., Simpson, G. D., Gardner, J. N., Reneau, S. L., Kolbe, T. R., Forman, S. L., and Wong, I. G., 1996, Late Pleistocene and possibly Holocene displacement along the Rendija Canyon fault, Los Alamos County, New Mexico, *in* Goff, F., Kues, B. S., Rogers, M. A., McFadden, L. D., and Gardner, J. N., eds., The Jemez Mountains region: New Mexico Geological Society Forty-Seventh Annual Field Conference Guidebook, p. 153-160.

Reneau, S. L., Kolbe, T., Simpson, D., Carney, J. S., Gardner, J. N., Olig, S. S., and Vaniman, D. T., 1995, Surficial materials and structure at Pajarito Mesa, *in* Reneau, S. L., and Raymond, R., Jr., eds., Geological site characterization for the proposed Mixed Waste Disposal Facility, Los Alamos National Laboratory: Los Alamos National Laboratory Report LA-13089-MS, Los Alamos, New Mexico, p. 31-69.

Stuiver, M., and Reimer, P. J., 1993, Extended ^{14}C data base and revised CALIB 3.0 ^{14}C age calibration: Radiocarbon, v. 35, p. 215-230.

Wong, I., Kelson, K., Olig, S., Kolbe, T., Hemphill-Haley, M., Bott, J., Green, R., Kanakari, H., Sawyer, J., Silva, W., Stark, C., Haraden, C., Fenton, C., Unruh, J., Gardner, J., Reneau, S., and House, L., 1995, Seismic Hazards Evaluation of the Los Alamos National Laboratory: unpublished report, Woodward-Clyde Federal Services, Oakland, California, January 1995, 3 volumes.

Figure Caption

Figure 1. Combined probability distributions for each of the nine radiocarbon analyses obtained from the 1997 Pajarito fault zone trenches. Distributions were calculated using CALIB 3.0.3 (Stuiver and Reimer, 1993), with 2σ uncertainty and an error multiplier of 2.0 on the original analyses. Vertical scale is arbitrary. Two alternatives for the timing of the most recent surface rupture event (MRE) are indicated.

Table 1

Radiocarbon Dates From 1997 Palarito Fault Zone Trenches, Camp May Road

Field Number	Laboratory Number	^{14}C Date (yr B.P.) *	$\delta^{13}C$ (o/oo)	Calibrated Age (CALIB 3.0.3) **	Depth (m)	Trench Distance (m)	Notes
Trench 3							
WJR-18	Beta-108400	1300 ± 80	-24.9	1260 cal BP (920-1520)	0.35	5.4	rocky colluvium, fine sand matrix
Trench 4							
WJR-20	Beta-108401	1690 ± 40	-23.2	1560 cal BP (1400-1800)	0.3	9.6	massive fine-grained deposit
WJR-21	Beta-108402	2230 ± 40	-23.3	2200-2310 cal BP (2000-2360)	0.25	2.4	rocky colluvial deposit, near fault
Trench 7							
WJR-15	Beta-108398	3960 ± 60	-22.3	4410 cal BP (4000-4820)	1.05	8.9	fine-grained deposit
WJR-16	Beta-108399	4020 ± 50	-23.6	4450-4510 cal BP (4160-4830)	1.5	8.6	basal Holocene deposit
WJR-25	Beta-113029	1510 ± 50	-24.2	1360-1390 cal BP (1260-1600)	1.0	11.0	lower Holocene section, at fault
WJR-27	Beta-113030	2580 ± 40	-22.8	2740 cal BP (2360-2840)	1.75	10.9	tuff rubble in fissure
WJR-28	Beta-113031	2870 ± 40	-23.4	2960 cal BP (2780-3220)	2.8	11.0	tuff rubble in fissure
WJR-29	Beta-113032	2200 ± 50	-23.8	2150-2290 cal BP (1940-2360)	3.6	11.0	tuff rubble in fissure

Notes:

* Reported dates were corrected for carbon isotope fractionation using $\delta^{13}C$ values, normalized a $\delta^{13}C$ of -25 o/oo. Uncertainties are 1σ.

** Calibrated ages obtained using computer program CALIB 3.0.3 (Stuiver and Reimer, 1993). Ages in parentheses indicate 2σ uncertainty, using an error multiplier of 2.0.

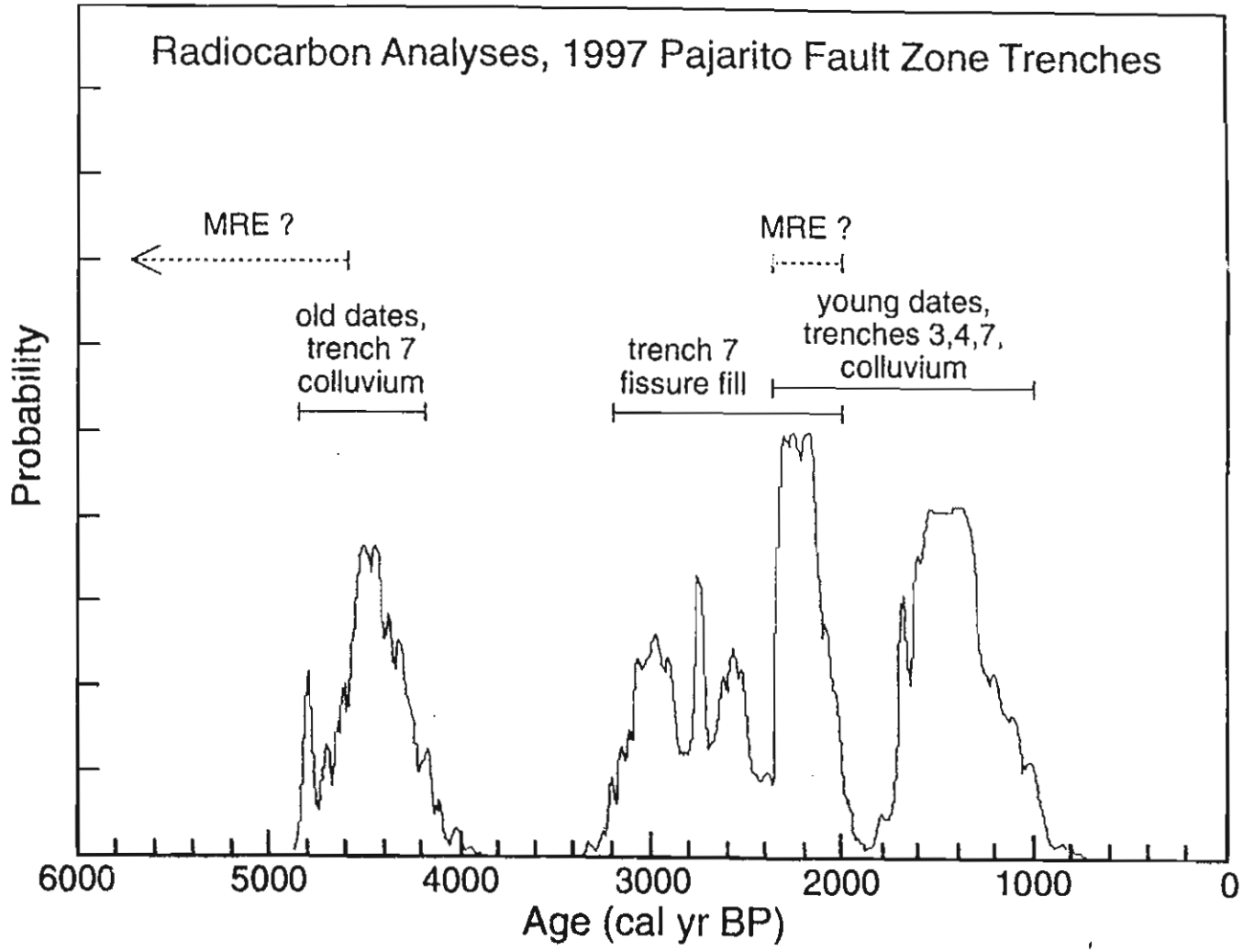
Radiocarbon Analyses, 1997 Pajarito Fault Zone Trenches
MRE ?
MRE ?
old dates,
trench 7
colluvium
trench 7
fissure fill
young dates,
trenches 3,4,7,
colluvium
Probability
6000
5000
4000
3000
2000
1000
0
Age (cal yr BP)

Figure 1.

APPENDIX D

Report by Steven L. Forman, University of Illinois-Chicago, on thermoluminescence (TL) dating.

Luminescence Dating

Luminescence geochronometry has been used previously to determine ages of up to 100,000 yr and older for sediments that received sufficient solar radiation prior to deposition (e.g., Huntley et al., 1993). Usually, exposure of sediment to sunlight for at least 8 hours eliminates most of an inherited TL signal from mineral grains, thus resetting the TL clock. Luminescence geochronology usually measures the time-dependant dosimetric properties of quartz and feldspar minerals. Exposure of these minerals to ionizing radiation from the decay of naturally occurring radioisotopes in sediments imparts a luminescence signal that accumulates during burial, after the sediment is shielded from further light exposure. The intensity of the TL signal, if calibrated against a known radiation dose in the laboratory, can be used as a measure of sample age. The age is calculated by dividing the laboratory determined dose (equivalent dose, ED) by an estimate of the radioactivity the sample received during burial (dose rate, DR).

Thermoluminescence Dating Methods Used in This Study:

The thermoluminescence signal was measured on the fine grained (4-11 um) polymineral fraction of sediments. All samples were analyzed by the total-bleach method, with the residual level defined as the TL remaining after an 8 hour exposure of a UV-dominated spectra from a 275-watt "sunlamp". which results in near total resetting of the TL signal. Dose rate estimates were derived from U and Th concentrations, inferred from thick-source alpha counting and the ^{40}K content calculated from the total potassium concentration.

Blue TL emissions (which are considered a time sensitive luminescence signal; Balescu and Lamothe, 1992) were selected for measurement, by placing a Corning 5/58 filter in front of the photomultiplier tube. All samples were preheated at 124 degrees C for at least 48 hours, prior to analysis to remove a potential instability (anomalous fading) in the laboratory induced TL signal. Each sample, post heating was also tested for anomalous fading, by storing irradiated (100 to 450 Gy) material for at least 32 days and comparing to the TL signal of an unstored aliquot. The anomalous fading tests reveal no instability in the preheated TL signal.

The rate of TL growth was evaluated by appling additional beta doses to the natural TL signal by a series of extended radiations with a calibrated 90Sr/90Y source. The highest radiation dose added to the natural TL signal was at least six times the calculated equivalent dose, which is sufficient to accurately interpolate an equivalent dose. The natural and additive dose data were fitted by an saturating double-exponential function to calculate an equivalent dose (cf. Huntley et al., 1988; Pierson, unpub. data). Equivalent dose values are calculated over a range of temperatures, usually between 250 to 350 degrees C or 250 to 400 degrees C which includes at least 90% of the measured TL signal and is also the temperature region that exhibits a pronounced plateau in equivalent dose values.

Aitken, M. J., and Bowman, S. G. E. 1975, Thermoluminescent dating: Assessment of alpha particle contribution. Archaeometry, 17, 132-138.

Balescu, S. and Lamothe M., 1992, The blue emissions of K-feldspar coarse grains and its potential for overcoming TL age underestimates: Quaternary Science Reviews, v. 11, p. 45-51.

Godfrey-Smith, L. I., Huntley, D. J. and Chen, W.-H., 1988, Optical dating studies of quartz and feldspar sediment extracts: Quaternary Science Reviews v. 7, p. 373-380.

Huntley, D. J., and Wintle, A. G., 1981,The use of alpha scintillation counting for measuring Th-230 and Pa-231 contents of ocean sediments. Canadian Journal of Earth Sciences, 18, 419-432.

Huntley, D. J., Hutton, J. T. and Prescott, J. R., 1993, The stranded beach-dune sequence of south-east sout Australia: A test of thermoluminescence dating, 0-800 ka: Quaternary Science Reviews v. 12, p. 1-20.

Table 1: Thermoluminescence Age Estimates for Pajarito Fault Trench Studies, Los Alamos National Laboratory New Mexico

Field No.	Lab sample No.	Strat. Unit	Equivalent Dose Method[1]	Light Exposure[2]	Temperature (°C)[3]	Equivalent Dose (grays)[4] est.	TL age (ka)[4]
PF97-2	UIC-635	colluvium	TL-Total Bleach	16h sun	250-400	494.11+/-17.54	105.5+/-10.0
			TL-Total Bleach	8h UV	250-400	503.21+/-17.63	107.5+/-10.0
PF97-3	UIC-633	colluvium	TL-Total Bleach	16h sun	250-350	445.32+/-15.25	69.5+/-6.0
			TL-Total Bleach	8h UV	250-350	449.43+/-15.28	68.5+/-6.0
PF97-4	UIC-637	colluvium	TL-Total Bleach	16h sun	250-400	293.61+/-3.79	94.0+/-9.0
			TL-Total Bleach	8h UV	250-400	289.94+/-3.85	93.0+/-9.0
PF97-5	UIC-634	colluvium	TL-Total Bleach	16h sun	250-400	206.41+/-10.31	43.0+/-4.5
			TL-Total Bleach	8h UV	250-400	206.11+/-10.41	43.0+/-4.5
PF97-7	UIC-638	colluvium	TL-Total Bleach	thermal reset	250-350 (close maximum estimate)	54.91+/-6.23	13.0+/-1.5*
PF97-8	UIC-639	colluvium	TL-Total Bleach	thermal reset	250-350 (close maximum estimate)	30.99+/-3.31	7.0+/-0.8*
PF97-10	UIC-636	colluvium	TL-Total Bleach	16h sun	250-350	707.11+/-32.02	133.0+/-12.0
			TL-Total Bleach	8h UV	250-350	703.21+/-31.96	132.0+/-12.0

[1]All TL measurements were made with a Corning 5/58 and HA-3 filters in front of the photomultiplier tube. Samples were preheated to 124 °C for 48 hrs prior to analysis.

[2]Hours of light exposure to define residual level. "Sun" is natural sunlight in Chicago, Illinois. UV is light exposure from 275 watt General Electric "sunlamp".

[3]Temperature range used to calculate equivalent dose.

[4] All errors are at one sigma and calculated by averaging the errors across the temperature range. A moisture content of 15 Ò 5% was assumed for all samples in the final age calculation.

* Preliminary age calculation.